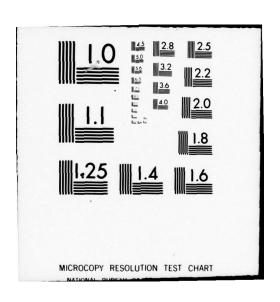
NAVAL OCEANOGRAPHIC OFFICE NSTL STATION MS
EASTERN ARCTIC AREA 15- AND 30-DAY ICE FORECASTING GUIDE. (U)
APR 79 P A MITCHELL AD-A072 930 F/6 8/12 N00-SP-266 UNCLASSIFIED NL 1 OF 3 ADA 072930



NAVAL OCEANOGRAPHIC OFFICE SPECIAL PUBLICATION 266



EASTERN ARCTIC AREA 15- AND 30-DAY
ICE FORECASTING GUIDE

APRIL 1979



AG 22 1979

Approved for public release, distribution unlimited

DEPARTMENT OF THE NAVY NSTL STATION BAY ST LOUIS, MS 39522

THE COPY

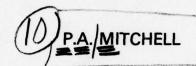
ABSTRACT

Procedures for preparing 15- and 30-day forecasts of ice conditions in the eastern North American Arctic which relate current and historical ice data to environmental parameters are given. Background data on environmental factors which influence the growth, movement, and decay of sea ice in the eastern Arctic region are detailed and include primary and secondary storm tracks, sea level pressure, surface air temperature, and surface currents. Analyses of historical sea ice distribution data which have been observed over the 18-year period from 1954 through 1971 are presented and include the mean, median, mean maximum, mean minimum, absolute minimum, and absolute maximum eastern and western positions of the pack ice edges at half-monthly intervals. Advancement and recession rates of ice edge movement computed for the entire year and analyses of mean ice concentrations and percentage of large floe sizes for the western Labrador Sea, Baffin Bay/Davis Strait region, and the east Greenland coastal regions are included. Data also include frost degree-day, related ice -growth, and estimated ice disintegration curves for 17 eastern Arctic coastal stations. Statistical methods for forecasting ice growth, movement, distribution, and decay are presented since these methods have been proven most successful.

14) NOO-SP-266

EASTERN ARCTIC AREA 15- AND 30-DAY

ICE FORECASTING GUIDE,





12) 263 P'



Special publication,

Approved for public release, distribution unlimited

250 450

NAVAL OCEANOGRAPHIC OFFICE NSTL STATION BAY ST LOUIS, MS 39522

250 450

79 08 20 121

set

FOREWORD

The U. S. Navy pioneered operational sea ice forecasting for arctic operations almost 3 decades ago. This important requirement exists to this day and presently supports both surface and subsurface operations. Using data gathered from satellite imagery, aerial reconnaissance, and snip and shore ice reports over the 18-year period from 1954 through 1971, this forecasting guide presents a summary of statistical long-range ice forecasting techniques available to the forecaster. Historical ice and environmental data for the eastern North America Arctic region as presented herein will prove to be valuable forecasting tools when used in conjunction with real-time information.

W.C. Palmer Captain, USN Commander

N2	cession For	Z
Un	C TAB	
By_Dis	ribution	目
Dist	Availand/	or
A	special	

CONTENTS

		P	age
ı.	INT	RODUCTION	1
II.	BACI	KGROUND INFORMATION	2
	A.	Physical Features	3
	В.	Storm Tracks	4
	C.	Sea Level Pressure	7
	D.	Surface Air Temperature	8
		1. Frost Degree Days	9
		2. Surface Temperature Distribution	9
	E.	Surface Currents	10
III.	HIST	TORICAL SEA ICE DISTRIBUTION	12
	A.	Annual Cycle	12
	В.	Pack Edge	13
		1. Semimonthly Positions and Ranges	13
		2. Advancement and Recession Rates	15
	C.	Ice Concentration and Large Floe Sizes	22
		1. Concentration Analysis	23
		2. Floe-Size Analysis	26
IV.	FORE	ECASTING TECHNIQUES	27
	A.	Forecasting Ice Edge Movement, Pack Concentration, and	
		Floe Size Coverage	28
		1. Davis Strait	29
		2. Western Labrador Sea	33
		3. Denmark Strait/Western Greenland Sea	37
	В.	Forecasting Freezeup and Ice Growth	39
		1. Increasing Ice Growth	41
			41
		b. Offshore Ice Pack	44
	c.	Forecasting Breakup and Decreasing Ice Thickness	45
Bibli	ograp	phy	48

FIGURES

				Page
1. Place I	V 01 E			51
	Name Chart Eas	stern North Americ	can Arctic · · · · ·	
3. Princip	pal Tracks of	Lows for January		53
4. Princip	pal Tracks of	Lows for April		54
5. Princip	al Tracks of	Lows for October		55
6. Surface	Currents -	Summer		56
			me Positions of the Pac	
			· · · · · · · · · · · · · · · ·	
	1st-15th of	month	16th-end o	f month
	Figure	Page	Figure	Page
January	8A	58	8B	59
February	9A	60	9в	61
March	10A		10B	63
April	11A		11B	
May	12A		12B	
June	13A		13B	
July	14A			71
August	15A		15B	
September	15B		15B	
October	15B		15B	
November	16A		16B	
December	17A	76	17B	77
18A. through	29B. Mean.	Median, and Extre	eme Positions of the Pa	ck
	Figure	Page	Figure	Page
January	18A	73	188	79
February	19A		19A	
March	20A		20В	83
April	21A	84	21B	85
May	22A	36	22В	87
June	23A	88	23В	89
July	24A	90	24B	
August	25A		25В	93
September	26A		26В	95
October	27A		27В	97
November	28A	• • 93	28B	99
December	29A	• • 100	29В	• • • 101
30A. through	41B. Mean.	Median, and Extra	eme Positions of the Pa	ck
	Fact Creenle			102 -11

FIGURES (con.)

	1st-15th of mo	nth	16th-end of	month	
	Figure	Page	Figure	Page	
January	30A	102	30в	103	
February	31A	104	31B		
March	32A		32B		
April April	33A		33В		
May	34A		34B		
June	35A		35B		
July	36A		36B		
August	37A		37В		
September	38A		38B		
October	39A		39B		
November	40A		40B		
December	41A		41B		
Section Section					
42A. Enrou	ign 53B. Mean,	Median, and E	xtreme Positions of	f the Pack	
Edge	- Southwest Co	ast of Greenl	and		. 126-137
	Figure	Page	Figure	Page	
January	42A	126	42B	126	
February	43A	127	43B	127	
March	44A	128	44B	128	
April	45A	129	45B		
May	46A	130	46B		
June	47A	131	47B		
July	48A	132	48B		
August	49A	133	49B	133	
September	50A	134	50B		
October	51A	135	51B		
November	52A	136	52B		
December	53A	137	53B		
54A. throu	gh 77A. Mean I	ce Concentrati	ion		. 138-184
54B. throu	gh 77B. Mean F	loe-Size Perce	entage		. 139-185
	Figure	Page	Figure	Page	
January 1-15	54A	• 138	54B	100	
16-31	55A		55B		
February 1-15				• • • 141	
16-28			57B		
March 1-15	58A		58B		
16-31	59A				
April 1-15	60A		59B		
16-30	61A		60B	• • • 151	
10-30	OIA	. 132	61B	• • • 153	

FIGURES (con.)

			m
	Figure		Figure Page
May 1-15	62A		62B 155
16-31	63A	156	63B 157
June 1-15	64A	158	64B 159
16-30	65A	160	65B 161
July 1-15	66A	162	66B 163
16-31	67A	164	67B 165
August 1-15	68A		68B 167
16-31	69A		69B 169
September 1-15	70A		70В 171
16-30	71A		71B 173
October 1-15	72A		72B 175
16-31	73A		73B 177
	74A		74B 179
November 1-15			
16-30	75A		75B 181
December 1-15	76A		76B 183
16-31	77A	184	77B 185
	Mean 700-Millibar Pr		
Normal Chart			• • • • • • 186
79. NOAA 30-Day N	Mean Sea Level Progra	ostic Chart (mb)	187
80. Location Char	t for Frost Degree-	Day, Ice-Growth,	and
Disintegrati	ion Curves		189
81A, through 97A.	Frost Degree-Day (urves	190-222
81R through 97R	Theoretical Ice-Gr	owth and Estimat	ed
Disintegrati	ion Curvos	owen and bottman	191-223
Distincegraci	ton curves		
Disintegrati			
Disintegraci	Figure		Figure Page
	Figure	Page	Figure Page
Angmagssalik	Figure 81A	Page	Figure Page 81B 191
Angmagssalik Aputiteq	Figure 81A	Page 190 192	Figure Page 81B 191 82B 193
Angmagssalik Aputiteq Cape Dyer	Figure 81A	Page 190 192 194	Figure Page 81B 191 82B 193 83B 195
Angmagssalik Aputiteq Cape Dyer Cartwright	Figure 81A	Page 190 192 194 196	81B 191 82B 193 83B 195 84B 197
Angmagssalik Aputiteq Cape Dyer Cartwright Clyde River	Figure 81A	Page 190 192 194 196 198	Figure Page 81B 191 82B 193 83B 195 84B 197 85B 199
Angmagssalik Aputiteq Cape Dyer Cartwright Clyde River Daneborg	Figure 81A	Page 190 192 194 196 198 200	Figure Page 81B 191 82B 193 83B 195 84B 197 85B 199 86B 201
Angmagssalik Aputiteq Cape Dyer Cartwright Clyde River Daneborg Egedesminde	Figure 81A	Page 190 192 194 196 198 200 202	Figure Page 81B 191 82B 193 82B 195 84B 197 84B 197 85B 199 86B 201 87B 203
Angmagssalik Aputiteq Cape Dyer Cartwright Clyde River Daneborg Egedesminde Frobisher Bay	Figure 81A	Page 190 192 194 196 198 200 202 204	Figure Page 81B 191 82B 193 82B 195 84B 197 84B 197 85B 199 86B 201 87B 203 88B 205
Angmagssalik Aputiteq Cape Dyer Cartwright Clyde River Daneborg Egedesminde Frobisher Bay Goose Bay	Figure 81A	Page 190 192 194 196 198 200 202 204 206	Figure Page 81B 191 82B 193 82B 193 83B 195 84B 197 85B 199 86B 201 87B 203 88B 205 89B 207
Angmagssalik Aputiteq Cape Dyer Cartwright Clyde River Daneborg Egedesminde Frobisher Bay Goose Bay Hopedale	81A 82A 83A 84A 85A 86A 87A 88A 90A	Page 190 192 194 196 198 200 202 204 206 208	Figure Page 81B 191 82B 193 83B 195 84B 197 85B 199 86B 201 87B 203 88B 205 89B 207 90B 209
Angmagssalik Aputiteq Cape Dyer Cartwright Clyde River Daneborg Egedesminde Frobisher Bay Goose Bay	81A 82A 83A 84A 85A 86A 88A 90A 91A	Page 190 192 194 196 198 200 202 204 206 208 210	81B 191 82B 193 83B 195 84B 197 85B 199 86B 201 87B 203 88B 205 89B 207 90B 209 91B 211
Angmagssalik Aputiteq Cape Dyer Cartwright Clyde River Daneborg Egedesminde Frobisher Bay Goose Bay Hopedale	81A 82A 83A 84A 85A 86A 88A 90A 91A 92A	Page 190 192 194 196 198 200 202 204 206 208 210 212	Figure Page 81B 191 82B 193 83B 195 84B 197 85B 199 86B 201 87B 203 88B 205 89B 207 90B 209
Angmagssalik Aputiteq Cape Dyer Cartwright Clyde River Daneborg Egedesminde Frobisher Bay Goose Bay Hopedale Kap Tobin	81A 82A 83A 84A 85A 86A 88A 90A 91A	Page 190 192 194 196 198 200 202 204 206 208 210 212	81B
Angmagssalik Aputiteq Cape Dyer Cartwright Clyde River Daneborg Egedesminde Frobisher Bay Goose Bay Hopedale Kap Tobin Resolution Island Sondrestrom St. Anthony	81A 82A 83A 84A 85A 86A 88A 90A 91A 92A	Page 190 192 194 196 198 200 202 204 206 208 210 212 214	81B 191 82B 193 83B 195 84B 197 85B 199 86B 201 87B 203 88B 205 89B 207 90B 209 91B 211 92B 213
Angmagssalik Aputiteq Cape Dyer Cartwright Clyde River Daneborg Egedesminde Frobisher Bay Goose Bay Hopedale Kap Tobin Resolution Island Sondrestrom St. Anthony	81A 82A 83A 84A 85A 86A 89A 91A 93A	Page 190 192 194 196 198 200 202 204 206 208 210 212 214 216	81B
Angmagssalik Aputiteq Cape Dyer Cartwright Clyde River Daneborg Egedesminde Frobisher Bay Goose Bay Hopedale Kap Tobin Resolution Island Sondrestrom St. Anthony Stephenville	Figure 81A	Page 190 192 194 196 198 200 202 204 206 208 210 212 214 216 218	81B 191 82B 193 83B 195 84B 197 85B 199 86B 201 87B 203 88B 205 89B 207 90B 209 91B 211 92B 213 93B 215 94B 217 95B 219
Angmagssalik Aputiteq Cape Dyer Cartwright Clyde River Daneborg Egedesminde Frobisher Bay Goose Bay Hopedale Kap Tobin Resolution Island Sondrestrom St. Anthony Stephenville Thule	Figure 81A	Page 190 192 194 196 198 200 202 204 206 208 210 212 214 216 218 220	81B 191 82B 193 83B 195 84B 197 85B 199 86B 201 87B 203 88B 205 89B 207 90B 209 91B 211 92B 213 93B 215 94B 217 95B 219 96B 221
Angmagssalik Aputiteq Cape Dyer Cartwright Clyde River Daneborg Egedesminde Frobisher Bay Goose Bay Hopedale Kap Tobin Resolution Island Sondrestrom St. Anthony Stephenville	Figure 81A	Page 190 192 194 196 198 200 202 204 206 208 210 212 214 216 218 220	81B 191 82B 193 83B 195 84B 197 85B 199 86B 201 87B 203 88B 205 89B 207 90B 209 91B 211 92B 213 93B 215 94B 217 95B 219
Angmagssalik Aputiteq Cape Dyer Cartwright Clyde River Daneborg Egedesminde Frobisher Bay Goose Bay Hopedale Kap Tobin Resolution Island Sondrestrom St. Anthony Stephenville Thule Upernavik	81A 82A 83A 85A 86A 87A 88A 90A 91A 92A 94A 95A 97A	Page 190 192 194 196 198 200 202 204 206 208 210 212 214 216 218 220 222	81B
Angmagssalik Aputiteq Cape Dyer Cartwright Clyde River Daneborg Egedesminde Frobisher Bay Goose Bay Hopedale Kap Tobin Resolution Island Sondrestrom St. Anthony Stephenville Thule Upernavik	## Figure ## 81A	Page 190 192 194 196 198 200 202 204 206 208 210 212 214 216 218 220 222 Thickness and S	Figure Page 81B
Angmagssalik Aputiteq Cape Dyer Cartwright Clyde River Daneborg Egedesminde Frobisher Bay Goose Bay Hopedale Kap Tobin Resolution Island Sondrestrom St. Anthony Stephenville Thule Upernavik	## Figure ## 81A	Page 190 192 194 196 198 200 202 204 206 208 210 212 214 216 218 220 222 Thickness and S	81B
Angmagssalik Aputiteq Cape Dyer Cartwright Clyde River Daneborg Egedesminde Frobisher Bay Goose Bay Hopedale Kap Tobin Resolution Island Sondrestrom St. Anthony Stephenville Thule Upernavik 98. Ice-Growth Gracumulations	## ## ## ## ## ## ## ## ## ## ## ## ##	Page 190 192 194 196 198 200 202 204 206 208 210 212 214 216 218 220 222 Thickness and S	81B 191 82B 193 83B 195 84B 197 85B 199 86B 201 87B 203 88B 205 89B 207 90B 209 91B 211 92B 213 93B 217 95B 219 96B 221 97B 223 mall Degree-Day 224
Angmagssalik Aputiteq Cape Dyer Cartwright Clyde River Daneborg Egedesminde Frobisher Bay Goose Bay Hopedale Kap Tobin Resolution Island Sondrestrom St. Anthony Stephenville Thule Upernavik 98. Ice-Growth Graccumulations 99. Ice-Growth Graccumulations	## ## ## ## ## ## ## ## ## ## ## ## ##	Page 190 192 194 196 198 200 202 204 206 208 210 212 214 216 218 220 222 Thickness and S	81B 191 82B 193 83B 195 84B 197 85B 199 86B 201 87B 203 88B 205 89B 207 90B 209 91B 211 92B 213 93B 217 95B 219 96B 221 97B 223 mall Degree-Day 224

TABLES

		Page
I	. Advancement and Recession Rates of Ice Edge for 15-Day Periods August 1-December 31 (1953-1971)	16
11	. Advancement and Recession Rates of Ice Edge for 15-Day Periods January 16-April 30 (1953-1971)	17
111	. Advancement and Recession Rates of Ice Edge for 15-Day Periods May 1-July 31 (1953-1971)	18
IV	. Advancement and Recession Rates of Ice Edge for 15-Day Periods August 1-January 31 (1953-1971) - Greenland Coast East of 45°W	19
V	. Advancement and Recession Rates of Ice Edge for 15-Day Periods February 1-July 31 (1953-1971) - Greenland Coast East of 45°W	20
VI	. Advancement and Recession Rates of Ice Edge for 15-Day Periods December 1-September 15 (1953-1971) - Greenland Coast West of 45 W	21
VII	. Breakup-Freezeup Dates for Coastal Stations	42
C-1	. 30-Day Degree-Day Modifications to Predicted Totals	257
	APPENDIXES	
A. M	ean Sea Level Pressure Charts, January-December, Eastern North American Arctic	
в. м	ean Monthly Surface Air Temperature Charts, January-December, Eastern North American Arctic	. 241
C. 7	00-Millibar Departure-from-Normal Thickness Derivation and 30-Day Degree-Day Modification Table to Predicted Totals	255

I. INTRODUCTION

In 1946, the U.S. Navy was assigned responsibility for the resupply of weather stations located in Labrador, Greenland, and the Canadian Arctic. During the late 1940's and through the mid-1950's when the stations comprising the Distant Early Warning (DEW) line were constructed in Greenland and along the northern reaches of Canada and Alaska, vast quantities of material had to be sealifted through ice infested waters. During this period the need for the U.S. Navy to conduct aerial ice reconnaissance and to promulgate analysis of sea conditions and ice forecasts in the North American Arctic was firmly established. An annual Navy requirement to sealift material to stations in the eastern North American Arctic and to provide operational sea ice forecasts and analyses in support of this requirement, and other Department of Defense polar missions as well, exists to this day.

Prior to the late 1960's, sea ice data were collected in the polar regions through the use of platforms such as marine vessels, land stations, and from both fixed-wing and rotor-driven aircraft. This information served as the source input for ice forecasts, but, as more and more detailed data became available, it also served to further the investigation into the development of improved and new forecasting techniques. In the late 1960's a new observation platform, earth-orbiting satellite, appeared. The data from this new platform, in combination with those obtained by ship, shore, and aerial reconnaissance ice observers, have made it possible to compile a detailed historical record of arctic ice conditions.

The purpose of this publication is to provide the operational ice forecaster with the procedures and necessary background data needed to prepare 15- and 30-day forecasts of sea ice growth, movement, distribution, and decay in the eastern North American Arctic (hereafter referred to as the eastern Arctic). Since knowledge relating to the average and extreme extents of sea ice and the average ice conditions existing within the pack ice cover for specific geographical areas and times of the year plays an essential role in the preparation of any ice forecast, the major portion of this guide is devoted to a detailed analysis of historical ice conditions in the eastern Arctic observed, for the most part, from 1954 through 1971. With these data at his disposal, the ice forecaster can immediately relate current ice conditions to normal and extreme conditions observed during a similar semimonthly time period.

An equally essential role in the predictive process is played by the various environmental elements which influence the growth, distribution, movement, and decay of sea ice. When preparing an ice forecast, the forecaster should be able to identify anomalous environmental conditions, either presently existing or forecasted, which will drastically change ice conditions. Although the majority of ice observations made in the eastern Arctic through calendar year 1971 was collected during the time period between breakup and freezeup, the ice conditions presented in this guide cover a 12-month period. Consequently, the number of observations made in late fall, winter, and early spring is small in comparison. As

observations are increased during these periods through the use of satellite imagery and additional aerial reconnaissance, the additional data will no doubt cause changes in average and extreme statistical values.

As with any forecasting procedure, it is desirable that the predictive techniques used to produce a 15- and a 30-day ice forecast are as objective as possible. However, in the case of ice forecasts, the forecaster is working in an area of the world where synoptic measurements of the environmental parameters needed to increase this objectivity are not routinely available. There is also che additional problem that even if the measurements were available, ice dynamists have not as yet solved the complex interrelationships between dynamic forces produced when these parameters act in concert on the polar ice pack. Subjectivity in the ice forecasting process, therefore, can never really be isolated to a large degree. The forecaster must rely heavily on his knowledge of the physical oceanographic and meteorological processes which influence sea ice formation and movement, as well as knowledge concerning sea ice distribution and its variability in both time and space. This knowledge will vary directly with the forecaster's experience and will therefore impart subjectivity to the final forecast. It also should be noted that although weather forecasting is now considered by many to be a science, it is generally agreed that a forecast more that 3 days in advance is not very reliable. Coordinated experiments in the field to measure ice dynamics and characteristics and the thermodynamic interaction between the atmosphere and sea ice, such as the Arctic Ice Dynamic Joint Experiment (AIDJEX) described by Untersteiner and Humkins (1969), will ultimately contribute greatly to development of numerical prediction models that will be necessary for a successful objective operational program. This will, however, involve results from many more field experiments in the years ahead.

The operational ice forecaster generally concerns himself with three types of forecasts. These are (1) short-range forecasts for the ensuing 24- to 48-hour period which, by necessity, provide detailed ice information since they usually provide close tactical support over a specific locality to ongoing polar missions; (2) long-range forecasts that estimate ice conditions during the ensuing 15 to 30 days and are used primarily for planning purposes in areas where ship operations are either underway or shortly planned; and (3) seasonal ice outlooks which cover periods from 60 to 90 days and are ordinarily updated by the 15- and 30-day forecasts. This guide deals specifically with 15- and 30-day long-range ice forecasts for the eastern Arctic region.

II. BACKGROUND INFORMATION

The annual cycles of the growth and decay of sea ice, as well as its movement and subsequent distribution, are governed by local topography, air temperature, storm surges, ocean currents, wind stress, and water density.

Variations in water density are a function of the preceding factors and need not be discussed separately. For the forecaster to understand the behavior of the everchanging pack ice, however, a thorough understanding of these parameters over both time and space in the eastern Arctic is necessary, especially since synoptic measurements of these elements over arctic waters and pack ice are not routinely available. As an aid in achieving this understanding, brief descriptions of these factors are presented along with charts depicting their mean conditions in the eastern Arctic.

In addition, the sea ice forecaster should have a working knowledge of average ice conditions in the forecast area, as well as minimum and maximum extents that pack ice has achieved in the past. The arctic sea ice forecaster is concerned primarily with ice conditions in the marginal sea ice zone, which may be defined as the area that undergoes an almost complete cycle of growth and decay within a single year. Fluctuations in this annual cycle, caused primarily by environmental factors, impart great spatial variability to the ice cover from year to year. This variability is depicted in figures *8A through 53B for the eastern Arctic by presenting absolute maximum and minimum extents, average maximum and minimum extents, and the median and mean positions of the pack edge along the latitudes lying within the areas of interest in the eastern Arctic. The numbers of years of observations along these latitudes are also given.

A. Physical Features

For this report the eastern Arctic region has been divided into three primary regions: the Labrador Sea and a portion of the neighboring North Atlantic Ocean which extends up to 250 nmi (463 km) seaward from the Labrador/Newfoundland coasts, the Baffin Bay - Davis Strait region north of 60°N, and Greenland coastal areas between 60°N and 72°N east of 45°W (including the Denmark Strait) and west of 45°W between 60°N and 65°N. An area placename chart for the eastern Arctic is presented as figure 1. The area depicted in figure 1 extends over a north-south distance of approximately 2,190 nmi (4,056 km). Extending as it does over this great north-south area, the environmental phenomena influencing this region show marked differences among themselves.

The Labrador Sea extends northward to 66°N adjacent to the rugged coastlines of Labrador and Newfoundland, which together form its western border. Its eastern border is a line from Cape St. Francis, Newfoundland, to Cape Farvel, Greenland. In the southern region, sea ice has been observed to extend over the western boundary into the North Atlantic Ocean in winter and early spring. Banks with depths of 110 fm (201 m) extend seaward from the Labrador coast for a distance of approximately 75 nmi (139 km). Beyond this point, depths increase to 2,250 fm (4,115 m) in the northwest Atlantic Mid-Ocean Canyon at a distance of approximately 350 nmi (649 km). Off the southeast coast of Newfoundland, the continental shelf widens drastically; and a series of banks, collectively known as the Grand Banks, extends seaward nearly 310 nmi (574 km). The average depths of these banks approach 30 fm (55 m) but in many instances reach 100 fm (183 m).

*The number of years of observation are indicated along left margin of each figure for figures 8A through 53B.

Baffin Bay and Davis Strait are neighboring bodies of water located north of 60°N between Greenland and Baffin Island. Baffin Bay extends northward from 70°N, the boundary between these bodies of water, and includes the narrow Nares Strait between northwest Greenland and Ellesmere Island. Baffin Bay has a deep level basin in its west-central region with depths of approximately 1,350 fm (2,468 m). To the east of this basin lie banks of 275 fm (503 m) or less which extend seaward from the western Greenland coast for nearly 120 nmi (222 km). On the western side of Baffin Bay, adjacent to Baffin Island, lies a narrow, shallow shelf less than 110 fm (271 m), which extends seaward for approximately 30 to 50 nmi (56 to 93 km). Davis Strait, which connects Baffin Bay with the Labrador Sea, extends southward from 70°N where its width approaches 250 nmi (463 km) to 66°30'N where it attains its narrowest width of nearly 180 nmi (333 km), thence to its southern border at 60°N where its width increases dramatically to approximately 500 nmi (927 km). In the northern region of the Davis Strait, the west Greenland coastal banks with depths of 275 fm (503 m) or less continue southward from Baffin Bay and extend seaward for 120 nmi (222 km) between 68°N and 70°N. From 68°N southward to 60°N, these banks become increasingly narrow and range from 90 nmi (167 km) just south of 68°N to 60 nmi (111 km) at 60°N. The narrow shelf along the east coast of Baffin Island extends from Baffin Bay to approximately 66°30'N, where it begins to widen appreciably to attain a maximum seaward extent of 150 nmi (278 km). The greatest depths in Davis Strait, 1,886 fm (3,450 m) are found in its south-central part which contains the northwest extension of the Atlantic Mid-Ocean Canyon. Northward from this area, depths decrease to a minimum of approximately 312 fm (571 m) in the center of its narrowest section at 66°30'N. Depths begin to increase again through its north-central region to reach a maximum of 1,150 fm (2,103 m) at the extreme northern boundary.

The east Greenland coastal region is characterized by an almost continuous shelf of 275 fm (503 m) or less which varies in width from 120 nmi (222 km) to 200 nmi (371 km) between 76°N and 80°N, from 70 to 80 nmi (130 to 148 km) between 70°N and 75°N, 35 nmi (65 km) at 69°N, from 80 to 140 nmi (148 to 259 km) between 64°N and 68°N, and from 25 to 35 nmi (46 to 65 km) between 60°N and 63°N. Depths in the Greenland Sea north of Jan Mayen Island increase from the shelf to a maximum of approximately 1,975 fm (3,613 m), while south of Jan Mayen the maximum depth approaches 1,148 fm (2,100 m). Depths in Denmark Strait, which connects the Greenland Sea with the North Atlantic, vary from 644 fm (1,178 m) in the north to just over 273 (500 m) in the south. In the North Atlantic adjacent to the east Greenland coast, maximum depths approach 1,695 fm (3,100 m) at a distance of 200 nmi (371 km).

B. Storm Tracks

Movement of sea ice is strongly influenced by wind and currents. Of these two parameters, winds by far produce the largest spatial and temporal changes in ice distribution, particularly if the direction of the resultant wind stress component coincides with that of a surface current. Storms, therefore, with their associated strong pressure gradients and higher-than-normal windspeeds will, over relatively short time spans, cause significant changes in the movement, distribution, and deformation of an ice cover. The principal tracks of lows for winter (January), spring (April),

summer (July), and autumn (October) are presented in figures 2 through 5 (Klein, 1957). In the eastern Arctic this effect can be clearly seen as storms move along or deviate from their principal tracks near the coastal regions of east Greenland and Labrador. A good example of this phenomenon occurred along the east Greenland coast in the summer of 1973 when the approaches to Angmagssalik on the east coast of Greenland at approximately 65°30'N failed to become clear of ice by mid-August as forecasted in the long-range seasonal ice outlook. In fact, ice remained in the approaches throughout summer and fall. If conditions had been normal, cyclones transiting from the Labrador/Newfoundland region and from the Gulf Stream area in the North Atlantic would have followed tracks similar to those shown for July (figure 4) to reinforce the semipermanent cyclone or "Icelandic Low" positioned in August as shown in figure A-8. However, the anticyclonic area normally situated over northern Greenland in August as shown in figure A-8 shifted southward and remained stationary for the most part over the Greenland ice cap between 70°N and 71°N. With high pressure centered over Greenland in this manner, an anomalous northerly windflow north of 70°N and a northeasterly windflow south of 70°N dominated the east Greenland coast during August rather than the more normal onshore flow as depicted in figure A-8. The blocking effect of the high also caused a corresponding eastward shift in the principal track of lows north of Iceland. As the cyclones passed to the east of their normal track, the flow in the strong gradient areas on the backside of these storms worked in concert with the anomalous longshore flow and the prevailing southward moving East Greenland Current to continually advect pack ice from areas north of Scoresby Sund along the southeastern Greenland coast.

The majority of storms affecting the eastern Arctic originates in Alberta, Canada, and subsequently moves eastward to join the paths of cyclones from the United States. The United States storms generally develop in the Great Basin, Northern Rockies, Central Plains, Colorado, Texas, Ohio Valley, and in warm waters along the eastern coastal states and in the western Gulf of Mexico. Cyclones migrating into the eastern Arctic tend to converge within the general area of the Icelandic Low. This convergence is most marked over the ocean immediately southwest of Iceland in the area bounded by 60°N and 65°N and 15°W and 30°W (Figures 2-5).

In winter (January), the Alberta cyclones move eastward to the upper Great Lakes region where they merge with storms from the United States. From the Great Lakes, these lows follow a common primary track across southern Canada to the Labrador/Newfoundland coastal region where they merge with storms migrating northeasterly along the east coast of the United States as shown in figure 2. Most of the Labrador/Newfoundland storms turn north-northwestward along a primary storm track toward southern Greenland. The high ice-covered Greenland plateau causes this storm track to split into two primary tracks causing the lows to move northwesterly into Davis Strait along the west Greenland coast or northeasterly along the east Greenland coast.

A small number of winter storms may also enter Davis Strait along a seldom travelled secondary track from Hudson Bay. The Alberta cyclones, moving northeasterly into the Icelandic region, are further joined by storms developing near the Gulf Stream south or east of Newfoundland and by those migrating from the Labrador/Newfoundland coastal regions. An additional secondary track which has its origin in the northern Beaufort Sea feeds lows through the Canadian Archipelago along 73°N into central Baffin Bay.

In spring (April), the tracks of lows from the United States and southern Canada leading into the eastern Arctic region as shown in figure 3 do not differ significantly from winter tracks. However, cyclonic activity in the North American Arctic reaches an annual minimum in April owing to intensification of polar anticyclones. There is also (1) a reduction to secondary importance of the track of lows migrating northeastward along the east Greenland coast into the approaches to Denmark Strait and (2) disappearance of the secondary track through the northern reaches of the Canadian Archipelago into Baffin Bay.

In summer (July), a pronounced northward shift in the general pattern of the principal storm tracks affecting the eastern Arctic becomes evident as shown in figure 4. This northward movement initially appears during June as the northward displacement of the track of Alberta Lows replaces the Hudson Bay secondary track. The number of Alberta storms also reaches annual maximum in June, with only a small decrease from this maximum in July. Storms originating in western Canada are now fed into Davis Strait along this primary track.

A corresponding northward shift is also evident in the upper Great Lakes primary track of lows which originates in July just south of Hudson Bay. The primary track from the Labrador/Newfoundland region feeding storms into Davis Strait is reduced to secondary status during July. Lows approaching the Icelandic region now transit two primary tracks, one from the Labrador coastal area and one from the Gulf Stream area east of the Island of Newfoundland. The secondary track which stretched across the northern Canadian Archipelago in winter reappears to feed the lows that pass across Siberia and along its north coast through the Bering Strait into northcentral Baffin Bay.

During autumn (October), the principal Canadian storm tracks which started moving northward in early summer begin to move back south as shown in figure 5. The only source of lows entering Davis Strait in October is the primary track cutting across southern Hudson Bay. Lows from the Labrador/Newfoundland region transit the Labrador Sea along a primary track and terminate near Iceland. The primary track of eastern United States coastal lows evident in the Newfoundland area in summer (July) is reduced to two secondary tracks in autumn.

C. Sea Level Pressure

The general large-scale circulation, or theoretical geostrophic windflow, over a specific area can be inferred with little error from the study of mean patterns of the sea level pressure field. For this reason, the mean monthly sea level pressure data for the eastern Arctic (U.S. Weather Bureau Technical Paper No. 21) are presented in appendix A (figures A-1 through A-12). When these data are compared with a current 30-day prognostic mean sea level pressure chart, the comparison will reflect either normal or anomalous forecasted conditions and, in this manner, provide the ice forecaster with an invaluable long-range predictive tool.

Throughout the year, mean monthly pressure patterns reflect the frequency, location, and intensity of cyclones which migrate into the eastern Arctic area from Canada, from the United States, and from the vicinity of the Gulf Stream in the western North Atlantic Ocean. The prominent climatic features evident on the monthly mean sea level pressure charts are (1) the semipermanent cyclone or "Icelandic Low" whose position generally oscillates throughout the year in a northeast-southwest direction between Iceland and the southern tip of Greenland and (2) the "polar high" or anticyclone which is normally situated over the Arctic Basin between the North Pole and the landmasses of the eastern Arctic.

During winter (December and January) the Icelandic Low is centered southwest of Iceland near 62°N, 36°W. Its average central pressure reaches an annual minimum value of 995 mb between mid-December and mid-January. polar high tends to remain stationary for long periods north of the Greenland landmass during winter. The pressure gradient around this huge dome of cold, dry air in winter is very steep over the ocean periphery of this area. For these reasons, winter in the eastern Arctic is characterized by intense atmospheric activity. By spring (March and April) the Icelandic Low begins to fill slightly and is positioned farther to the southeast in the vicinity of 58°N, 33°W. In addition, the strong gradient associated with the polar high in winter begins to weaken in early spring and its influence on the circulation is primarily felt only in northern regions. Although still prominent in summer (July and August), the Icelandic Low weakens to a point where it takes on the appearance of an elongated trough, stretching in a northeast-southwest direction from Iceland to the southern portion of Davis Strait. The average pressure for this weak cyclonic circulation reaches its annual maximum of approximately 1009 mb near 65°N, 25°W. In late spring and summer atmospheric activity, in contrast to the colder months, becomes comparatively quiet; and northward migrating cyclones are more shallow and slower moving. In summer the polar high tends to move southeastward from its winter location and position itself over the extreme northeast coast of Greenland. By autumn (September through November) the change to winter conditions takes place more abruptly than the transition from colder to warmer months. This is evident from the mean pressure distribution in October (figure A-10) which indicates a considerably more intense contrast in atmospheric pressure than that which prevails during April (figure A-4). During autumn the Icelandic Low begins to fill as the polar high builds and begins its migration northwestward to its winter polar location.

The large-scale circulation over the eastern Arctic from December through April (figures A-12 and A-1 through A-4), as indicated by the mean pressure distribution, is predominately alongshore towards the southeast over the Labrador/Newfoundland coastal regions; onshore toward the west and west-southwest over the entire east Greenland coast; onshore toward the southwest over the northeast coast of Baffin Island; and southward over the southern portion of Davis Strait. This circulation occurs when ice growth is at its peak and normally results in the drift of pack ice from Davis Strait southward along the Labrador/Newfoundland coasts. Under normal conditions, it also produces a relatively narrow, dense band of ice adjacent to the east Greenland coast particularly south of 70°N and an increase in pack ice concentration adjacent to the northeast coast of Baffin Island.

The May through September (figures A-5 through A-9) circulation in the Baffin Bay/Davis Strait and Labrador/Newfoundland regions undergoes some changes in magnitude and direction. The geostrophic flow, which normally varies from 6 km (11 km/h) or less in April to as high at 16 km (30 km/h) in February, decreases in strength to a maximum of 7 km (13 km/h) over both regions during the warmer months; and the circulation over Labrador/Newfoundland changes from an alongshore to an offshore east to east-southeasterly flow. During the early part of this period when temperatures are rising, this offshore circulation over the western Labrador Sea results in a loosening of ice pack and aides its disintegration.

Circulation in Baffin Bay remains onshore while that over Davis Strait shifts from toward the south to the southeast transporting pack ice away from the colder southerly Labrador Current into warmer waters. Normal geostrophic flow over east Greenland coastal regions during this time also moderates from a maximum of 11 kn (20 km/h), generally in evidence during the colder months of December and January, to a minimum of 7 kn (13 km/h) in May and 4 kn (7 km/h) or less during the remainder of the period. The mean circulation pattern over this area as depicted in appendix A, however, generally remains onshore throughout the year with the flow fluctuating from easterly to east-northeasterly.

In October and November the geostrophic flow increases over all areas and generally varies from 6 km (11 km/h) to 9 km (17 km/h) as the pressure gradients build to their winter strengths. For the most part, circulation patterns in the Baffin Bay/Davis Strait and the Labrador/Newfoundland regions during these transition months are not much different from those in summer with only a slight movement toward the winter and spring patterns discernible.

D. Surface Air Temperature

Air temperature is the parameter that exerts the most influence upon the growth and decay of sea ice, particularly during freezeup and disintegration. In the period between these two stages air temperature will, at the very least, affect the subsequent rate of growth of sea ice and, therefore, is an important input into a 15- and 30-day ice forecast. One prediction technique relating air temperature to ice thickness utilizes the concept of converting air temperature into accumulated frost degree days (FDD).

1. Frost Degree Days

In the early 1940's a Russian geographical scientist, N.N. Zubov, formulated an ice growth equation as a function of air temperature alone and based on his empirical observations of ice formation along portions of the northern Russian arctic coast. Air temperatures can be translated into accumulated frost degree days from which theoretical ice thicknesses are calculated using the following modification of Zubov's equation:

$$\sqrt{817.96 + 5.808\Sigma \text{Fdd}_{1}}_{\text{Tj}} = \frac{1}{2.904} -9.85$$

where Tj is the ice thickness in inches for day j, and Fdd is the frost degree day accumulation in degrees Fahrenheit on day i (Gerson, 1975).

A frost degree day is defined as a day with a mean temperature of 1F° below an arbitrary base. The base most commonly used is the freezing point of freshwater (32°F). If, for example, the mean temperature on a given day is 5F° below freezing, then five frost degree days are registered for that day. These frost degree days are then added to those collected the next day to obtain an accumulated value, which is then added to the number of degree days collected the following day. This process is repeated daily throughout the ice growing season. A mean monthly value for accumulated frost degree days can also be obtained from the mean monthly temperature. For example, a mean monthly temperature of -10°F transforms into an accumulation of 1,302 Fdd during a 31-day month (42 FDD x 31). Examples utilizing frost degree days to compute ice thickness for a 15- and 30-day ice forecast are presented in section IV, Forecasting Techniques.

The relationship between frost degree-day accumulations and theoretical ice-growth curves at 17 eastern Arctic stations are graphically presented in figures 81A through 97B.

2. Surface Temperature Distribution

The distribution of mean monthly air temperature (°F) over the eastern Arctic regions (U.S. Navy Chief of Naval Operations, 1963) is presented in appendix B (figures B-1 through B-12). Extending as it does over a large north-south distance, the eastern Arctic region experiences great air temperature differences. Depending upon the specific area, minimum air temperatures occur in either January or February over the Labrador/Newfoundland coastal area and adjacent to the east Greenland coast. North of 70°N, surface air temperatures reach a minimum in January. In contrast, along the east Greenland coast south of 70°N and in the Baffin Bay/Davis Strait regions the minimums occur in February. During the spring months of April through June, temperatures increase along with a weakening of the horizontal temperature gradient due primarily to a decrease in atmospheric activity over the area. Higher temperatures are brought about by northward advection of warm air from the south by cyclones moving over the area. In late spring this advection is accelerated as the pack ice begins to break up. Also aiding breakup and increased air temperature are the effects of extended

insolation during this period and northward movement of warmer waters from the south. Isotherms presented in figures B-1 through B-12 indicate the general effect of currents on the geographic distribution of the temperature regime in all seasons. Two major examples of this are bending of isotherms in the western Davis Strait and Labrador Sea regions as the cold Labrador Current flows southward along the coastal areas.

Air temperatures generally reach their annual maximum in July for all areas except in southern Davis Strait and along the Labrador/Newfoundland coastal region where they occur in August. With acceleration of pack ice breakup during summer, the absence of the cooling effect of ice results in increased rate of warming. During July and August, freezing temperatures in the form of the 32°F isotherm are located north of 80°N in the eastern Arctic. By mid-September, freezing temperatures are present in northern Baffin Bay and extend southward along the east Greenland coast to 72°N. By mid-November the majority of the eastern Arctic, which will eventually be ice covered, is under the influence of freezing temperatures (< 32°F). Even as air temperatures decrease in fall, they remain relatively higher during this period than they are in spring owing to less extensive ice cover in the fall. This is particularly evident in the Baffin Bay/Davis Strait area where air temperatures in April, as opposed to those in October, average between 10°F lower in the southern sector of this region to over 20°F lower in the northern sector. In the other primary areas of the eastern Arctic the contrast is not as great, averaging between 5° and 10°F lower in the Labrador region and approximately 5°F lower along the east Greenland coast.

Temperatures over the entire eastern Arctic during winter are closely associated with the extent of ice-covered ocean areas extending southward from the Arctic Basin. As ocean areas become ice covered they, along with the Greenland ice cap, assume continental characteristics. The polar high then exerts its influence, particularly in the northern regions, as low temperatures extend far to the south when the pressure field causes a southward flow of arctic air. As long as the oceans or any continental areas in the region remain snow or ice covered, the average air temperature cannot rise above the freezing point for any extended period of time.

E. Surface Currents

Summer and winter distributions of surface currents in the eastern Arctic are presented in figures 6 and 7. Current directions and magnitudes are based on H.O. Pub 705, Part II (1958), Chief of Naval Operations publication NAVAIR 50-1C-528 (1974), and sailing directions for various arctic locales. Knowledge of the speed and set of currents in various geographic areas throughout the eastern Arctic is important, because their effects can either impede or reinforce redistribution of the ice cover. During periods of light winds, currents are the dominant force acting on ice distribution.

The North American Arctic has two major circulation regimes. First is the Pacific Gyre, which is not located in the Pacific Ocean as implied but in the Arctic Ocean between Alaska and the North Pole and affects the surface circulation in the western North American Arctic. The second major current system, the Trans-Polar Drift Stream, flows across the Arctic Basin from Siberia to the Greenland Sea. As this current flows southward on or just along the East Greenland Shelf between Greenland and Spitsbergen, it is referred to as the East Greenland Current or Drift Stream and comprises the principal outflow of ice and water from the Arctic Ocean. This current continues southward through the Denmark Strait parallel to and along the entire east Greenland coast. It then rounds Greenland's southern tip and joins with currents flowing north from the Atlantic to form the West Greenland Current which flows northward into Davis Strait and Baffin Bay.

North of 70°N the East Greenland Current follows the edge of the continental shelf southward attaining speeds of between 0.5 and 0.7 kn (0.9 to 1.3 km/h) over the continental slope, with lower speeds of 0.3 to 0.5 kn (0.6 to 0.9 km/h) in the shoal areas over the shelf during winter and summer. As the current flows southwesterly along the east Greenland coast south of 70°N, the speed varies from 0.3 to 0.5 kn (0.6 to 0.9 km/h) during summer to 0.5 to 0.7 kn (0.9 to 1.3 km/h) during winter. North of Iceland, a branch of the East Greenland Current turns eastward to form a counterclockwise circulation in the Greenland Sea with speeds ranging from 0.1 to 0.5 kn (0.2 to 0.9 km/h) just north of Iceland to 0.5 to 0.7 kn (0.9 to 1.3 km/h) in the gyre north of Jan Mayen Island.

In its northward course through eastern Davis Strait adjacent to the west Greenland coast, the West Greenland Current sends off branches along its seaward margin which turn westward into western Davis Strait and the habrador Sea. Speeds of this current generally range from 0.1 to 0.5 km (0 to 0.9 km/h) in summer to 0.3 to 0.7 kn (0.6 to 1.3 km/h) in winter. Inshore portions of this current continue to flow northward at a reduced rate (0.1 to 0.2 km (0.2 to 0.4 km/h)) through northern Davis Strait along the continental slope to the northern reaches of Baffin Bay. It then turns westward at this point to merge with currents flowing from Kane Basin, Jones Sound, and Lancaster Sound to form the southeast to southward setting Baffin Island Current in western Baffin Bay and western Davis Strait. This current is stronger and more voluminous than the West Greenland Current in the Baffin Bay region with speeds in winter and summer ranging from 0.4 to 0.5 km (0.7 to 0.9 km/h) in northwestern Baffin Bay to 0.1 to 0.2 kn (0.2 to 0.4 km/h) in southwestern Baffin Bay and northwestern Davis Strait. Before this current reaches Labrador coastal regions, it merges with a southeast setting current from Hudson Strait to form the Labrador Current, which flows southeastward along the Labrador coast. The Labrador current flows at an average speed of 0.5 km (0.9 km/h) in summer and generally averages between 0.1 to 0.5 km (0.2 to 0.9 km/h) during winter.

III. HISTORICAL SEA ICE DISTRIBUTION

A. Annual Cycle

Ice cover in the three primary areas in this guide experiences, under normal conditions, a complete seasonal cycle of growth and decay. Because pack ice limits may vary greatly about a mean position in a particular area from year to year owing to anomalous environmental factors, the annual cycle of ice decay may not be complete in areas such as the east Greenland coastal region and in Baffin Bay. The northeast coastal sections of east Greenland are never completely free of ice, irrespective of the severity of the ice growing season.

During late winter and early spring when ice conditions are generally maximum, ice covers, on the average, the entire Baffin Bay region, northern and western Davis Strait, the waters along the entire Labrador/Newfoundland east Greenland coastal regions, and areas as far north as 65°N along the western Greenland coast. The coastal region of the Island of Newfoundland contains thin first-year ice (12-28 in (30-71 cm)) near the end of its normal growth cycle, whereas the Labrador coastal areas north of 52°N generally attain medium first-year growth (28-48 in (71-122 cm)). In Baffin Bay and Davis Strait, the ice cover consists of predominately medium and thick first-year growth (greater than 48 in (122 cm)) during most of the growth cycle. During some years, second-year ice (greater than one year's growth) and/or multi year ice (ice which has survived at least two summers' melt and at least 118 in (300 cm) thick) may be present in Baffin Bay and northern Davis Strait owing to incomplete melt in these areas during unusually short or cool summer seasons. The ice cover in the western Greenland Sea consists not only of large quantities of locally formed ice, but also multi-year pack ice which has been advected from the Arctic Ocean via the East Greenland Current. Ice growing locally at east Greenland stations south of 70°N attains a thickness equivalent to medium first-year ice during winter. North of 70°N, thick first-year ice dominates the pack ice in the Greenland Sea at the end of its normal growth cycle. Owing to the strong longshore flow of the East Greenland Current, however, both multi-year and thick first-year ice are distributed along the entire length of the east Greenland coast during winter and spring.

Normally, by early summer, the southern portion of the Labrador/
Newfoundland coastal region south of 55°N is essentially ice-free. During
the same period, ice concentrations in the northern portions of this area
and in southern Davis Strait begin to decrease rapidly and the pack ice
in eastern Baffin Bay begins to retreat westward forming a 40 to 60 nmi
(74 to 111 km) wide ice-free passage adjacent the west Greenland coast to
73°N. By midsummer the pack ice has retreated from the western Labrador
Sea and southern Davis Strait, and the disintegration of ice in northern
Davis Strait begins to accelerate. At the same time the ice pack in eastern
Baffin Bay retreats farther to the west as sea ice disintegration in this
region also accelerates and, under normal conditions, eastern Baffin Bay
is free of ice resulting in an ice-free passage to the north-central reaches
of Baffin Bay. The pack ice concentrations along the east Greenland coast
south of 72°N during this period begin to decrease causing a westward retreat

of the ice edge and the southeast coastal area south of 64°N to become ice free by late summer. During early autumn (last half of September), northern Davis Strait and western Baffin Bay is completely free of ice with the exception of some ice remaining in a narrow belt adjacent the Baffin Island east coast.

During early fall, beginning in late September in the east Greenland region and in mid-October in western Baffin Bay, the pack ice begins to grow with a corresponding small eastward movement of the pack edge in both regions. By the end of October new ice growth appears off the Baffin Island coast in western Davis Strait, and the ice-free passage to northern Baffin Bay is blocked as ice grows rapidly and covers nearly the entire western portion of Baffin Bay. In the western Greenland Sea, sea ice also reaches the southern tip of Greenland. Ice makes its initial appearance in the northern Labrador coastal area during the first half of December as seawater begins to freeze and as ice drifts southward in the Labrador Current from Davis Strait.

The ice edge in Davis Strait reaches its maximum eastward position during early April as the result of freezing and the drift of pack ice from Baffin Bay. The east Greenland ice edge also attains its maximum eastward extent during this time. Southeasterly drift of pack ice in the Labrador Current during winter causes the ice edge along the Labrador/Newfoundland coastal area to reach its maximum seaward extent in late February.

B. Pack Edge

The mean, median, and extreme semimonthly positions of pack ice edges as shown in figures 8A through 53B were extracted from aircraft, ship, and satellite observations of the pack edge contained in annual Naval Oceanographic Office reports of the arctic ice observing and forecasting program covering the period from 1954 through 1971. Ice conditions were generally shown in these reports by 6-day periods. Positions of the ice edge along the Labrador/Newfoundland coastal region during January and February are also based on data extracted from eastern Arctic sea ice analyses charts compiled by the U.S. Navy Fleet Weather Facility between 1972 and 1976. The position of the ice pack edge was recorded for every degree of latitude between 47°N and 76°N and for each 6-day period. A mean ice edge was computed from the three 6-day periods within each semimonthly period with the midmonthly (13-18) period included in both semimonthly periods for each month. For these data the mean, median, and ranges of the 15-day means and extreme eastern and western portions of the pack edge were computed for each semimonthly period. The pack edge was defined by an ice concentration of one okta (eighth) or more.

1. Semimonthly Positions and Ranges

The normal width of the pack ice in the western Labrador Sea reaches its 15-day maximum of approximately 190 nmi (352 km) during the latter half of February at 55°N, 53°30'W with its easternmost position located at approximately 48°%, 50°20'W (figure 9B). By the end of April

(figure 11B), the mean pack edge width has decreased to approximately 110 nmi (204 km), and by the end of June (figure 13B) to 90 nmi (167 km). By early August (figure 15A), the western Labrador Sea is essentially ice free except for some scattered strips and belts of rotten ice remaining along the immediate coastal areas.

The normal seaward extent and width of the ice cover in southern Davis Strait attain their 15-day maximums during early April (figure 21A). At this time the width of the ice edge averages approximately 160 nmi (297 km) as it runs parallel to the southeast coast of Baffin Island and intersects the west coast of Greenland in the vicinity of 67°30'N. By mid-May the ice cover in nothern Davis Strait normally retreats from the west Greenland coast to form an ice-free passage along the coast as far north as Disko Island as shown in figure 22A. As the spring and summer seasons progress, the ice pack in eastern Baffin Bay also begins its westward retreat from the Greenland coast, extending the west Greenland ice-free passage northward to Cape York at the western end of Melville Bay by the end of July (figure 24B). The widths of the pack in southern and northern Davis Strait are at this time approximately 130 nmi (241 km) and 63 nmi (117 km), respectively. By mid-September southern Davis Strait is essentially ice free and the northern Davis Strait ice pack has retreated to an average width of only 30 nmi (56 km). Only a narrow pack, 49 nmi (92 km) wide lying parallel to the northeast Baffin Island coast, remains in western Baffin Bay. By the end of September, the ice covers in western Baffin Bay and northern Davis Strait have retreated to their minimum westward positions, leaving a narrow 15-nmi (23 km) discontinuous belt of ice adjacent to the northeast Baffin Island coast. Refreezing with a corresponding eastward movement of the ice cover begins during the first half of October in eastern Baffin Bay and during the first half of November in northern and southern Davis Strait.

The normal seaward extent of the ice cover which lies parallel to the east Greenland coast normally attains its 15-day maximum during the last half of April (figure 33B), particularly between 65°N and 70°N. The average width of the pack in this area approaches 120 nmi (222 km). Investigation of figures 30A through 41B shows that the mean position of the ice cover south of 63 N, during the ice growth season (October through May) and beyond, does not vary over a range greater than 30 nmi (56 km). It also shows that the variation of the mean between 63°N and 65°N averages less than 66 nmi (122 km). By mid-June (figure 35A) the pack edge has retreated westward leaving an average ice pack width of nearly 105 nmi (195 km) between 65°N and 70°N and 42 nmi (78 km) between 60°N and 65°N. By mid-August (figure 37A) these pack widths are further reduced to 58 nmi (107 km) and 26 nmi (48 km), respectively. The pack reaches its minimum 15-day width of less than 35 nmi (65 km) during the first half of September (figure 38A) as the coast south of 65°N becomes ice free and a sometimes discontinuous belt of decaying pack ice remains along the coastal areas between 65 N and 70 N. By the end of September (figure 38B), the pack north of 65 N begins to grow and advance seaward and by the end of October (figure 39B) pack ice stretches southward to the tip of Greenland at 60 N.

Pack ice is transported around the south tip of Greenland and then northward along the west Greenland coast by the West Greenland Current. The initial appearance of ice in this area generally occurs during late November or early December. By mid-April (figure 45A) the southwest Greenland pack ice normally reaches its northernmost position at 65°N and 63°W; however, its furthest seaward extent (75 nmi (139 km)) occurs during the last half of May (figure 46B). By the end of September (figure 50B), the disappearance of the southwest Greenland ice pack is usually complete owing to the absence of ice which may be advected around the south Greenland tip from the eastern coastal regions south of 64°N.

2. Advancement and Recession Rates

Examination of the mean and median positions of the ice pack edges in figures 8A throught 53B graphically indicates that the pack edge does not retreat or advance along each parallel at a uniform rate. In addition it is evident that during many 15-day periods portions of the same ice edge retreat while others advance, particularly during freezeup and breakup periods. Both of the aforementioned effects are due primarily to environmental factors interacting in varying combinations yet to be determined at specific geographical locations and to the large north-south distance covered by the ice in the eastern Arctic. Mean and median advancement and recession rates in nautical miles per day computed for each 15-day period along each parallel where an ice edge was observed in the three primary areas of interest are presented in tables I through VI.

Mean conditions in the western Labrador Sea indicate that the ice edge advances rapidly between mid-January and mid-February at a rate of 0.7 to 4.7 nmi/d (1.3 to 8.7 km/d), being greatest between 1 and 15 February south of 550N. Between 550N and 600N, the edge advances most rapidly between 16 and 31 January with rates varying from 1.3 to 2.0 nmi/d (2.4 to 3.7 km/d). The edge becomes nearly static during late February as its advancement rate decreases to an average of 1.2 nmi/d (2.2 km/d). In the Baffin Bay/Davis Strait region the ice pack edge begins its eastward advance in early autumn. Throughout the ice growing season, advancement rates vary from 0.9 to 11.0 nmi/d (1.7 to 20.4 km/d) in Baffin Bay and from 0 to 7.6 nmi/d (0 to 14 km/d) in Davis Strait with the maximum rates occuring between 1 and 15 November in both areas. The pack ice advances eastward to its maximum extent in early winter as it covers Baffin Bay entirely and as the ice edge stabilizes in eastern Davis Strait during March and April. The east Greenland pack ice begins to grow during the latter half of September as the ice edge advances eastward at rates ranging from 0 to 11.3 nmi/d(0 to 21 km/d) through April. During this period, movement of the east Greenland ice edge shows considerable annual variation over the same 15-day periods owing to the combined effects of ocean currents and atmospheric activity. Table IV shows that between 1 and 15 December when the maximum advancement rate of 11.3 nmi/d is attained at 72°N, the edge between 62°N and 66°N is simultaneously receding at rates varying from 0.3 to 3.1 nmi/d (0.6 to 5.7 km/d). Further examination of the 15 semimonthly periods in tables IV and V during which the ice edge should be advancing shows that the edge actually advances eastward along its entire length during only three of these semimonthly periods (20% of the total). The three periods are 1 to 15 November, 16 to 30 November, and 1 to 15 March. This reinforces

Table I. Advancement and Recession Rates of Ice Edge for 15-Day Periods August 1 - December 31 (1953-1971) (nmi/d)

		_			1		1		1		1		1			1_	_	1		.1.	•	01	
		٥	'		L	-	1	'		1		'	1	-		2.4	0	2	2 6	1			1
		62	-2.0	-2.8	9.0-	0		1		1		1	1	•		2.2	0	1.4	0	4.5			1
	;	63	1.1-	-0.8	-1.1	8.0-		1		1		,	1	,		6.0	0.0	3.0	2	7.7	2 6	2	,
	;	òla	-3.0	-5.2	-0.9	4.0-				1	0		,	1.0-	0.0	6.0	1.3	1.6	2.2	5.3	, ,		1
	,	1	14.0	4.7	1.0	1.4	-1.0	9.0	9.0	0.0	0.0	0		1.0	0.0	3.8	4.2	1.3	1.7	1.5	1.7		,
	77	-		3.0	-0.9	1.6 -		0.0	0.0	0.0	0.5	0	,	1:0	0.0	3.2	8.4	8.0	8.0		7.0	-	
		1		3	S	2	9	8	-		1_	0.0	+	_	-	4	<u>۔</u> ٣	8	7	8	8	-	5
	7.7		1	4	9	-0-	0-	-1	0-	0.0	0				· A	2.	3	1	1.	2.	-	2.	3.
	8	100	7.7	7	-1.8	-2.0	-1.2	-4.4	-1.3	0.0	-0.1	0.0	1		-	4.8	9.9	2.8	1.8	4.6	4.8	0.4	1.5
(N)	09	-30		2.7	-1.5	-3.6	-2.8	-5.8	-1.6	0.0	4.0-	0.2	7		2	9./	6.6	2.2	2.0	6.2	7.7	1.5	0.0
Latitude	7.0	-2.2	7		1.3	1.7	_	-6.1	9.	0.	.3	0.0	0	-	•1	7.0	8.7	2.7	1.7	3.8		1.0	1.
Lat		1-10	-	1	-	-	8	3	-0-	0	2 -	_		0	ļ	_	-					-	-
	7.1	-3	-		-1-	-3.		-8	-1-	0.0	0	•		~	•	0	9.3	1.6	0.8	7.5	7.6	0.7	-1.9
	72	9.4-	2	•	0.7-	-2,3	-4.1		-2.8	0.0	3.4	9.0	2.7	2 7		1.,	13.5	1:1	0.0	4.1	3.9	1	1
	73	0.9-	6 7	٠l	0.0	•	6.4-	œ	2.3	0.0	8.5	3.0	1.5	3.7	-	2.1	0.0	2.4	6.2	1.0	2.3	1	1
		4	7		<u>_</u>	1	-	+	-		0	-	1 -	7	-	-	7	5			1		1
	74	-6.	-4-	-	2 1		-6.1	-8.5	-	0	6	او	e,	2	=	:::	13.7	1.5	0.0	ı	-	•	1
	7.5	-7.8	-12.0	-3 3		14:	2.0	0.0	0.3	4.0	8.6	4:1	4.3	12.5	2		2:0		1	•		ı	
	.91	-5.7	0.2	8 9-		7.7	0.1.	7.0	4.0	0.0	80.0	17.0	6.1	4.2	7 0-			•	1		1	,	-
		15		•	_		2		200			1	31		Т	_	1	200	1	0	1	31	1
Semimonthly	lods	Aug 1-Aug 15		Aug 16-Aug 31	0	1	cr dac-r dac	100	oc dac-or dac	1	oct 1-0ct 13		o Oct 16-Oct 31		Nov 1- Nov 15		1	NO TO-NO 30	1	nec 1-nec 15	1	nec 10-nec 31	
minc	Periods	8 1-		2 16		1	· T d	1.6	or d	1	-T 2	1	t 16		V 1-		1	10	1	-T -	1	10	
Se	1	Au		Au		15	0	10	מ	18	00	1	00		No		1	NO	1	ne	1	n n	1
												-											

Positive values indicate rate of advancement. Negative values indicate rate of recession.

Top value in each box is a mean rate. Bottom value in each box is a median rate.

Table II. Advancement and Recession Rates of Ice Edge for 15-Day Periods January 16 - April 30 (1953-1971) (nmi/d)

						Latitude		(N)					
Semimonthly	1 y												
Periods	1	70°	69	89	67	99	65	64	63	62	61	09	59
Jan 16-Jan 31	n 31	1	1	1	1	1	-	1.7	1.8	0.5	1.3	1.7	1.9
								1.7	0.9	1.4	1.5	0.7	0.0
Feb 1-Feb 15	15		1	1	ı	1.2	-5.0	0.1	9.0	6.0-	2.8	1.0	0.7
						1.2	-5.0	0.4	2.7	-1.9	1.3	0.0	0.0
Feb 16-Feb 28	b 28	1	1	1		2.0	-1.5	-2.7	-1.0	0.0	1.2	0.7	-0.7
						3.2	-1.5	-2.0	0.0	0.0	2.7		0.7
Mar 1-Mar 15	15		1	•	•	-1:1	9.4	6.4	-0.2	2.2	-4.7		-2.3
						-1.6	5.0	3.5	-1.8	0.9	0.9-		-0.7
Mar 16-Mar 31	r 31	•	7.0-	0.0	-0.1	0.5	0.4	-0.4	2.3	-0.2	-0.3		-0.3
			0.0	0.0	-0.4	0.0	0.0	6.0	6.0	6.0	1.9		-1.0
Apr 1-Apr 15	15	-0.1	-0.8	-0.2	-0.1	-0.4	0.1	1-0.4	6.0	0.3	0.0	-0.3	0.5
		0.0	0.0	-0.7	0.8	-0.3	-0.3	3 0.0	1.1	0.0	-1.5		-0.3
Apr 16-Apr 30	r 30	0.0	-1.5	-0.5	-0.5	-0.3	-0.1	-0.4	9.0-	0.0	0.3	1	0.5
		0.0	-2.8	0.0	-1.2	-0.5	0.0	-2.0	-0.5	-0.3	9.0-	0.2	1.0

47	-		-		0.0	0.0	0.0	-3.7	0.2	0.0	-1.4	0.0	-0.2	0.0	an rate
8 7			3.5	6.7	1.5	-1.0	-6.3	0.9-	6.0	0.7	0.0	-0.7	-0.5	0.0	is a media
64	0.7	0.0	4.7	7.3	0.7	0.0	-3.7	-5.7	0.5	2.1	-0.7	-1.4	-1.6	-2.1	h box
50	3.6	5.3	4.5	5.7	1.5	0.0	-4.7	-5.0	2.9	4.0	-2.7	-3.5	0.4	6.0-	in each
51	4.0	5.3	3.5	4.3	0.0	-0.7	-4.7	-4.7	1.3	0.7	-0.7	-3.3	-1.7	1.3	Top value Bottom val
52	2.2	4.7	4.3	4.5	0.7	0.0	-5.7	0.6-	2.1	3.8	9.0-	9.0-	9.0-	-1.9	Top
53	2.8	5.0	4.7	1.9	8.0-	0.0	-5.3	0.9-	1.9	4.3	-1.0	-2.5	9.0-	9.0-	
54	4.3	5.3	2.7	2.0	0.5	0.0	0.4-	-3.3	0.0	0.0	-0.2	9.0-	-0.2	-1.0	
55	4.7	2.9	2.3	0.8	1.3	3.0	0.4-	-5.7	0.2	9.0-	8.0	0.8	-0.2	0.0	ement. ion.
56	2.0	2.7	0.7	0.0	1.0	0.0	-2.0	-2.0	9.0-	9.0-	0.0	9.0	0.0	0.0	advancement recession.
57	1.3	1.3	0.7	0.0	0.7	-0.7	-2.0	-1.3	-1.1	-0.9	7.0	0.7	-0.4	-1.5	rate of rate of
58°	1.3	0.0	-0.7	0.0	1.2	0.0	-1.7	-0.7	-1.6	-1.1	0.4	-0.2	-0.2	-0.2	indicate indicate
	Jan 16-Jan 31		Feb 1-Feb 15		Feb 16-Feb 28		Mar 1-Mar 15		Mar 16-Mar 31		Apr 1-Apr 15		Apr 16-Apr 30		Positive values indicate rate Negative values indicate rate

Advancement and Recession Rates of Ice Edge Perfods May 1 - July 31 (1953-1971) (nm1/d) Table III. for 15-Day

Latitude (N)

76° 75	75		74	73	72	1	70	0	0	67	99	65	64	63
1	1	1		;	1	-3.6	-1.0	-2.9	-2.2	-1.3	-1.2	-1.5	-1.3	-1.2
1		-		,	1 ,	-1.6	-1.7	-1.4	-1.2	-1.4	-1.1	-1.3	-1.6	-2.1
1	1	ı		1	-2.0	-2.9	-1.5	-1.6	-1.2	-1.2	-1.7	-2.1	-2.2	-1.8
	1	_	77	96	-1.1	-1.3		-0.9		-0.8	-0.5	00		-0.8
-3.8 -3.0 -3.3 -1 0.0 -1.4 -2.1 -1	0 -3.3	3.3	1-1-	.5	-1.4	-1.3	-1.3	-0.8	-1.2	-0.5	-0.3	-1.1	-1.3	-1.4
-3.8 -2.	-2. -2.	2.	-10	.3	-0.9	-1.2	-1.8	-1.5	-1.6	-1.7	-0.4	0.0	-0.9	-0.6
62° 61 60	09			59	58	57	56	55	54	53	52	51	50	
$\begin{array}{c ccccccccccccccccccccccccccccccccccc$	8 0.0	.0	0-	.3	0.4	0.2	-0.2	-1.4	-2.4	-2.1	-3.0	-3.0	-4.2	
-0.2	8 -0.2	.2	-	0.3	0.2	0.2	0.2	0.2	0.6	0.2	0.0	0.0	0.0	
5 -1.	5 -1.2	. 5	-1	2	-1.4	-1.3	-1.1	-2.1	-1.8	-1.0	-1.3	-1.7	-2.2	
-0.5 -0.8 -0.2 -0 -0.6 -1.1 -0.3 -1	8 -0.2	3.5	7 7	7.0	-0.4 -0.5	4.0-	-1.3	-1.6	-1.4	-1.9 -1.0	-1.3	!	-	
-2.2 -3.2 -2.3 -1 -2.0 -1.6 -1.5 -0	-2.3 -1.5	. 5	-1	0.0	6.0-	-0.7	-1.9	-1.8	-1.4	ı	i		1	
-1.2 -4.2 -2.0 - -1.2 -4.5 -2.7 -	2 -2.0	0.	1 1	2.1	-2.1	-2.2	-1.9	-1.8	ı	i	1	ı	,	
			١		1		-	-	1					

Positive values indicate rate of advancement. Negative values indicate rate of recession.

Bottom value in each box is a median rate. Top value in each box is a mean rate.

Table IV. Advancement and Recession Rates of Ice Edge for 15-Day Periods August 1 - January 31 (1953-1971) (nm1/d) Greenland Coast East of 45°W

		1	_	T	_	T	_	T		T		T		7	-	ī	-	i		Γ.	-	1-		1	
	59					1		i		!		:		-		1				,		2.9	2.9	0.7	0
	09		0.5		-1.2		0.2	1		•		:				0.2	0.0	0.7	0.7		-0.2		-1.0	0.8	
	61			0.3		1-0.5	-0.3	1		-		-		0.0	-0.3	0.0		0.5	1.1		0.0		-0.5	0.3	-0 3
	62	-1.4	-1.6		-1.7	-C , 3	•	,		-		,		0.2		0.5		-0.3			0.9	0.3	8.0-	0.0	0
	63			0.0		9.0-	•	-		,		-				0.0		-0.3	-0.3		-0.2		0.0	0.0	-0 2
	99	-2.5	1-2.9		9.0-	-0.7	-0.2	-0.2	-0.3		•	0.0			0.7	0.7	0.4	-1.5	-1.0	0.0		0.7	0.1	0.0	
	65		-2.8	0	-1.1	-0.7	0.3	0.0	0.0		0.0	1.0	•	1.5	•	2.2	•	9.4-	-4.2	2.6	2.1	1.6	0.4	0.3	7 6
(N)	99	-2.9	-3.6	-2.4	-2.5	-1.1	6.0-	1.3	1.5		-2.1		1.1		2.4		2.5	-3.1	-3.9	1.5	3.6	1.2	-0.1	-1.3	-1.2
tude	29	-3.7	-9.1	-0.1	-0.9	-5.8	-1.7	4.1	9.0	0.5	-0.3	2.2	4.0	1.4	5.9	2.0	6.0	0.5	2.0	-1.5	-2.3		6.0-	3.5	9.0
	89	-2.6	-1.5	-2.6	-1.1	4.2-	0.4-	5.0	0.6	2.7	2.0	0.0	7.0	2.9	1.2	1.1	0.1	2.4	2.6	0.0	-1.1	-1.3	-0.4	2.7	3.8
	69	-1.3	1.6	-2.1	-4.4	6.0-	•	1.2	1.3			9.0	•		0.2	1.1	0.8	2.0		0.7	-6.5	-2.1	-2.5	2.7	3.6
	70	-1.6	-1.4	6.0	•	•	•	0.0	•	•	•	•	0.7			1.0		4.3	4.6	0.2		-3.0	-3.1	4.7	6.7
	71	-2.0	-0.1	1.3	1.0	-1.4	-0.8	9.0	0.2	1.8	1.3	0.3	1.3	0.3	-0.3	1.1	0.7	5.5		9.0		,	-	-	
	72°	-1.4	-0.9	2.0	2.5	-1.2	-1.8	9.0-	-0.4	3.1	2.7	-0.2	8.0-	1.0	9.0	1.3	1.8	11.3	15.8	-2.9	-8.6			-	
h1.y	1	g 15		ug 31		p 15		Sep 16-Sep 30		t 15		ct 31	-	v 15		ov 30		c 15	-	ec 31		n 15		an 31	
Semimonthly	Periods	Aug 1-Aug		Aug 16-Aug 31		Sep 1-Sep 15		16-5		Oct 1-0ct 15		Oct 16-0ct 31		Nov 1-Nov 15		Nov 16-Nov 30		Dec 1-Dec 15		Dec 16-Dec 31		Jan 1-Jan 15		Jan 16-Jan 31	
Sem	P	Aug	-	Ang		Sep		Sep		Oct		Oct		Nov		Nov		Dec		Dec		Jan		Jan	

Positive values indicate rate of advancement. Negative values indicate rate of recession.

Top value in each box is a mean rate. Bottom value in each box is a median rate.

Table V. Advancement and Recession Rates of Ice Edge for 15-Day Periods February 1 - July 31 (1953-1971) (nm1/d) Greenland Coast East of 45°W

Latitude (N)

Semimonthly		1													
Periods	72°	7.1	70	69	89	67	99	65	49	63	62	61	09	59	
Feb 1-Feb 15	•	1.7	4.5	-0.2	-2.3	-3.7	0.3	-2.2	1.4	0.3	9.0		-0.5	2.9	
		2.4	1.0	-4.7		•	•	-2.9	1.0	0.5	•	۲.	0.7	2.2	
Feb 16-Feb 28	1	2.6	2.3	2.0	1.1	-C.7	8.0	9.0		-0.2	-0.4	7.	1.0	-2.8	
		1.6	0.5	7.4	1.0	•	•	•	-0.5	-0.5	-0.9	6.0-	4.0-	-1.8	
Mar 1-Mar 15	2.9	0.3	1.1	0.2	2.4	5.9	6.0	1.3	2.6		0.0	0.0	0.0	0.7	1
	2.7	1.0	-0.1	0.9	5.9	2.0	3.2	1.0	•	8.0	2.3	1.4	0.5	6.0	
Mar 16-Mar 31	-2.0	-3.3	-2.2	-1.5		6.0-	1.3	1.0	0.0	0.0	6.3		0.5	-0.2	T
	3.7	-4.2	6.0-		-	-0.5	6.9	0.7	0.9	•	0.2	0.0	0.2	-0.7	
Apr 1-Apr 15	-1.1	-2.2	-1.2	0.8	1.7	1.0	1.5	0.1	•	-0.3	-1.6	c	-0.7		T
	-4.0	-1.5	-2.6	3.0	-1		3.2	1.1	-1.0		0.0	0.0	-0.3	6.0-	
Apr 16-Apr 30	-1.6	1.9	0.3	0.5	0.0	0.0	0.8	0.8	0.1	0.0	0.0	0	0.2		1
	-5.1	3.0		-0.9	•		•	0.3	-0.1		-0.2	.2	-0.2		_
May 1-May 15	-5.1	-3.6	-1.8	•	-1.5	-1.0	-2.3	7.0	0.0	-0.3	-0.3	-0.5	-0.7	-1.6	
	-6.2	-6.1	-1.6	-2.0	-3.5	-2.2	-1.6	•	4.0-	•	•	-		-2.6	_
May 16-May 31	9.0	2.1	0.2	-0.2	0.2	-1.2	1.7	-1.8	-0.1	0.0	0.3		0.5		
	2.0	3.0	-1.1	-1.3	3.9	-0.3	1.3	-1.5	0.1	-0.1		8.0		0.7	
Jun 1-Jun 15	3.9	-1.6	0.0	-0.2	-0.7	-0.2	-0.7	1.4	9.0	0.3	0.2	-0.3		0.0	ī
	4.8	0.0	1.3	-0.4	-3.2	-0.2	-0.7	0.0	2.2	8.0	8.0-	-0.2	-0.2	0.9	_
Jun 16-Jun 30	-6.2	-2.3	-1.2	-0.1	-0.2	8.0-	-1.2	-1.1	-0.1	-0.2		0.3	-0.2	0.2	
	-8.3	-4.8	-1.6	1.2	0.7	1.0	6.0-	0.1	-0.4	0.0	0.5	-	0.0	-0.2	_
Jul 1-Jul 15	0.5	2.0	9.0-	.1.9	-0.9	1.4	-0.1	-1.0	1.0	-1.1	0.0	0.2	0.2	1.4	_
	0.6	-2.7	9.0-	-1.5	-1.1	3.1	0.1	1.0	1.0	0.3	•	-0.2	0.3	1.4	-
Jul 16-Jul 31		-1.3	-1.1	-0.2	-1.1	-2.6	0.8	9.0	6.0-	6.0	0.2	-0.3	0.0	-1.7	Γ-
	-2.9	-1.4	9.0-	-1.2	9.0-	-1.5	2.0	-0.81	-1.3	-0.3	0.0	0.0	-0.3	-0.7	-
															1

Positive values indicate rate of advancement. Negative values indicate rate of recession.

Top value in each box is a mean rate. Bottom value in each box is a median rate.

Table VI. Advancement and Recession Rates of Ice Edge for 15-Day Periods December 1 - September 15 (1953-1971) (nmi/d) Greenland Coast West of 45°W

Latitude (N)

	imonthly						
	eriods	64°	63	62	61	60	59
	1-Dec 15	-	-		-	0.8	-
						1.0	
	16-Dec 31	-	-	-	-	1.0	-
						1.5	
	1-Jan 15	-	-	-	-	4.3	-
						3.7	
	16-Jan 31	-	-	-	1.6	0.2	-
					1.5	1.0	
	1-Feb 15	-	-	-	0.2	-0.2	-
					0.3	-0.8	
	16-Feb 28	-	-	-	-1.9	0.5	-
					-1.9	1.5	
	1-Mar 15	-	-	-	1.0	1.3	1.9
					1.1	1.2	2.1
	16-Mar 31	-	-	2.1	1.8	0.5	1.9
				2.2	1.5	0.3	3.3
Apr	1-Apr 15	-	-	1.7	-1.0	0.2	0.4
				1.4	0.2	0.7	-1.4
	16-Apr 30	-	-1.8	0.8	0.6	0.5	1.7
			-1.5	1.1	0.0	-0.5	1.7
	1-May 15	-	2.4	-2.6	-0.2	-0.8	-2.1
			1.7	-3.6	-0.2	0.7	-2.2
	16-May 31	-	0.6	0.3	0.8	1.5	0.5
			0.0	1.2	0.8	2.3	1.0
	1-Jun 15	-	0.9	0.0	-0.2	-0.5	-0.9
			2.0	-0.6	-1.0	-1.8	-0.5
	16-Jun 30	-	-0.3	1.1	0.5	-0.8	-
			-1.2	1.2	-0.2	0.2	
	1-Jul 15	-	1.8	-0.3	-0.3	-0.7	0.2
			0.8	-0.9	0.2	0.2	-0.4
	16-Jul 31	-0.4	-0.8	0.5	-0.5	0.7	-
		0.4	0.6	0.0	0.6	0.0	
	1-Aug 15	-2.9	-2.4	-1.6	-0.8	-1.8	-
		-3.6	-2.7	-1.2	-2.1	-2.7	
	16-Aug 31	-	-	-0.2	-1.6	-0.3	-
				0.3	-0.8	-0.8	
Sep	1-Sep 15	-	-	•	0.5	-0.8	-
					0.5	0.3	

Positive values indicate rate of advancement.
Negative values indicate rate of recession.
Top value in each box is a mean rate.
Bottom value in each box is a median rate.

the contention made earlier that the ice forecaster must have a working knowledge of basic oceanographic and meteorological processes which influence the behavior of sea ice.

The ice edge in the western Labrador Sea begins to recede during the first half of March as recession rates vary from 0 to 6.3 nmi/d (0 to 11.7 km/d) through the end of April, with the maximum occurring between 1 and 15 March along 48°N. By the end of April, recession of the Davis Strait ice edge is well underway. Between May and the end of September, the Davis Strait recession rates vary from 0 to 4 nmi/d (0 to 7.4 km/d) with the maximum rate occurring in the first half of August. The pack ice in Baffin Bay begins to recede westward in earnest during June as its ice edge recession rates range from 0.9 to 7.8 nmi/d (1.7 to 14.5 km/d) through late September when the edge begins to advance eastward in the northern portion of the bay. Maximum recession rates during spring and summer for the east Greenland ice edge vary from 0 to a maximum of 6.2 nmi/d (11.5 km/d), which occurs during the latter half of June along the 72°N parallel. However, on the average, the edge attains its highest net recession rates during May and August. The same forces interacting on the east Greenland ice edge during autumn and winter, causing the edge to advance along some parallels and recede along others simultaneously, also interact in a like manner during spring and summer. Only during the first half of the months of August and September does the ice edge come close to receding along each parallel during the same semimonthly period where an ice edge position was observed.

The mean rates of advancement and recession of the pack ice edges have been explained in detail to provide an understanding of year-round variability. Median advancement and recession rates are also given for the entire year in tables I through VI.

C. Ice Concentration and Large Floe Sizes

Mean ice concentrations in oktas and mean percentages of area covered with large floes were computed for the western Labrador Sea, the Davis Strait/ Baffin Bay region, and the east Greenland coastal area for the 18-year period from 1954 through 1971. The primary sources for these data were aerial ice reconnaissance and satellite observations supplemented by icebreaker data. Since floe size information could not be ascertained from available satellite imagery, satellite data were used only to determine ice concentrations. Concentration and floe size data were analyzed by one-degree geographic squares for all semimonthly periods. Means presented for ice concentrations and floe size percentages were computed from data sources which did not equally cover the areas of interest in either time or space. Therefore, normal increases in ice concentration and floe size coverage during the icegrowth season and their subsequent decrease during spring and summer may not be apparent for all areas from one semimonthly period to the next. However, examination of the concentration and floe size percentage charts for each semimonthly period should provide the ice forecaster with a general picture of breakup and freezeup in the eastern Arctic.

Concentration and floe size percentages were not computed when ice covered less than 50 percent of a one-degree square. Means were computed for the three 6-day periods in each semimonthly period with the midmonthly

6-day (13th through 18th) period included in both semimonthly periods of each month for computational purposes. The mean semimonthly concentration data representing each one-degree square and year were averaged, and the resultant values were plotted and analyzed. Figures 54A through 77A show these analyses for successive semimonthly periods.

Semimonthly floe size data were treated in a similar fashion, and a mean large floe size percentage value was computed, plotted, and analyzed for each semimonthly period. For the purpose of this study, big (1,640 ft (500 m) to 1.1 nmi (2 km)), vast (1.1 nmi (2 km) to 5.4 nmi (10 km)), and giant floes (greater than 5.4 nmi (10 km) have been grouped collectively and designated as "large floes." Values are plotted as percentages of a one-degree square area covered with large floes rather than as a percentage of the total amount of ice present. For example, if 5 oktas of ice were observed in a one-degree square and 4 oktas consisted of large floes, 50 percent of the area was covered with big, vast, or giant floes. Percentages of large floes for each semimonthly period are presented in figures 54B through 77B.

1. Concentration Analysis

Ice concentrations in the eastern Arctic generally reach a maximum during the first half of September (figure 70A) with some sea ice normally remaining in western Davis Strait, west-central and northern Baffin Bay, and adjacent to the east Greenland coast north of 64°N. Mean concentrations during this period range from 1 to 3 oktas in Davis Strait and central Baffin Bay, 1 to 4 oktas in northern Baffin Bay between 75°N and 77°30'N, 5 to 6 oktas north of 77°30'N, 1 to 3 oktas adjacent to the east Greenland coast south of 70°N, and 1 to 6 oktas between 70°N and 75°N. As a rule, the eastern Arctic ice-growth season begins during the latter half of September (figure 71A) as the pack ice begins to advance with a corresponding increase in ice concentrations. In October (figures 72A and 73A), western and central Baffin Bay freezes over as the ice edge advances southward in western Davis Strait and along the southeast Greenland coast. During November (figures 74A and 75A), concentrations in western Davis Strait approach 4 to 6 oktas with some areas of 7 to 8 oktas appearing in its northwest section and areas of 2 to 4 oktas immediately adjacent to the ice edge. Concentrations in the main pack of Baffin Bay, which is almost completely ice covered at this time, range from 6 to 8 oktas. Adjacent to the east Greenland ice edge, concentrations range from 1 to 3 oktas while those farther to the west are primarily 4 to 6 oktas north of 67°30'N and 3 to 5 oktas to the south. By the end of December (figure 77A), concentrations in the main pack bodies of Baffin Bay and northern Davis Strait are 7 to 8 oktas with concentrations of mainly 1 to 5 oktas evident in a 5-nmi (9.3 km)-wide band in their extreme eastern portions between 66°30'N and 73°N. Concentrations in southwestern Davis Strait at this time are primarily 6 to 8 oktas as the ice pack begins to advance toward the northern Labrador coastal region. Concentrations adjacent

to the east Greenland coast north of 67°N generally range from 6 to 8 oktas, decreasing to 2 to 5 oktas along the pack ice edge. Between 65°N and 67°N in this area, concentrations generally vary from 3 to 5 oktas while those south of 65°N range from 1 to 4 oktas. In January and February (figures 54A through 57A), the pack edge advances southward rapidly along the Labrador and Newfoundland coasts while the east Greenland pack edge north of 66°N remains fairly static. Ice concentrations in Baffin Bay remain at 7 to 8 oktas with some areas of 6-okta concentration in the extreme southeast portion. Ice concentrations in western and northern Davis Strait normally attain their maximum of 7 to 8 oktas by the end of February (figure 57A) while those along the Labrador coast generally reach their maximum of 5 to 8 oktas by mid-February (figure 56A). By the end of January (figure 55A), pack ice is present to the east, west, and southwest of Newfoundland with concentrations generally ranging from 1 to 5 oktas. By the end of February (figure 55A) pack ice is present to the east, west, and southwest of Newfoundland with concentrations generally ranging from 1 to 5 oktas. By the end of February (figure 57A), these concentrations have increased to their normal maximum of 3 to 8 oktas with 1 to 2 oktas present along the eastern ice pack edge. Ice concentrations along the east Greenland coast generally range from 4 to 8 oktas with concentrations of 1 to 4 oktas adjacent to the ice edge.

During March and through mid-April (figures 58A through 60A), Baffin Bay attains its maximum concentrations of 8 oktas with small 7-okta areas in the extreme southeast corner and in the vicinity of the North Water* area between 76°N and 78°N. During March and April (figures 58A through 61A), heavier concentration areas of 6 to 8 oktas continue to be in evidence in the main pack ice bodies of northern and western Davis Strait. Areas of 2 to 6 oktas adjacent to the west Greenland coast north of 65°N and 1 to 5 oktas adjacent to the ice edge south of 65°N develop as the ice edge advances eastward causing loosening within the ice pack. Concentrations along the Labrador/Newfoundland coastal regions during March and April (figures 58A through 61A) decrease to 4 to 7 oktas along both coasts and to 1 to 3 oktas adjacent to the ice edge. Concentrations within an average of 125 nmi (232 km) of the east Greenland coast north of 65°N increase in March and April to 6 to 8 oktas with the remaining pack concentrations north of 65°N ranging from 1 to 5 oktas. South of 65°N, 6 to 7 oktas occur adjacent to coastal areas with 1 to 5 oktas along the ice edge.

^{*}North Water - the large semipermanent polynya during winter in northwestern Baffin Bay, Smith Sound, and portions of Lancaster and Jones Sounds.

Breakup in the eastern Arctic initially occurs in late April (figure 61A) and the first half of May (figure 62A). The ice pack in the southern portion of the region begins to recede during the latter half of April (figure 61A) with a corresponding decrease in ice concentrations of the Labrador/Newfoundland area. Concentrations of 8 oktas decrease to 7 oktas in many areas of northwest and southeast Baffin Bay by 1 May (figure 62A). During May (figures 62A and 63A), concentrations in the Baffin Bay/Davis Strait and the Labrador/Newfoundland regions continue to decrease as the pack ice edge remains fairly static. By 1 June (figure 64A), ice concentration in the Baffin Bay main pack body is predominately 7 oktas with concentrations ranging from 2 to 6 oktas in the North Water and in the east-central and southeast areas of the bay. In Davis Strait, main pack concentrations vary from 4 to 7 oktas with concentrations ranging from 1 to 3 oktas adjacent to the ice pack edge. Along the Labrador coast north of 54°N, concentrations of the inner half of the ice pack vary from 4 to 6 oktas while those of the outer half range from 1 to 3 oktas. Concentrations and the pack edge along the east Greenland coast remain fairly static during May (figures 62A and 63A) with the exception of a slight decrease from 7 to 8 oktas to 6 to 7 oktas in concentrations along the coast north of 64°N.

During June (figures 64A through 65A), the pack edge recedes northward away from the Newfoundland coast and westward along the Labrador coast, in western and northern Davis Strait, and in eastern Baffin Bay. Concentrations in the main pack body of Baffin Bay remain heavy at 7 oktas as lighter concentrations in its northern and eastern regions continue to expand over greater areas. In western Davis Strait, concentrations in the inner half of the ice pack range from 4 to 7 oktas with 1 to 3 oktas predominant in the outer half as ice-free conditions extend along the west Greenland coast as far north as Disko Island. Along the Labrador coast there is a general decrease in ice concentrations during June (figures 64A and 65A) with maximum significant concentrations of 5 to 6 oktas located along its northern The predominant maximum ice concentrations along the east Greenland coast north of 64°N continue to decrease slightly and vary from 5 to 6 oktas by 1 July. There is a general westward recession of the east Greenland ice edge of approximately 75 nmi (139 km) north of 65°N during June; however, the ice edge south of 65°N remains fairly static. Disintegration rapidly accelerates in July and August (figures 66A through 69A) as the pack edge recedes in all areas during both months, except for the east Greenland ice edge south of 65°N which remains fairly stable during July. By 1 August (figure 68A), concentrations along the Labrador coast vary from 1 to 2 oktas, and by mid-August (figure 69A) the coastal area is free of ice. Maximum significant concentrations in Baffin Bay by the end of July vary from 5 to 6 oktas as ice-free conditions develop in the northwest sector and along the west Greenland coast to 74°N. The maximum concentration present in western Davis Strait at this time is 5 oktas. East Greenland coastal ice concentrations generally decrease to 4 to 5 oktas with concentrations adjacent the ice edge ranging from 1 to 3 oktas by 1 August. By the end of August (figure 69A), overall ice concentrations in western Davis Strait, central and northeastern Baffin Bay, and south of 70°N along the east Greenland coast have decreased to 1 to 3 oktas as concentrations in the western Greenland Sea north of 70°N remain stable at 1 to 6 oktas.

2. Floe-Size Analysis

Figures 54B through 77B show that mean large floe percentages are generally minimum in the eastern Arctic during September (figures 70B and 71B). As autumn progresses, increases in mean large floe percentages appear initially in the northern sector of the forecast region in such areas as northern Baffin Bay and in the northwestern Greenland Sea as freezing alters the structure of the pack ice. During the latter half of October (figure 73B), high percentages of large floes (60-100 percent) cover Smith Sound and Kane Basin in northern Baffin Bay as percentages of 20 to 30 percent begin to appear in western Baffin Bay and along the east Greenland Coast north of 68°N. Large floe percentages increase rapidly in central Baffin Bay and northwestern Davis Strait during November (figures 74B and 75B) and range as high as 80 to 90 percent in the main pack bodies by 1 December.

During December and January (figures 76B, 77B, 54B and 55B), high percentages of large floes (80 to 100 percent) become predominant in central Baffin Bay and northern Davis Strait. In western Davis Strait large floe coverage is primarily in the 40- to 60-percent range. Lower percentages (<10 to 30 percent) can be expected at this time along the Labrador/Newfoundland coastal region and along the east Greenland coast south of 70°N.

During the latter half of winter (February through mid-March, figures 56B through 58B), predominant percentages remain high (80 to 100 percent) in the central and extreme northern sectors of Baffin Bay. In western and northern Davis Strait primary mean floe percentages vary from 40 to 90 percent while the maximum percentages adjacent to the Labrador coast reach the 40- to 60-percent range at times. During late February (figure 57B) and again in late March (figure 59B), large floe percentages in the western Greenland Sea north of 67°N are concentrated in small areas adjacent to the coast and in the pack north of Iceland.

In April (figures60B and 61B), the mean percentage of large floes in Baffin Bay has decreased slightly to the 80- to 90-percent range, with 100-percent coverage present only in Kane Basin. As spring begins in western Davis Strait, mean floe percentages in the inner half of the ice pack range primarily from 40 to 60 percent with lower percentages (<10 to 30 percent) evident within the outer half. Maximum large floe percentages along the east Greenland coast remain in the 40- to 60-percent range while those along the Labrador coast decrease to 20 percent by 1 May. During May and June (figures 62B through 65B), there is a general decrease in large floe coverage throughout the region as mean percentages range from 80 to 100 percent in Kane Basin; 20 to 40 percent in northwestern and eastern Baffin Bay; 40 to 80 percent in central Baffin Bay, northwestern Davis Strait, and along the east Greenland coast; and less than 10 to 20 percent in southern Davis Strait and along the Labrador/Newfoundland coasts. During July (figures 66B and 67B), further decreases occur in large floe coverage as the predominant percentages in central Baffin Bay range from 10 to 30 percent with small areas of 40 to 60 percent adjacent to the

Baffin Island and east Greenland coasts and in Smith Sound. The highest percentages (60 to 80 percent) continue to be present in Kane Basin, while over the remainder of the eastern Arctic mean percentages range from less than 10 percent to 20 percent. In August and September (figures 68B through 71B), when area minimums are approached, large floe percentages are mostly less than 10 percent in Baffin Bay, western Davis Strait, and within the majority of the east Greenland ice pack. Exceptions to this are mean floe percentages of 10 to 20 percent adjacent to the east Greenland coast north of 70°N and percentages of 10 to 30 percent in the extreme northern portion of Baffin Bay.

IV. FORECASTING TECHNIQUES

Long-range forecasting of growth, movement, and decay of arctic sea ice is presently far from being an exact science. Not only are the number of available forecasting techniques limited, but the number of detailed ice observations including measurements of ice thickness, topography, and floe size is also limited. There is an additional deficiency present, because the reliability of meteorological predictions decreases significantly beyond three days.

The three primary forecasting techniques available to the forecaster include: (1) dynamic numerical models, (2) analog methods, and (3) statistical methods. The major shortcoming inherent in a dynamic model has been the lack of directly measurable meteorological and oceanographic parameters which simultaneously act on the ice cover and which serve as the primary source inputs to the model. This has necessitated estimation of various forces known to act on the ice cover during ice redistribution and drift. Ice dynamicists are continually attempting to model the movement of polar ice and to improve their knowledge of pack ice dynamics through programs such as the ongoing Arctic Ice Dynamic Joint Experiment (AIDJEX). AIDJEX was conceived in 1969 as a joint Canadian and American project to determine interactions between drifting pack ice, atmosphere, and ocean. A major deficiency in attempting to utilize numerical models was summed up by some of the major AIDJEX investigators (Maykut et al., 1972) who stated: "to describe, and hence predict, the behavior of the ocean-ice-atmosphere system in quantitative terms it would be necessary to know the initial status of all three media, as well as the physical laws describing their behavior and interaction. Neither of these requirements can be met today." Current literature (Atkinson, 1976) indicates that an ocean-data-computer model delivered from the AIDJEX project will soon be available and "may be useful" in forecasting ice pack movement. Results from project such as AIDJEX should, someday, raise the use of dynamic ice forecasting models to a practical level.

Until such a time, the statistical and analog forecasting techniques should be utilized to produce the majority of long-range ice forecasts. These two techniques have proven useful, particularly the statistical approach when given the information presented in this guide. The analog method is the least complex of the two techniques since it generally involves a comparison of current ice conditions with those observed during a similar time period for previous years. For example, if ice conditions on 1 June 1974 appeared very similar to those which existed on 10 June 1972 and the

current 30-day meteorological prognostic charts were forecasting near-normal conditions, forecasted ice conditions for 15 and 30 June 1974 would approximate conditions observed on 25 June and 10 July 1972, respectively.

A major disadvantage inherent in this technique is that in its simplest form no allowances are made during the forecast period for unusual environmental conditions such as a major storm or anomalous temperatures that may drastically change ice conditions. This inadequacy, however, can be overcome somewhat by careful examination, if possible, of synoptic meteorological conditions during the analog period to determine if any anomalous conditions did indeed exist. This examination also provides the opportunity to compare past conditions with the current 30-day mean prognostic charts.

The forecasting procedures described in this guide approach the problem of predicting changes in ice distribution and ice edge movement based on a statistical technique. Application of statistical methods to long-range sea ice forecasting has been shown in recent years to produce the best results without accounting for various unavailable meteorological and oceanographic parameters that ultimately determine sea ice behavior (Potocsky, 1975).

The primary products from a long-range sea ice forecast, in the majority of cases, are the position of the ice edge and determinations of concentration and floe size coverage within the pack ice for a specific location. Since the growth, movement, and decay of sea ice for a specific locality are dependent largely upon effects produced by large-scale environmental factors such as mean monthly air temperatures, mean sea level pressure patterns, mean set and magnitude of surface currents, and location of primary and secondary storm tracks, these essential parameters should be carefully examined during the prediction process. Preparation of 15- and 30-day sea ice forecasts should make optimum use of all current and historical ice concentration and floe size data. The 30-day mean meteorological prognostic charts issued by the long-range prediction group of the National Weather Service also serve as primary inputs to a long-range sea ice forecast. This section of the guide describes the procedures and techniques used in preparing long-range (15- and 30-day) ice forecasts in support of operations in the eastern sector of the North American Arctic.

A. Forecasting Ice Edge Movement, Pack Concentration, and Floe Size Coverage

Utilizing a statistical approach to forecast advancement or recession of the ice edge and change in pack concentration and floe size coverage in the western Labrador Sea, Davis Strait/Baffin Bay, and east Greenland regions for specific periods throughout the year requiresthat different emphasis be placed on the various environmental parameters. At any given time, a single oceanographic or meteorological parameter, depending upon the season, will exert greater or lesser influence on the pack ice than other parameters. For example, during breakup or freezeup the effect of temperature on the ice cover may be more important than the effect of wind or current drift. However, between breakup and freezeup light and variable winds or, going to the other

extreme, indications of a strong gradient on the monthly mean prognostic pressure chart along an active storm track will imply that wind or current drift are the dominant forces influencing pack ice movement. Often, a combination of several environmental factors exerts forces simultaneously on the ice cover. It is then the prime responsibility of the ice forecaster to weigh the importance of each factor.

In order to relate ice edge advancement and recession rates as given in tables I through VI to forecasted conditions, the forecaster should consider the 30-day mean sea level prognostic chart as the primary input source when preparing long-range forecasts of pack edge movement. The prognostic chart will indicate the strength of the geostrophic wind over the areas of interest, and will enable the forecaster to assess normal or anomalous conditions along specific parallels where advancement and recession rates are given. Examination of the mean monthly sea level pressure charts presented in appendix A indicates that windspeeds of 7 km (13 km/h) or less are most frequently observed in the three primary areas of the eastern Arctic from March through October. Winds over the Labrador/Newfoundland region normally average between 8 and 12 km (15 and 22 km/h) during November and December and between 13 and 16 km (24 and 30 km/h), while winds in Baffin Bay and the east Greenland coastal region during the same time period range from 8 to 11 km (15 and 20 km/h). With the preceding winds considered normal for these areas during the time periods detailed, lighter forecasted geostrophic winds will equate to less-than-normal advancement or recession rates, while stronger forecasted geostrophic winds will equate to abovenormal rates.

Another primary source input to a long-range ice forecast is the 30-day mean 700-mb prognostic height departure-from-normal (D.N.) chart which can be used for two specific purposes. First, it can be used as an indicator of a forecasted warming or cooling trend which can then be used to qualitatively modify the mean conditions shown by the ice concentration and floe size percentage charts (figures 54A through 77B). Secondly, it can be used to increase or decrease 15- and 30-day projected degree-day totals by utilizing the metric conversion table presented in appendix C. Reliability of the final product will not only depend heavily upon the aforementioned long-range prognostic charts, but also on the way in which the ice forecaster evaluates the current synoptic ice data at his disposal. The suggested solution for each of the following problems is one of several possible solutions. Since many of the techniques involved are subjective by nature, the same data input used by different forecasters will yield various, but similar, results.

1. Davis Strait

The pack edge in the Davis Strait/Baffin Bay area normally begins to recede in a westerly direction after April. Under normal conditions the "middle passage"ship route to northern Baffin Bay opens to navigation during the latter part of July. The middle passage route extends northward in eastern Baffin Bay from 70°N to 72°45′N, approximately 30 nmi seaward, and then northwestward to 76°N approximately 75 nmi seaward. Ice pack recession generally continues through mid-August.

EXAMPLE 1

Given: The pack edge was observed by satellite imagery on 14 April to extend between 62°N and 70°N as shown in forecast example figure 1A. The 30-day mean 700-mb prognostic height D.N. chart issued by the National Meteorological Center (NMC) of the National Oceanic and Atmospheric Administration (NOAA) on 11 April 1975 is shown as figure 78. According to this prognostic chart, above-normal heights are expected over the forecast area during the next 30 days. The 30-day mean sea level prognostic chart (figure 79) also issued by NMC on 11 April 1975 depicts a light geostrophic windflow toward the southwest over the forecast area. Although other prognostic height and mean sea level charts will be referred to in subsequent forecast problems, the charts for 11 April 1975 are the only examples illustrated in this report.

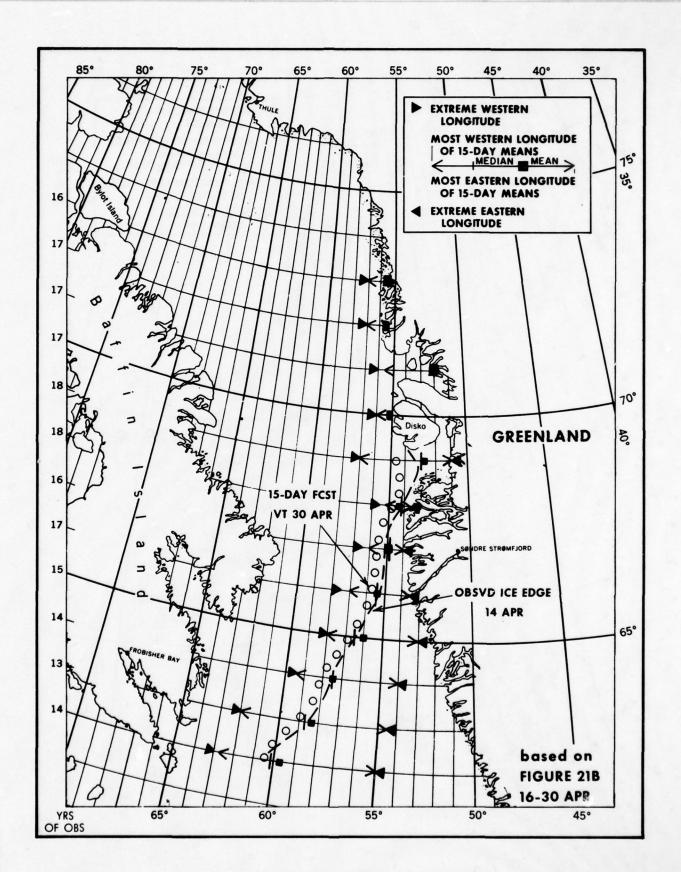
Find: (a) Position of the ice edge on 30 April and 15 May within the Davis Strait region, and

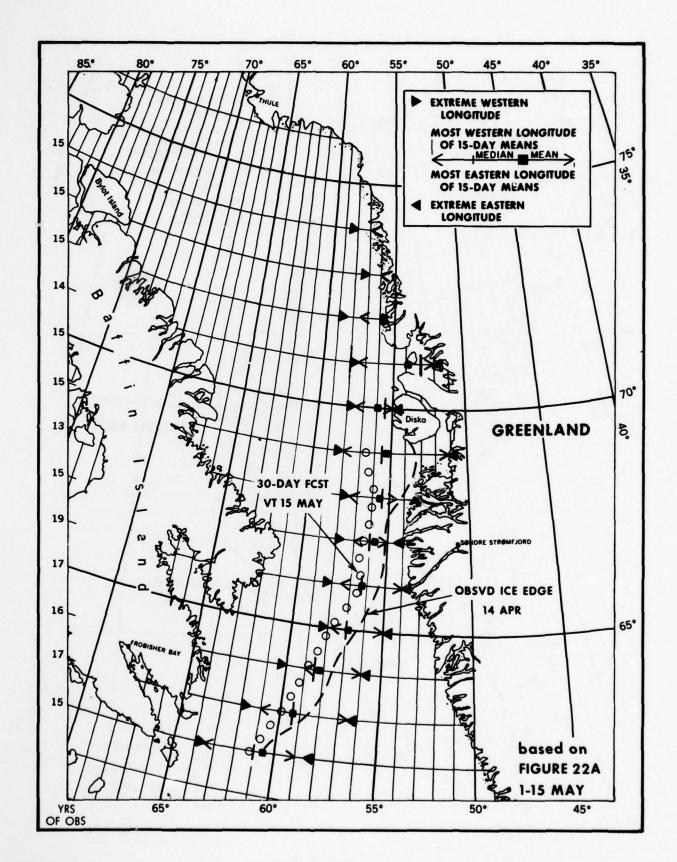
(b) Concentration and floe size coverages within the pack ice for the same dates.

Solution: (a) The prognosticated mean sea level pressure pattern over the forecast area (figure 79) compares vary favorably with the area's normal isobaric conditions and geostrophic flow for the months of April and May as shown in figures A-4 and A-5 of appendix A. Comparison of the position of the observed ice edge with its expected normal position for this date (figure 21A) indicates that is has, for the most part, attained a less-than-normal position. Examination of earlier observed positions of the ice edge during the preceding 4 or 5 months indicates that this was due primarily to the less-than-normal growth of the pack ice during a relatively mild winter. Therefore, using the appropriate mean recession rates for 16-30 April as given in table 1, the forecast ice edge by 30 April can be expected to recede farther westward and by 15 May be positioned as shown in forecast example 1B.

(b) The concentrations (shown in forecast examples 1A and 1B) within the pack ice were also observed by the 14 April satellite imagery to be slightly less than normal in contrast with the mean conditions shown in figure 60A. A 30- to 50-nmi (56 to 93 km) band of 4 to 6 oktas of ice extended from 62°N to approximately 65°30'N adjacent to the ice edge, becoming a 5-to 7-okta band of the same width from 65°30'N to 70°N. The main pack concentration was 7 to 8 oktas. Floe sizes in this instance were not discernible from current satellite imagery; however, since all other factors indicate less-than-normal conditions, it can be safely assumed that current floe size coverages are also less by a similar degree than the mean conditions shown in figure 60B.

The primary input to this portion of the forecast is, of course, the observed ice concentration and floe size conditions described above. Since the 30-day mean 700-mb prognostic height D.N. chart depicts a slight warming trend over the forecast area and a normal windflow pattern is forecasted, the normal rate of decrease in ice concentration and floe size coverage





FORECAST EXAMPLE 1B

between the mean conditions shown in figures 60A and 61A and between figures 60B and 61B should be increased slightly for the 30 April forecast. Therefore, by 30 April a 40-to 60-nmi (74 to 111 km) band of 3 to 5 oktas of ice will be located just inside the ice edge between 62°N and 66°N, increasing to a 4-to 6-okta band between 64°N and 69°N. Within this band of ice, 10 to 30 percent of the area will be covered by large floes (big floe or larger (500 m to > 10 km)) with the remainder consisting of brash (<20 m), small (20-100 m) and medium (100-500 m) floes. Within the main pack, large floes will cover 30 to 60 percent of the area. The remainder can be predominately medium floe with some small floe.

Continuing with the predicted warming trend over the forecast area for the next 15-day period and referring to figure 22A, concentrations within the first 50 to 70 nmi (93 to 130 km) of the ice pack will range from 2 to 4 oktas with some scattered areas of 1-okta or less concentration immediately adjacent to the ice edge by 15 May. Predominant concentrations within the remainder of the pack ice beyond the initial 70 nmi (130 km) can be expected to range from 6 to 7 oktas with some 5-okta areas along the boundary separating the higher and lower concentrations. Floe size coverages shown in figure 62B indicate that 10 to 20 percent of the area of 2- to 4-okta concentration adjacent to the ice edge will be covered by large floes. The area within the main pack will have 30 to 50 percent of its surface covered by large floes. The remaining floe sizes in both areas will vary from brash to medium floe.

2. Western Labrador Sea

Sea ice may begin to appear along the extreme northern portion of the Labrador coast in scattered strips and belts during the latter half of October as a result of ice drifting southward from the Davis Strait under the influence of the south-setting Labrador Current or through in-situ growth as coastal seawater reaches its freezing point. However, a continuous pack edge is not generally observed to extend along the entire Labrador coast until the latter half of December. Sea ice will, on the average, remain adjacent to some portions of the Labrador coastal regions through July, approaching a mean maximum seaward extent of between 120 nmi (222 km) in the north and 150 nmi (278 km) in the south.

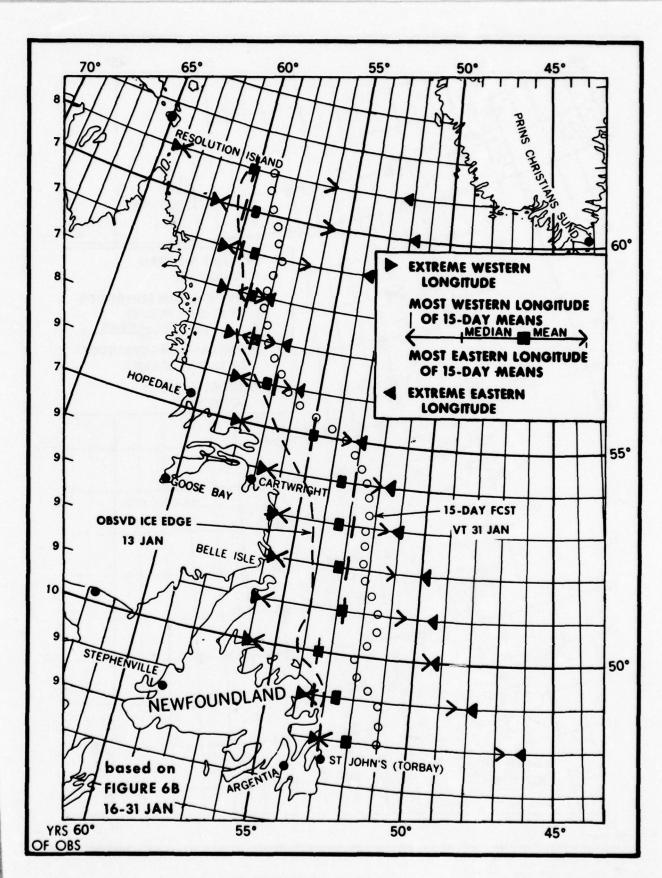
EXAMPLE 2

Given: On 13 January the pack edge in the western Labrador Sea, as well as the inner pack concentrations and floe-size coverage distributions, were observed by aerial reconnaissance from approximately 51°20'N to 61°N. The 30-day mean 700-mb prognostic height D.N. chart issued by NMC on 15 January indicates below-normal heights are expected over the entire forecast area. In addition, the 30-day mean sea level prognostic chart depicts that a moderate anomalous west-southwesterly geostrophic windflow will prevail over the Labrador coastal area.

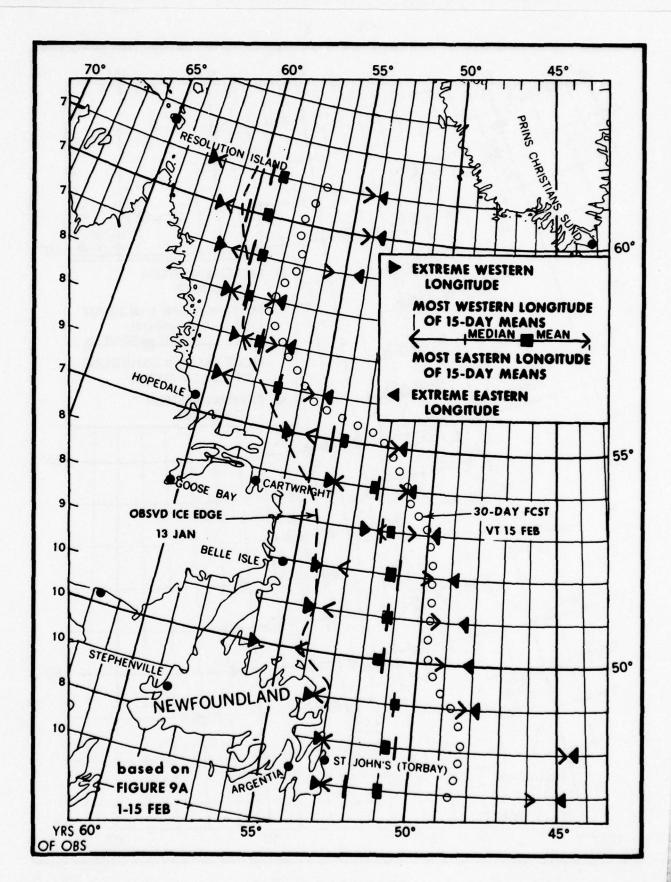
- Find: (a) Position of the ice edge on 1 and 15 February, and
- (b) Pack concentrations and floe size coverages within the pack edge for the same dates.

Solution: (a) The position of the observed pack edge as shown in forecast example 2A coincides closely with the expected normal position for this date as shown in figure 8A. However, the below-normal heights forecasted on the D.N. chart suggest a cooling trend over the entire Labrador coastal area, and, as stated above, the 30-day mean sea level prognostic chart is forecasting an anomalous offshore windflow. These anomalous conditions acting in concert imply increased ice growth and a much faster-than-normal advancement of the pack edge. Under these conditions it would not be unusual for the ice edge to approach or reach its historical maximum limits. Therefore, the ice edge by 1 February can be expected to be located as shown in forecast example 2A. The ice edge will continue to advance seaward, again at faster-than-normal rates than those given in table II, and by 15 February will be positioned as shown in forecast example 2B.

(b) The ice concentrations and floe size coverages observed on 13 January also compare very favorably with the mean conditions for these parameters as shown in figures 54A and 54B. Figure 55A shows that between 54^oN and 61^oN an ice concentration of 6 to 8 oktas would normally be expected within the main pack, with 2 to 5 oktas generally expected adjacent to the ice edge between $54^{\circ}N$ and $58^{\circ}N$ and in the remainder of the forecast area pack south ot 54°N by 1 February. However, since the 30-day mean 700-mb prognostic height D.N. chart indicates below-normal heights over the forecast area and, therefore, a cooling trend and an anomalous offshore windflow is forecasted, the normal ice-growth cycle from one semimonthly period to the next will not take place. Taken by itself, the effect of the cooling trend would normally cause a slight increase in overall ice concentrations, floe size coverages within the pack ice, and normal ice edge advancement rates. however, the effect of the moderate offshore windflow not only will cause the ice edge to advance at an above-normal rate but also will cause dispersion of ice within the pack leading to decreased ice concentrations, particularly immediately adjacent to the ice edge. Therefore, as effects of the cooling trend and anomalous windflow oppose and complement each other to a certain degree, by 1 February an area of 1- to 2-oktas concentrations can be expected adjacent to the ice edge south of 580N with large flce size percentages ranging from less than 10 percent south of 550N to 10 to 15 percent between 550N and 580N. Ice concentrations of 3 to 6 oktas will be present over the inner half of the pack adjacent to the coast south of 540N with less than 10 percent of the area covered by large floes, in the middle third of the pack between 540N and 580N with large_floes percentages varying from 10 to 20 percent, and over the outer third of the pack adjacent to the edge between 58°N and 61°N with 20- to 30-percent large floes. The remainder of the pack adjacent to the coast between 54°N and 61°N will consist of 6 to 8 oktas with large floe percentages of 20 to 30 south of 58°N and 30 to 40 between 580N and 610N. With moderate to strong offshore flow present, discontinuous areas of ice-free to open water areas will also develop along coastal regions affected by the anomalous flow.



FORECAST EXAMPLE 2A



FORECAST EXAMPLE 2B

By February 15 the continuing anomalous trend will cause forecasted ice conditions to differ from the mean conditions depicted in figures 56A and 56B. Ice concentrations in the outer one-third of the pack adjacent to the edge will vary from 1 to 2 oktas south of 54°N to 2 to 4 oktas between 54°N and 61°N with floe size percentages in these areas ranging from less than 10 south of 54°N to 10 to 15 between 54°N and 61°N. In the middle third of the ice pack, concentrations will increase to 3 to 5 oktas south of 55°N and to 5 to 7 oktas between 55°N and 61°N with corresponding increases in floe size coverages to 10 to 15 percent in the southern area and to 20 to 30 percent in the northern area. Over the remaining inner third of the pack ice adjacent to the coast, predominate ice concentrations can be expected to range from 6 to 8 oktas north of 55°N and from 5 to 7 oktas south of 55°N with large-floe percentages of 20 to 40 in both areas.

3. Denmark Strait/Western Greenland Sea

Sea ice along the east coast of Greenland south of $72^{\circ}N$ attains its minimum extent during early fall and, for the most part, lies adjacent to the coastal regions north of $65^{\circ}N$ year-round. Coastal areas south of $65^{\circ}N$ during September and the first half of October are generally ice free; however, by late October ice again forms along the entire east Greenland coast. Maximum conditions usually occur during the first half of March, particularly in the pack north of $65^{\circ}N$. The pack generally remains relatively narrow year-round south of $65^{\circ}N$, usually attaining a maximum mean width of approximately 60 nmi (111 km) during March. Between $65^{\circ}N$ and $72^{\circ}N$ the pack extends much farther seaward at this time with the maximim mean width approaching 310 nmi (574 km).

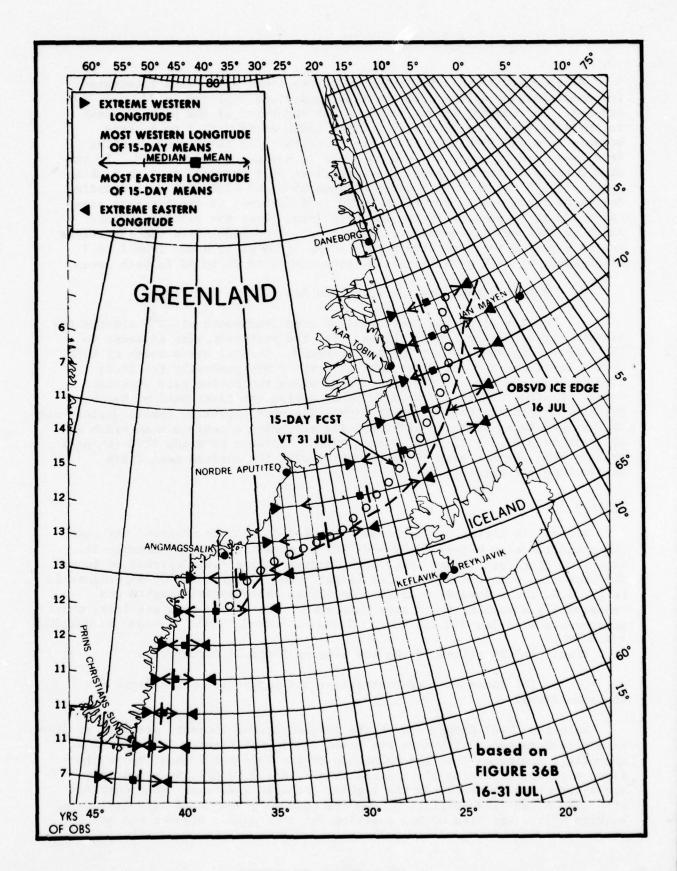
EXAMPLE 3

Given: An aerial reconnaissance mission on 16 July observed the east Greenland ice edge between 64°N and 72°N as shown in forecast example 3A. Floe size distribution and inner pack concentrations (not depicted in fugure 3A) were also observed during this flight. The 30-day mean 700-mb prognostic height D.N. chart issued on 15 July indicated above-normal heights and consequently a warming trend over this area. The 30-day mean sea level chart geostrophic windflow for 15 July indicated a normal, light onshore geostrophic windflow.

Find: (a) Positions of the ice edge on 1 and 15 August, and

(b) Inner pack concentrations and large-floe percentages for the same dates.

Solution: (a) Comparison of the prognosticated isobaric pressure gradient as depicted on the 30-day mean sea level chart with figures A-7 and A-8 of appendix A indicates that the magnitude of the forecasted geostrophic windflow, although remaining light (less than 7 km (13 km/h)), is slightly above-normal as evidenced by the tighter isobaric gradient. When compared with figure 36A, the position of the ice edge observed on 16 July is located seaward of its expected normal position for this date. Figures 66A and 66B



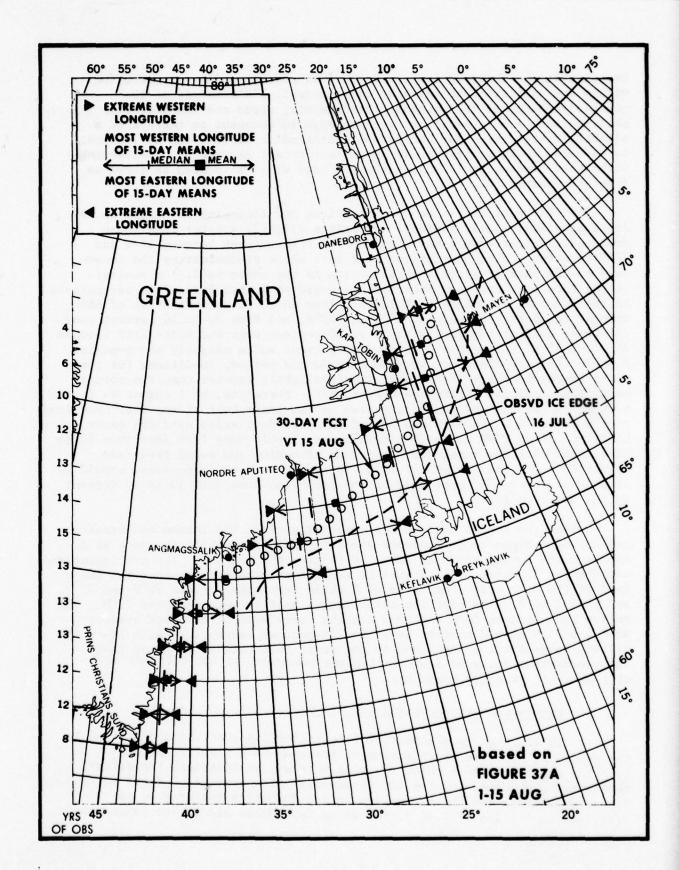
reveal that the observed ice concentrations and large-floe distribution within the pack are both slightly above-normal. As a result of the combined effects of the prognosticated warming trend and the slightly above-normal onshore windflow, the ice edge is forecast to retreat at a slightly faster rate than the normal indicated in table V and by 1 August is expected to be positioned as shown in forecast example 3A. Continuing with these trends, by 15 August the ice edge will be located as shown in forecast example 3B.

(b) Observations of ice concentrations and floe-size coverages on 16 July, as stated above, indicate conditions slightly greater than those depicted in figures 66 A and 66B. Aerial observations between 640N and 72 N reported ice concentrations of 5 to 7 oktas predominating the inner half of the pack and 2 to 4 oktas of ice in the outer half. An analysis of the floe size coverage observations would show that large-floe percentages in the forecast area vary as follows: from 10 to 20 percent south of 660N, from 10 to 30 percent between 66°N and 70°N, and from 30 to 50 percent over the inner half of the pack with 20 to 30 percent over the outer half between 70°N and 72 N. With only a mild warming trend and a slightly above-normal onshore windflow expected over the next 30-day period, conditions for the first 15-day forecast period will remain slightly greater than the normal conditions depicted in figures 67A and 67B. Therefore, by 1 August 4- to 6-oktas concentrations can be expected in the inner half of the east Greenland pack between 640N and 720N and 20 to 3 oktas predominating over the outer half. South of 70°N large-floe percentages should vary from less than 10 to 15 percent with the remainder consisting of medium and small floes and lesser forms of ice. North of 70°N, 30- to 50-percent large floes should be in evidence over the inner half of the pack with less than 10 to 20 percent in the outer half.

During the second half of the forecast period, the forecasted warming trend should begin to predominate and ice conditions within the pack will approach the normal state as shown in figures 68A and 68B. Ice concentrations can then be expected by 15 August to range from 3 to 4 oktas over the inner half of the pack with some areas of 5 oktas remaining between 70 N and 72 N, and from 1 to 2 oktas over the entire outer half between 64 N and 72 N. The entire pack between 64 N and 68 N and the outer half of the pack between 68 N and 72 N should contain less than 10-percent large floes with 10-to 20-percent large floes being found in the inner half between 68 N and 72 N. The predominant forms of ice covering the remainder of the forecast area will be small floe and brash ice.

B. Forecasting Freezeup and Ice Growth

In addition to the task of forecasting ice conditions described in the preceding examples, forecasting of freezeup in a specific arctic location and the rate at which ice will increase in thickness thereafter remain major problems for the ice forecaster. The concept of frost degreeday accumulations and their relation to ice formation and growth, as discussed in section II.D.1, serves as an invaluable aid to ice forecasters.



FORECAST EXAMPLE 3R

Bilello (1960), using observations of ice thickness and air temperature at five Canadian Arctic Archipelago stations derived an empirical method for determining the date of initial ice formation based on an earlier investigation by Rodhe (1952). This method was adapted through automated data processing techniques to near real-time routine operational applications by the U.S. Naval Oceanographic Office through its Numerical Ice Forecasting System (NIFS) as described by Gerson (1975). This numerical forecasting system is capable of producing daily automated outputs of degree-day accumulations and related ice thickness for 62 arctic and subarctic stations based on daily air temperature data received from the National Oceanic and Atmospheric Administration (NOAA) (Gerson and Perchal, 1973). An effective ice-growth forecast can be based on the NIFS output or the ice forecaster's own degreeday accumulation data and the frost degree-day and theoretical ice-growth curves shown in figures 81A through 97B. Figure 80 shows the locations of eastern Arctic stations for which curves are available. As in the preceding forecast examples, the two 30-day NOAA environmental prognostic charts will serve as forecast aids to determine whether conditions will inhibit or accelerate freezeup and ice-growth processes.

The earliest, average, and latest dates of initial ice formation (freezeup and breakup) for 17 eastern Arctic shore stations are presented in table VII to assist the forecaster.

1. Increasing Ice Growth

When forecasting the frost degree-days (FDD) that will accumulate over the next 15- or 30-day period and the corresponding increase in ice thickness over the same timespan at a specific station, these are suggested:

- (a) Determine the current frost degree-day totals for the 1st or 15th of the month for the station in question.
- (b) Using the slope of the normal frost degree-day accumulation curve for that station, project a value for the degree-day accumulations for the next 15- or 30-day period.
- (c) Using the 30-day mean 700-mb prognostic height D.N. chart, make a determination of how much cooling or warming will occur at the appropriate stations. Specific procedures for completing this step are outlined in the following ice-growth forecast examples.

a. Coastal Stations

EXAMPLE 1

Given: Frost degree-day accumulations at two stations (Goose Bay and Hopedale) along the Labrador coastal area totaled 2220 and 1930, respectively, on 31 January.

Table VII. Breakup-Freezeup Dates for Coastal Stations

		Breakupa	a dh	Yrs		Freezeup	qdna	Yrs
Station	Earliest	Average	Latest	Data	Earliest	Average	Latest	Data
Angmagssalik	7-15	8-18	9-12	23	9-30	11-03	11-26	17
Aputiteq	80-8	8-23	9-13	7	10-14	10-27	11-20	2
Cape Dyer	7-15	8–16	10-03	11	10-03	10-27	11-20	12
Cartwright	5-18	6-14	7-03	19	11-12	12-08	12-24	14
Clyde River	8-02	8-29	9-28	18	10-01	10-21	11-11	14
Daneborg	8-22	*	*	7	*	*	*	
Egedesminde	5-18	90-9	6-13	&	11-08	11-26	12-17	۲
Frobisher Bay	90-2	8-07	8-28	20	10-09	10-29	11-25	16
Goose Bay	5-25	6-25	7-23	30	10-20	11-17	12-09	54
Hopedale	6-12	7-08	90-8	17	11-12	11-30	12-20	13
Kap Tobin	8-15	8-23	8-29	∞	9-23	10-09	10-24	2
Resolution Island	6-30	7-22	8-25	20	10-09	11-13	12-03	15
Sondrestrom	5-22	6-07	6-18	24	10-08	11-01	11-07	15
St. Anthony	5-03	6-11	7-13	10	11-30	12-19	1-08	&
Stephenv111e	4-14	4-24	5-11	5	1-28	1-31	2-14	2
Thule	7-08	7-25	8-16	56	9-19	10-10	11-01	21
Upernavík	90-9	6-23	7-10	10	11-05	11-14	11-25	2

 $^{^{}a}\!\text{When ice-free conditions developed and persisted}$ $^{*}\!D_{\lambda}$ bConcentration of 1 okta or more

*Data not available

Find: (a) The number of frost degree-days accumulated at Hopedale and Goose Bay by 15 February and 1 March, and

(b) Corresponding ice thickness values at these stations for the same dates.

Solution: (a) Using the appropriate frost degree-day curves for Goosebay (figure 89A) and Hopedale (figure 90A), plot the current frost degree-day accumulation values. Then, assuming a slope similar to that of the normal frost degree-day curves, project the accumulations on 15 February and 1 March for each station. The 30-day mean 700-mb prognostic height D.N. chart shows a -40 meter value at Goose Bay and a -30 value at Hopedale. Table C-1 in appendix C transforms the meter values on the D.N. chart into frost degree-days for a 30-day period. Therefore, a -40 value at Goose Bay transforms into 61 FDD for the 30-day period and one-half this value, or 30 FDD, for the 15-day period. In the case of Goose Bay, if the projected FDD value for 15 February is 2610 add 30 for a final answer of 2640 FDD. For the 30-day period, the projected value for 1 March would be 3000 under normal conditions. Adding the full value of 61, the final answer for 1 March would be 3061 FDD. The same procedure is followed using the projected and computed D.N. values for Hopedale.

(b) To determine corresponding ice thickness values for the FDD accumulation values computed above, it is preferable to use the maximum FDD and ice thickness curves. In the case of Goose Bay, find the dates on the maximum FDD curve of figure 89A where the FDD values equal 2640 and 3061. Ice thickness values on 15 February and 1 March can then be determined by matching the dates determined above with thickness values on the Goose Bay maximum ice thickness curve. For this example, the correct ice thickness values for Goose Bay are 33.5 and 37.5 in (85.1 and 95.3 cm), respectively, for the 15- and 30-day periods.

EXAMPLE 2

Given: On 15 March the frost degree-day accumulations at Clyde River and Upernavik were 5805 and 3550, respectively. The 30-day mean 700-mb prognostic height D.N. chart for 15 March showed a warming trend over southern Baffin Bay north of $70^{\circ}N$.

Find: (a) The number of frost degree days accumulated by 1 and 15 April at the two stations, and

^{*}Values in table C-1 reflect 30 percent of the derived values since forecast experience has shown this yields the best results (Potocsky, 1975).

(b) Corresponding ice thickness values at these stations for the same dates.

Solution: (a) As in the preceding example, plot the 15 March FDD values for Clyde River and Upernavik on the FDD curves (figures 85A and 97A) and project the FDD accumulation at the stations on 1 and 15 April by assuming a slope similar to that of each station's normal FDD curve. For Clyde River, the projected values would equate to 6600 and 7150. A check of the 30-day mean 700-mb prognostic height D.N. chart showed a +15-meter value at Clyde River and +20 meters at Upernavik. Utilizing table C-1 a +15-meter value transforms into 24 FDD for the 30-day period or 12 FDD for the 15-day period. Since the area will be under the influence of a forecasted warming trend, the FDD accumulation for 1 April would be computed by subtracting 12 from 6600 for a value of 6588. For 15 April the forecasted FDD accumulation at Clyde River would be 7150 minus 24, or 7126. Corresponding values can be computed for Upernavik by following the same procedure.

(b) To determine the corresponding ice thickness values for the FDD accumulation values computed in (a) find the points on each station's maximum FDD curves (figures 85B and 97B) where the FDD accumulations equal those computed. The ice thickness values for 1 and 15 April at Clyde River and Upernavik will be qual to those values located on each station's maximum ice thickness curves at the dates computed above.

b. Offshore Ice Pack

Since reports of environmental parameters are usually not available for the offshore arctic ice pack and observations of ice thickness are randomly scattered in both time and space, the forecasting of ice growth in these areas requires a different approach from that outlined in the preceding section.

EXAMPLE 1

Given: On 1 November a Canadian icebreaker measured the thickness of ice just inside the pack ice edge near $67^{\circ}N$, $60^{\circ}W$ to be 12 inches (30.5 cm). The 30-day mean 700-mb prognostic height D.N. chart for 30 October indicates an intense cooling trend during the last week of October is forecasted to continue through November. In addition a -45-meter value is shown at $67^{\circ}N$, $60^{\circ}W$.

Find: How much additional ice growth will accumulate at this offshore location by 15 November and 30 November.

Solution: Owing to the absence of observations over the offshore location, the FDD accumulation rate must be estimated by utilizing data from the nearest shore station. In this instance, the station nearest 67°N, 60°W is Cape Dyer on Baffin Island. Examination of data from Cape Dyer showed that this station had accumulated 598 FDD by 1 November. With this value as a starting point, FDD values are then calculated for 15 and 30 November at Cape Dyer using procedures outlined previously and equal 950 and 1390 frost degree-days, respectively. For offshore locations it is assumed that frost degree-days are accumulated at rates similar to those at nearby shore stations with an

adjustment made for changes indicated by the 30-day mean 700-mb prognostic height D.N. chart. From table C-1 the 45-meter value indicated by this chart at 67°N, 60°W transforms to 69 FDD for the entire 30-day period or 35 FDD for the 15-day period. Taking into account these effects for the cooling trend, FDD accumulations at the offshore site are 985 for 15 November and 1459 for 30 November. After locating the one-foot (30.5 cm) curve on figure 98, since Io = 1 foot in this instance because of the 598 FDD accumulated, trace the curve to a point where the FDD value equals 387 (985 minus 598). At this point the ice thickness increment is equivalent to 5.2 in (13.2 cm), thereby giving an answer of 17.2 in (43.7 cm) for 15 November. At this point Io = 17.2 in (43.7 cm) for the next forecast period and a new curve equal to this value is drawn by interpolating between the Io = 1 foot (30.5 cm) and the Io = 2 foot (61 cm) curves. The point on this newly drawn curve where FDD equals 474 (1459 minus 985) reveals an ice thickness increment of approximately 5.4 in (13.7 cm). The ice thickness, therefore, would have increased to 22.6 in (57.4 cm) by 30 November.

C. Forecasting Breakup and Decreasing Ice Thickness

Forecasting breakup of the ice cover and the rates at which ice thickness decreases at various locations throughout the eastern Arctic after maximum ice growth has been attained presents a unique problem to the ice forecaster. In many respects, the breakup and ice disintegration forecast is one of the more complex tasks facing the forecaster since many environmental parameters besides air temperature act simultaneously upon ice to aid in its decay. Additional factors include water temperature, winds, currents, and oceanic tides (Potocsky and Mitchell, 1972).

The ice disintegration curves extrapolated on the ice-growth curves in figures 81B through 97B were estimated for each station primarily from satellite data supplemented by observed historical ice data. No effort was made to isolate individual environmental factors affecting disintegration, and the curves were drawn with the assumption that all factors were acting upon the ice at any given time. These curves can be used to project a gross rate of decreasing ice thickness at various coastal stations. Table VII indicates the progress of breakup at various eastern Arctic shore stations by listing time periods over which breakup has occurred. The forecaster, however, must be certain to take into account all additional updated ice information received from the field and modify the disintegration rates at a specific locality as necessary. Such additional information may include reconnaissance observations of variable concentrations and the percent of puddling or thaw holes in an icefield. Experience has shown that relatively thick ice of up to 24 in (61 cm) or more in thickness can undergo rapid disintegration if it has become "honeycombed" with numerous thaw holes or covered with puddles. This decay is further accelerated if strong winds facilitate breakup of individual ice floes.

EXAMPLE 1

Given: On 13 June, examination of FDD accumulation records showed that a maximum accumulation of 6843 FDD, corresponding to an ice thickness of approximately 60 in (152.4 cm), occurred on 3 June at Cape Dyer. The latest aerial reconnaissance of the area reported pack ice consisting of 7 to 8 oktas predominately thick, first-year ice with no puddling. Air temperatures at the station exceeded 32°F (0°C) on 4 June and have remained above freezing for the past 10 days. The 30-day mean 700-mb prognostic height D.N. chart issued on 13 June indicated that normal conditions would prevail over the Cape Dyer area for the next 30 days.

Find: Ice thickness at Cape Dyer on 1 and 15 July.

Solution: On figure 83B, plot the maximum ice thickness value of 60 in (152.4 cm) for 3 June and compare it with normal and minimum ice-growth curves. Since conditions for the next 30 days are forecasted to be normal, project from the plotted value a disintegration curve parallel to the normal and minimum disintegration curves in figure 83B. Forecasted ice thickness values can now be read directly from this projected curve. The values for 1 and 15 July, therefore, would be 48 and 37 in (121.9 and 94.0 cm), respectively.

EXAMPLE 2

Given: FDD accumulation at Resolution Island reached 6605 on 20 June, corresponding to an ice thickness value of approximately 58 in (147.3 cm). During the next 10 days the air temperature oscillated above and below 32°F (0°C). Aerial reconnaissance on 28 June reported 6 to 7 oktas of predominately thick, first-year ice with many puddles and a few thaw holes. The 30-day mean 700-mb prognostic height D.N. chart issued on 28 June indicated a slight warming trend over the area.

Find: Ice thickness at Resolution Island on 15 and 30 July.

Solution: Using an approach similar to that described in the preceding example, plot the maximum ice thickness value of 58 in (147.3 cm) on figure 92B and compare it with normal ice growth. The plotted thickness falls between the normal and maximum ice-growth curves. Since air temperatures have been observed oscillating above and below 32°F (0°C), project the plotted value along a line parallel to the nearest ice-growth curve until 30 June is reached. From this point a new disintegration curve should be drawn Owing to the forecasted warming trend and deteriorating condition of the ice the newly projected curve should not be drawn exactly parallel to the normal and maximum disintegration curves, but with a steeper slope. Ice thickness at Resolution Island for 15 and 30 July taken from this projected curve should approximate 46 and 30 in (116.8 and 76.2 cm), respectively.

EXAMPLE 3

Satellite imagery on 14 May showed that ice concentrations in the approaches to Thule varied from 7 to 8 oktas. Ice thickness calculation based on the total number of FDD accumulated at Thule by 15 May shows a growth of 64 in (162.6 cm). The 30-day mean 700-mb prognostic height D.N.

chart for 13 April indicated a cooling trend over the area with a -10 meter value at Thule and a -12.5 meter value offshore near 76°30'N, 72°W. Mean daily temperatures at Thule for the week preceding 15 May have been ranging between 6° and 8°F (3.3° and 4.4°C) below freezing. Ice growth at an offshore location near 76°30'N, 72°W was calculated during the previous forecast period to be 56 in (142.2 cm) by 15 May.

- Find: (a) Ice thickness at Thule on 1 and 15 June.
 - (b) Ice thickness offshore at 76°30'N, 72°W on 15 June.

Solution: (a) Plot the 15 May ice thickness value on the curves in figure 96B and compare with normal conditions. Since a cooling trend is forecast and temperatures at Thule have not as yet risen above 32°F (0°C), maximum ice thickness of 65 in (165.1 cm) is forecast for 5 June by assuming normal ice growth along a line starting from the 64 in (162.6 cm) value on 15 May and extending parallel to the normal ice growth curve. Ice thickness is 65 in (165.1 cm) along this line for 1 June. Using the value of 65 in (165.1 cm) on 5 June as the starting point, a projected disintegration curve is drawn subjectively allowing for the forecasted cooling trend by slightly flattening the slope of the projected curve. From this curve, ice thickness at Thule for 15 June is approximately 60.5 in (153.7 cm).

(b) As in the forecast examples for offshore pack ice, ice thickness at an offshore area is assumed to increase or decrease at rates similar to those at nearby coastal stations with modifications made for differing predicted amounts of warming or cooling over the offshore locations as shown by the height D.N. chart. Since the cooling trend over the offshore site in this instance is predicted to be greater than that at the shore station, the forecaster must consider this fact when projecting a new disintegration curve for the offshore ice. By 5 June the offshore ice would have grown another inch (2.54 cm) in thickness as had the ice at Thule. Therefore, using 57 in (144.8 cm) and 5 June as a starting point, project a disintegration curve on figure 96B with a slightly flatter slope than that of the normal disintegration curve to allow for the cooling trend. The ice thickness on 15 June at 76°30'N, 72°W approximates 52 in (132.1 cm).

BIBLIOGRAPHY

- Atkinson, H.T., Scientists study polar gyrations: may predict safe paths through ice, Ocean Industry, vol. 11 (9), 225-234, 1976.
- Bilello, M.A., Formation, growth, and decay of sea ice in the Canadian Arctic Archipelago, <u>Research Report 65</u>, 35 pp, U.S. Army Corps of Engineers, Snow, Ice, and Permafrost Research Establishment, 1960.
- Gerson, D.J., A numerical ice forecasting system, Reference Pub. RP-8, 138 pp, Nav. Oceanogr. Office, Washington, D.C., 1975.
- Gerson, D.J., and R.J. Perchal, Sea ice growth in potential arctic minefield areas, <u>Tech. Note 7700-11-73</u>, 16 pp, Nav. Uceanogr. Office, Washington, D.C., 1973.
- Klein, W.H., Principal tracks and mean frequencies of cyclones and anticyclones in the northern hemisphere, <u>Research Paper No. 40</u>, 60 pp, U.S. Weather Bureau, Washington, D.C., 1957.
- Kniskern, F.E., Report of the arctic ice observing and forecasting program 1966, Special Pub. SP-70 (66), 91 pp, Nav. Oceanogr. Office, Washington, D.C., 1968.
- Kniskern, F.E., Report of the arctic ice observing and forecasting program 1969, Special Pub. SP-70 (69), 173 pp, Nav. Oceanogr. Office, Washington, D.C., 1970.
- Maykut, G.A., A.D. Thorndike, and N. Untersteiner, AIDJEX scientific plan, AIDJEX Bull. No. 15, 1-62, Univ. of Washington, Seattle, 1972.
- Mitchell, P.A., Report of the arctic ice observing and forecasting program 1971, Special Pub. SP-70 (71), 216 pp, Nav. Oceanogr. Office, Washington, D.C., 1974.
- Perchal, R.J., Report of the arctic ice observing and forecasting program 1968. Special Pub. SP-70 (68), 104 pp, Nav. Oceanogr. Office, Washington, D.C., 1969.
- Potocsky, G.J., Alaskan area 15-and 30-day ice forecasting guide, Special Pub. SP-263, 190 pp, Nav. Oceanogr. Office, Washington, D.C., 1975.
- Potocsky, G.J., Report of the arctic ice observing and forecasting program 1967, Special Pub. SP 70 (67), 79 pp, Nav. Oceanogr. Office, Washington, D.C., 1972.
- Potocsky, G.J., Report of the arctic ice observing and forecasting program 1970, Special Pub. SP-70 (70), 249 pp, Nav. Oceanogr. Office, Washington, D.C., 1972.

- Potocsky, G.J., and P.A. Mitchell, Frost degree-day and related theoretical ice thickness curves for selected Russian Arctic stations, <u>Tech. Note 7700-8-72</u>, 35 pp, Nav. Oceanogr. Office, Washington, D.C., 1972.
- Rodhe, B., On the relation between air temperature and ice in the Baltic, Geografiskei Annaler, 39, 175-202, 1952.
- Untersteiner, N. and K.L. Hunkins, Arctic ice deformation joint experiment, Final Report ONR Contract NOO014-67-A-0103-0004, 39 pp, University of Washington, Seattle, 1969.
- U.S. Naval Oceanographic Office, Report of the arctic ice observing and forecasting program 1960, Special Pub. SP-70 (60), 208 pp, Washington, D.C., 1962.
- U.S. Naval Oceanographic Office, Report of the arctic ice observing and forecasting program 1961, Special Pub. SP-70 (61), 174 pp, Washington, D.C., 1965.
- U.S. Naval Oceanographic Office, Report of the arctic ice observing and forecasting program 1962, Special Pub. SP-70 (62), 172 pp, Washington, D.C., 1965.
- U.S. Naval Oceanographic Office, Report of the arctic ice observing and forecasting program 1963, Special Pub. SP-70 (63), 188 pp, Washington, D.C., 1965.
- U.S. Naval Oceanographic Office, Report of the arctic ice observing and forecasting program 1964, Special Pub. SP-70 (64), 188 pp, Washington, D.C., 1965.
- U.S. Naval Oceanographic Office, Report of the arctic ice observing and forecasting program 1965, Special Pub. SP-70 (65), 166 pp, Washington, D.C., 1967.
- U.S. Naval Oceanographic Office, Sailing directions for Labrador and Hudson Bay, H.O. Pub. 15, 312 pp, Washington, D.C., 1965.
- U.S. Naval Oceanographic Office, Sailing directions for west coast of Greenland, H.O. Pub. 16, 429 pp, Washington, D.C., 1968.
- U.S. Navy, Chief of Naval Operations, Marine climatic atlas of the world, Vol. I, North Atlantic Ocean, NAVAIR 50-1C-528, Washington, D.C., 1974.
- U.S. Navy, Chief of Naval Operations, Marine climatic atlas of the world, Vol. VI, Arctic Ocean, NAVWEPS 50-1C-533, Washington, D.C., 1974.
- U.S. Navy, Chief of Naval Operations, Marine climatic atlas of the world, Vol. VI, Arctic Ocean, NAVWEPS 50-1C-533, Washington, D.C., 1963.
- U.S. Navy Hydrographic Office, Oceanographic atlas of the polar seas, Part II, Arctic. H.O. Pub. 705, 149 pp, Washington, D.C., 1958.

- U.S. Navy Hydrographic Office, Report of the ice observing and forecasting program 1954, Tech. Report TR-49, 164 pp, Washington, D.C., 1955.
- U.S. Navy Hydrographic Office, Report or the ice observing and forecasting program 1955, <u>Tech. Report TR-50</u>, 155 pp, Washington, D.C., 1956.
- U.S. Navy Hydrographic Office, Report of the ice observing and forecasting program 1956, Tech. Report TR-51, 163 pp, Washington, D.C., 1957.
- U.S. Navy Hydrographic Office, Report of the ice observing and forecasting program 1957, <u>Tech. Report TR-52</u>, 147 pp, Washington, D.C., 1958.
- U.S. Navy Hydrographic Office, Report of the ice observing and forecasting program 1958, <u>Tech. Report TR-66</u>, 148 pp, Washington, D.C., 1959.
- U.S. Navy Hydrographic Office, Report of the ice observing and forecasting program 1959, Tech. Report TR-69, 121 pp, Washington, D.C., 1961.
- U.S. Navy Hydrographic Office, Sailing directions for east Greenland and Iceland, H.O. Pub. 17, 432 pp, Washington, D.C., 1951.
- U.S. Weather Bureau, Normal weather charts for the northern hemisphere, <u>Tech. Paper No. 21</u>, 74 pp, Washington, D.C., 1952.
- Zubov, N.N., On the maximum thickness of sea ice of many years' growth, Meteorologiia i Gidrologiia 4, 123-131, 1938.

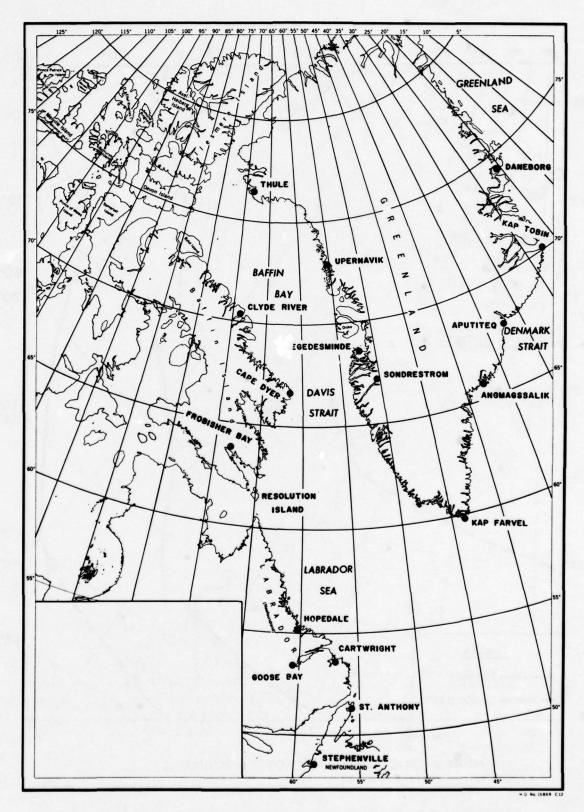


FIGURE 1 PLACE NAME CHART EASTERN NORTH AMERICAN ARCTIC

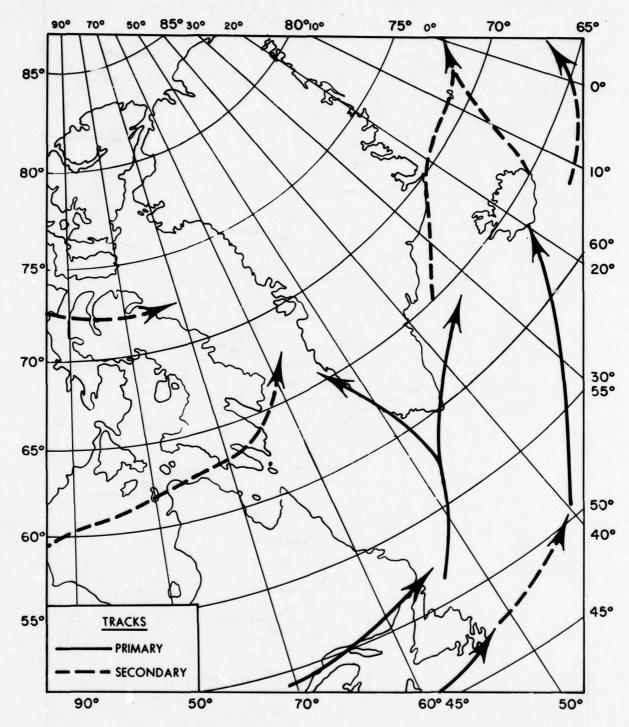


FIGURE 2 PRINCIPAL TRACKS OF LOWS - JANUARY

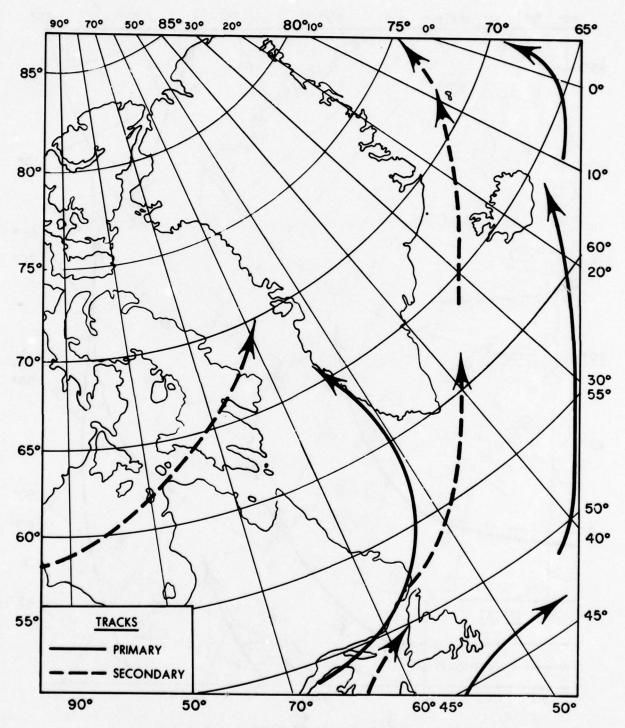


FIGURE 3 PRINCIPAL TRACKS OF LOWS - APRIL

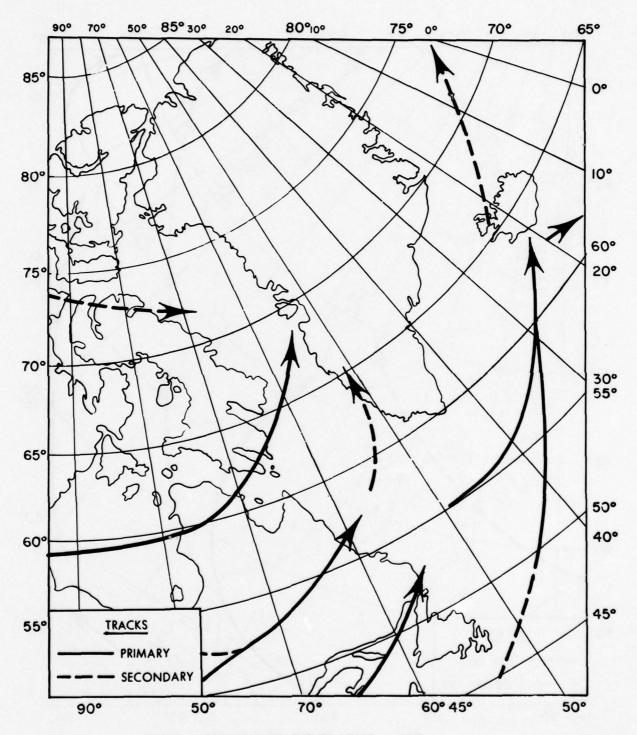


FIGURE 4 PRINCIPAL TRACKS OF LOWS - JULY

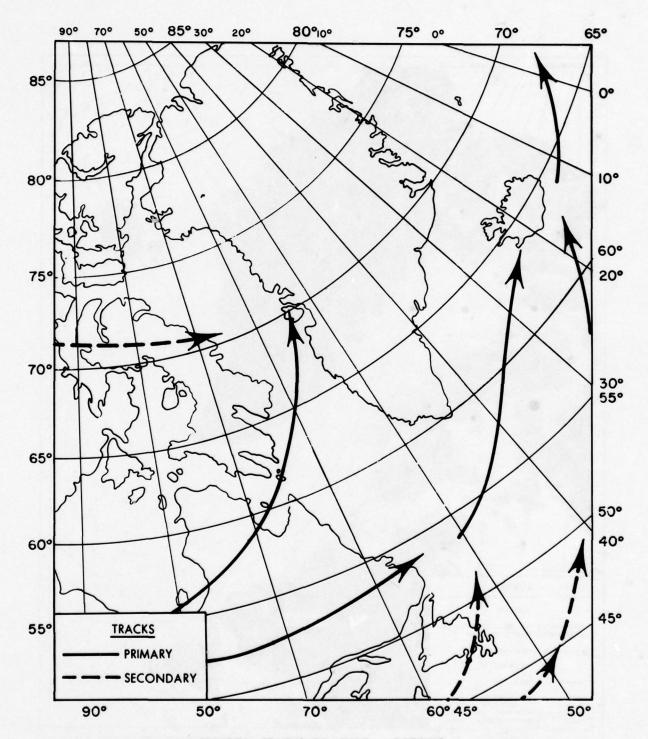


FIGURE 5 PRINCIPAL TRACKS OF LOWS - OCTOBER

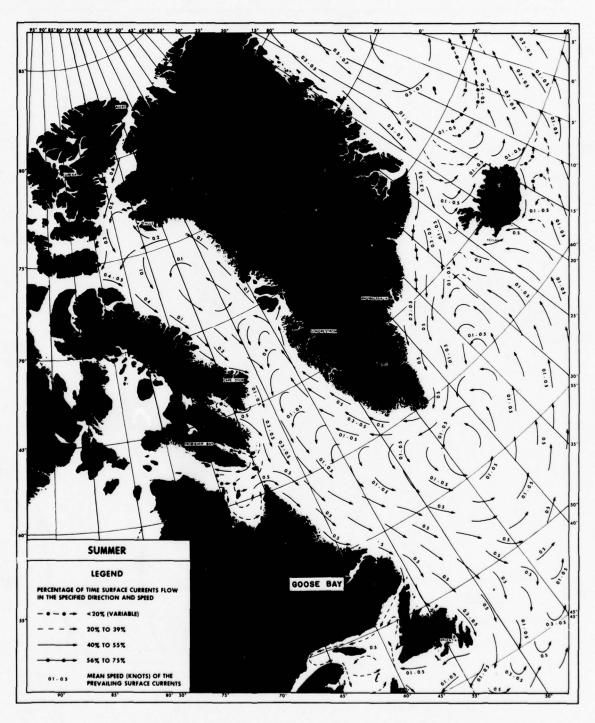


FIGURE 6 EASTERN ARCTIC SURFACE CURRENTS (KNOTS)—SUMMER

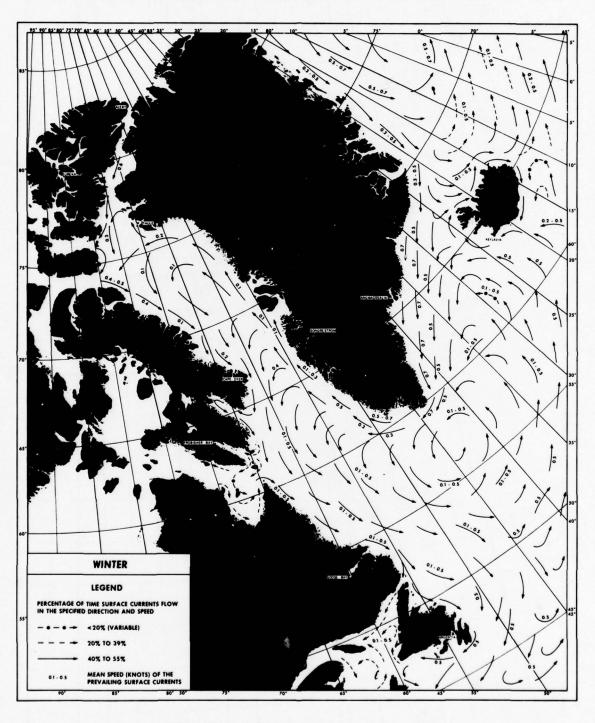


FIGURE 7 EASTERN ARCTIC SURFACE CURRENTS (KNOTS)—WINTER

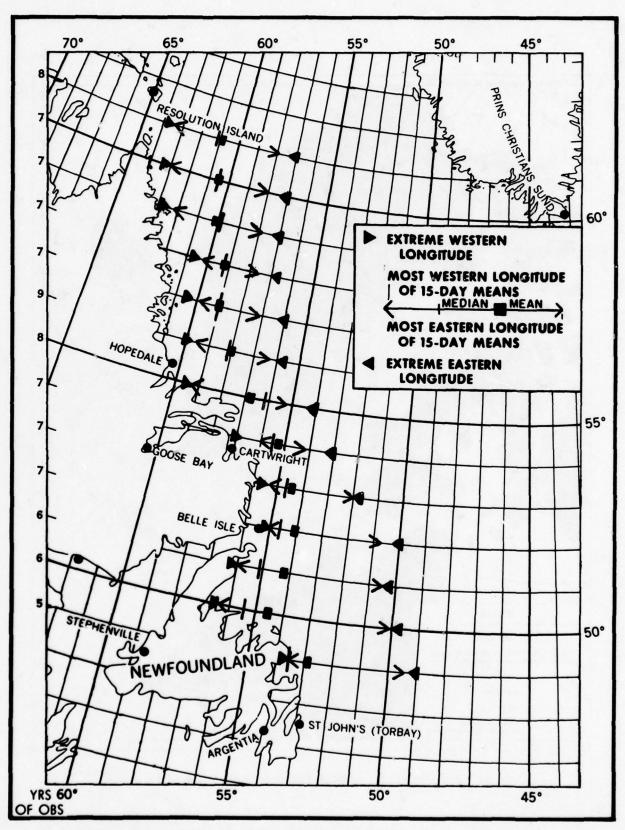


FIGURE 8A MEAN, MEDIAN AND EXTREME POSITIONS OF PACK EDGE 1-15 JANUARY

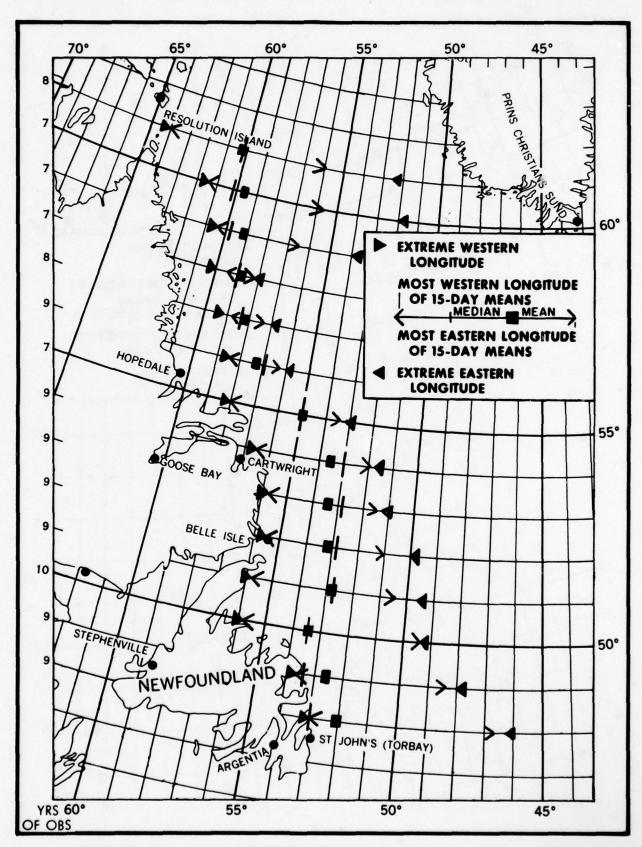


FIGURE 8B MEAN, MEDIAN AND EXTREME POSITIONS OF PACK EDGE 16-31 JANUARY

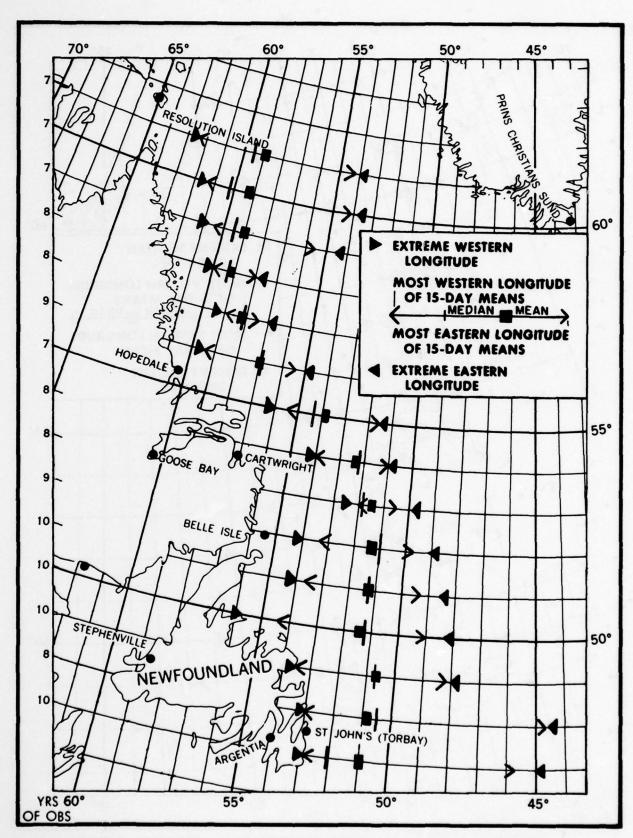


FIGURE 9A MEAN, MEDIAN AND EXTREME POSITIONS OF PACK EDGE 1-15 FEBRUARY

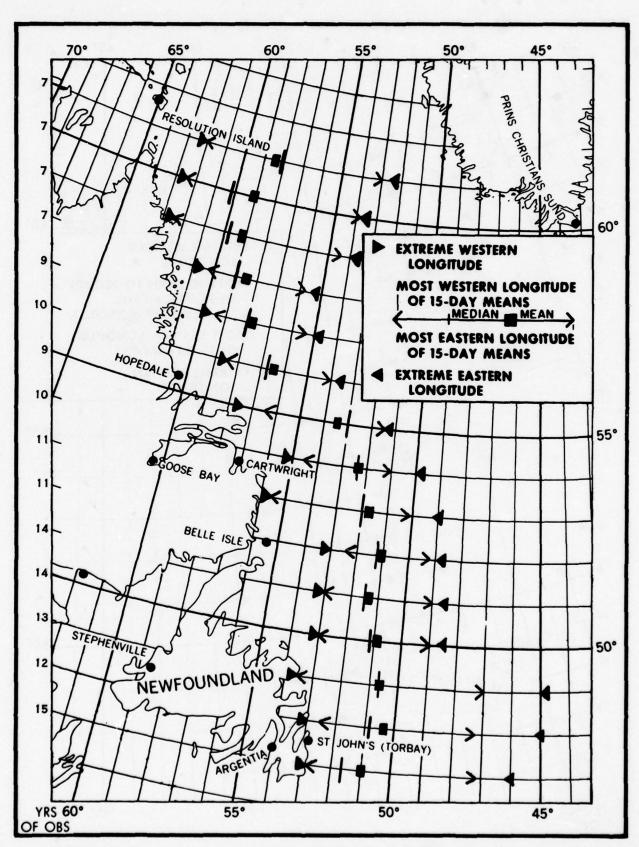


FIGURE 9B MEAN, MEDIAN AND EXTREME POSITIONS OF PACK EDGE 16-28 FEBRUARY

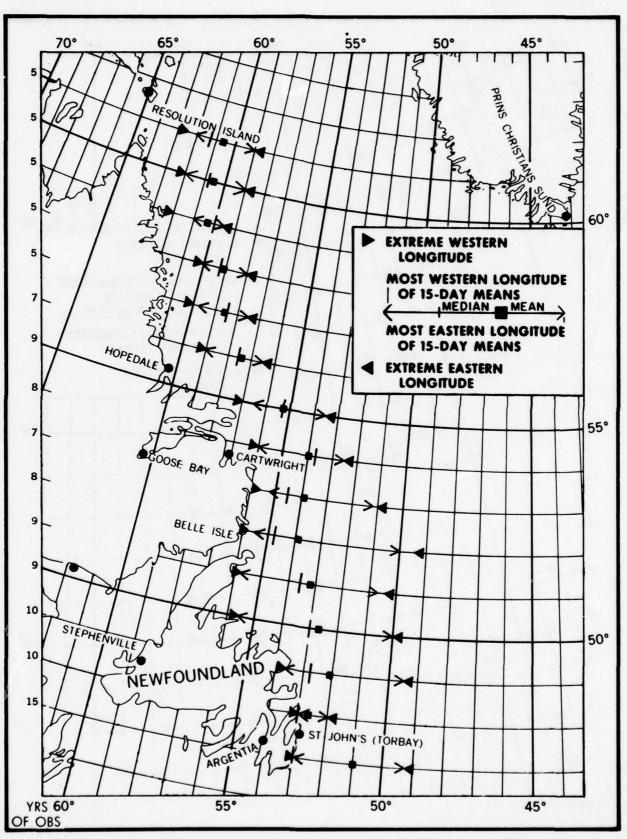


FIGURE 10A MEAN, MEDIAN AND EXTREME POSITIONS OF PACK EDGE 1-15 MARCH

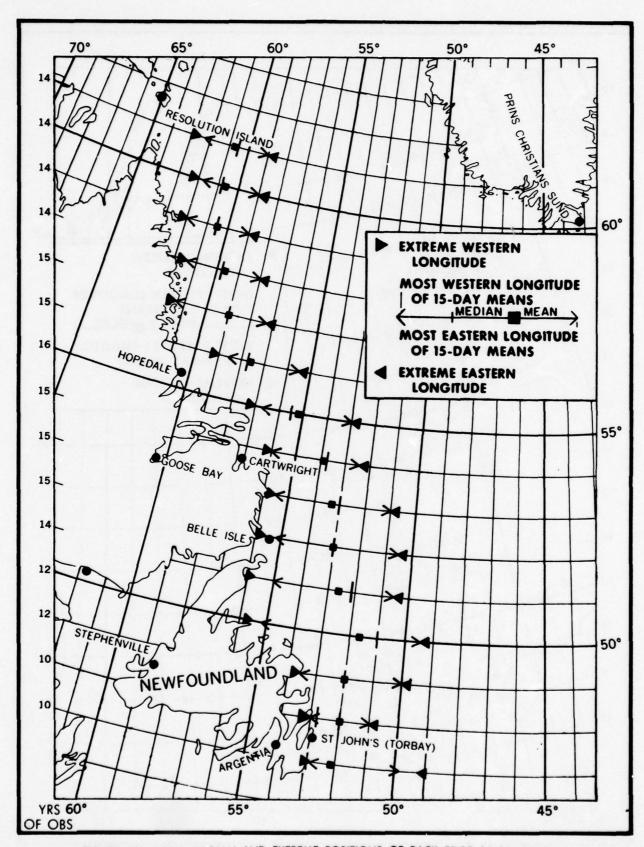


FIGURE 10B MEAN, MEDIAN AND EXTREME POSITIONS OF PACK EDGE 16-31 MARCH

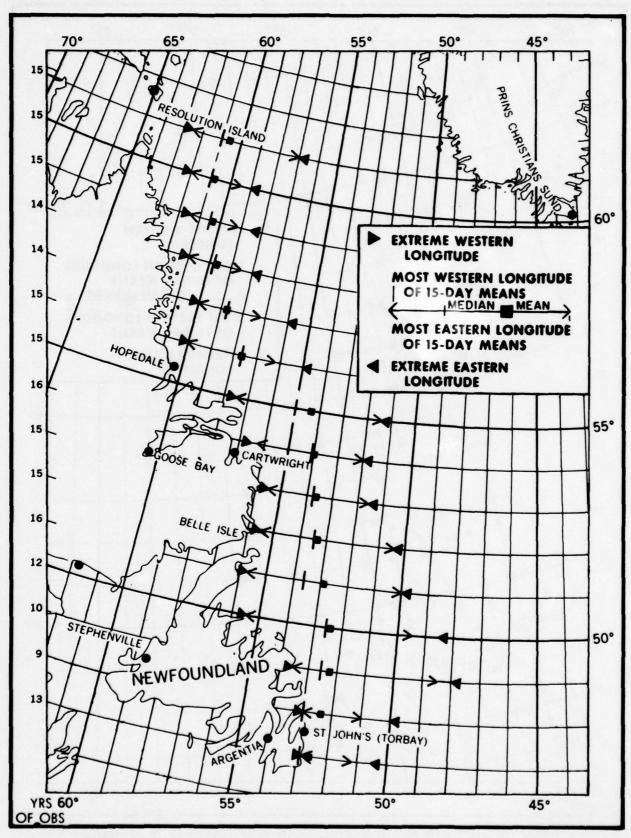


FIGURE 11A MEAN, MEDIAN AND EXTREME POSITIONS OF PACK EDGE 1-15 APRIL

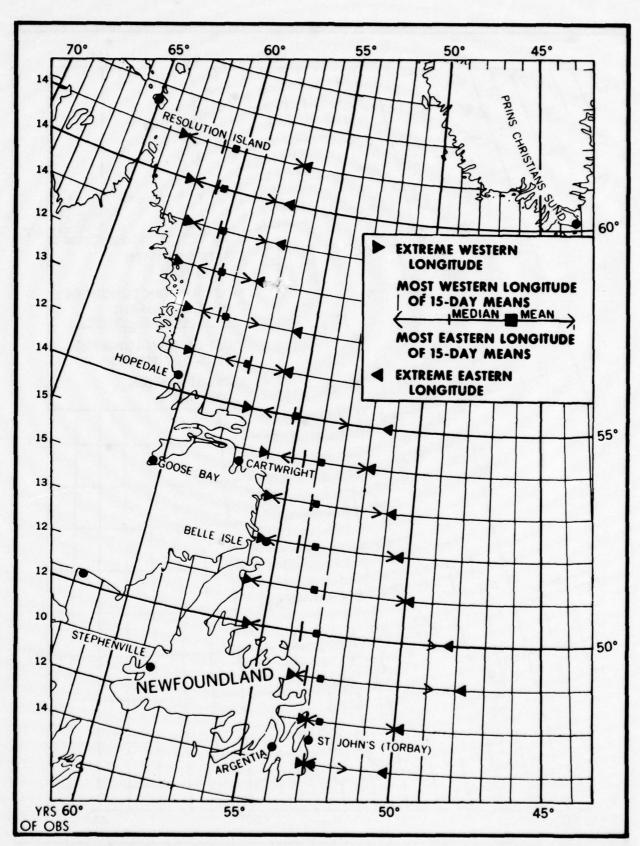


FIGURE 11B MEAN, MEDIAN AND EXTREME POSITIONS OF PACK EDGE 16-30 APRIL

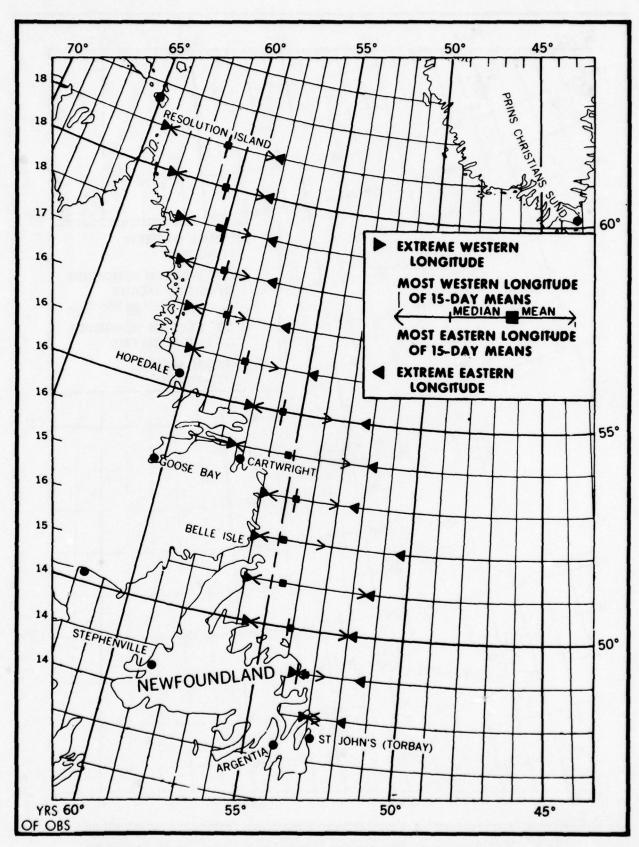


FIGURE 12A MEAN, MEDIAN AND EXTREME POSITIONS OF PACK EDGE 1-15 MAY

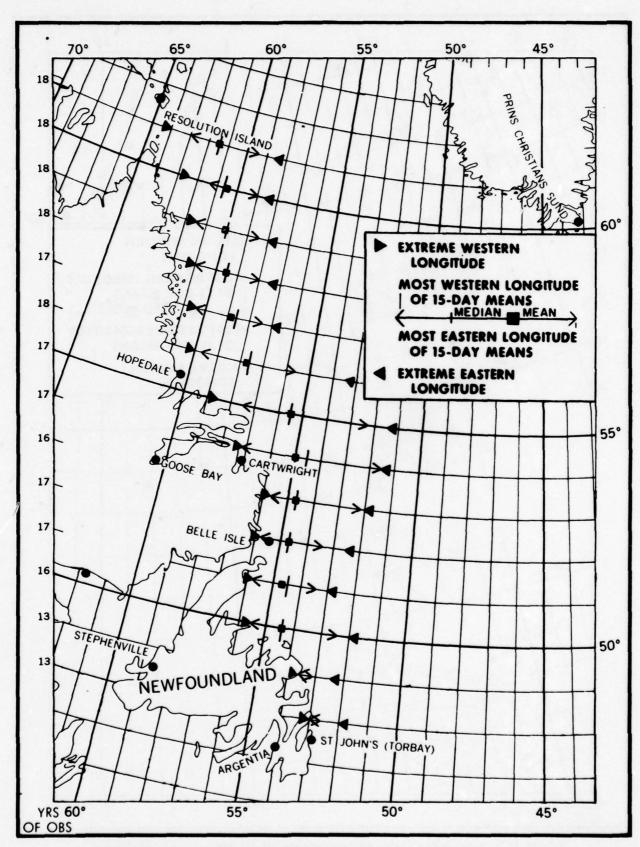


FIGURE 12B MEAN, MEDIAN AND EXTREME POSITIONS OF PACK EDGE 16-31 MAY

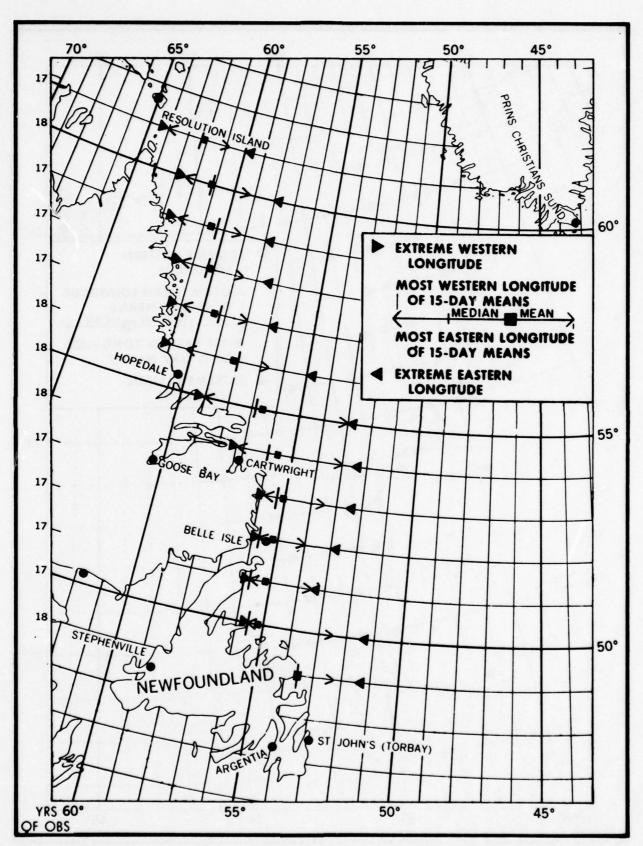


FIGURE 13A MEAN, MEDIAN AND EXTREME POSITIONS OF PACK EDGE 1-15 JUNE

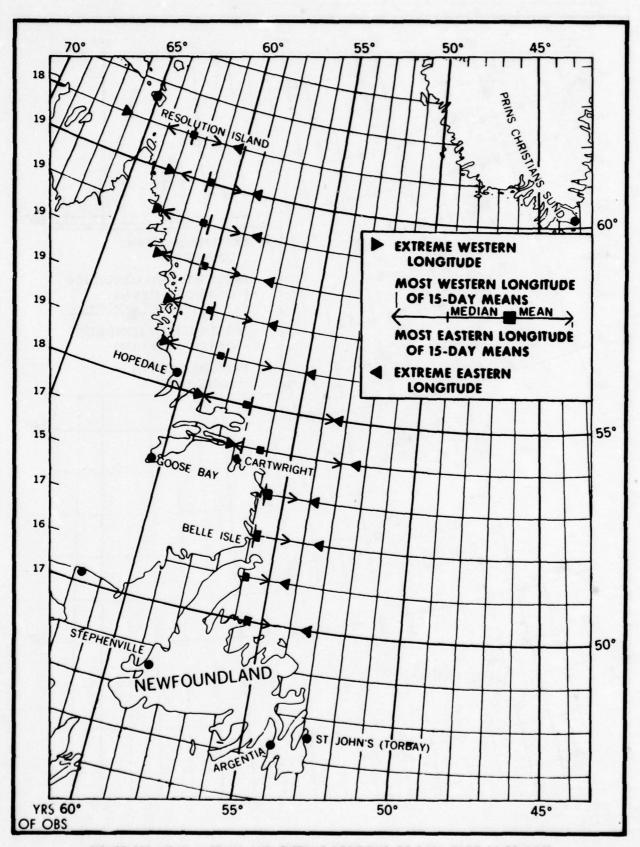


FIGURE 13B MEAN, MEDIAN AND EXTREME POSITIONS OF PACK EDGE 16-30 JUNE

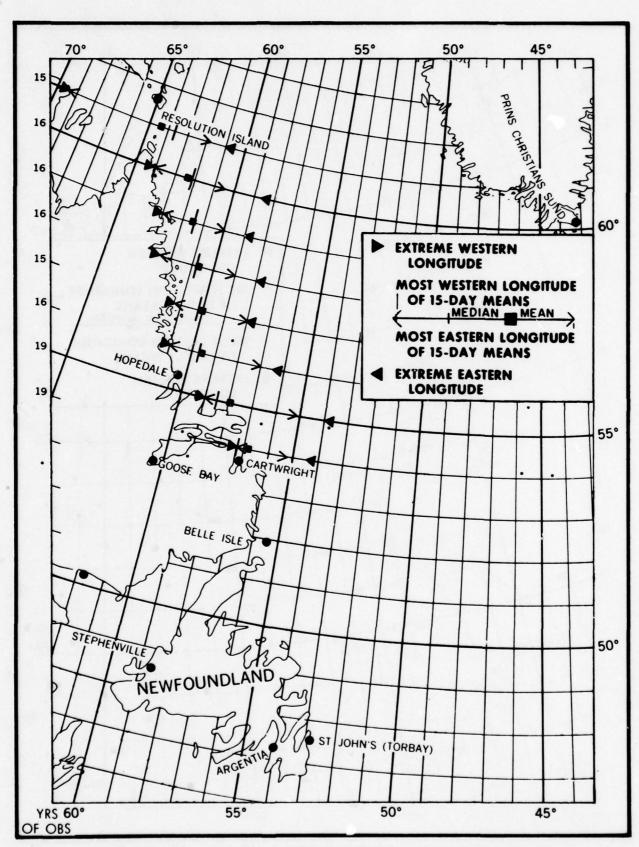


FIGURE 14A MEAN, MEDIAN AND EXTREME POSITIONS OF PACK EDGE 1-15 JULY

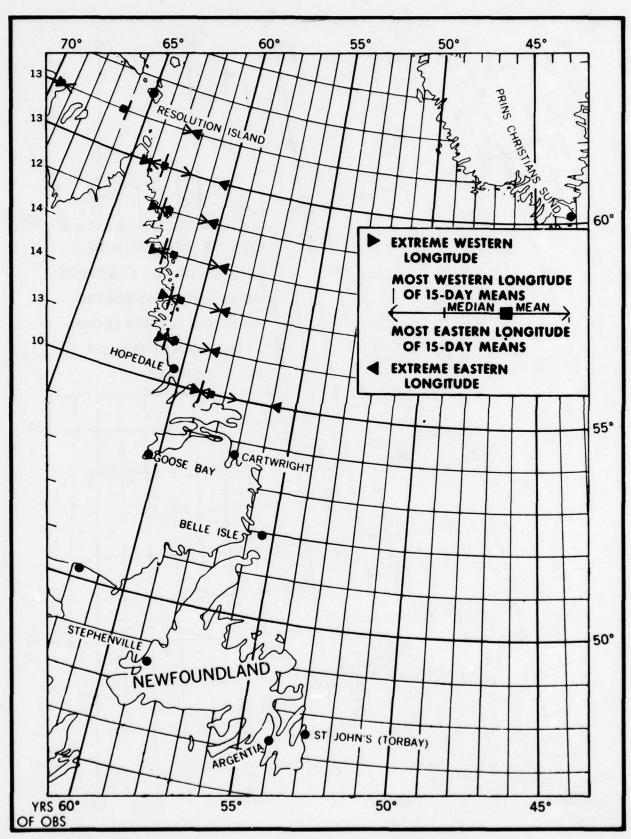


FIGURE 14B MEAN, MEDIAN AND EXTREME POSITIONS OF PACK EDGE 16-31 JULY

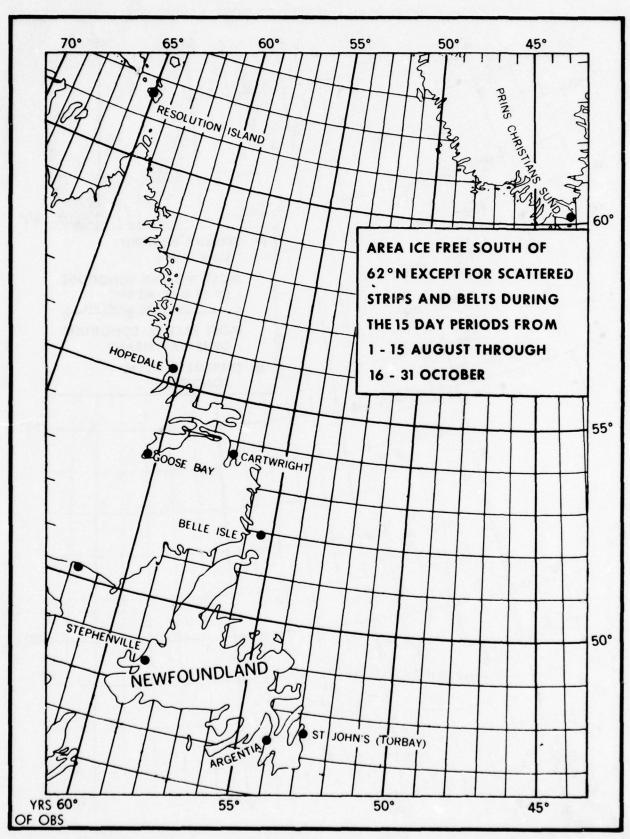


FIGURE 15A MEAN, MEDIAN AND EXTREME POSITIONS OF PACK EDGE 1-15 AUGUST

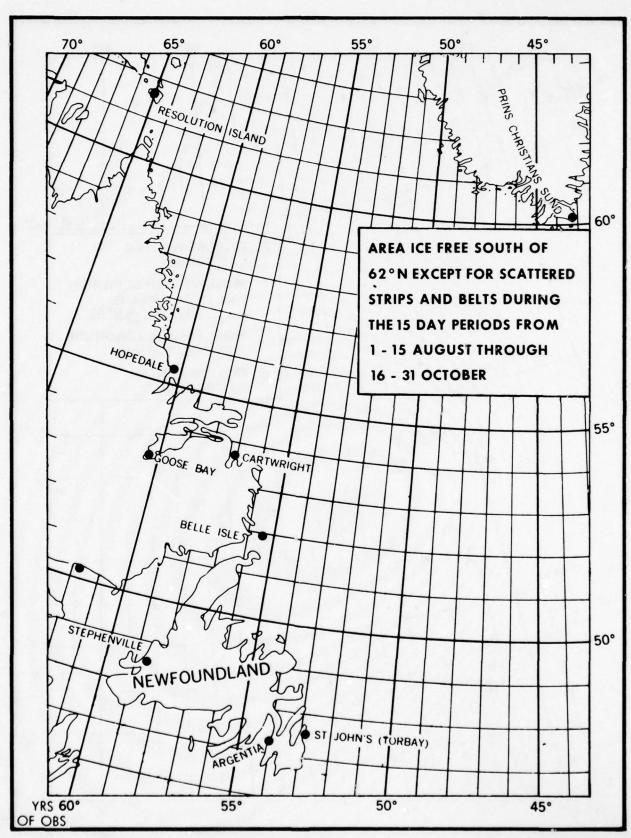


FIGURE 15B MEAN, MEDIAN AND EXTREME POSITIONS OF PACK EDGE 16 AUGUST-31 OCTOBER

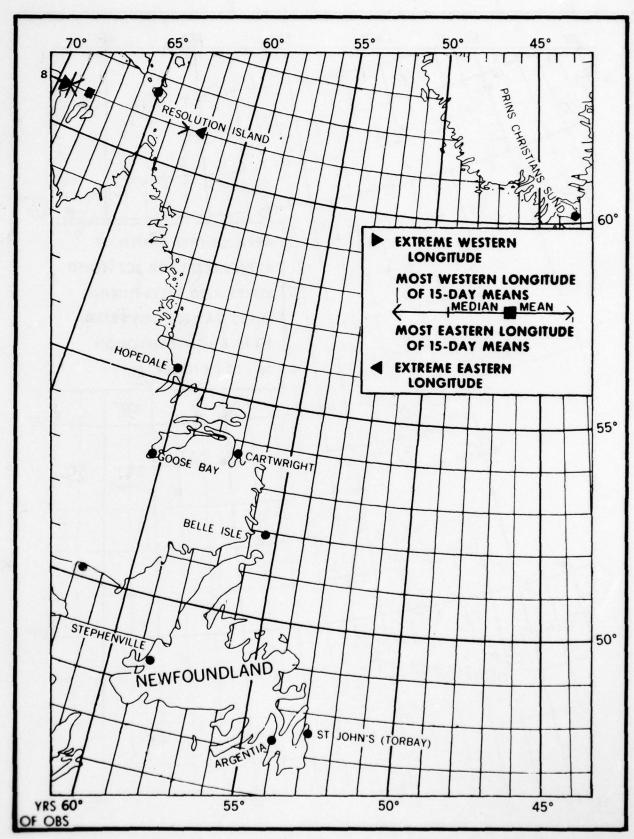


FIGURE 16A MEAN, MEDIAN AND EXTREME POSITIONS OF PACK EDGE 1-15 NOVEMBER

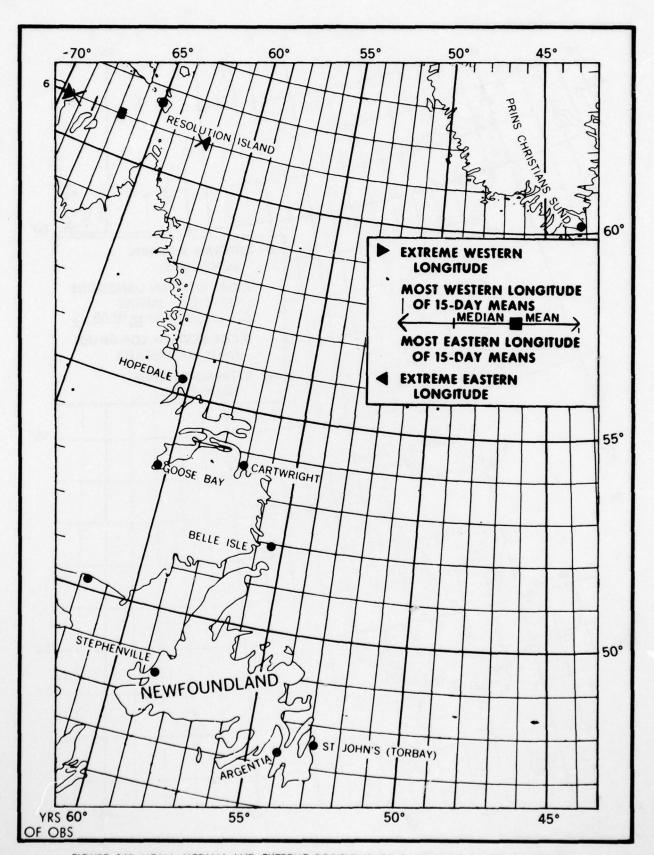


FIGURE 16B MEAN, MEDIAN AND EXTREME POSITIONS OF PACK EDGE 16-30 NOVEMBER

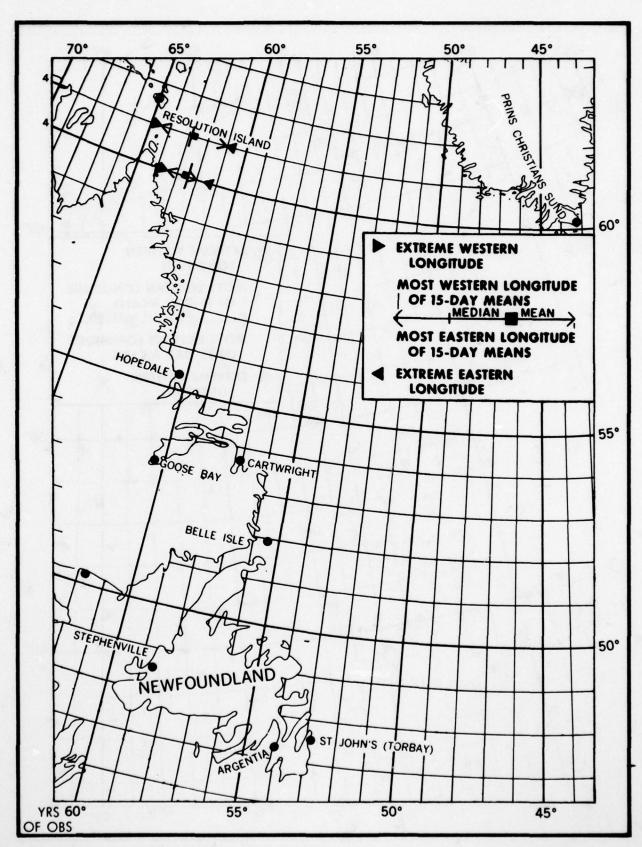


FIGURE 17A MEAN, MEDIAN AND EXTREME POSITIONS OF PACK EDGE 1-15 DECEMBER

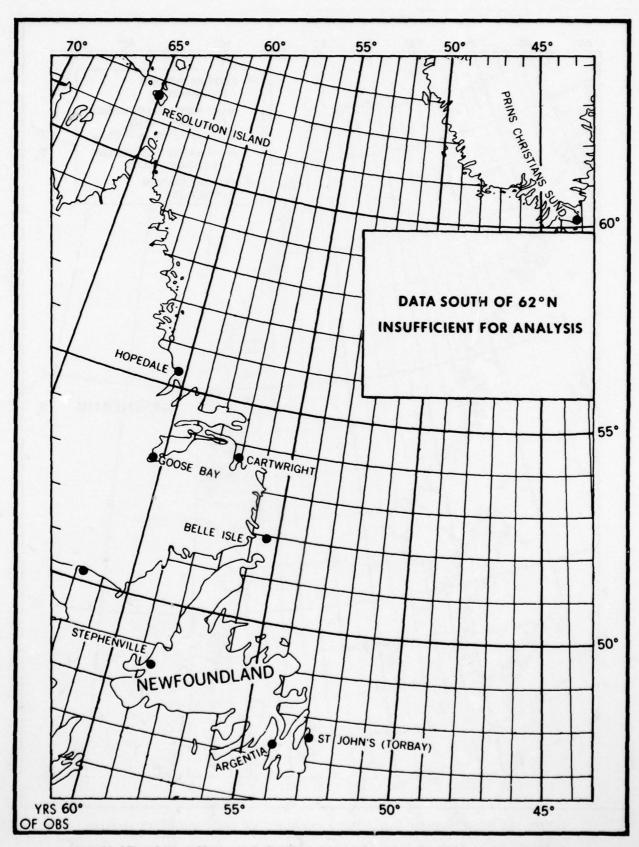


FIGURE 178 MEAN, MEDIAN AND EXTREME POSITIONS OF PACK EDGE 16-31 DECEMBER

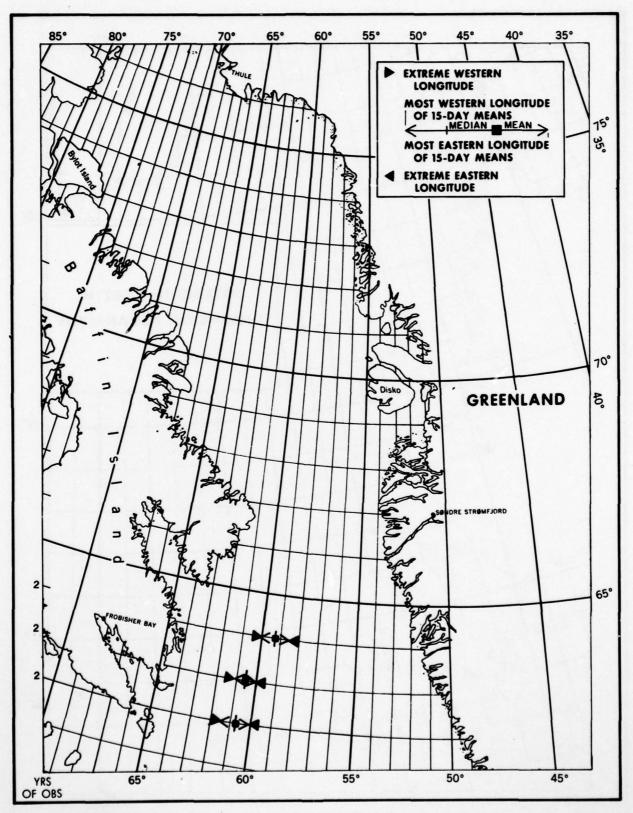


FIGURE 18A MEAN, MEDIAN AND EXTREME POSITIONS OF PACK EDGE 1-15 JANUARY

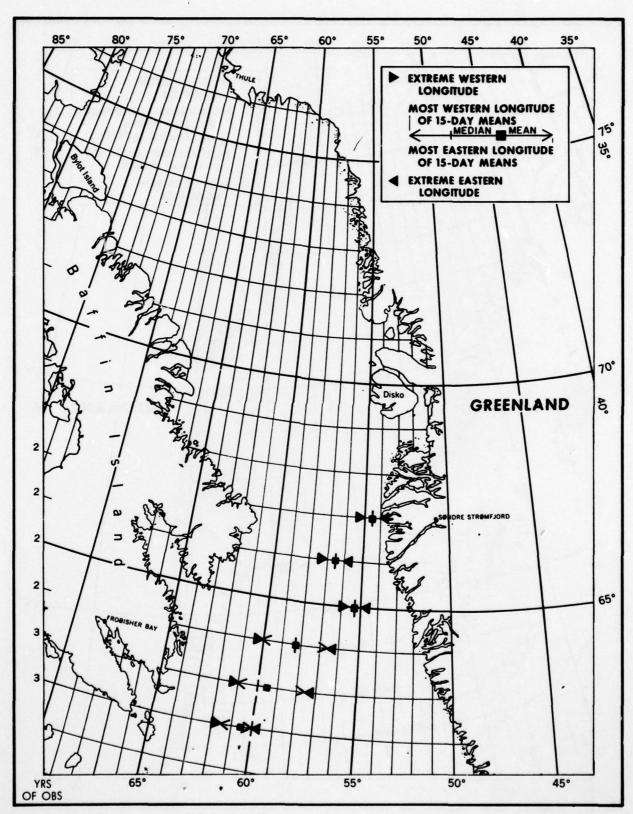


FIGURE 188 MEAN, MEDIAN AND EXTREME POSITIONS OF PACK EDGE 16-31 JANUARY

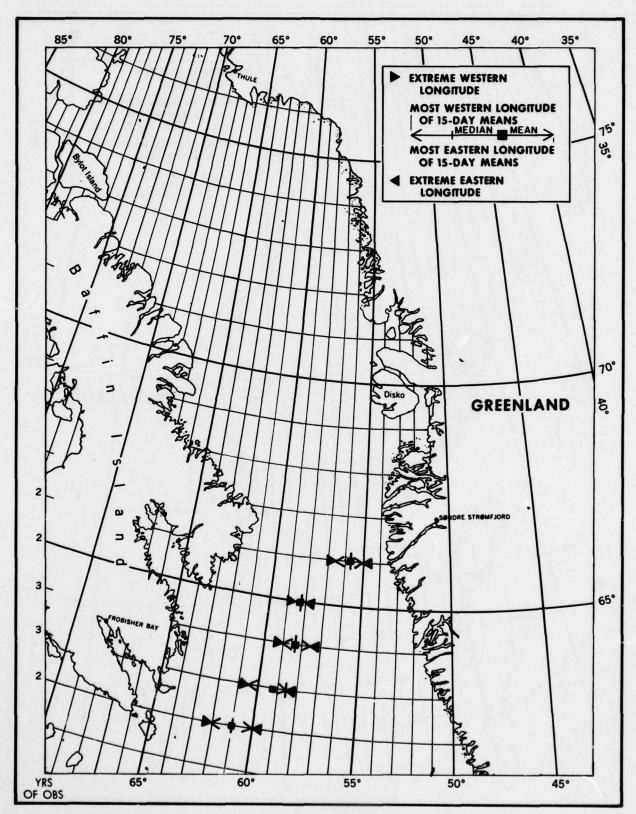


FIGURE 19A MEAN, MEDIAN AND EXTREME POSITIONS OF PACK EDGE 1-15 FEBRUARY

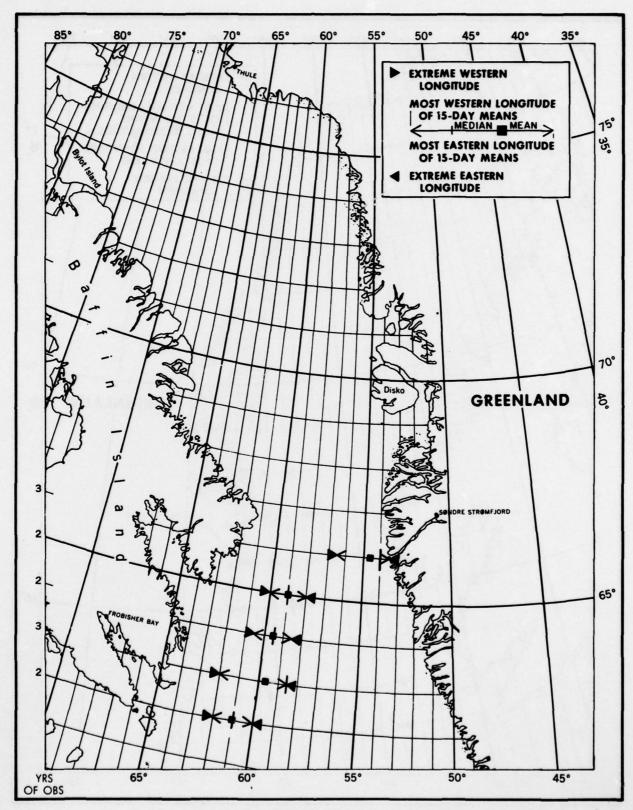


FIGURE 198 MEAN, MEDIAN AND EXTREME POSITIONS OF PACK EDGE 16-28 FEBRUARY

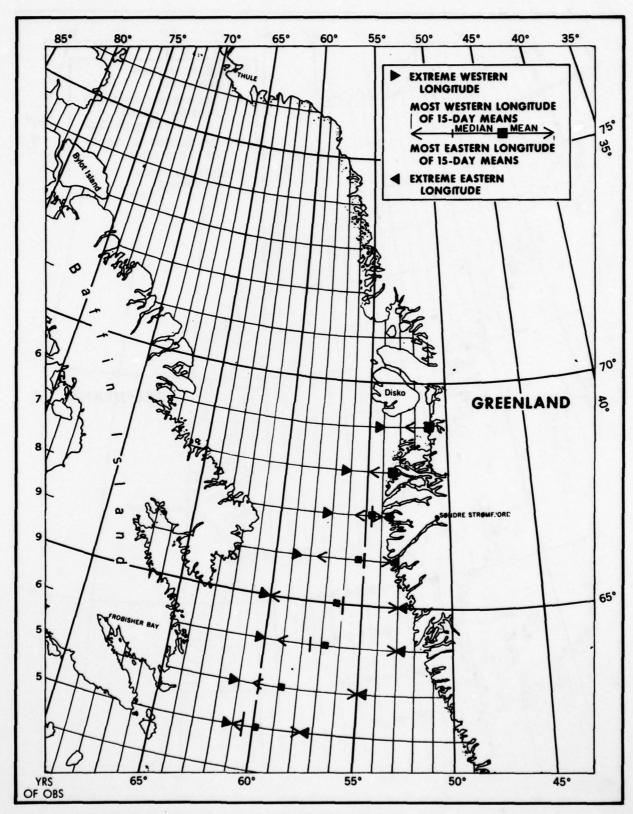


FIGURE 20A MEAN, MEDIAN AND EXTREME POSITIONS OF PACK EDGE 1-15 MARCH

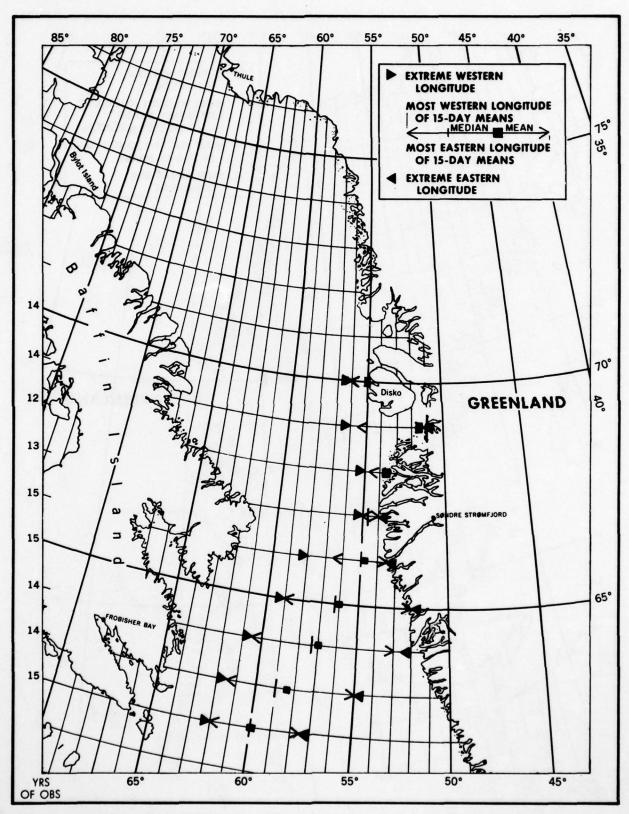


FIGURE 208 MEAN, MEDIAN AND EXTREME POSITIONS OF PACK EDGE 16-31 MARCH

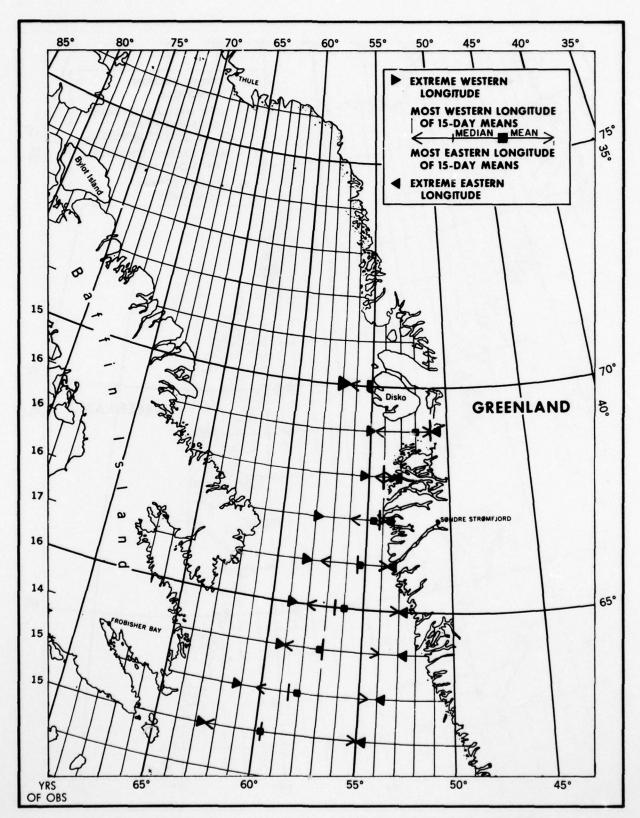


FIGURE 21A MEAN, MEDIAN AND EXTREME POSITIONS OF PACK EDGE 1-15 APRIL

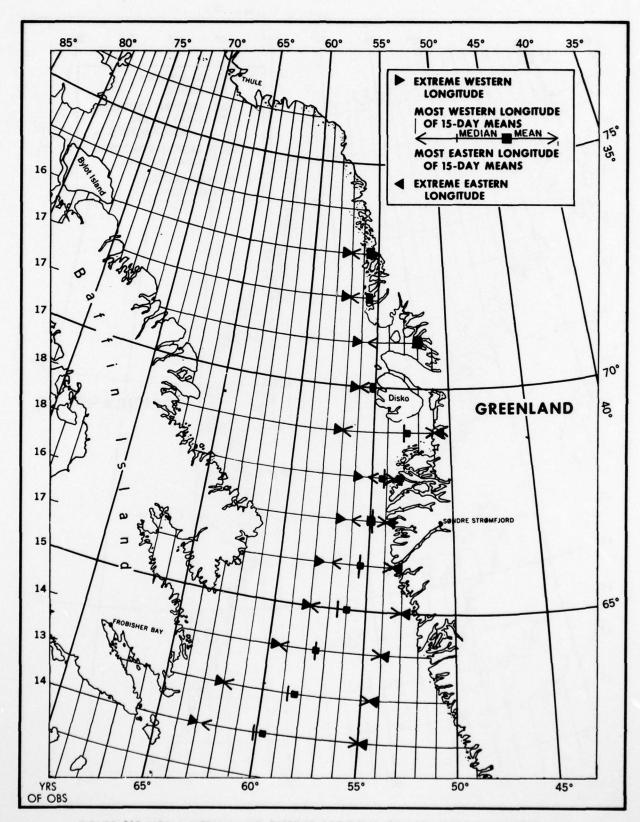


FIGURE 21B MEAN, MEDIAN AND EXTREME POSITIONS OF PACK EDGE 16-30 APRIL

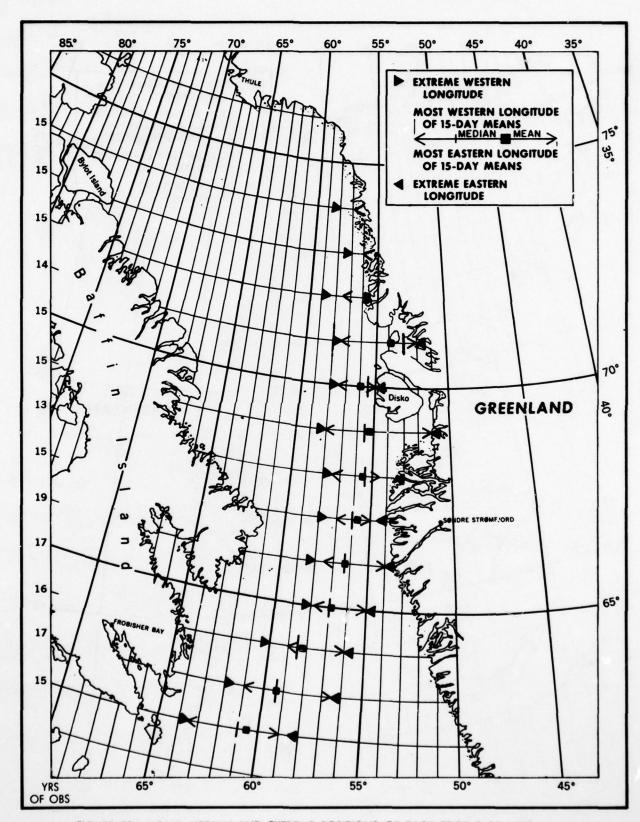


FIGURE 22A MEAN, MEDIAN AND EXTREME POSITIONS OF PACK EDGE 1-15 MAY

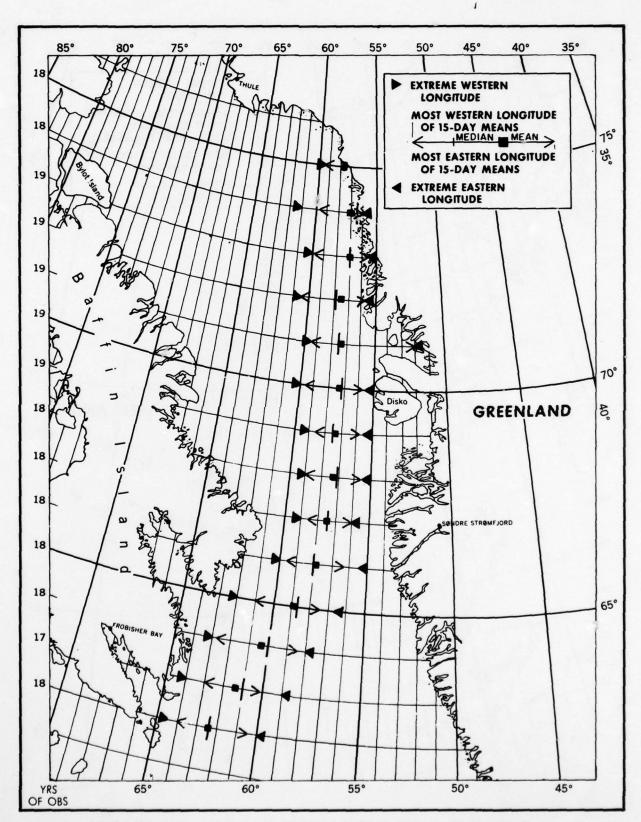
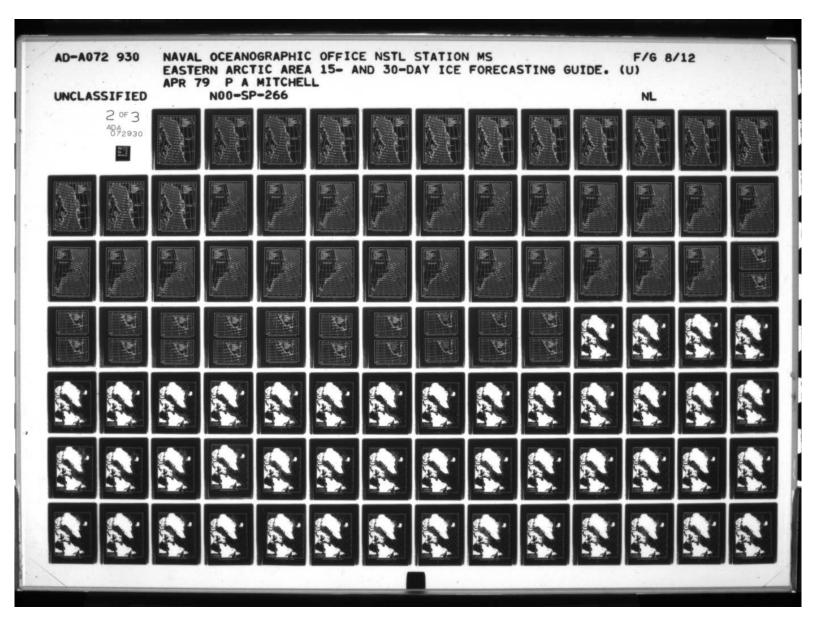
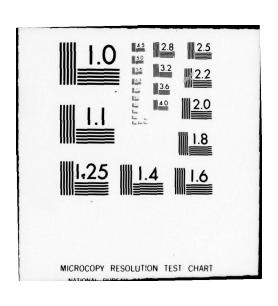


FIGURE 23A MEAN, MEDIAN AND EXTREME POSITIONS OF PACK EDGE 1-15 JUNE





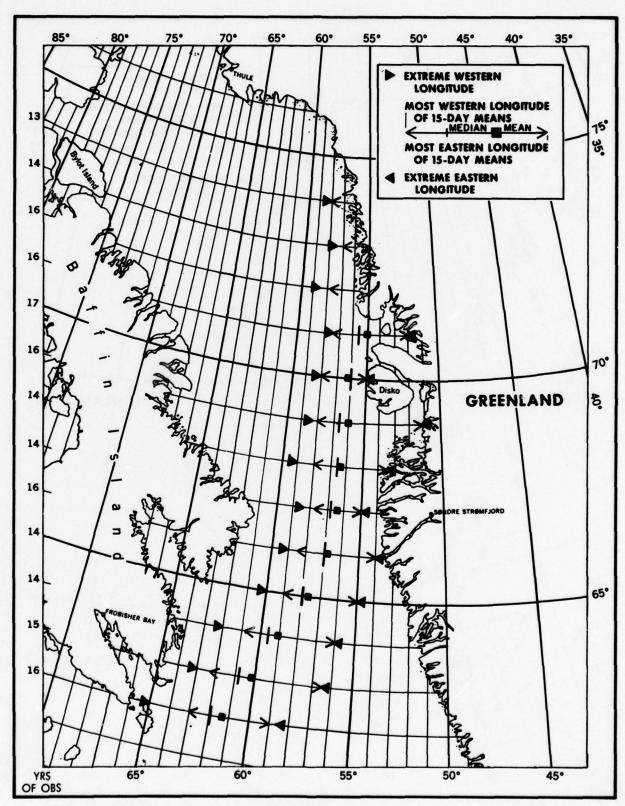


FIGURE 22B MEAN, MEDIAN AND EXTREME POSITIONS OF PACK EDGE 16-31 MAY

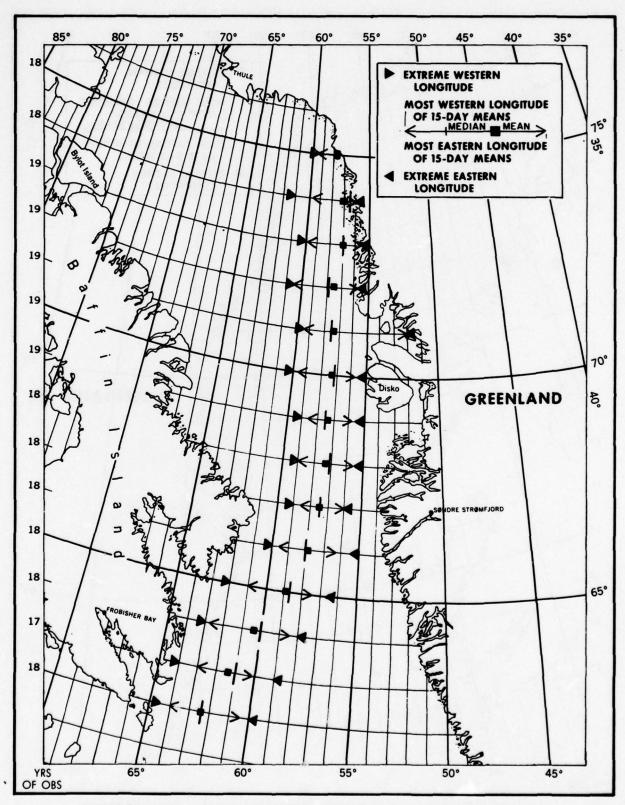


FIGURE 23A MEAN, MEDIAN AND EXTREME POSITIONS OF PACK EDGE 1-15 JUNE

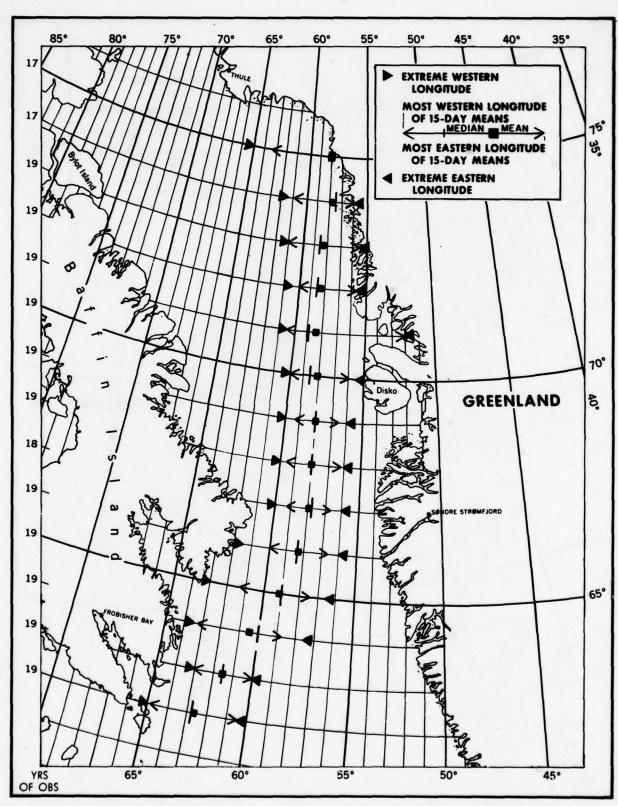


FIGURE 23B MEAN, MEDIAN AND EXTREME POSITIONS OF PACK EDGE 16-30 JUNE

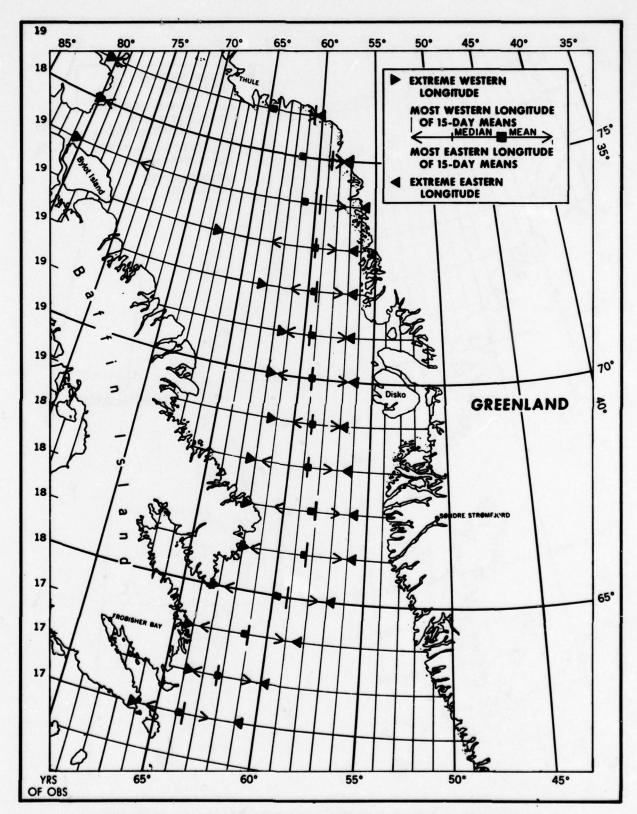


FIGURE 24A MEAN, MEDIAN AND EXTREME POSITIONS OF PACK EDGE 1-15 JULY

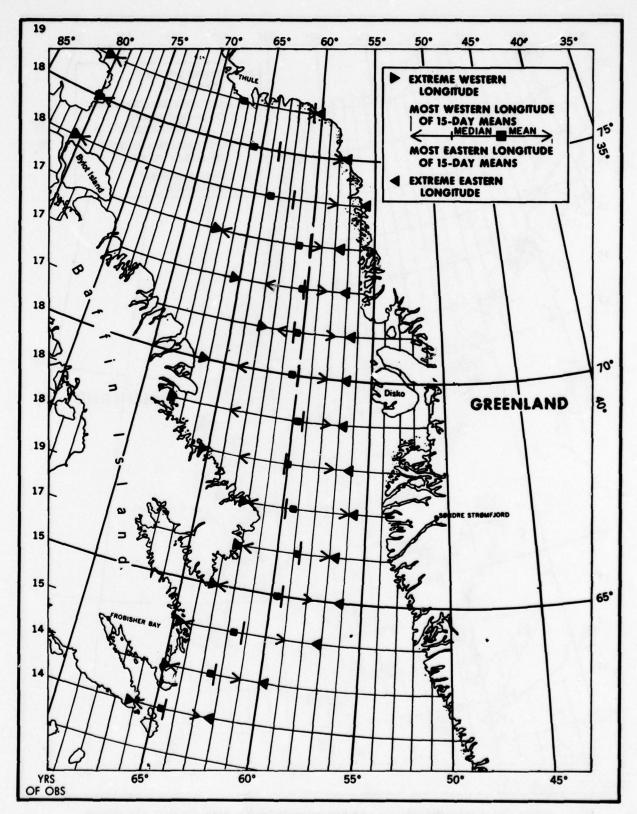


FIGURE 24B MEAN, MEDIAN AND EXTREME POSITIONS OF PACK EDGE 16-31 JULY

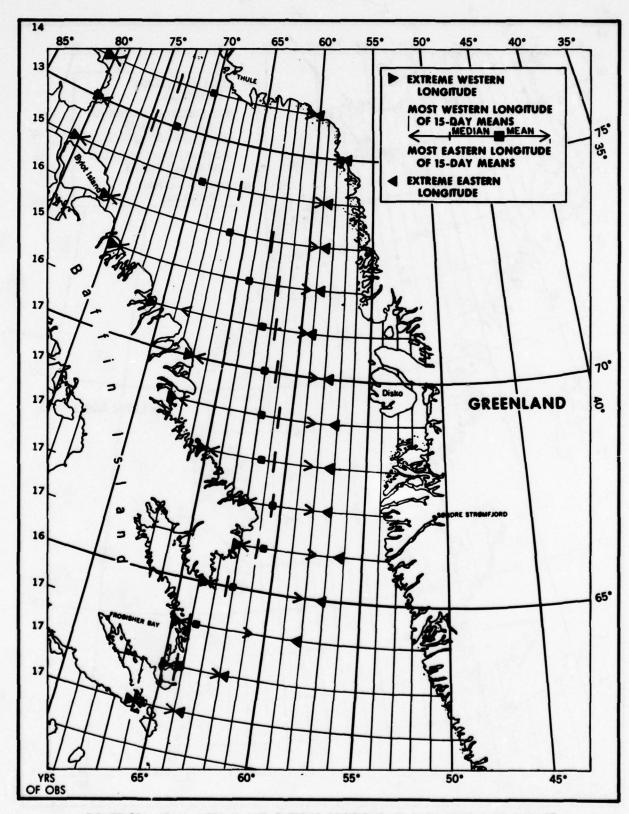


FIGURE 25A MEAN, MEDIAN AND EXTREME POSITIONS OF PACK EDGE 1-15 AUGUST

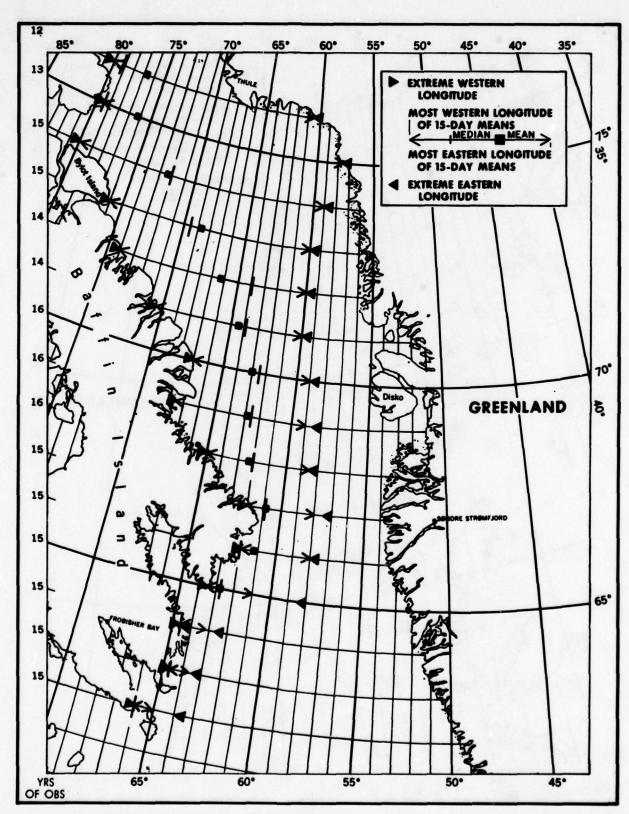


FIGURE 25B MEAN, MEDIAN AND EXTREME POSITIONS' OF PACK EDGE 16-31 AUGUST

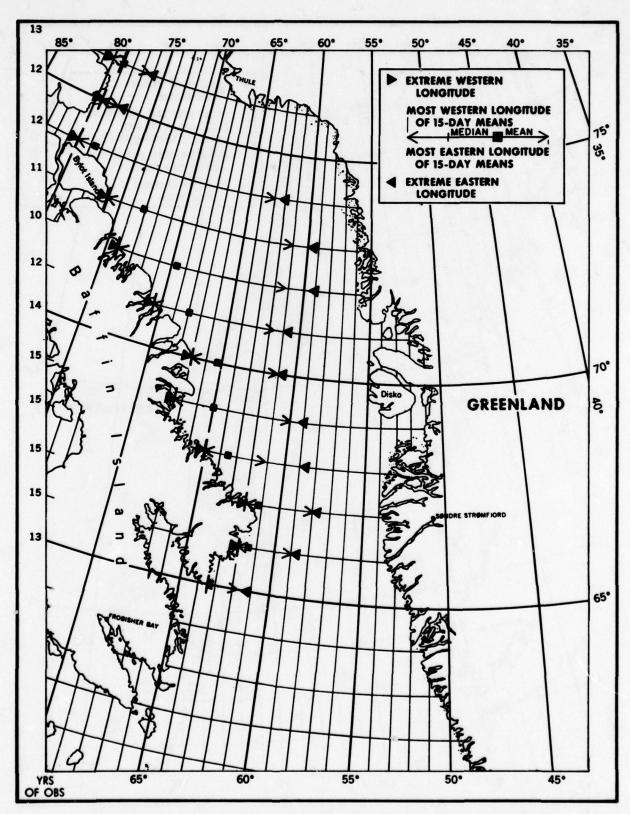


FIGURE 26A MEAN, MEDIAN AND EXTREME POSITIONS OF PACK EDGE 1-15 SEPTEMBER

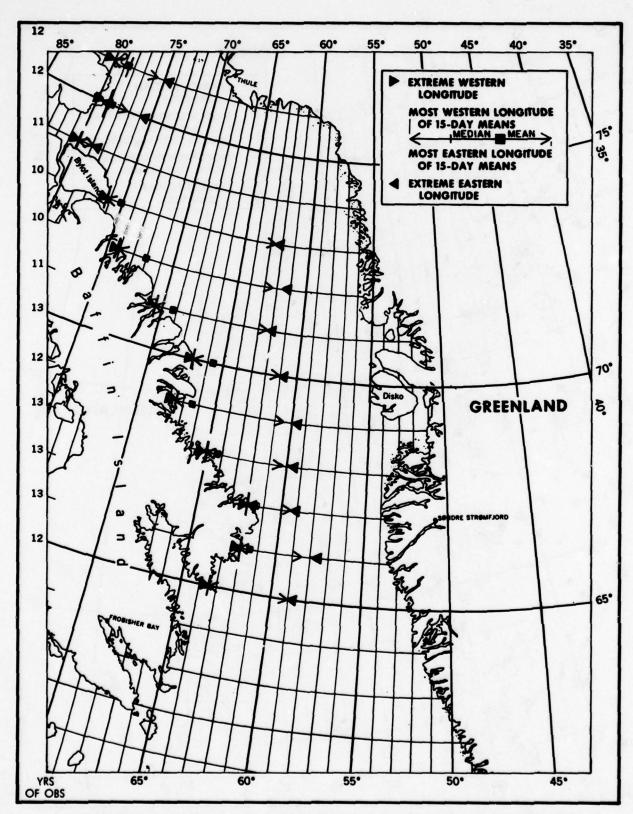


FIGURE 268 MEAN, MEDIAN AND EXTREME POSITIONS OF PACK EDGE 16-30 SEPTEMBER

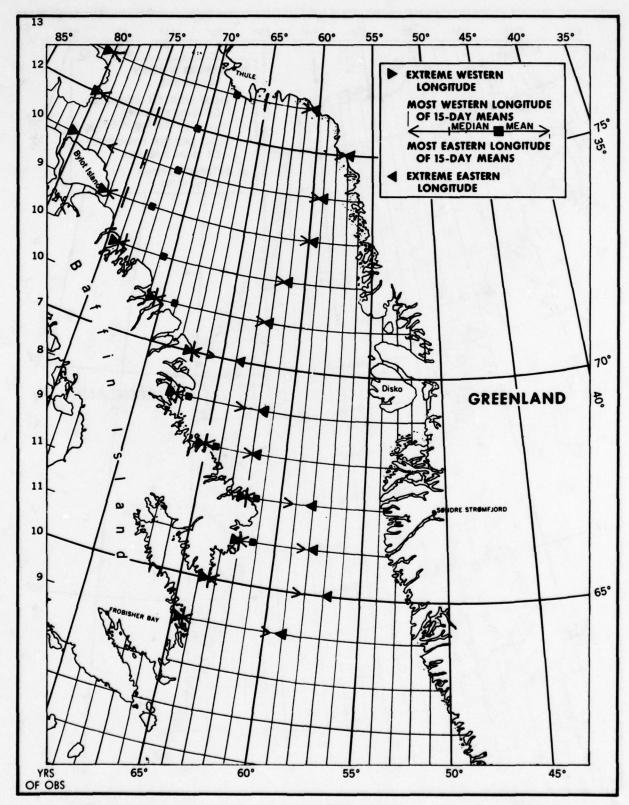


FIGURE 27A MEAN, MEDIAN AND EXTREME POSITIONS OF PACK EDGE 1-15 OCTOBER

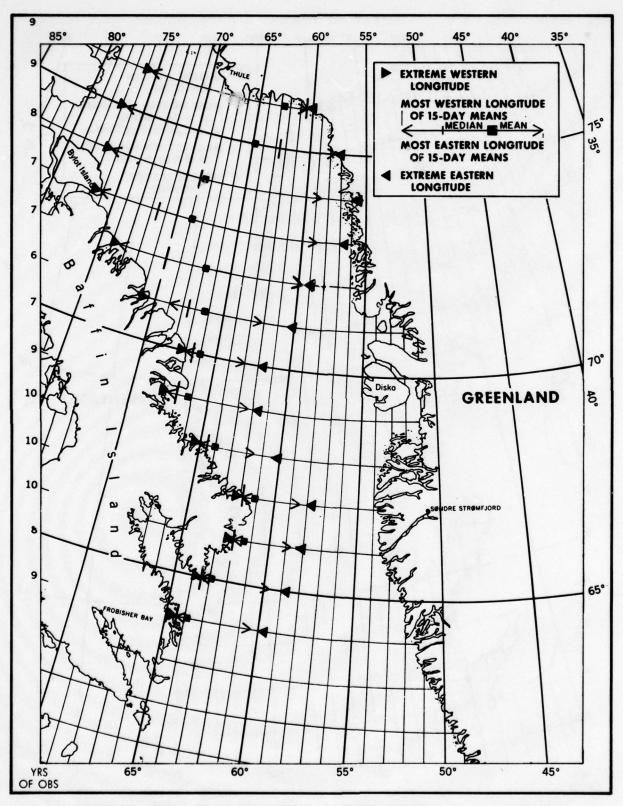


FIGURE 27B MEAN, MEDIAN AND EXTREME POSITIONS OF PACK EDGE 16-31 OCTOBER

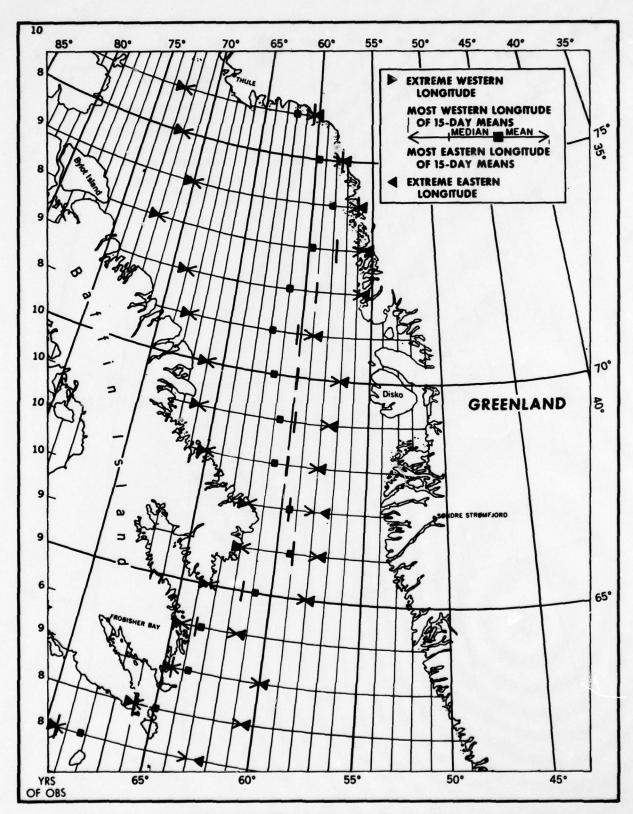


FIGURE 28A MEAN, MEDIAN AND EXTREME POSITIONS OF PACK EDGE 1-15 NOVEMBER

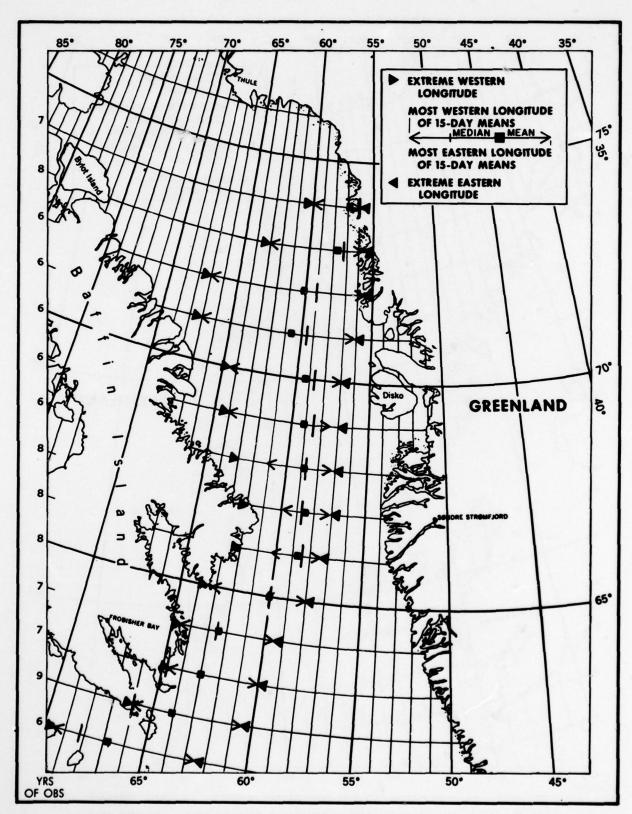


FIGURE 28B MEAN, MEDIAN AND EXTREME POSITIONS OF PACK EDGE 16-30 NOVEMBER

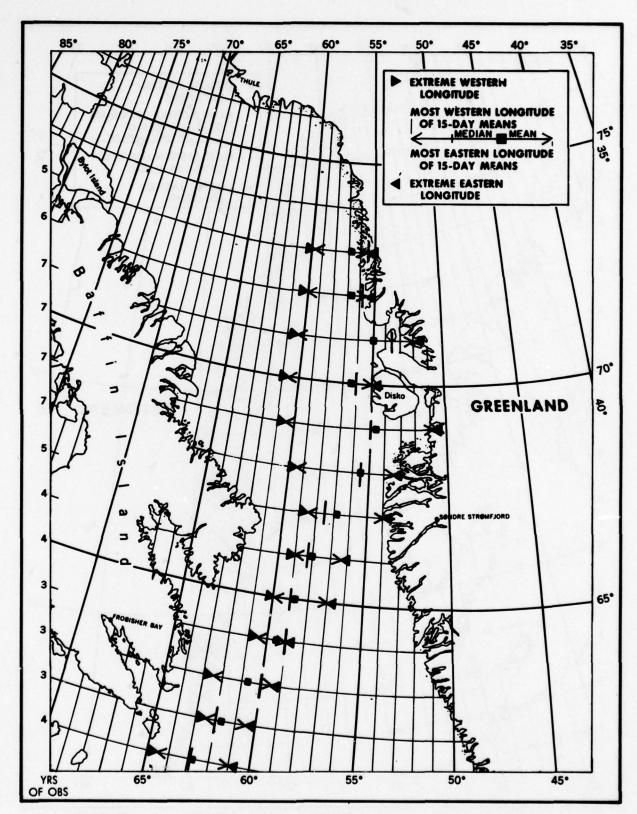


FIGURE 29A MEAN, MEDIAN AND EXTREME POSITIONS OF PACK EDGE 1-15 DECEMBER

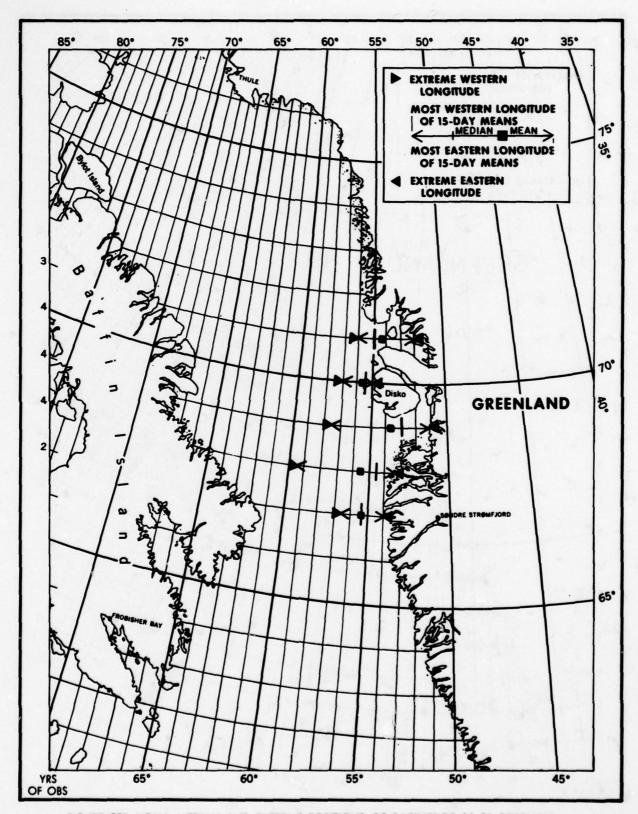


FIGURE 29B MEAN, MEDIAN AND EXTREME POSITIONS OF PACK EDGE 16-31 DECEMBER

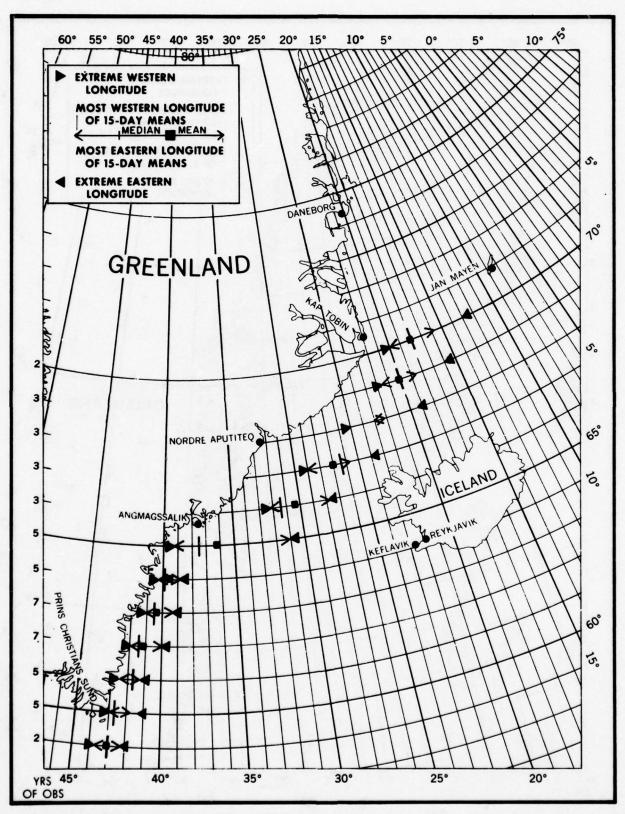


FIGURE 30A MEAN, MEDIAN AND EXTREME POSITIONS OF PACK EDGE 1-15 JANUARY

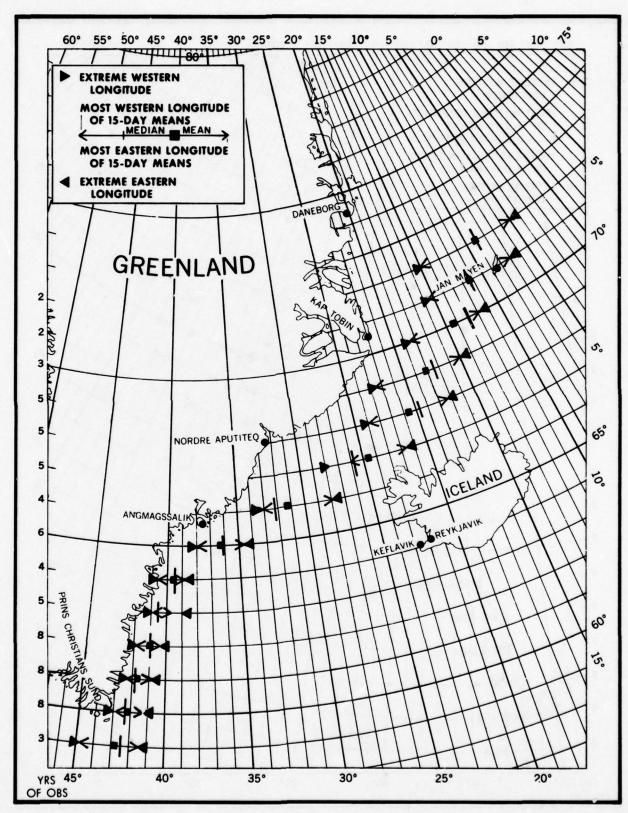


FIGURE 30B MEAN, MEDIAN AND EXTREME POSITIONS OF PACK EDGE 16-31 JANUARY

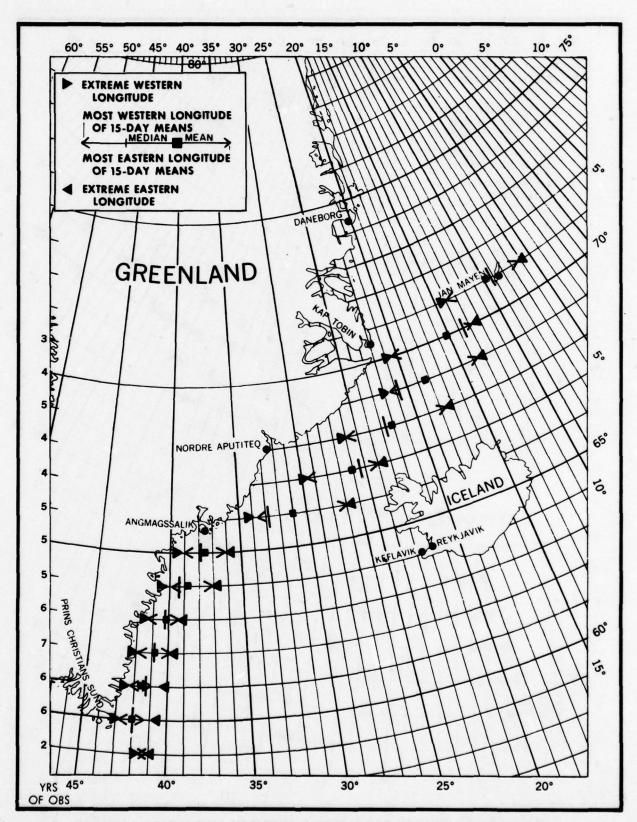


FIGURE 31A MEAN, MEDIAN AND EXTREME POSITIONS OF PACK EDGE 1-15 FEBRUARY

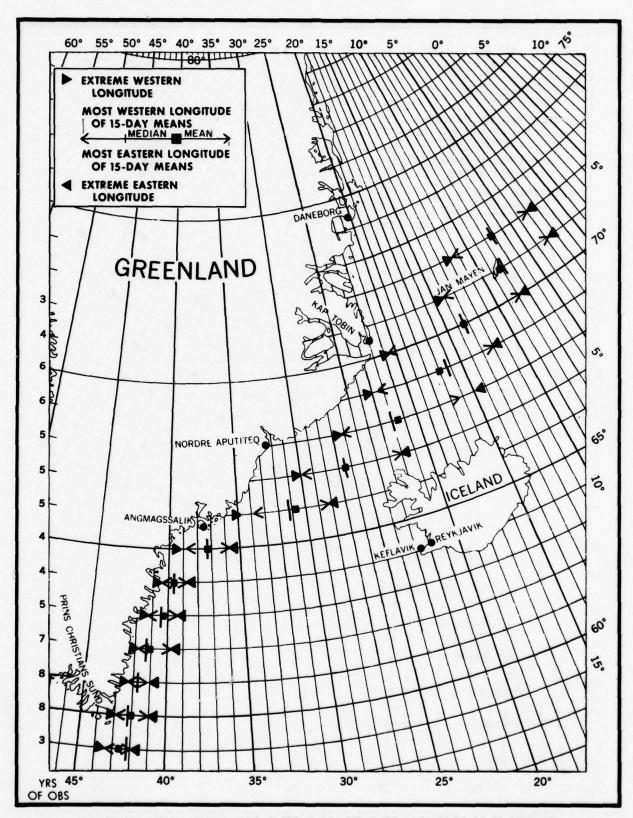


FIGURE 31B MEAN, MEDIAN AND EXTREME POSITIONS OF PACK EDGE 16-28 FEBRUARY

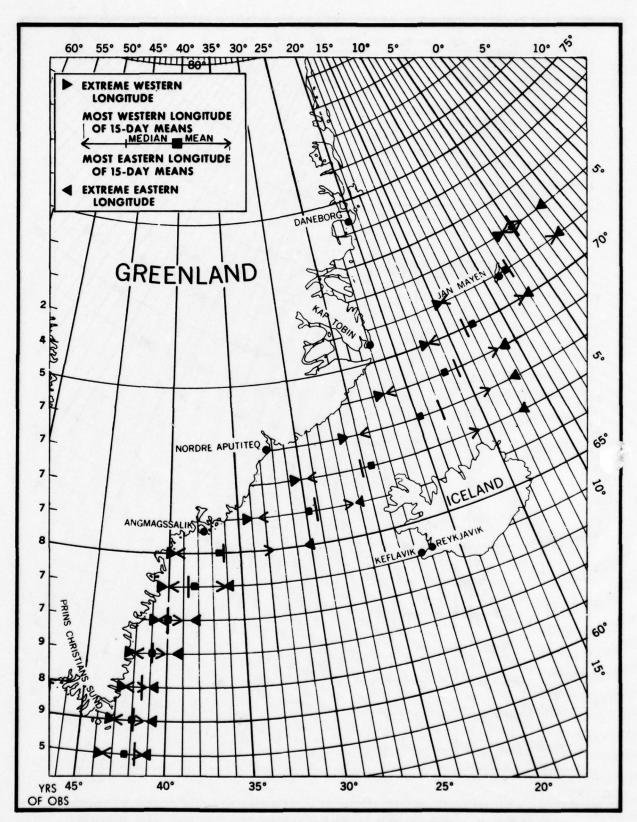


FIGURE 32A MEAN, MEDIAN AND EXTREME POSITIONS OF PACK EDGE 1-15 MARCH

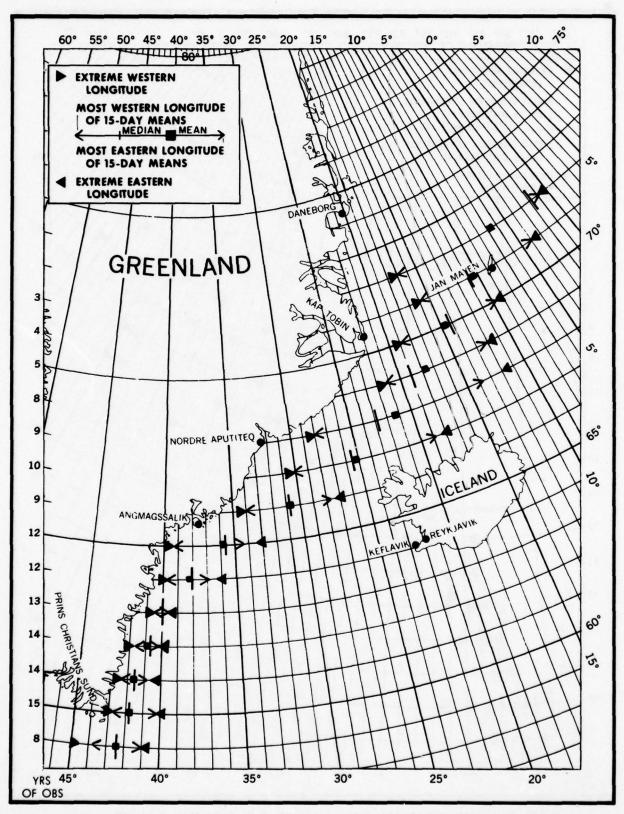


FIGURE 32B MEAN, MEDIAN AND EXTREME POSITIONS OF PACK EDGE 16-31 MARCH

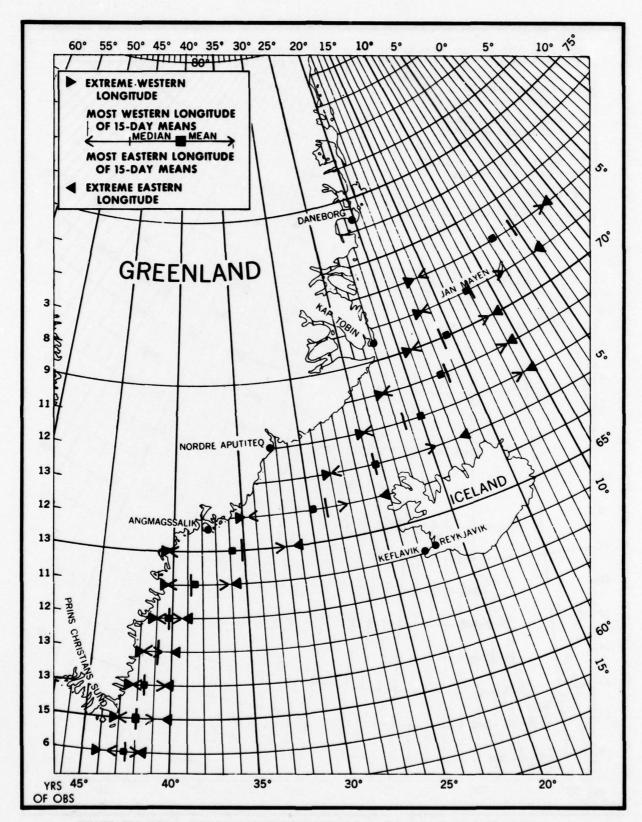


FIGURE 33A MEAN, MEDIAN AND EXTREME POSITIONS OF PACK EDGE 1-15 APRIL

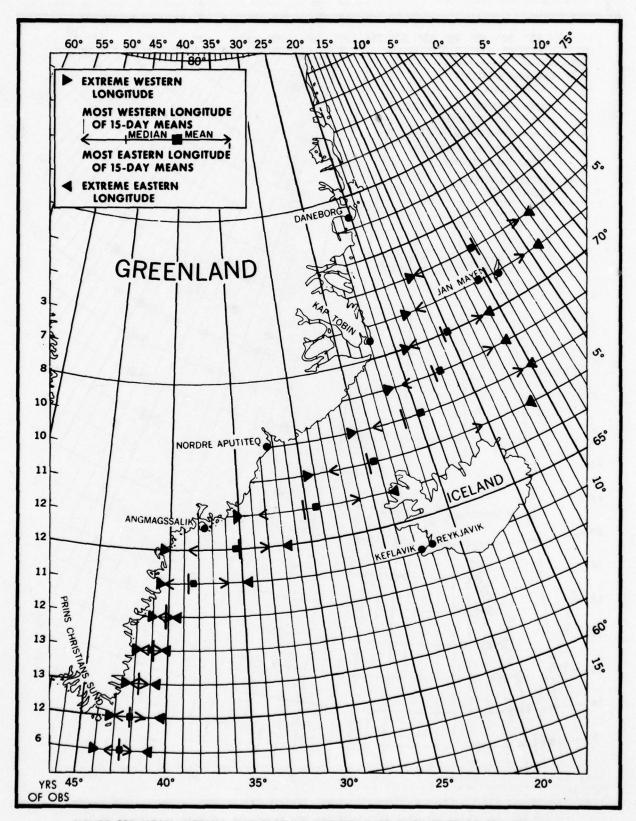


FIGURE 33B MEAN, MEDIAN AND EXTREME POSITIONS OF PACK EDGE 16-30 APRIL

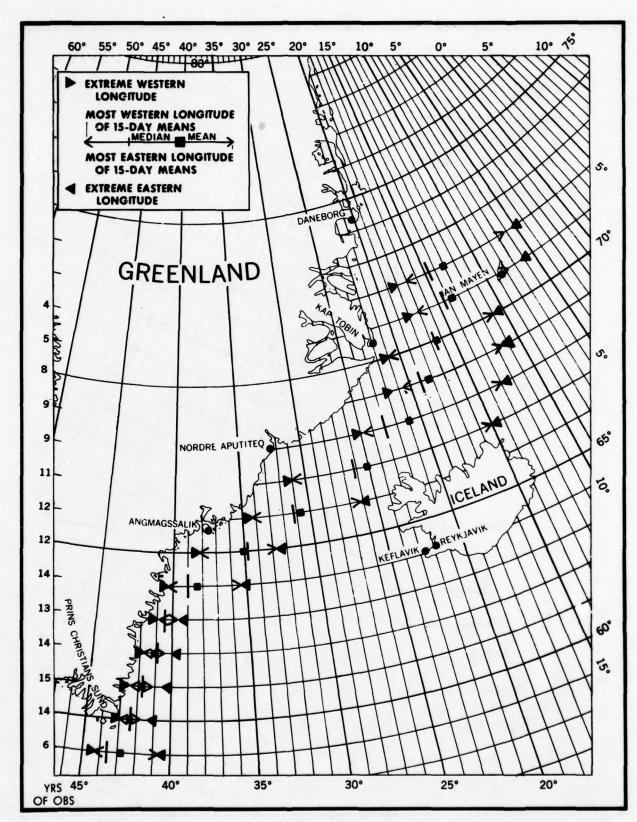


FIGURE 34A MEAN, MEDIAN AND EXTREME POSITIONS OF PACK EDGE 1-15 MAY

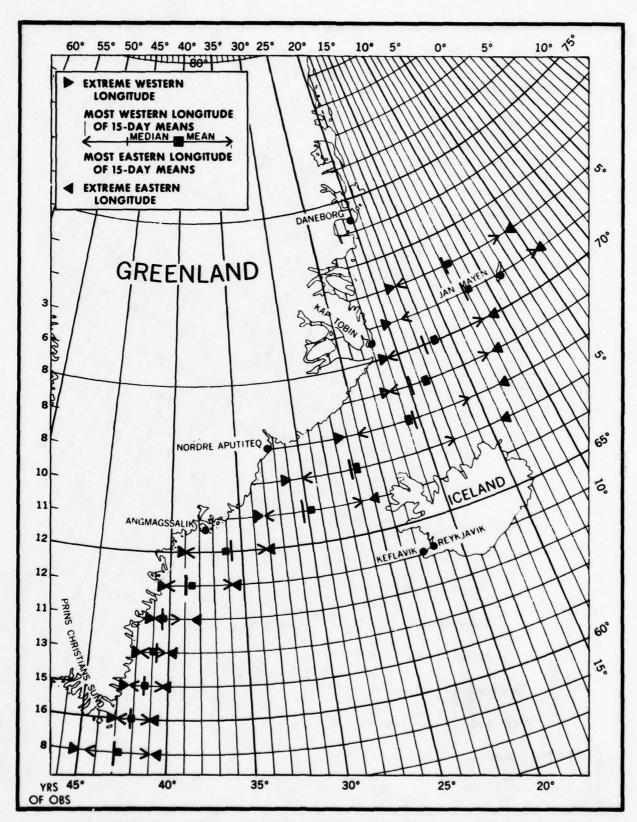


FIGURE 348 MEAN, MEDIAN AND EXTREME POSITIONS OF PACK EDGE 16-31 MAY

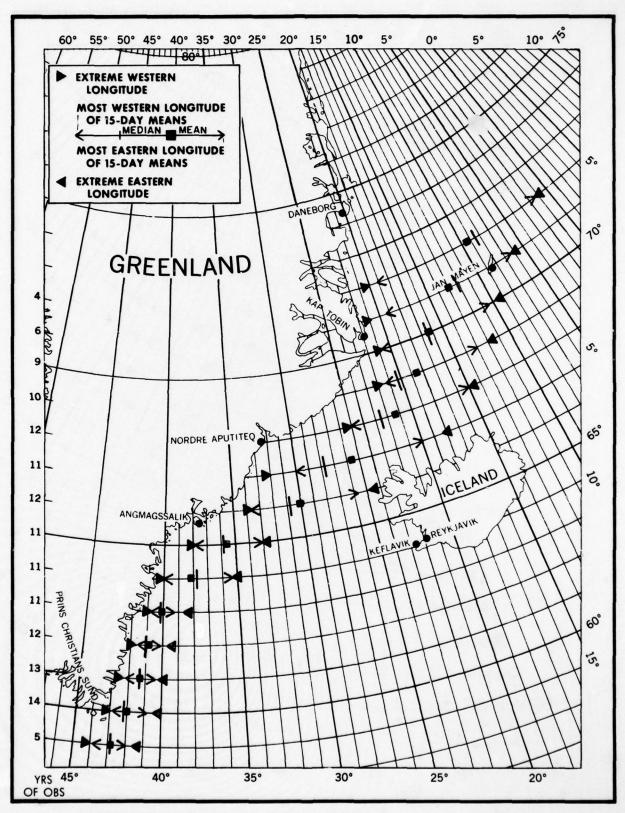


FIGURE 35A MEAN, MEDIAN AND EXTREME POSITIONS OF PACK EDGE 1-15 JUNE

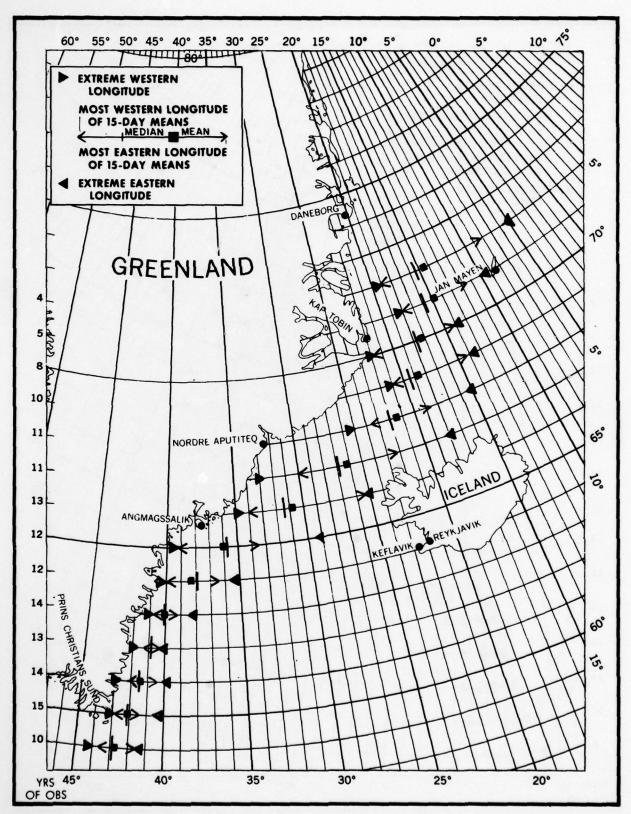


FIGURE 35B MEAN, MEDIAN AND EXTREME POSITIONS OF PACK EDGE 16-30 JUNE

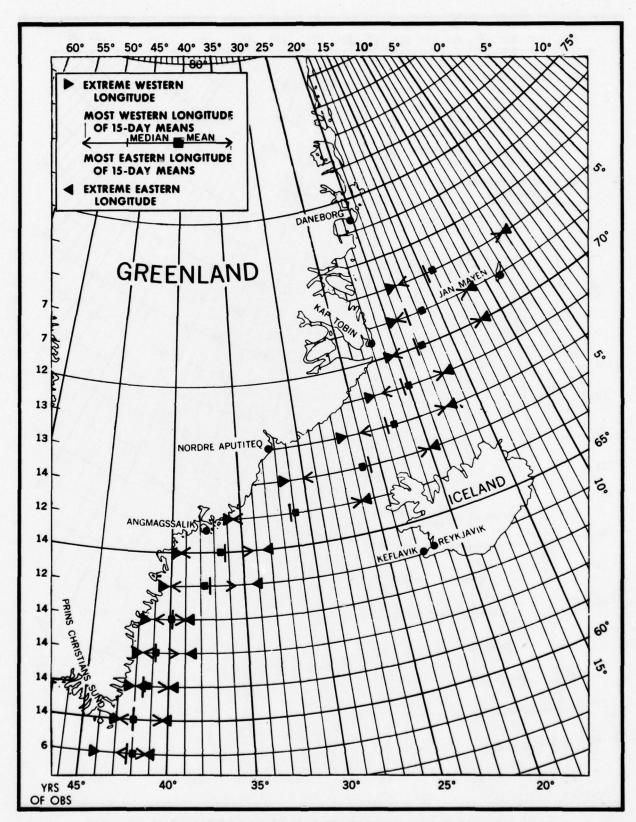


FIGURE 36A MEAN, MEDIAN AND EXTREME POSITIONS OF PACK EDGE 1-15 JULY

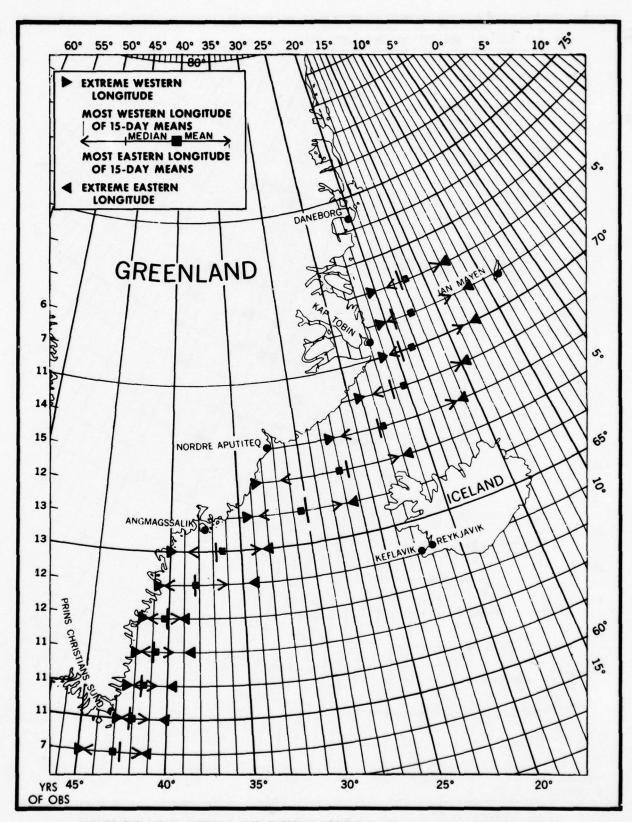


FIGURE 36B MEAN, MEDIAN AND EXTREME POSITIONS OF PACK EDGE 16-31 JULY

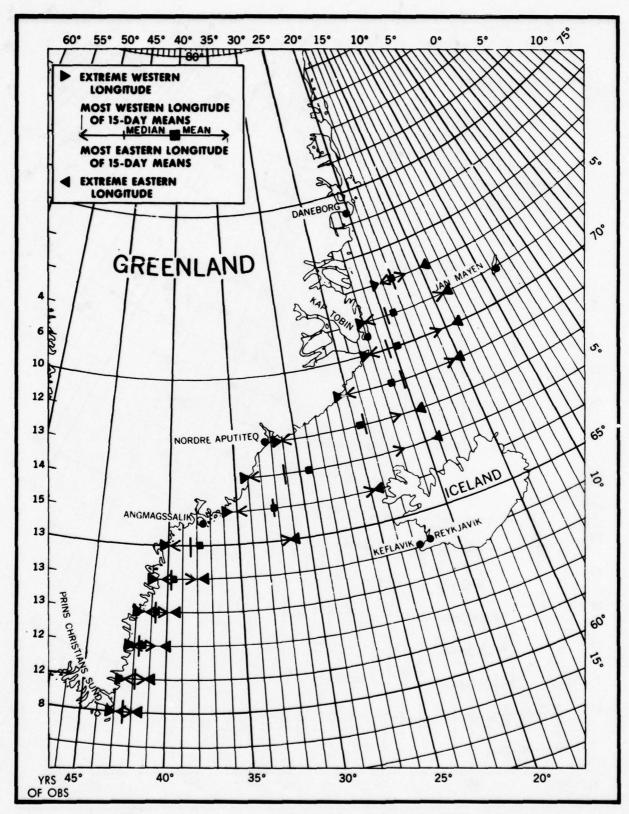


FIGURE 37A MEAN, MEDIAN AND EXTREME POSITIONS OF PACK EDGE 1-15 AUGUST

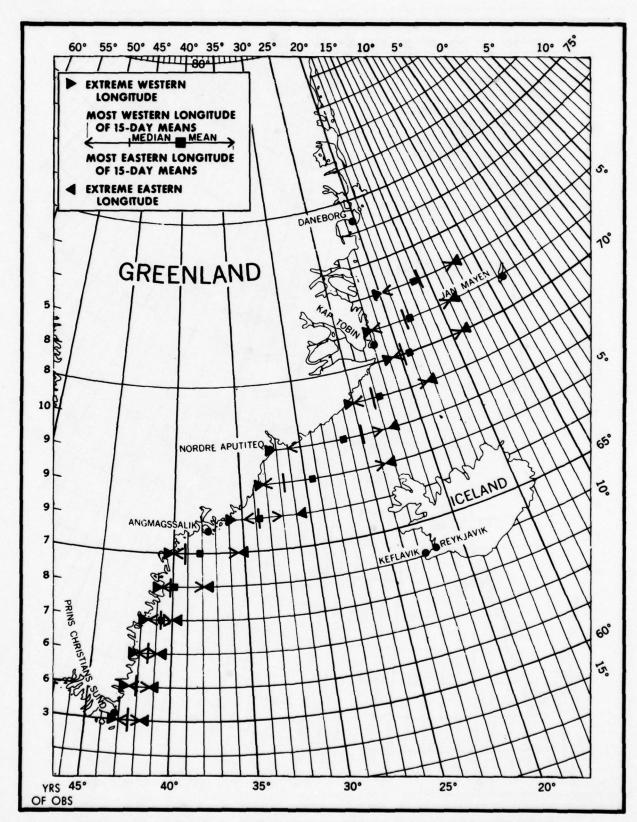


FIGURE 37B MEAN, MEDIAN AND EXTREME POSITIONS OF PACK EDGE 16-31 AUGUST

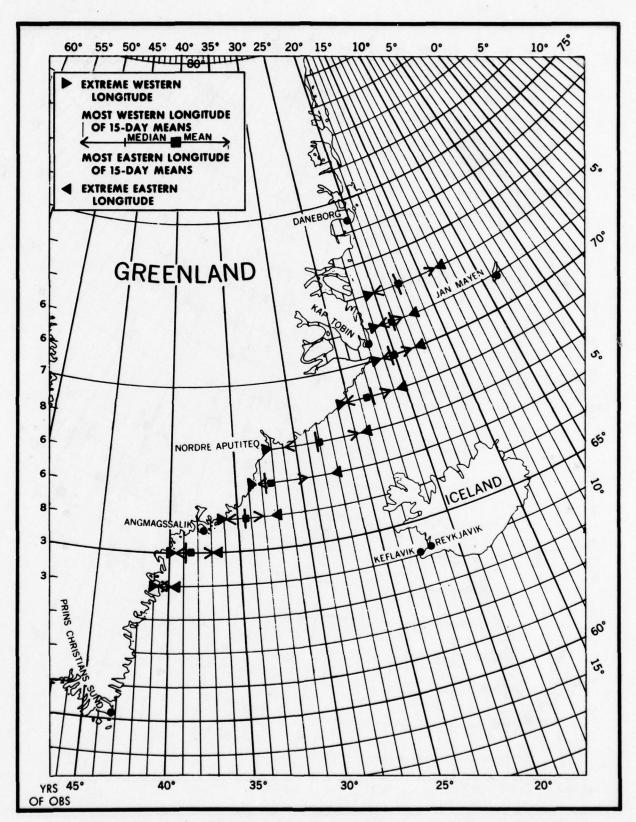


FIGURE 38A MEAN, MEDIAN AND EXTREME POSITIONS OF PACK EDGE 1-15 SEPTEMBER

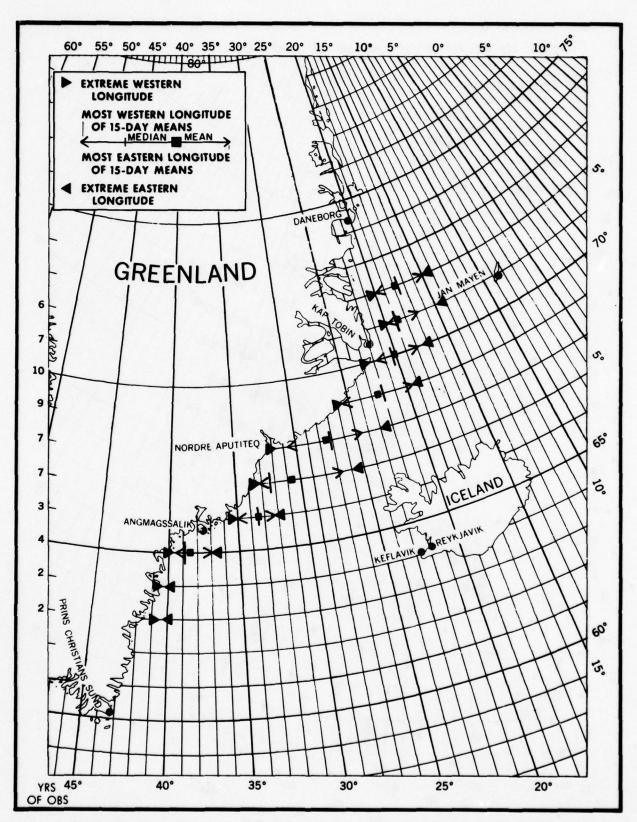


FIGURE 38B MEAN, MEDIAN AND EXTREME POSITIONS OF PACK EDGE 16-30 SEPTEMBER

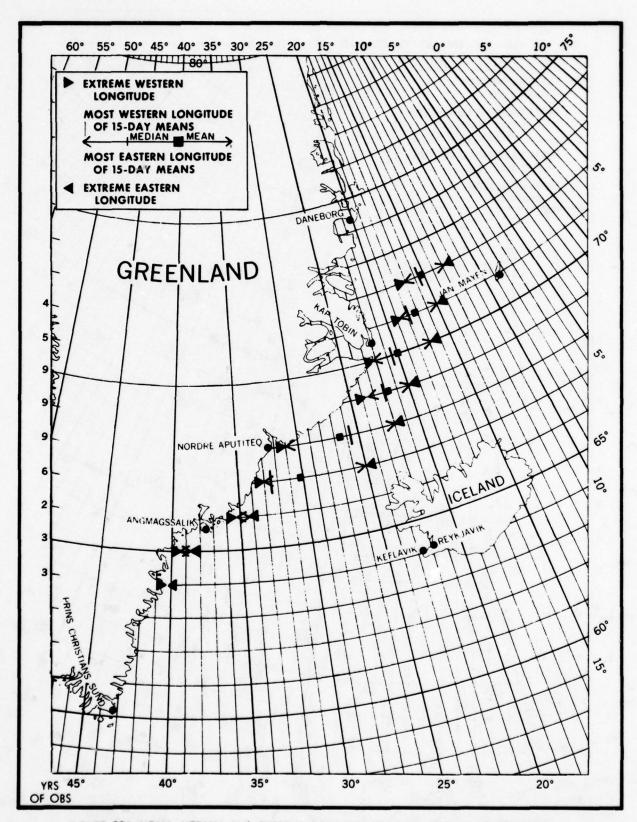


FIGURE 39A MEAN, MEDIAN AND EXTREME POSITIONS OF PACK EDGE 1-15 OCTOBER

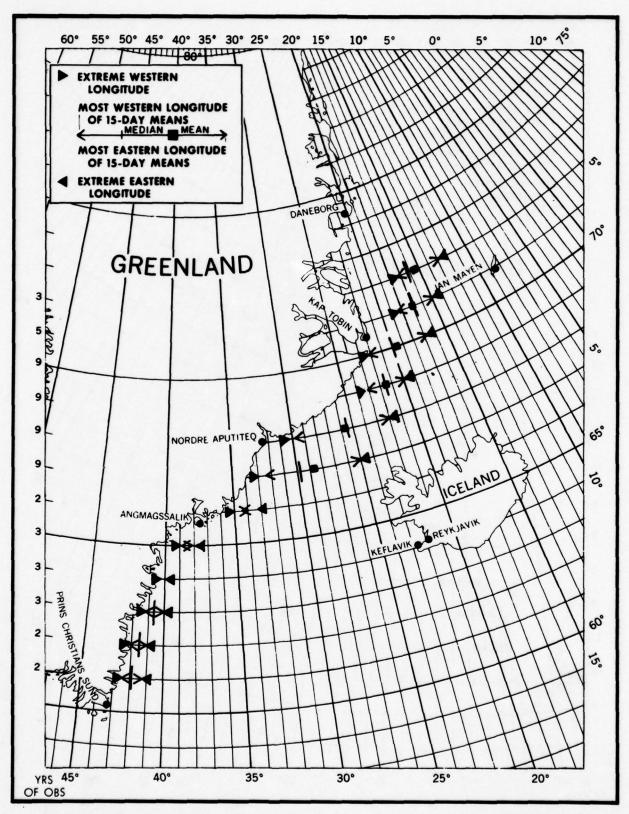


FIGURE 39B MEAN, MEDIAN AND EXTREME POSITIONS OF PACK EDGE 16-31 OCTOBER

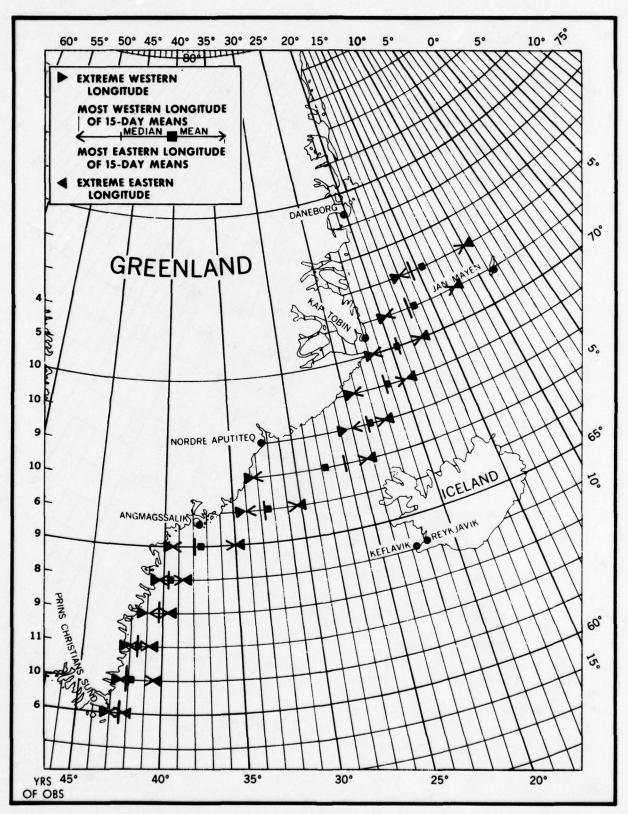


FIGURE 40A MEAN, MEDIAN AND EXTREME POSITIONS OF PACK EDGE 1-15 NOVEMBER

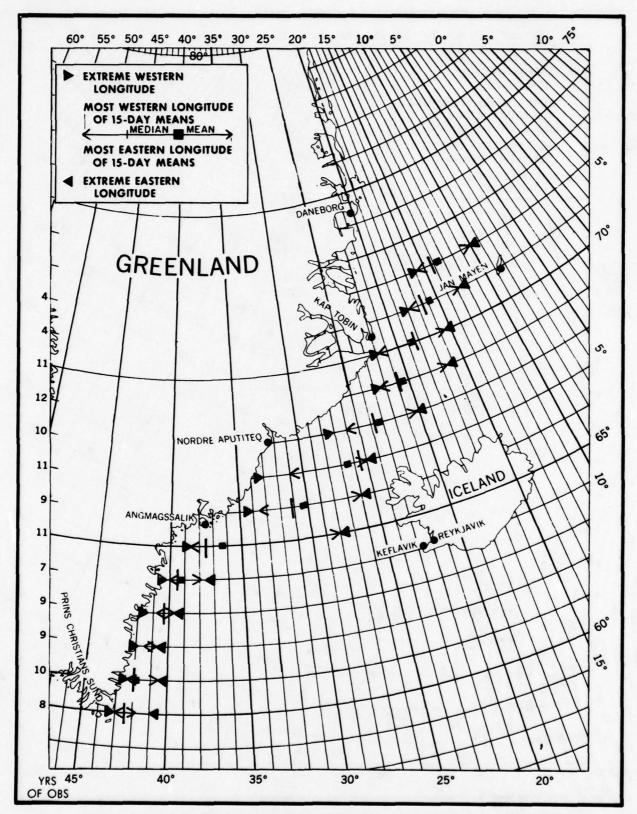


FIGURE 40B MEAN, MEDIAN AND EXTREME POSITIONS OF PACK EDGE 16-30 NOVEMBER

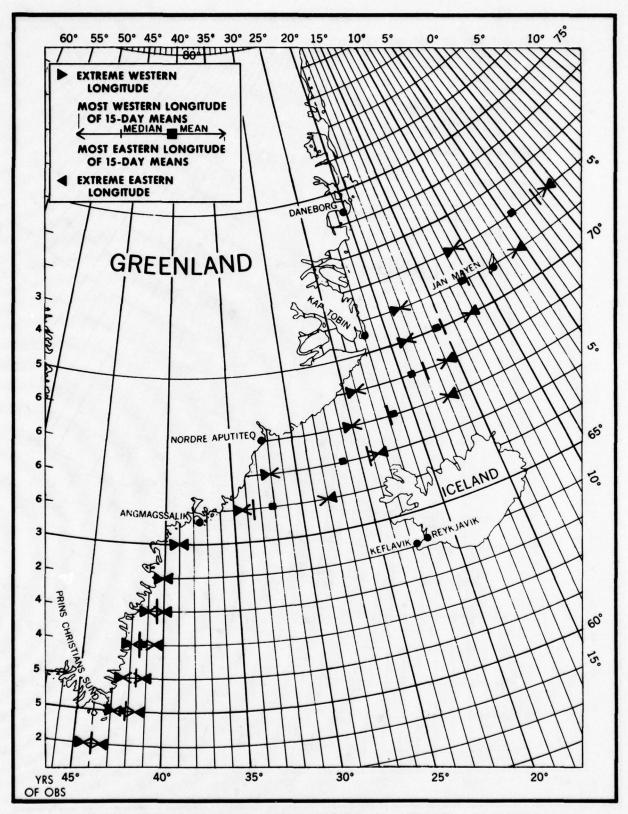


FIGURE 41A MEAN, MEDIAN AND EXTREME POSITIONS OF PACK EDGE 1-15 DECEMBER

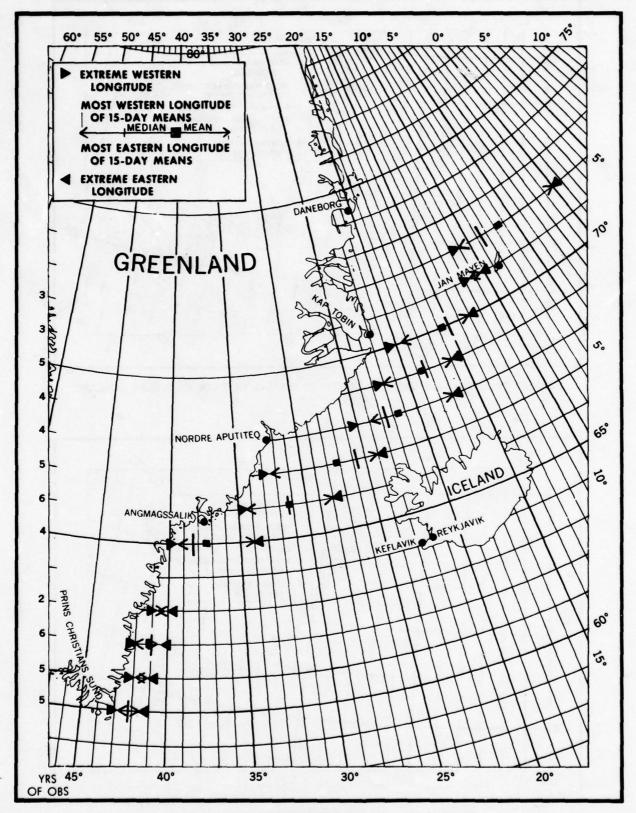


FIGURE 41B MEAN, MEDIAN AND EXTREME POSITIONS OF PACK EDGE 16-31 DECEMBER

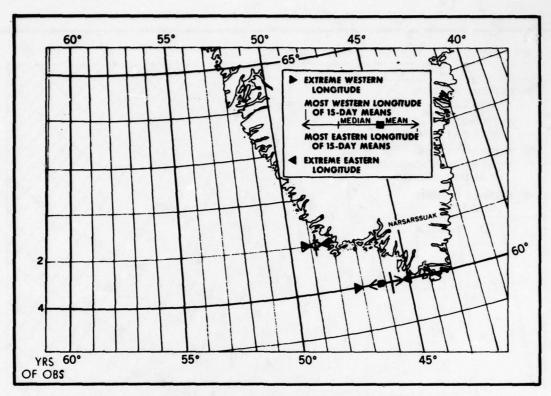


FIGURE 42A MEAN, MEDIAN AND EXTREME POSITIONS OF PACK EDGE 1-15 JANUARY

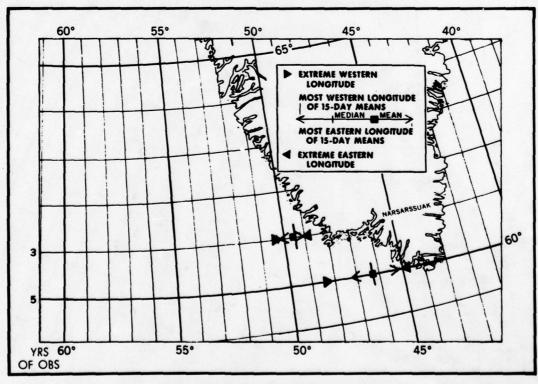


FIGURE 42B MEAN, MEDIAN AND EXTREME POSITIONS OF PACK EDGE 16-31 JANUARY

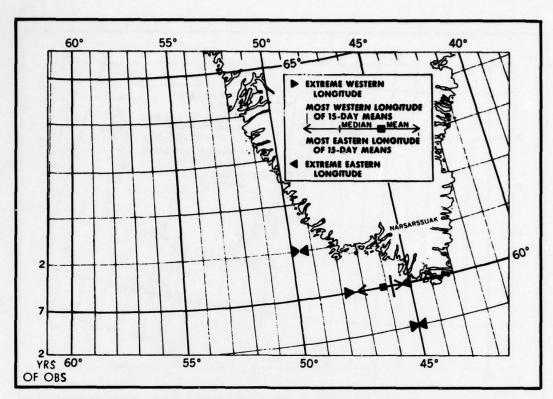


FIGURE 43A MEAN, MEDIAN AND EXTREME POSITIONS OF PACK EDGE 1-15 FEBRUARY

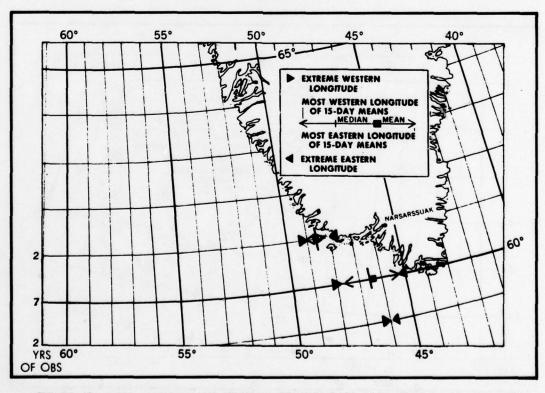


FIGURE 43B MEAN, MEDIAN AND EXTREME POSITIONS OF PACK EDGE 16-28 FEBRUARY

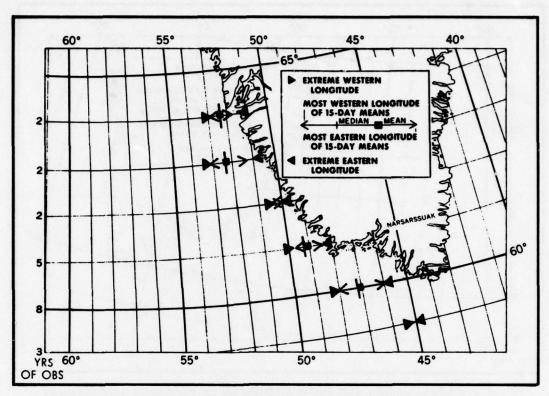


FIGURE 44A MEAN, MEDIAN AND EXTREME POSITIONS OF PACK EDGE 1-15 MARCH

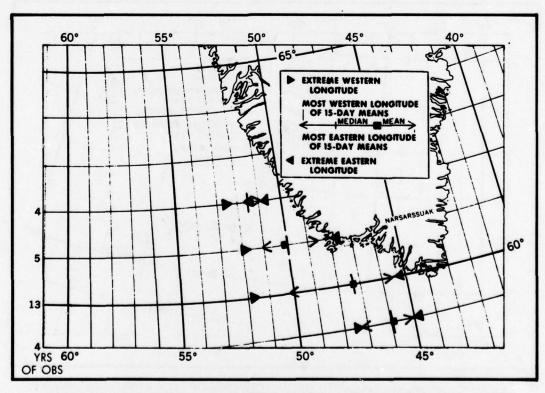


FIGURE 44B MEAN, MEDIAN AND EXTREME POSITIONS OF PACK EDGE 16-31 MARCH

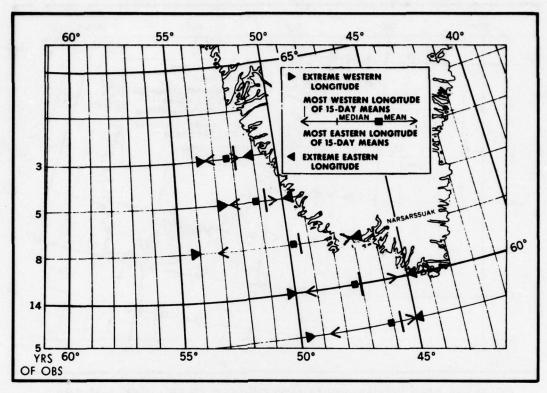


FIGURE 46A MEAN, MEDIAN AND EXTREME POSITIONS OF PACK EDGE 1-15 MAY

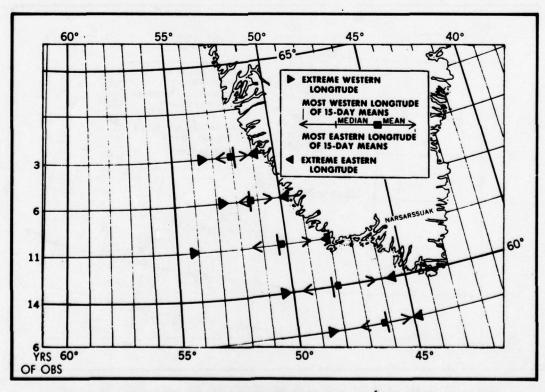


FIGURE 468 MEAN, MEDIAN AND EXTREME POSITIONS OF PACK EDGE 16-31 MAY

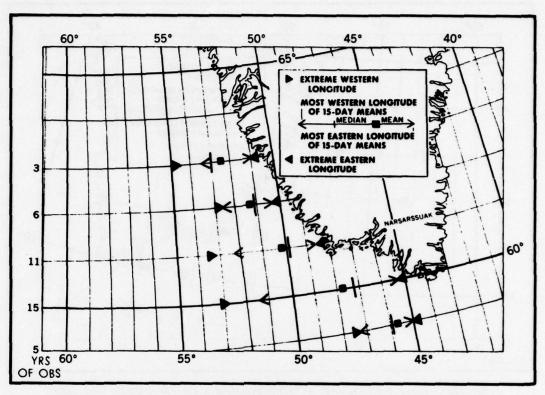


FIGURE 47A MEAN, MEDIAN AND EXTREME POSITIONS OF PACK EDGE 1-15 JUNE

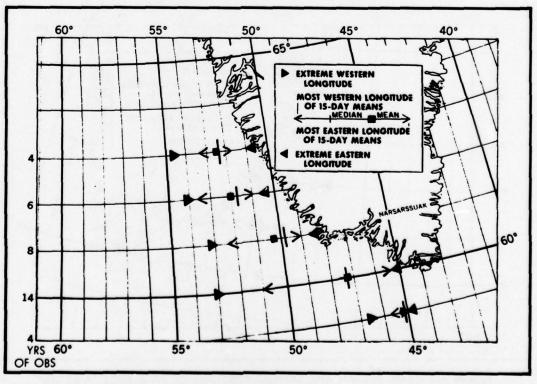


FIGURE 478 MEAN, MEDIAN AND EXTREME POSITIONS OF PACK EDGE 16-30 JUNE

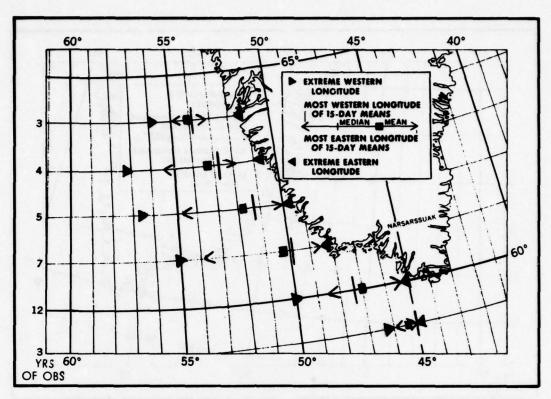


FIGURE 48A MEAN, MEDIAN AND EXTREME POSITIONS OF PACK EDGE 1-15 JULY

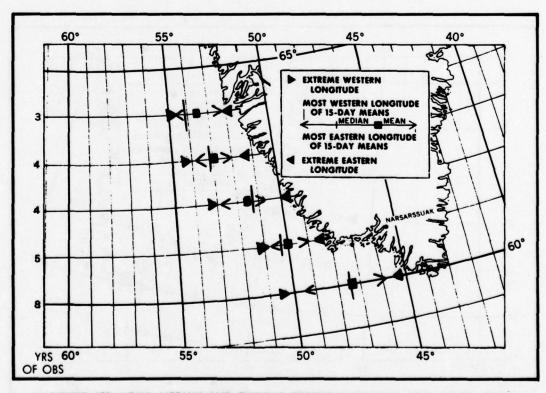


FIGURE 48B MEAN, MEDIAN AND EXTREME POSITIONS OF PACK EDGE 16-31 JULY

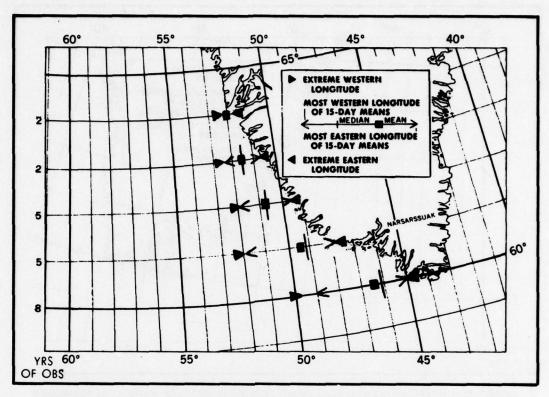


FIGURE 49A MEAN, MEDIAN AND EXTREME POSITIONS OF PACK EDGE 1-15 AUGUST

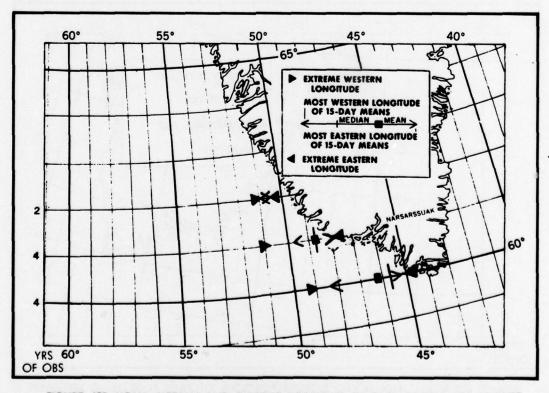


FIGURE 49B MEAN, MEDIAN AND EXTREME POSITIONS OF PACK EDGE 16-31 AUGUST

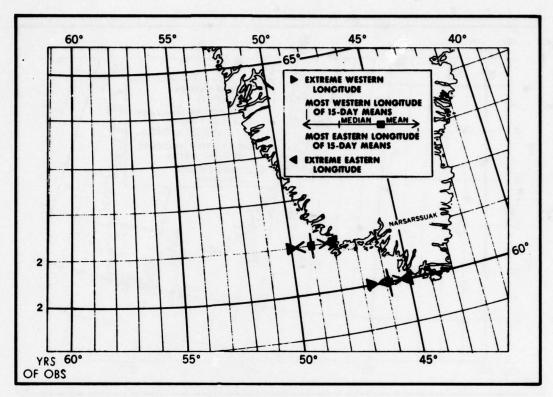


FIGURE 50A MEAN, MEDIAN AND EXTREME POSITIONS OF PACK EDGE 1-15 SEPTEMBER

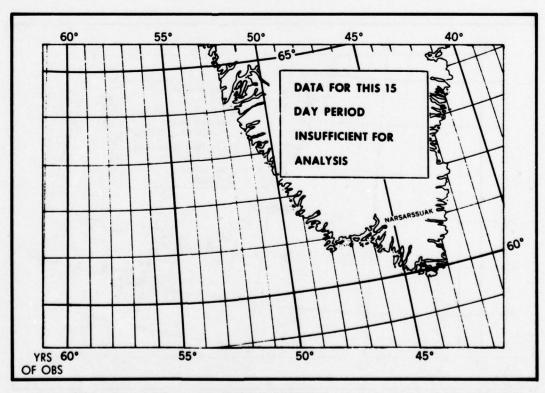


FIGURE 508 MEAN, MEDIAN AND EXTREME POSITIONS OF PACK EDGE 16-30 SEPTEMBER

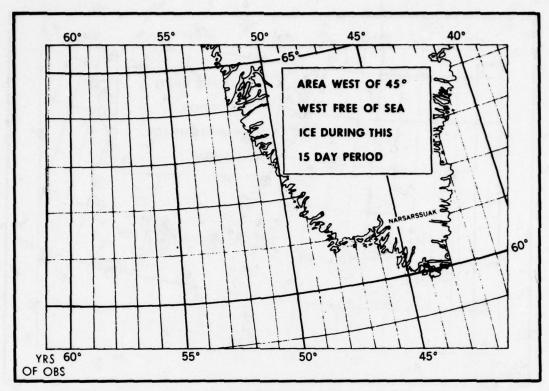


FIGURE 51A MEAN, MEDIAN AND EXTREME POSITIONS OF PACK EDGE 1-15 OCTOBER

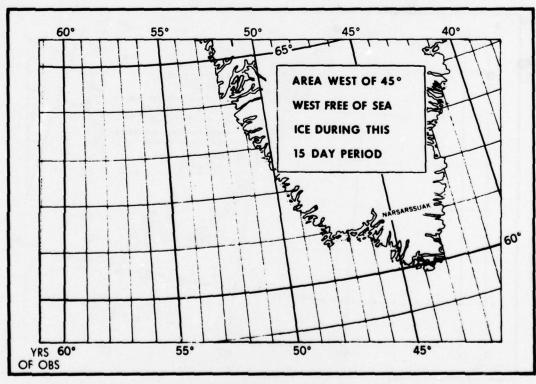


FIGURE 518 MEAN, MEDIAN AND EXTREME POSITIONS OF PACK EDGE 16-31 OCTOBER

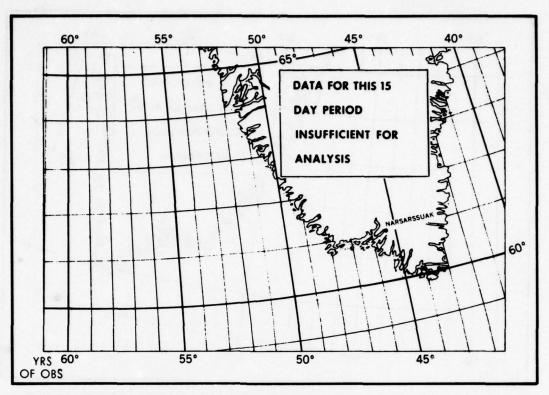


FIGURE 52A MEAN, MEDIAN AND EXTREME POSITIONS OF PACK EDGE 1-15 NOVEMBER

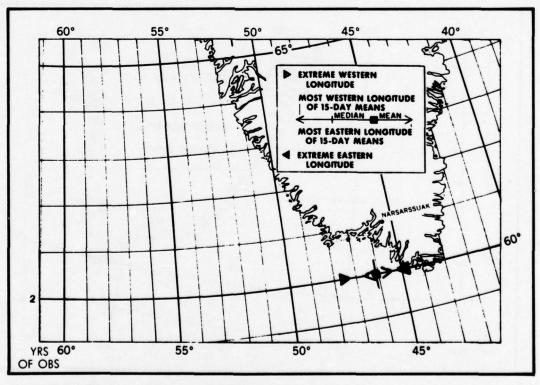


FIGURE 52B MEAN, MEDIAN AND EXTREME POSITIONS OF PACK EDGE 16-30 NOVEMBER

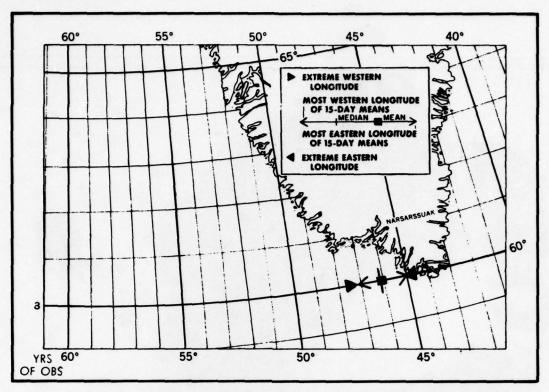


FIGURE 53A MEAN, MEDIAN AND EXTREME POSITIONS OF PACK EDGE 1-15 DECEMBER

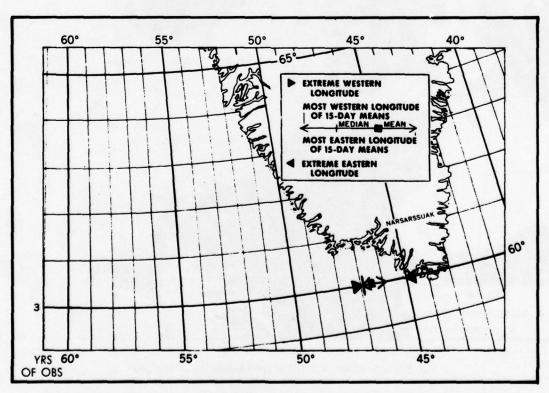


FIGURE 53B MEAN, MEDIAN AND EXTREME POSITIONS OF PACK EDGE 16-31 DECEMBER

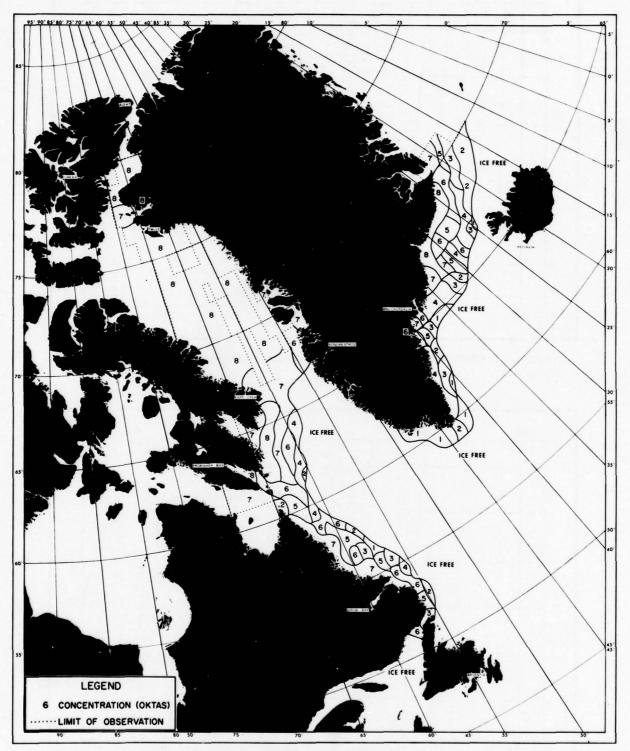


FIGURE 54A MEAN ICE CONCENTRATION 1-15 JANUARY

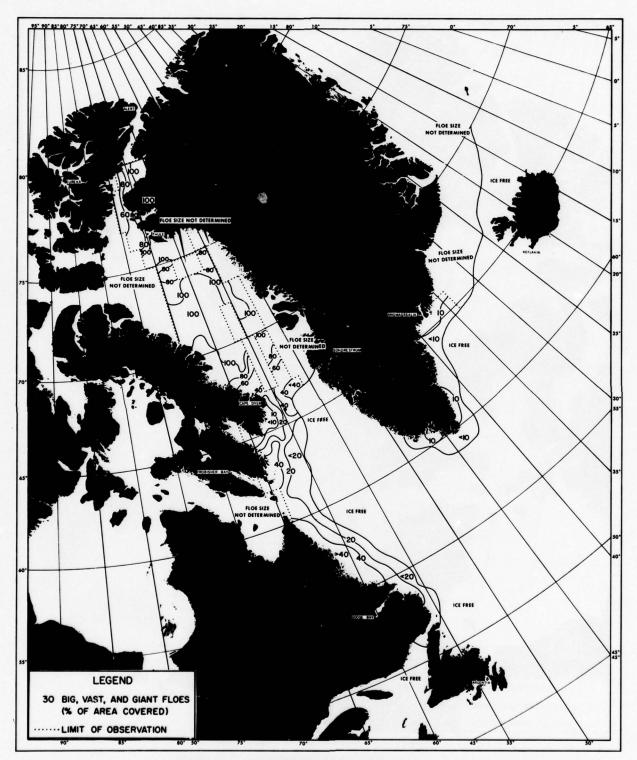


FIGURE 54B MEAN FLOE SIZE PERCENTAGE 1-15 JANUARY

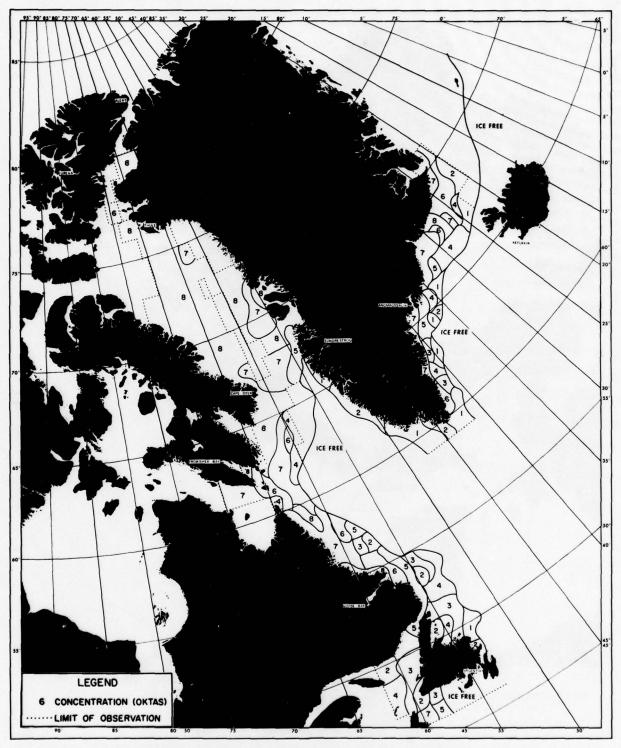


FIGURE 55A MEAN ICE CONCENTRATION 16-31 JANUARY

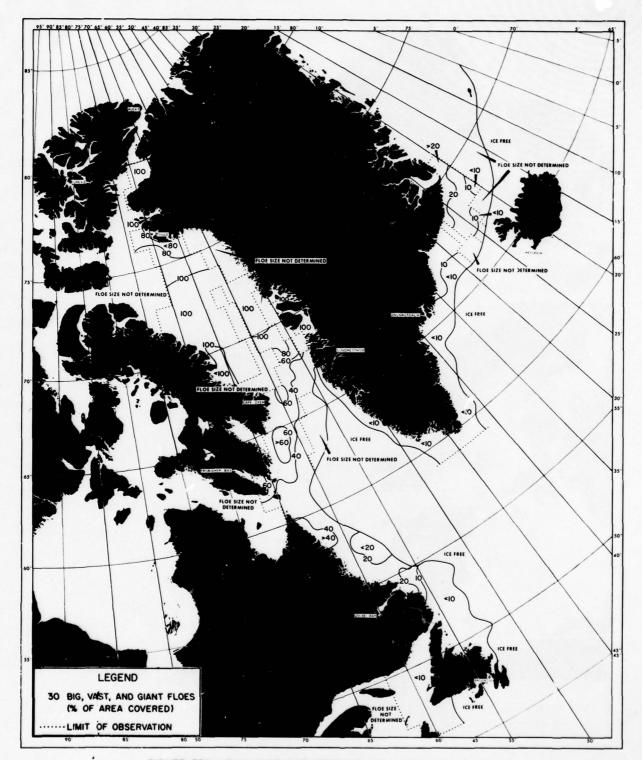


FIGURE 55B MEAN FLOE SIZE PERCENTAGE 16-31 JANUARY

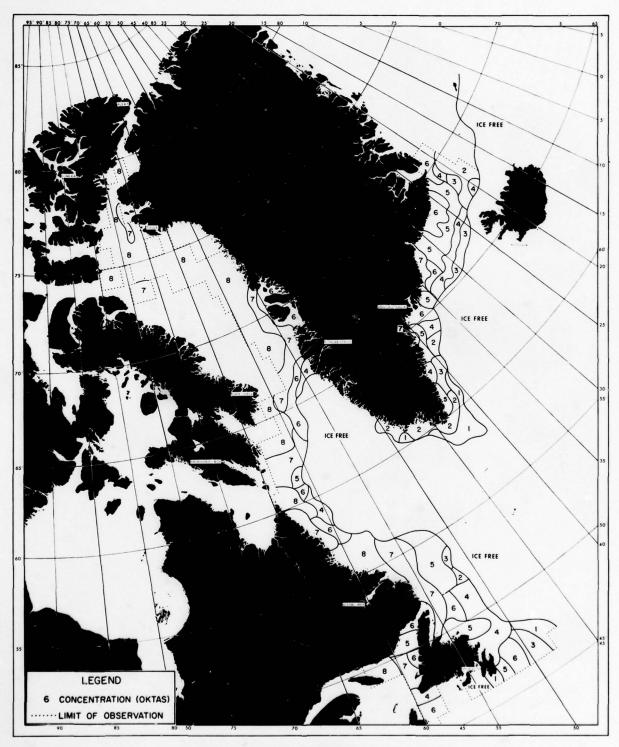


FIGURE 56A MEAN ICE CONCENTRATION 1-15 FEBRUARY

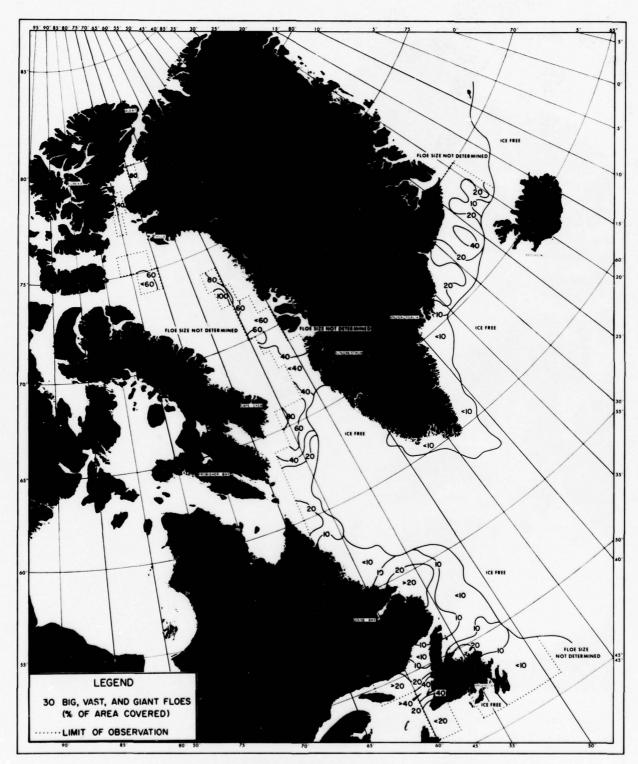


FIGURE 568 MEAN FLOE SIZE PERCENTAGE 1-15 FEBRUARY

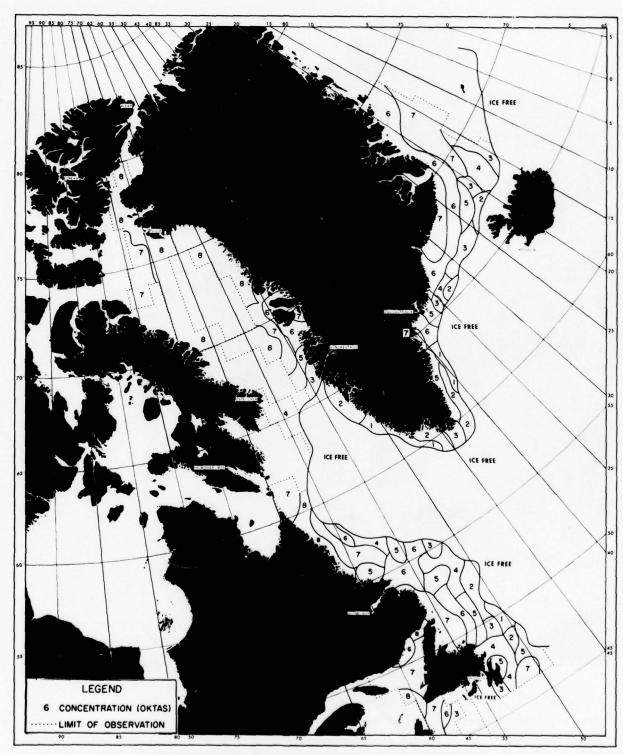


FIGURE 57A MEAN ICE CONCENTRATION 16-28 FEBRUARY

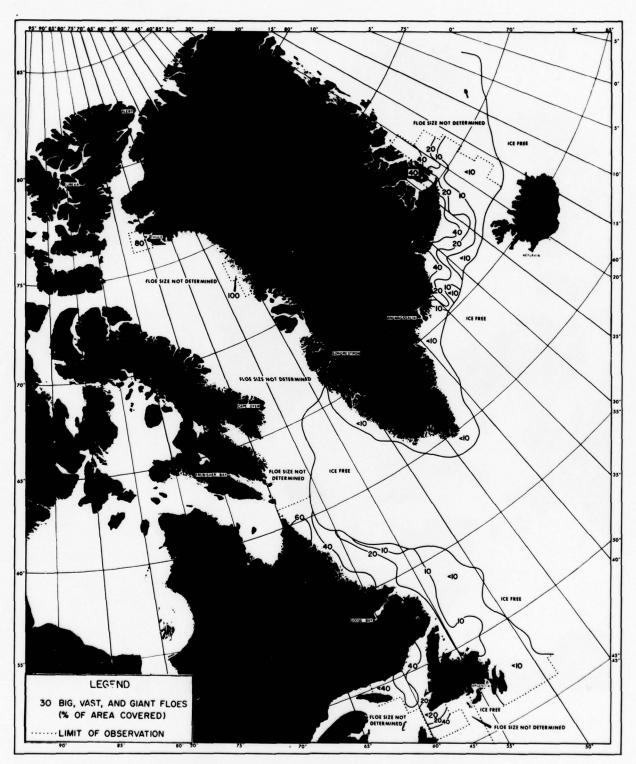


FIGURE 57B MEAN FLOE SIZE PERCENTAGE 16-28 FEBRUARY

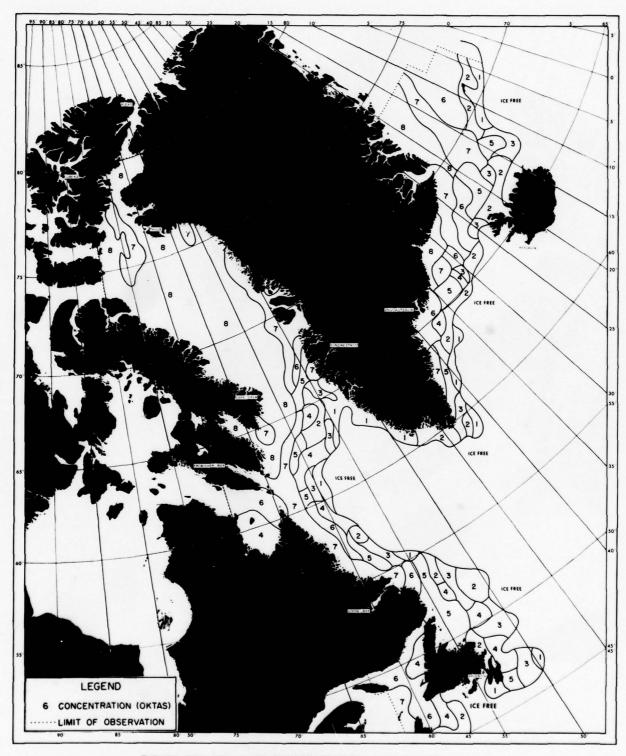


FIGURE 58A MEAN ICE CONCENTRATION 1-15 MARCH

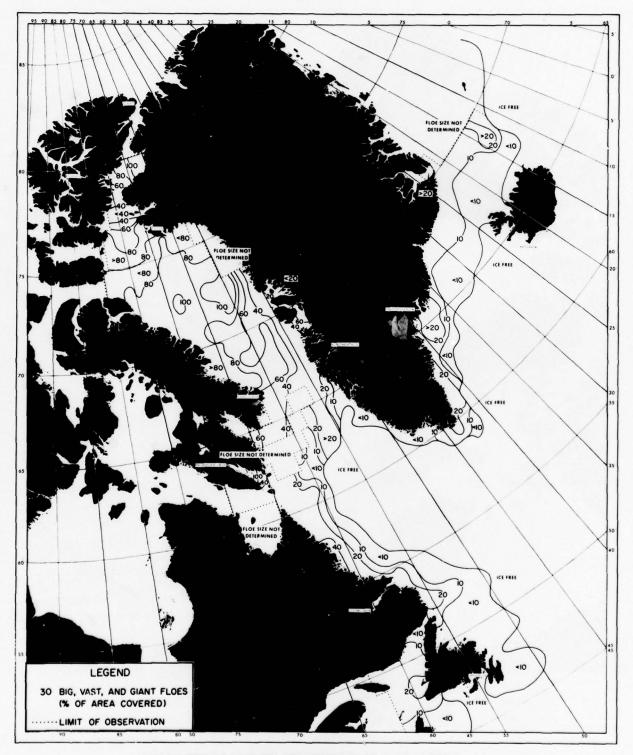


FIGURE 588 MEAN FLOE SIZE PERCENTAGE 1-15 MARCH

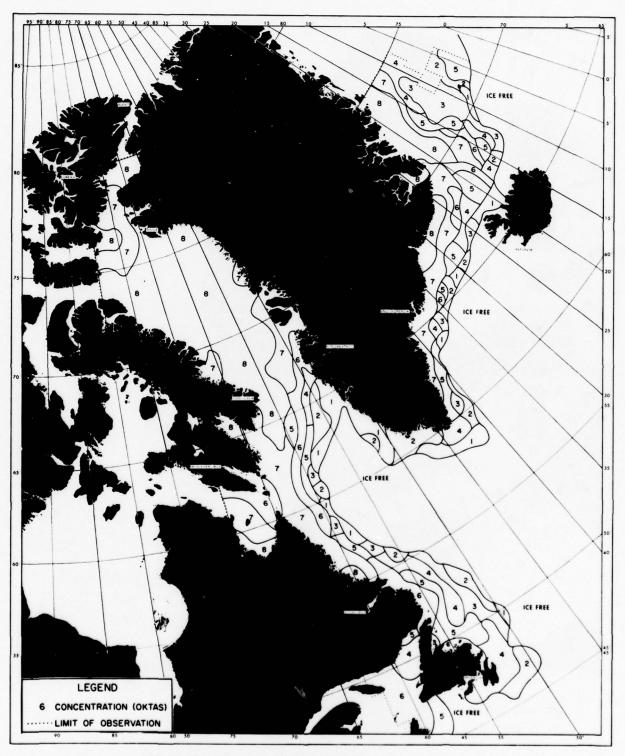


FIGURE 59A MEAN ICE CONCENTRATION 16-31 MARCH

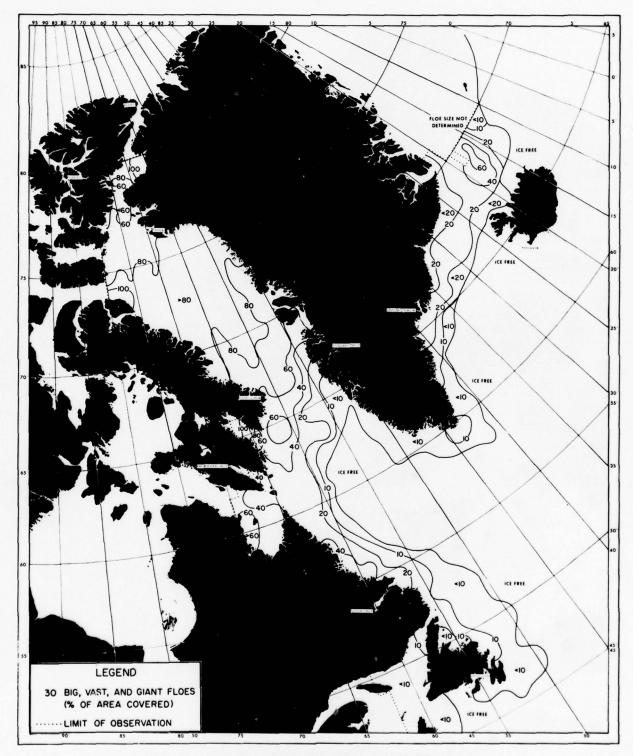


FIGURE 598 MEAN FLOE SIZE PERCENTAGE 16-31 MARCH

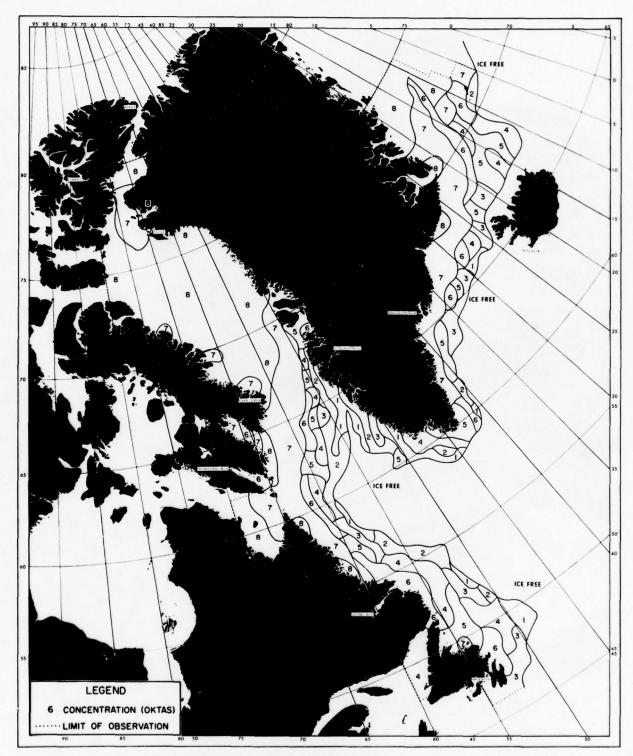


FIGURE 60A MEAN ICE CONCENTRATION 1-15 APRIL

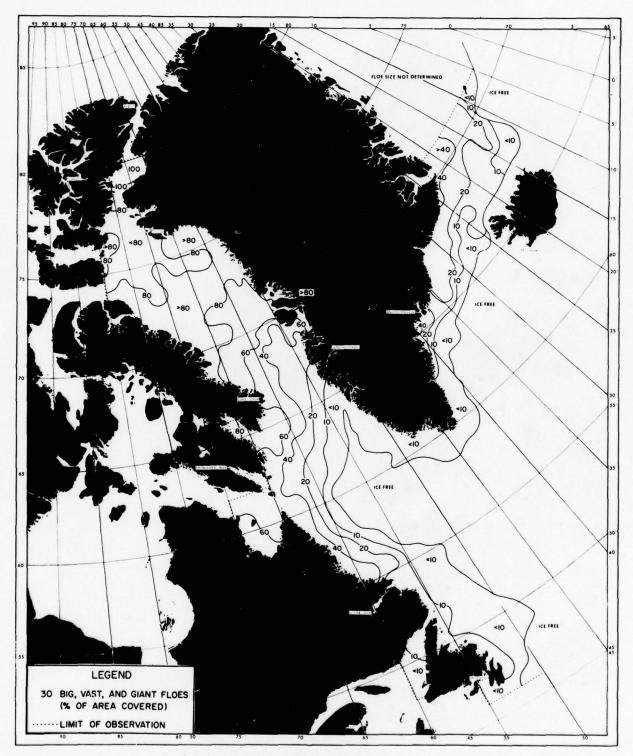


FIGURE 60B MEAN FLOE SIZE PERCENTAGE 1-15 APRIL

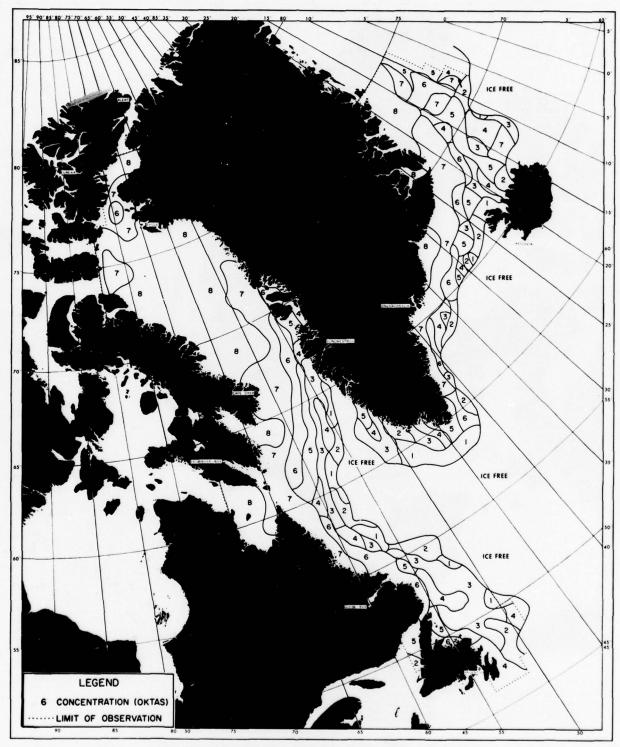


FIGURE 61A MEAN ICE CONCENTRATION 16-30 APRIL

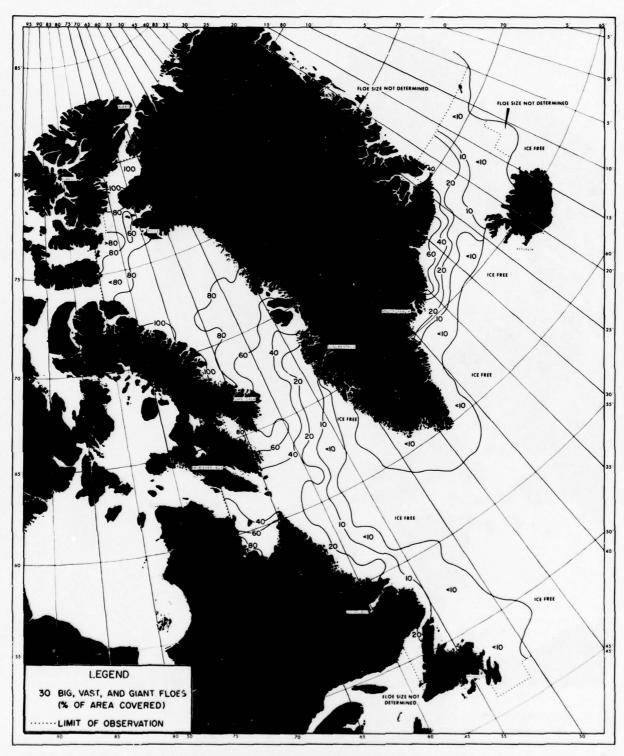


FIGURE 61B MEAN FLOE SIZE PERCENTAGE 16-30 APRIL

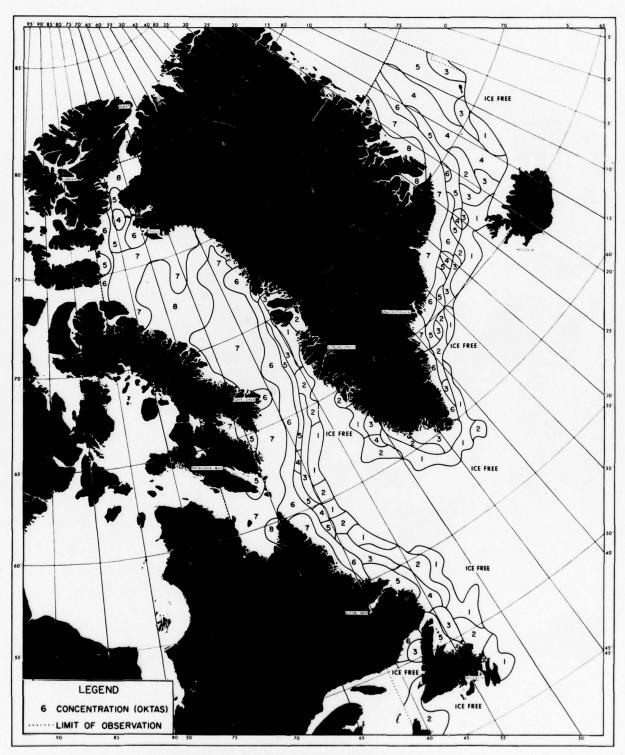


FIGURE 62A MEAN ICE CONCENTRATION 1-15 MAY

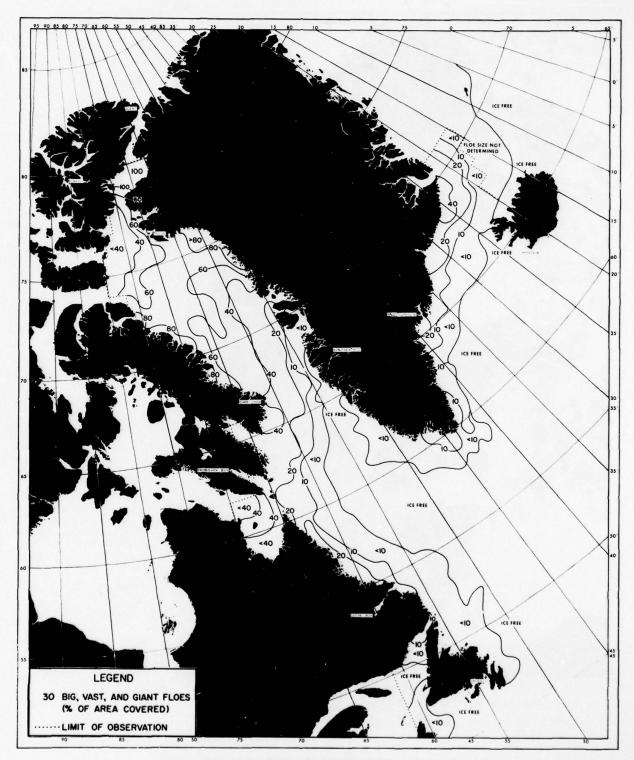


FIGURE 62B MEAN FLOE SIZE PERCENTAGE 1-15 MAY

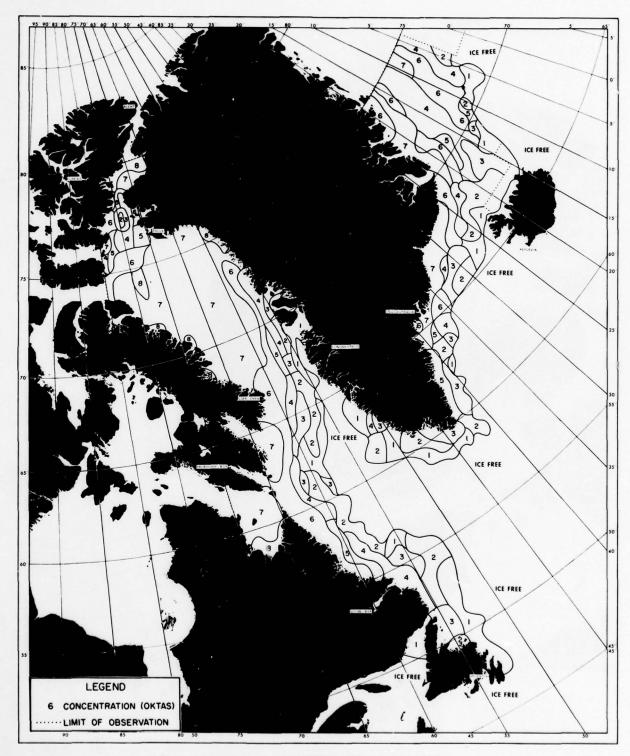


FIGURE 63A MEAN ICE CONCENTRATION 16-31 MAY

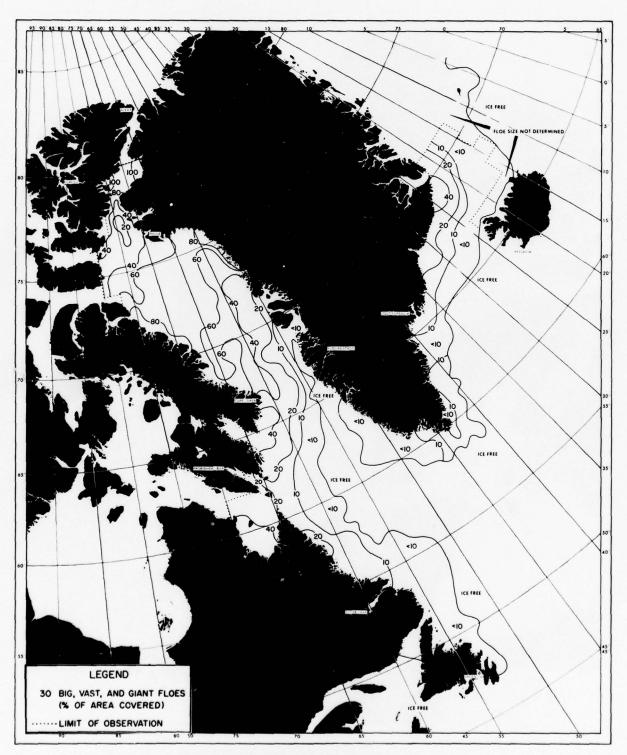


FIGURE 63B MEAN FLOE SIZE PERCENTAGE 16-31 MAY

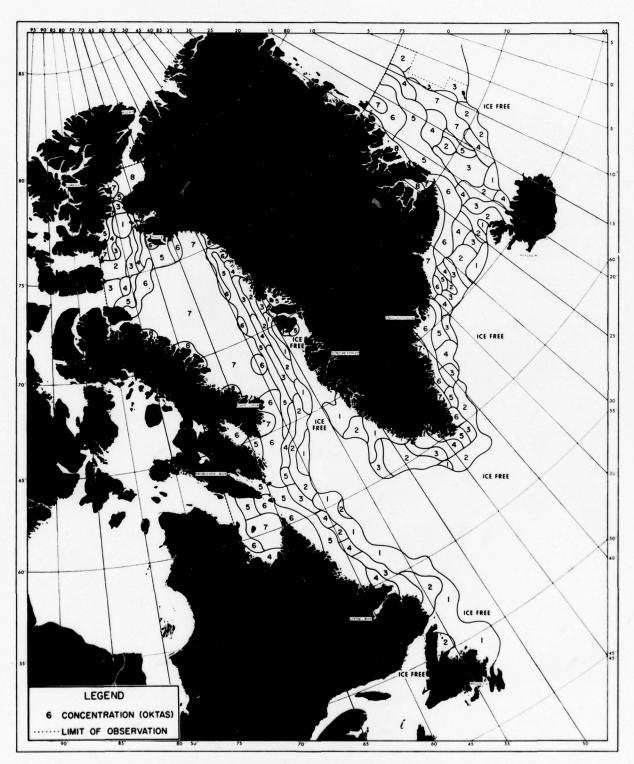


FIGURE 64A MEAN ICE CONCENTRATION 1-15 JUNE

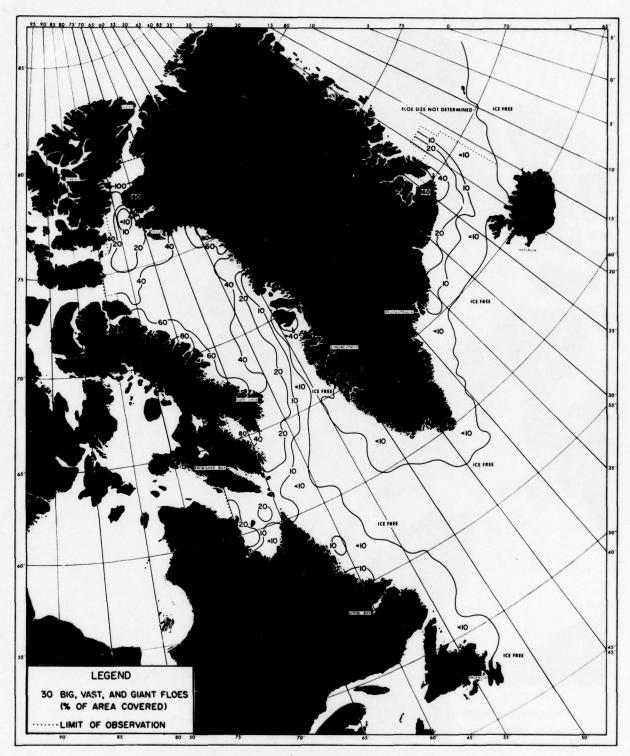


FIGURE 648 MEAN FLOE SIZE PERCENTAGE 1-15 JUNE

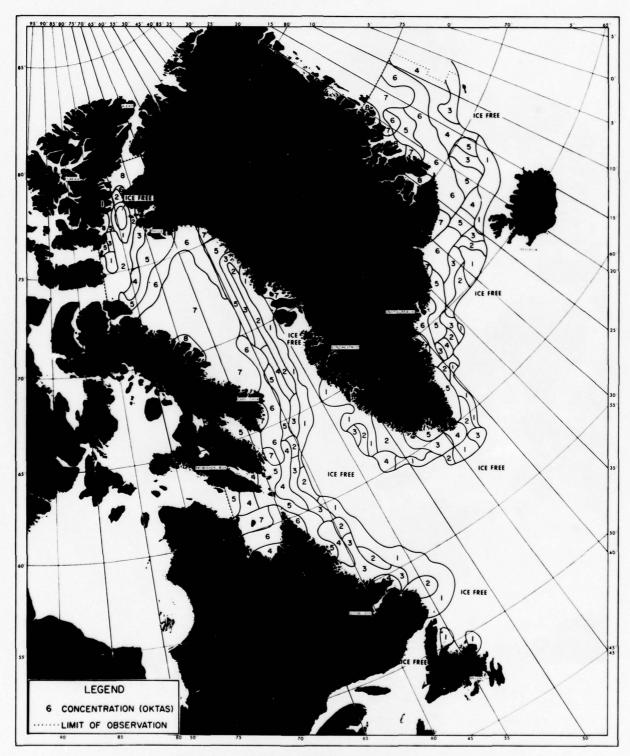


FIGURE 65A MEAN ICE CONCENTRATION 16-30 JUNE

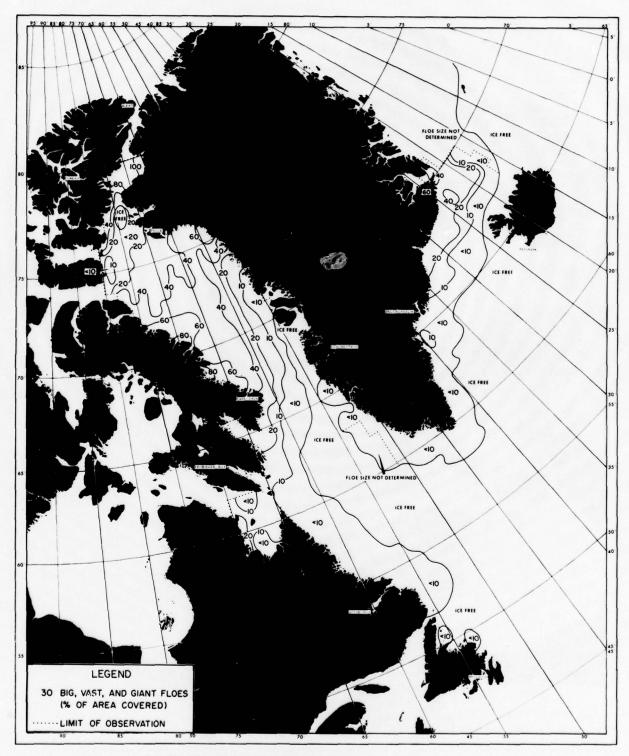


FIGURE 65B MEAN FLOE SIZE PERCENTAGE 16-30 JUNE

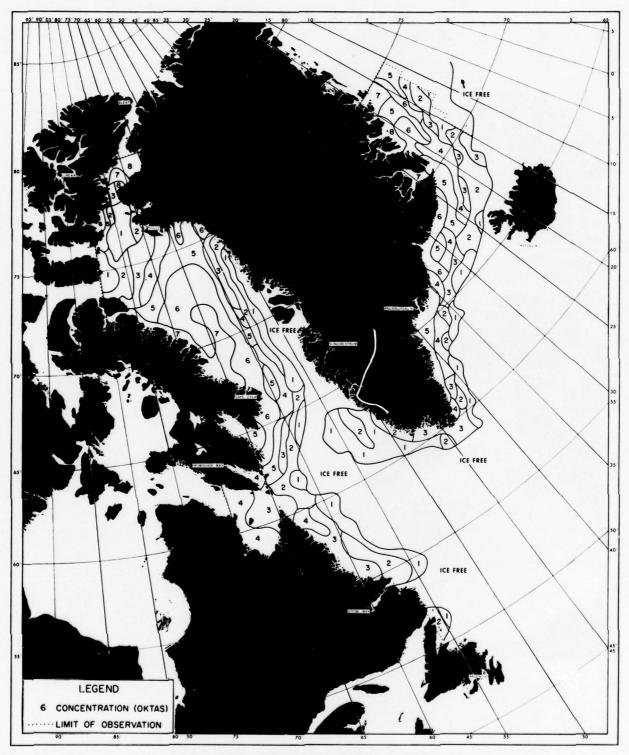


FIGURE 66A MEAN ICE CONCENTRATION 1-15 JULY

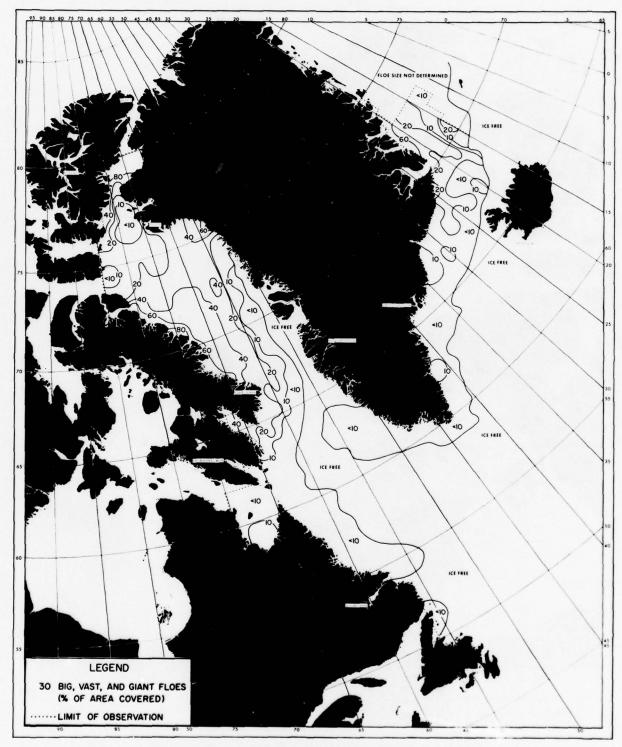


FIGURE 66B MEAN FLOE SIZE PERCENTAGE 1-15 JULY

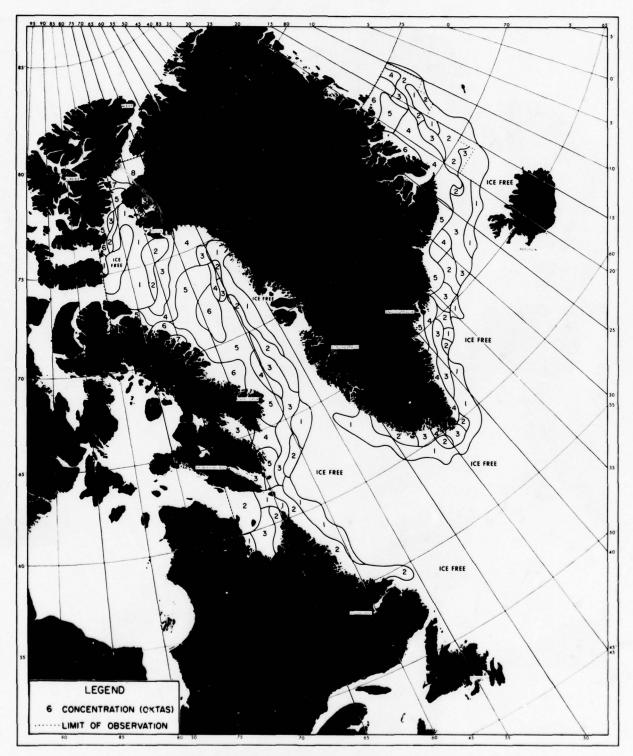


FIGURE 67A MEAN ICE CONCENTRATION 16-31 JULY

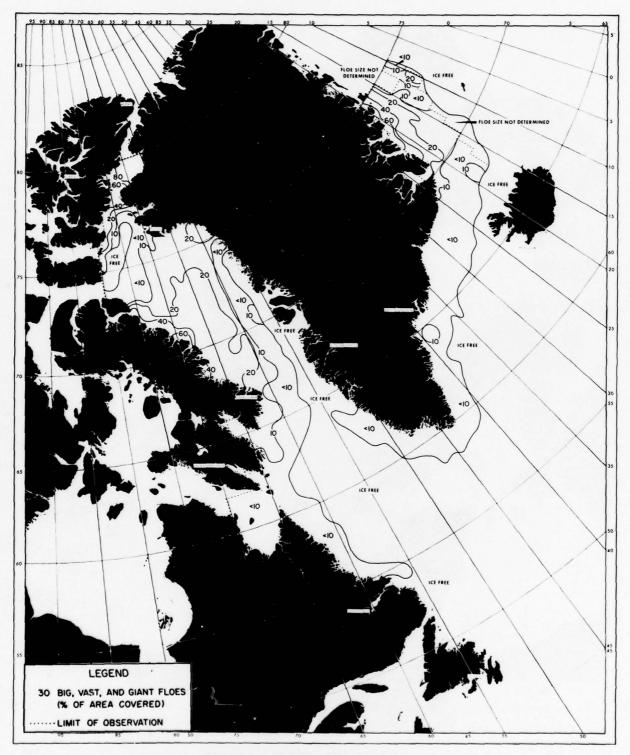


FIGURE 67B MEAN FLOE SIZE PERCENTAGE 16-31 JULY

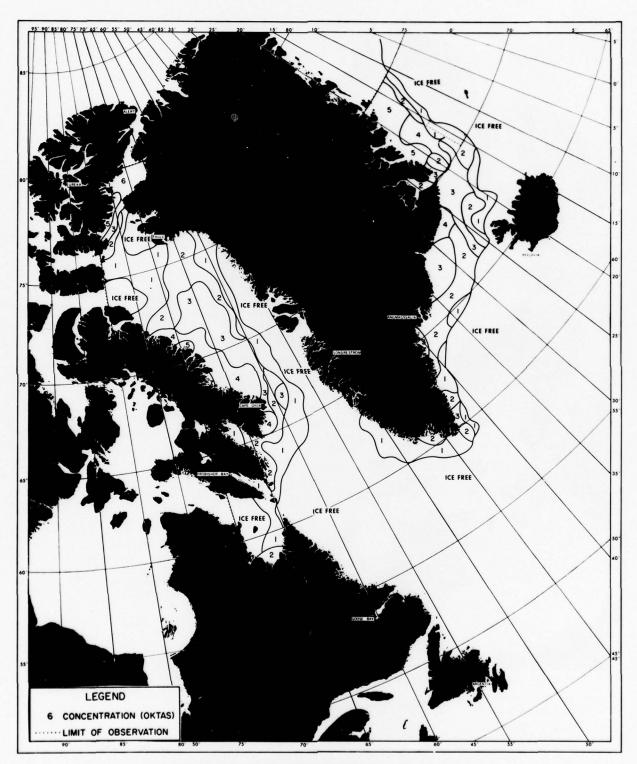


FIGURE 68A MEAN ICE CONCENTRATION 1-15 AUGUST

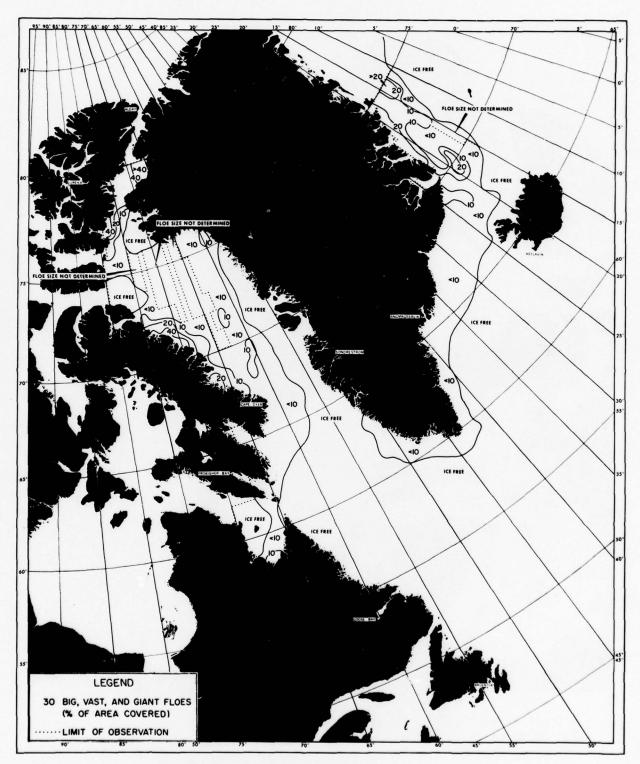


FIGURE 68B MEAN FLOE SIZE PERCENTAGE 1-15 AUGUST

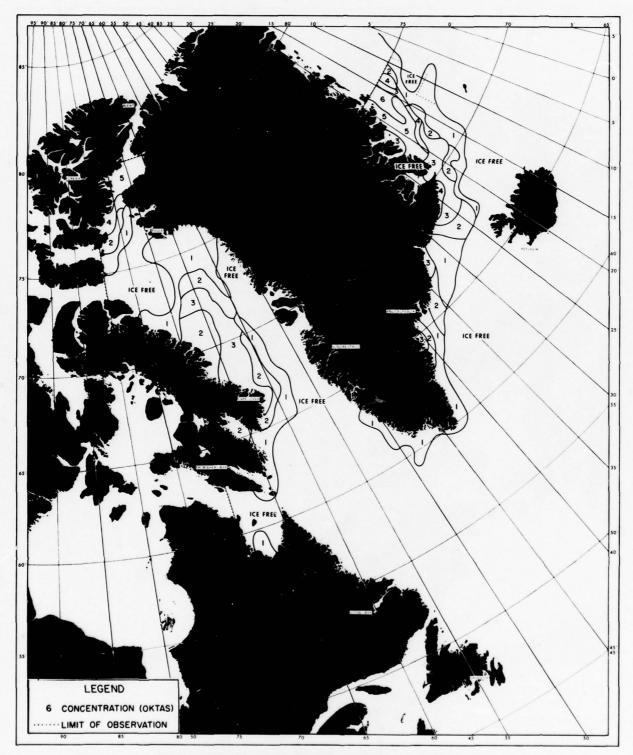


FIGURE 69A MEAN ICE CONCENTRATION 16-31 AUGUST

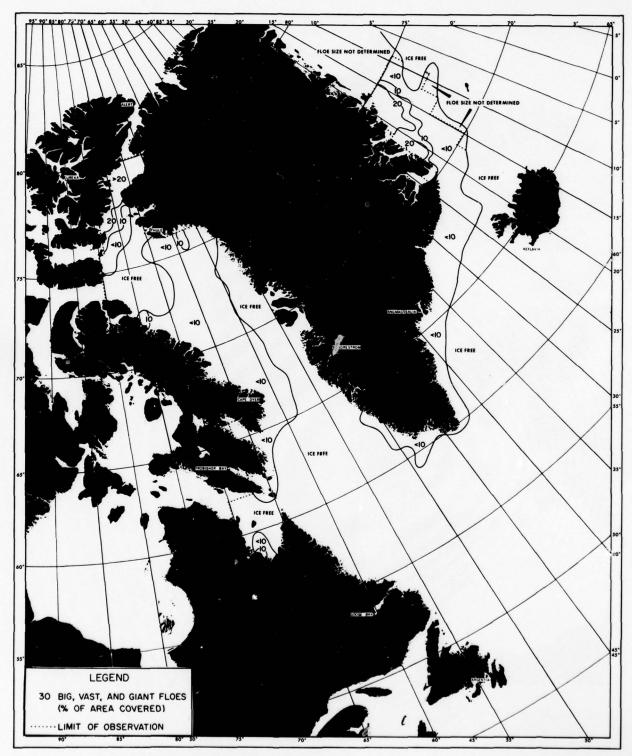


FIGURE 69B MEAN FLOE SIZE PERCENTAGE 16-31 AUGUST

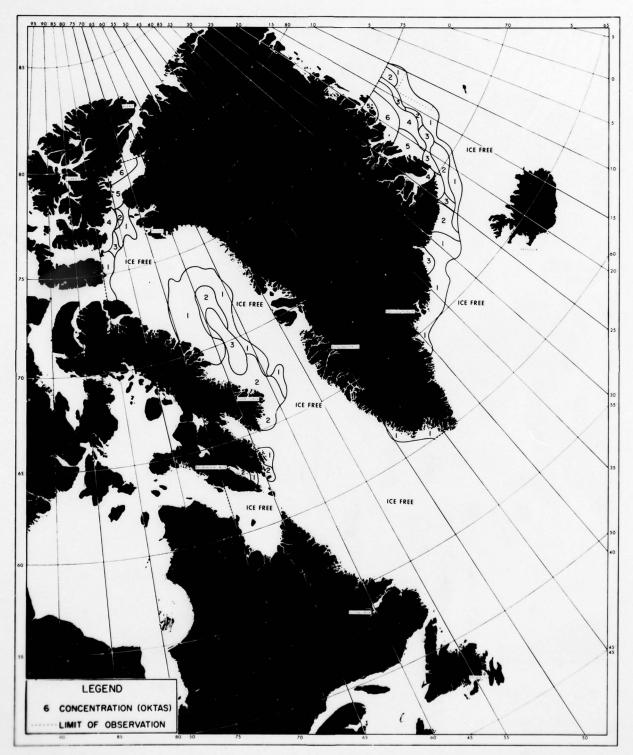


FIGURE 70A MEAN ICE CONCENTRATION 1-15 SEPTEMBER

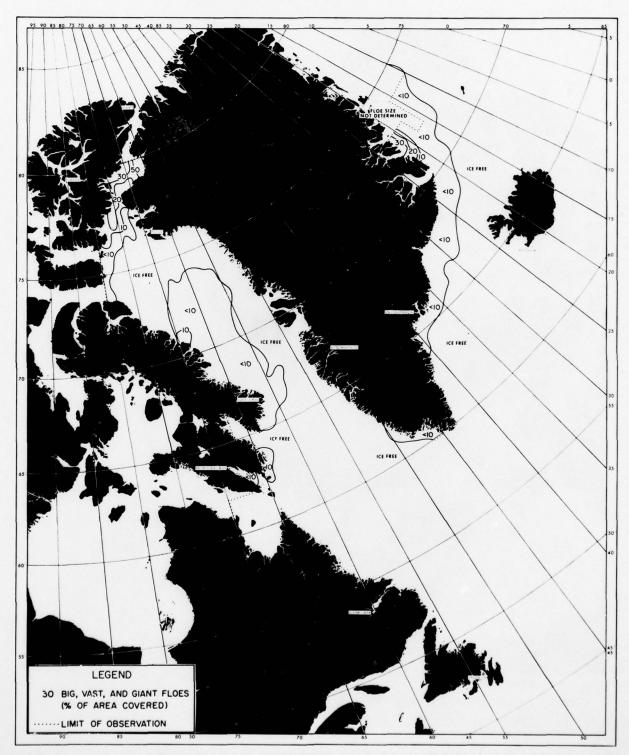


FIGURE 70B MEAN FLOE SIZE PERCENTAGE 1-15 SEPTEMBER



FIGURE 71A MEAN ICE CONCENTRATION 16-30 SEPTEMBER

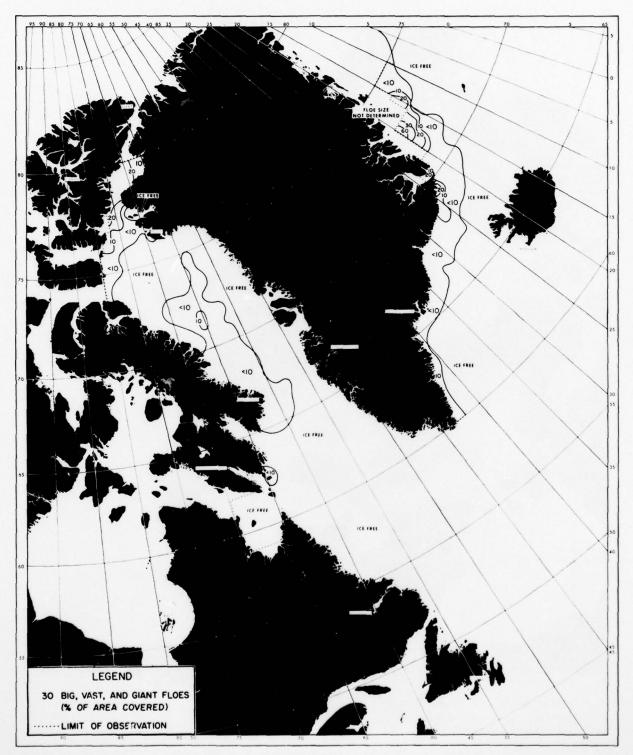


FIGURE 71B MEAN FLOE SIZE PERCENTAGE 16-30 SEPTEMBER

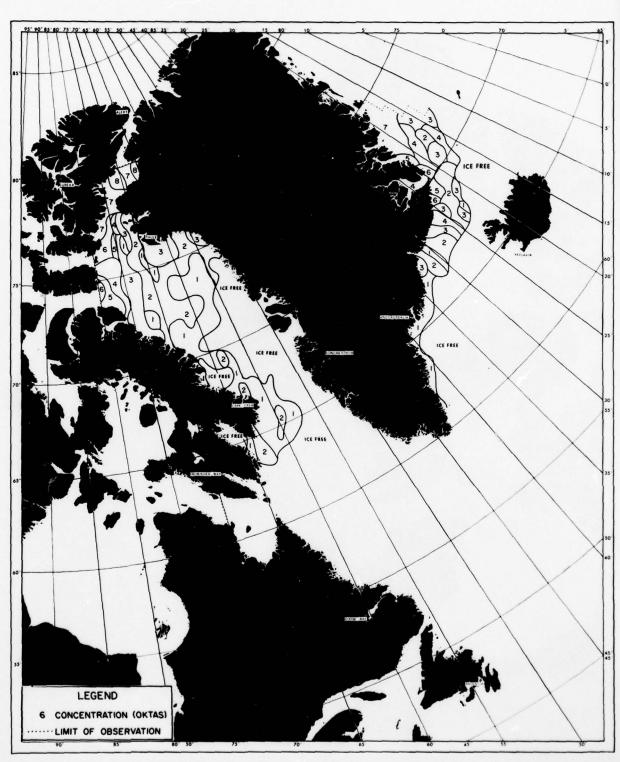


FIGURE 72A MEAN ICE CONCENTRATION 1-15 OCTOBER

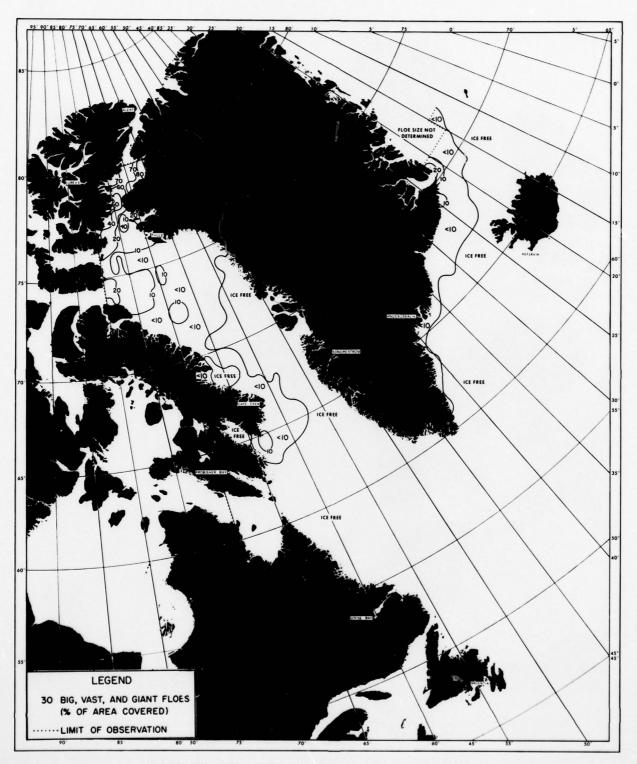


FIGURE 72B MEAN FLOE SIZE PERCENTAGE 1-15 OCTOBER

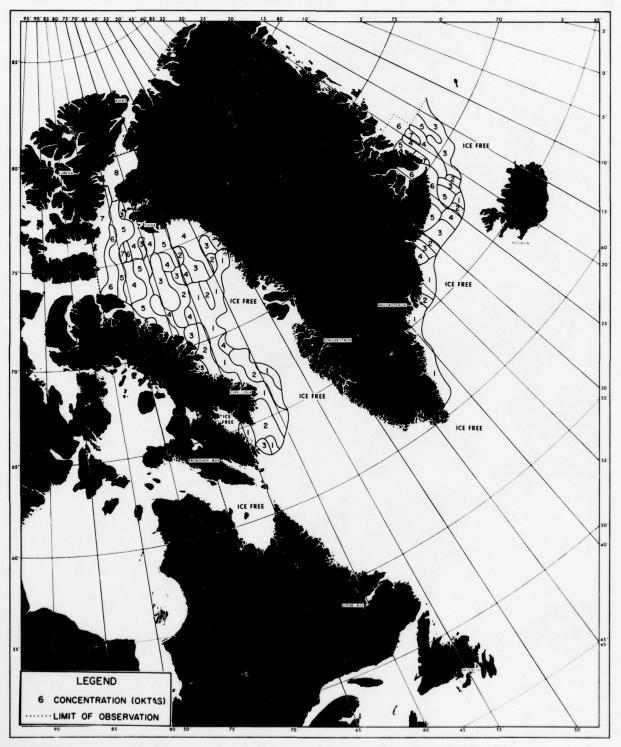


FIGURE 73A MEAN ICE CONCENTRATION 16-31 OCTOBER

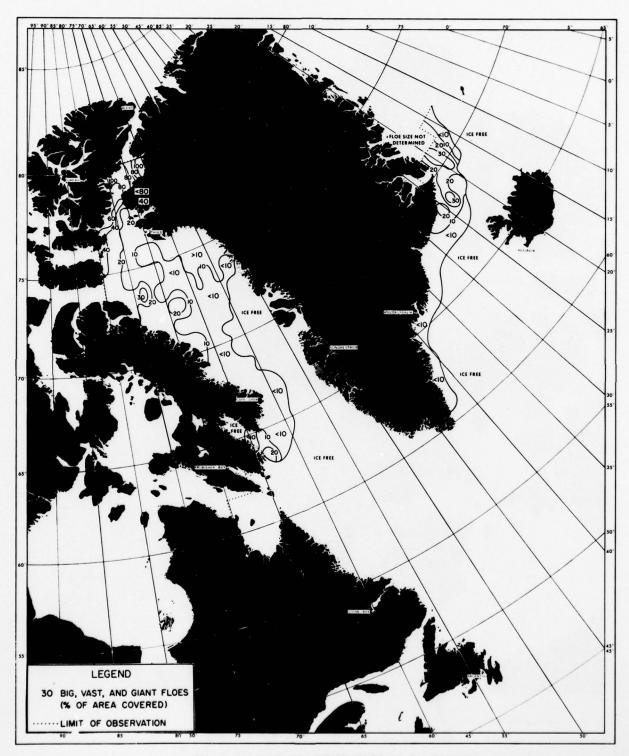


FIGURE 73B MEAN FLOE SIZE PERCENTAGE 16-31 OCTOBER

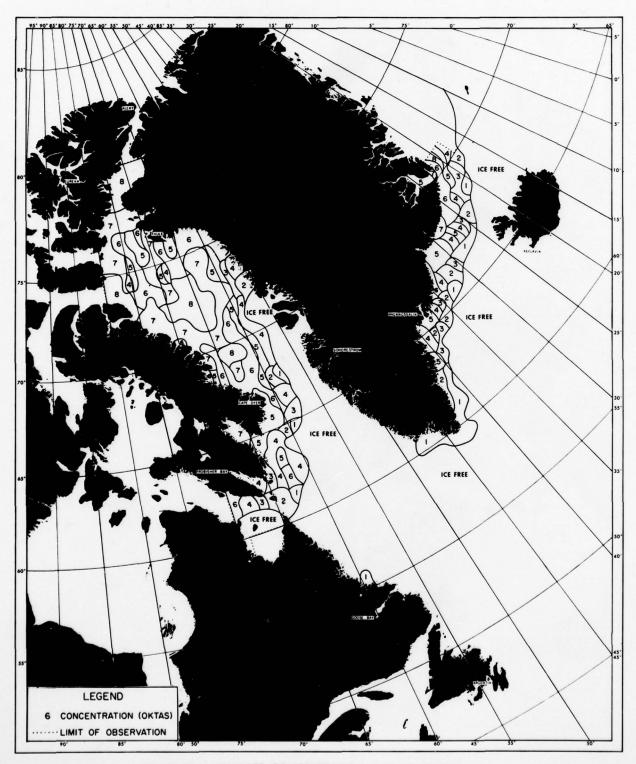


FIGURE 74A MEAN ICE CONCENTRATION 1-15 NOVEMBER

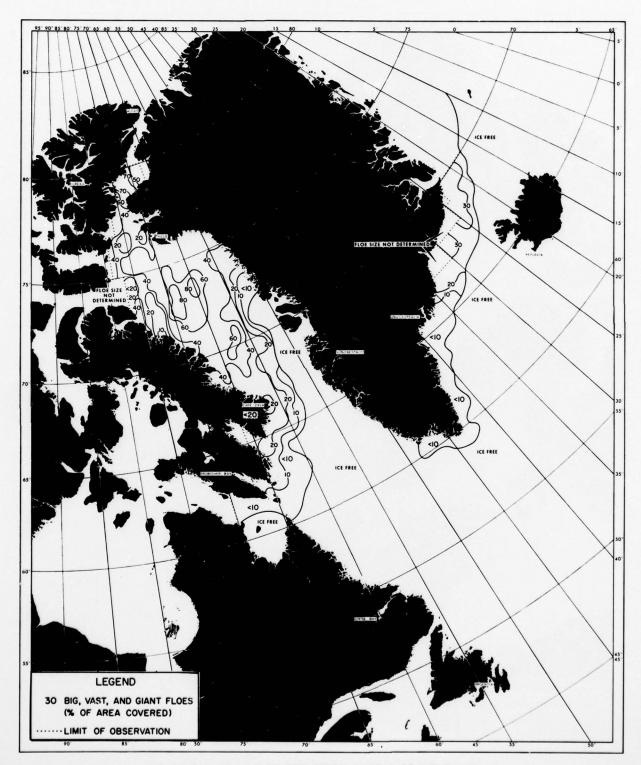


FIGURE 74B MEAN FLOE SIZE PERCENTAGE 1-15 NOVEMBER

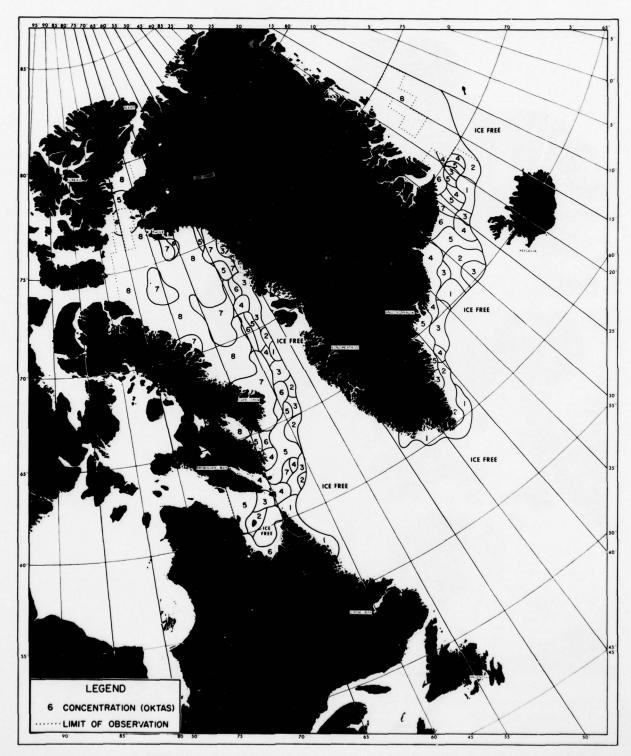


FIGURE 75A MEAN ICE CONCENTRATION 16-30 NOVEMBER

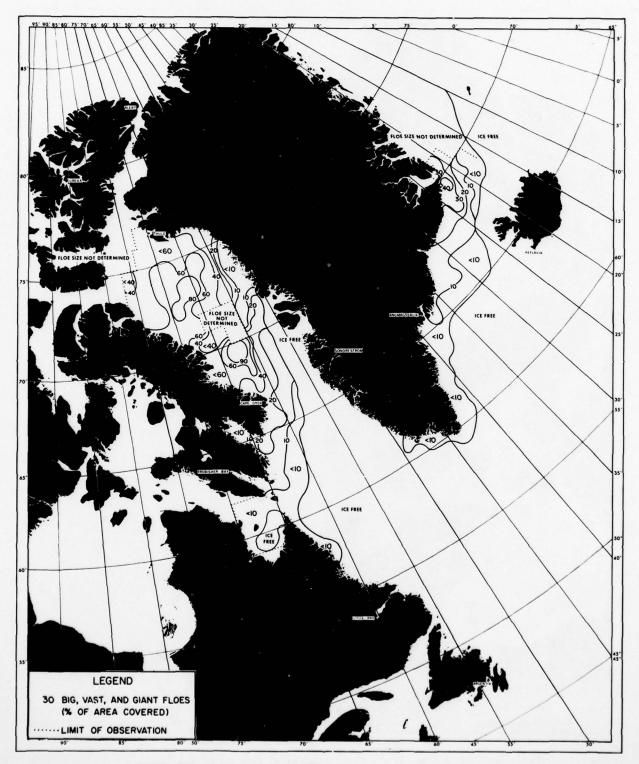


FIGURE 75B MEAN FLOE SIZE PERCENTAGE 16-30 NOVEMBER

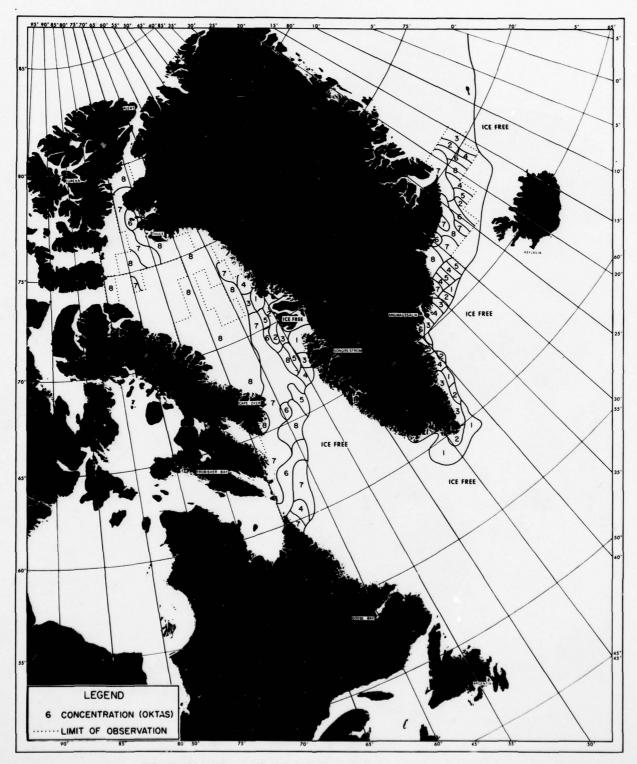


FIGURE 76A MEAN ICE CONCENTRATION 1-15 DECEMBER

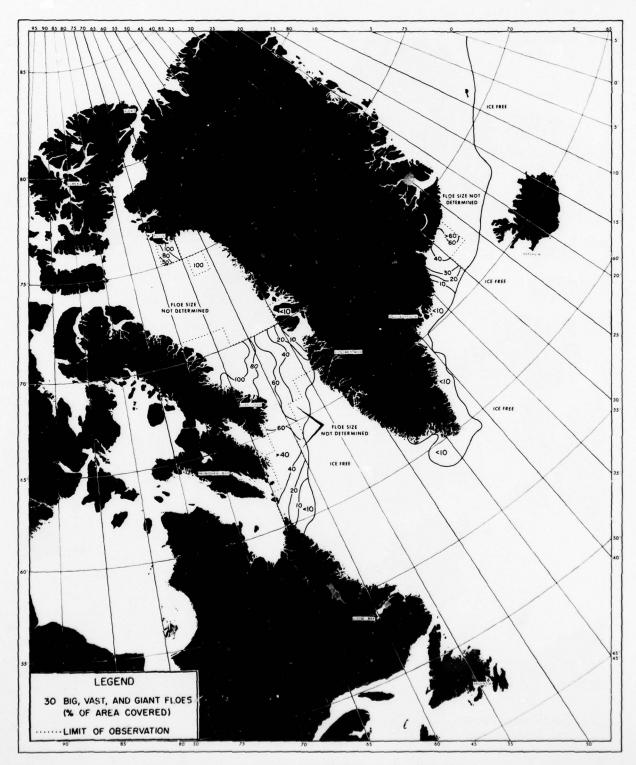
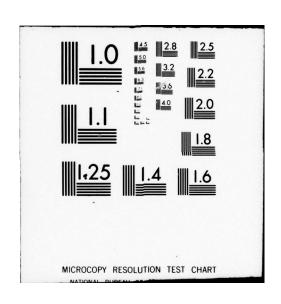


FIGURE 76B MEAN FLOE SIZE PERCENTAGE 1-15 DECEMBER

NAVAL OCEANOGRAPHIC OFFICE NSTL STATION MS
EASTERN ARCTIC AREA 15- AND 30-DAY ICE FORECASTING GUIDE. (U)
APR 79 P A MITCHELL
N00-SP-266 F/6 8/12 AD-A072 930 UNCLASSIFIED NL 3 of 3 ADA 072930 END DATE FILMED 9-79 DDC



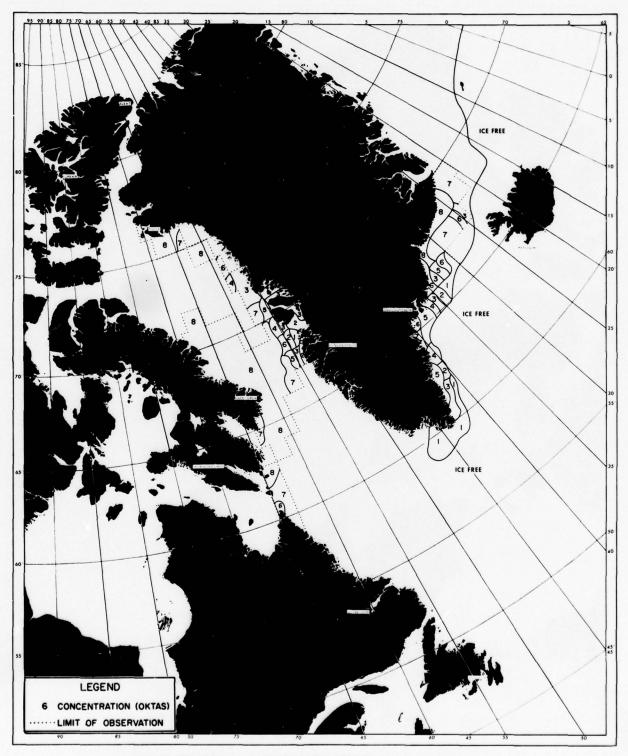


FIGURE 77A MEAN ICE CONCENTRATION 16-31 DECEMBER

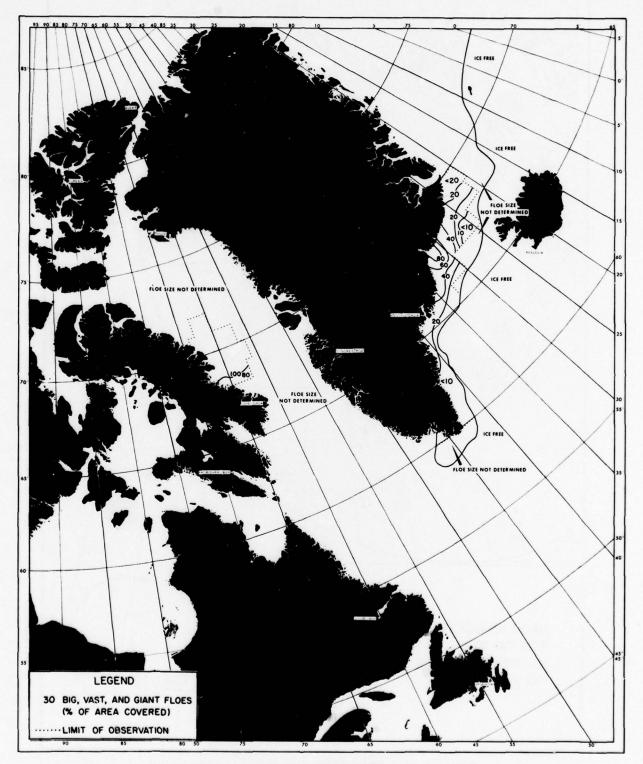


FIGURE 778 MEAN FLOE SIZE PERCENTAGE 16-31 DECEMBER

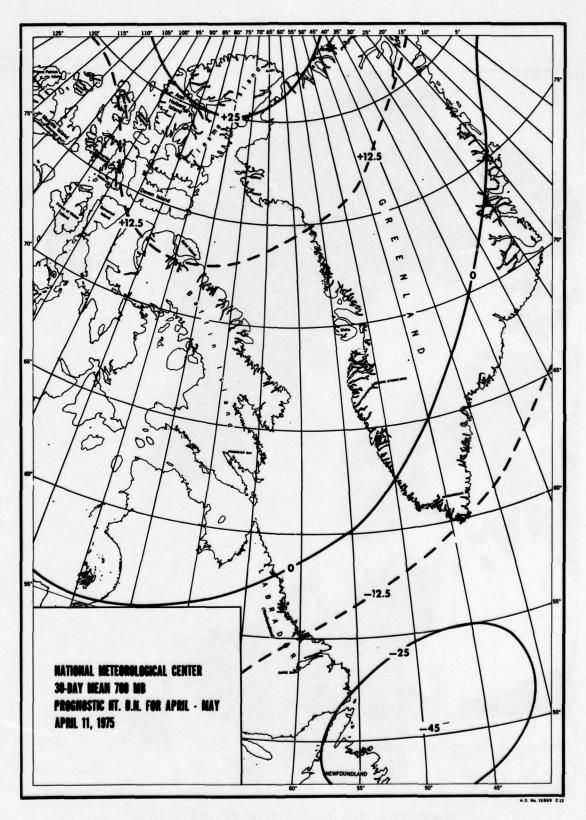


FIGURE 78 NOAA 30-DAY MEAN 700-MILLIBAR PROGNOSTIC HEIGHT DEPARTURE-FROM-NORMAL CHART (IN METERS)

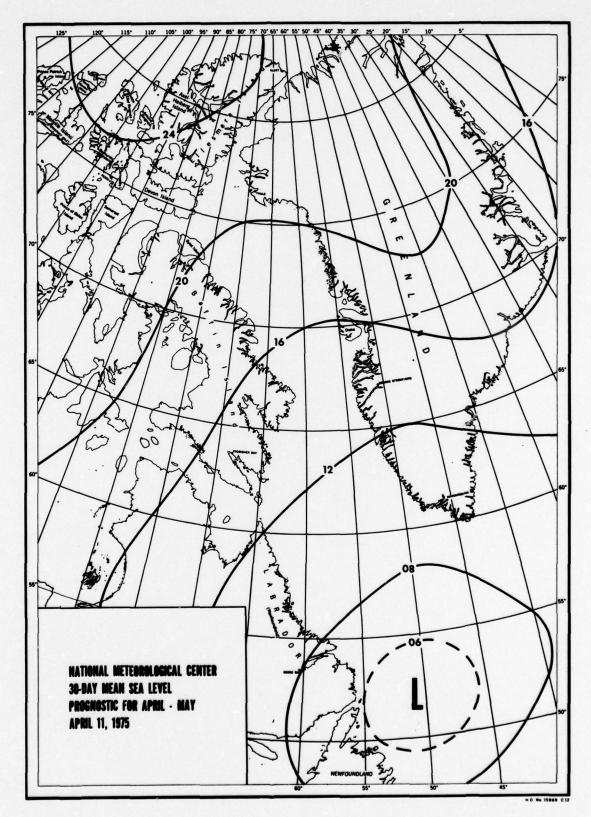


FIGURE 79 NOAA 30-DAY MEAN SEA LEVEL PROGNOSTIC CHART (MB)

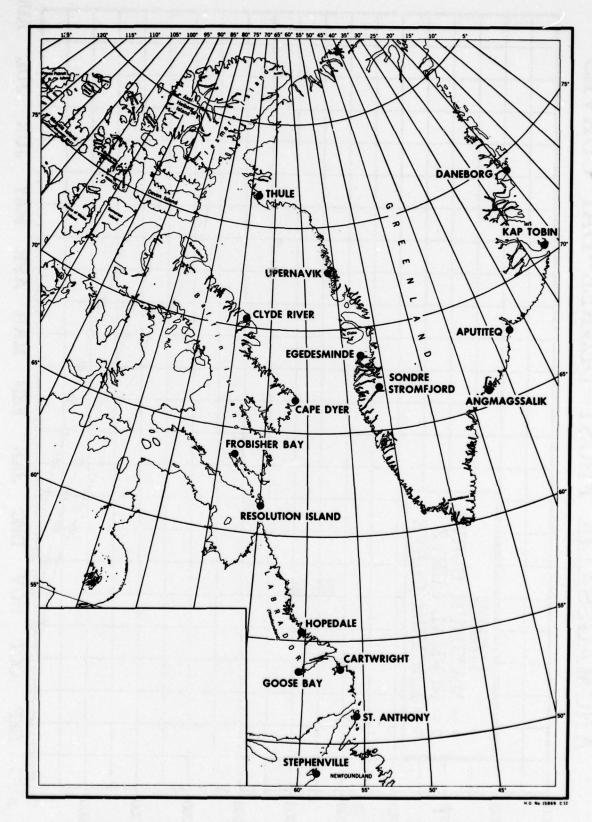


FIGURE 80 LOCATION CHART FOR FROST-DEGREE-DAY, ICE-GROWTH, AND DISINTEGRATION CURVES

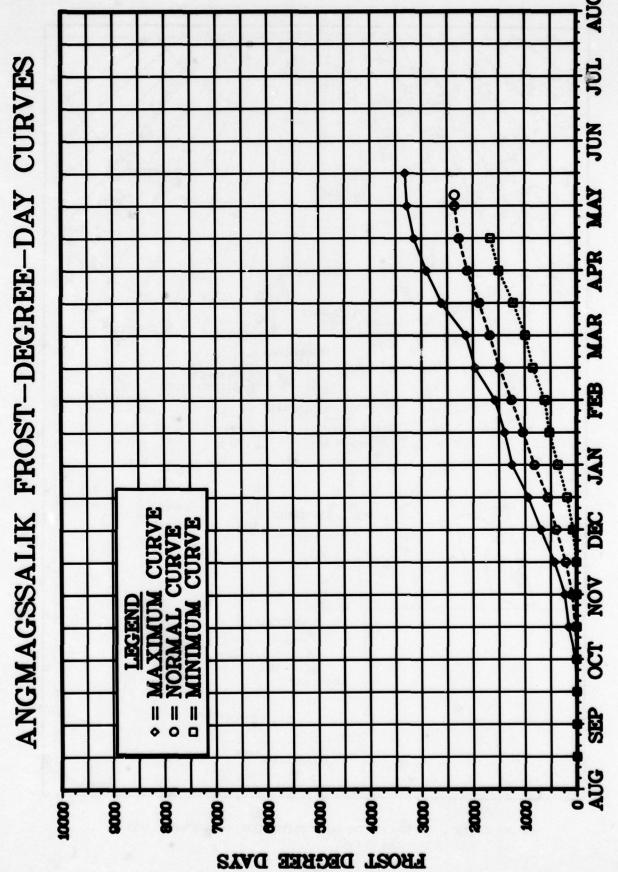


FIGURE 818

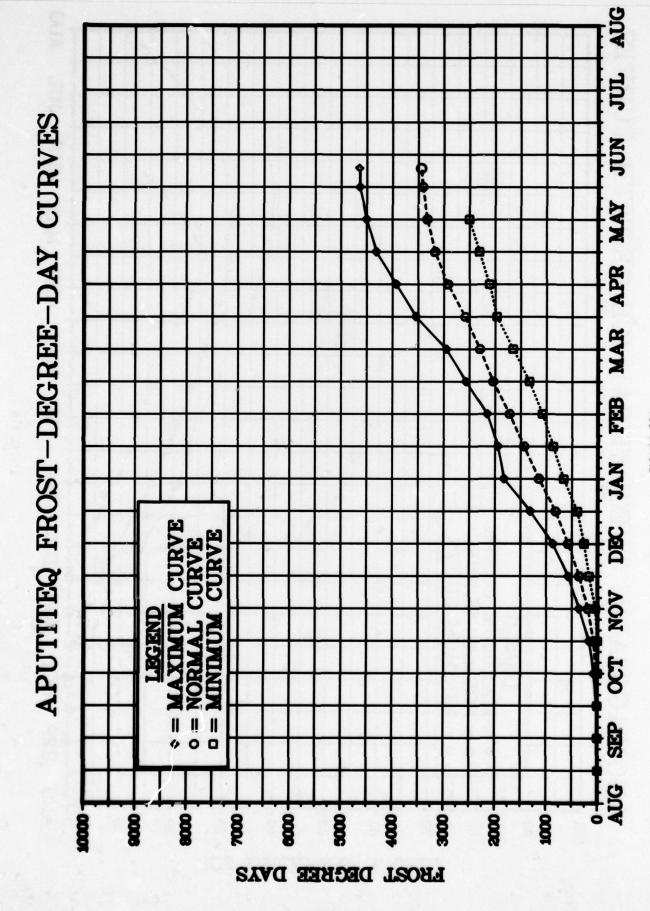
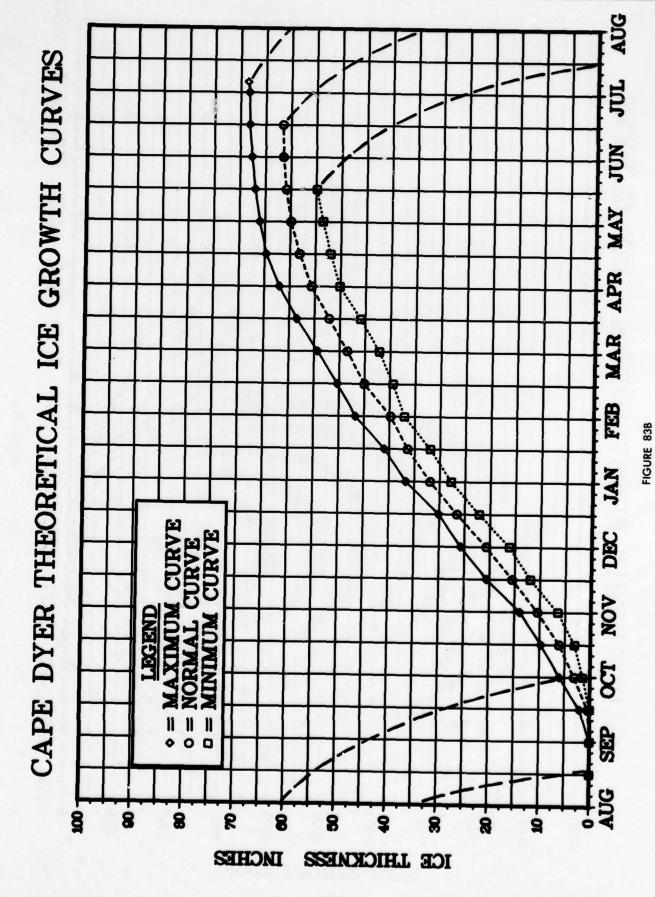
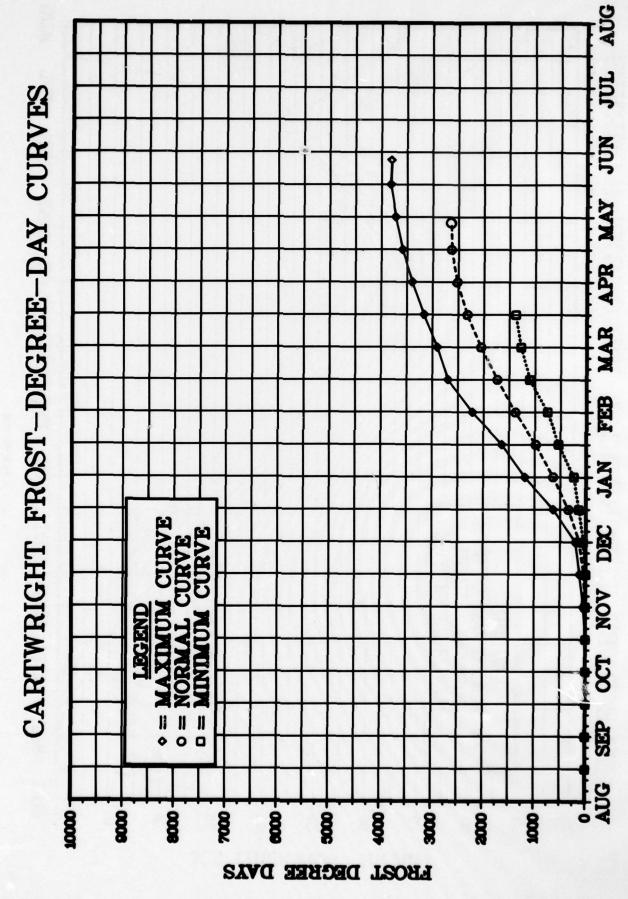


FIGURE 828

193

FIGURE 83A





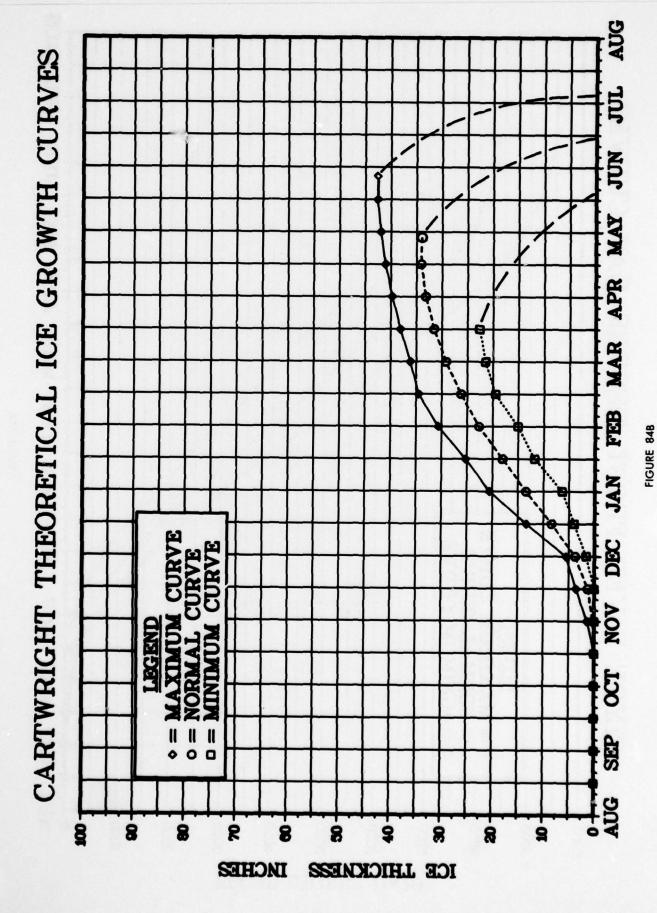
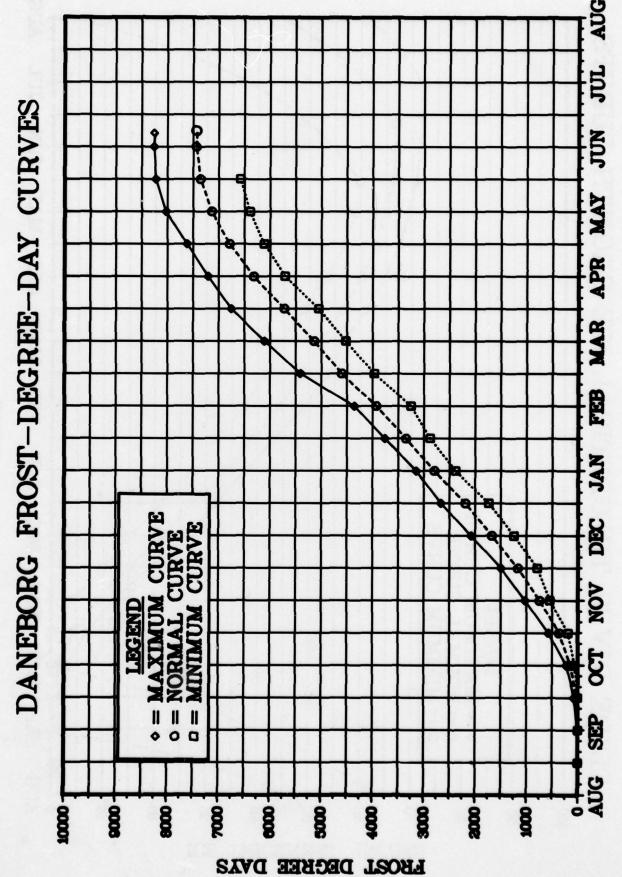


FIGURE 85A

FIGURE 85B



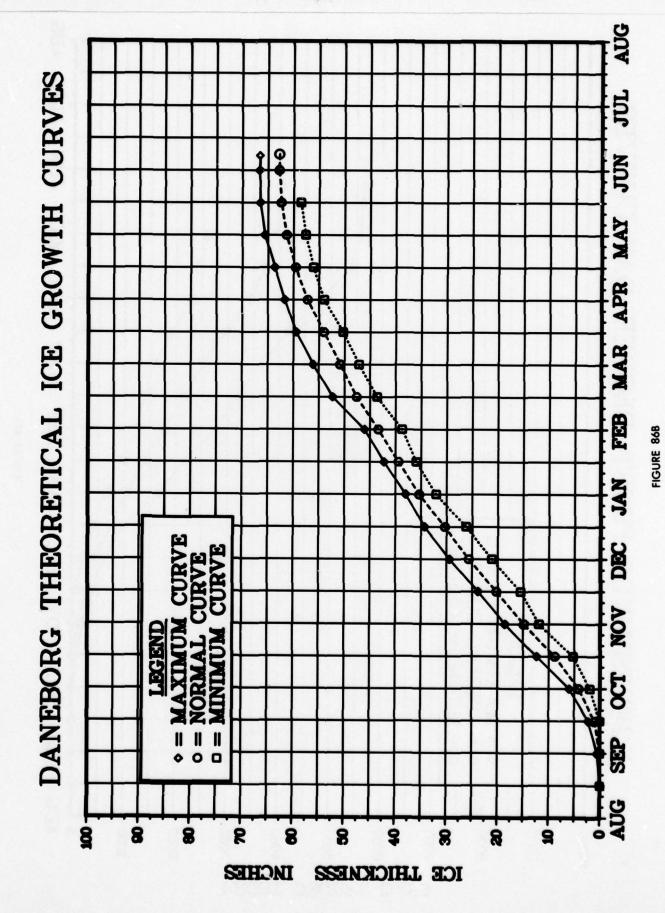
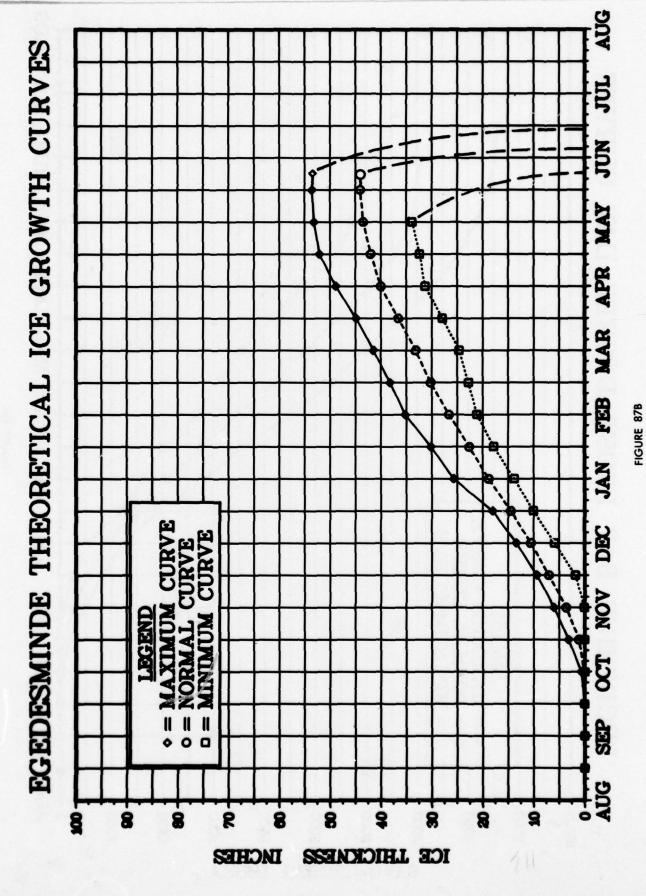
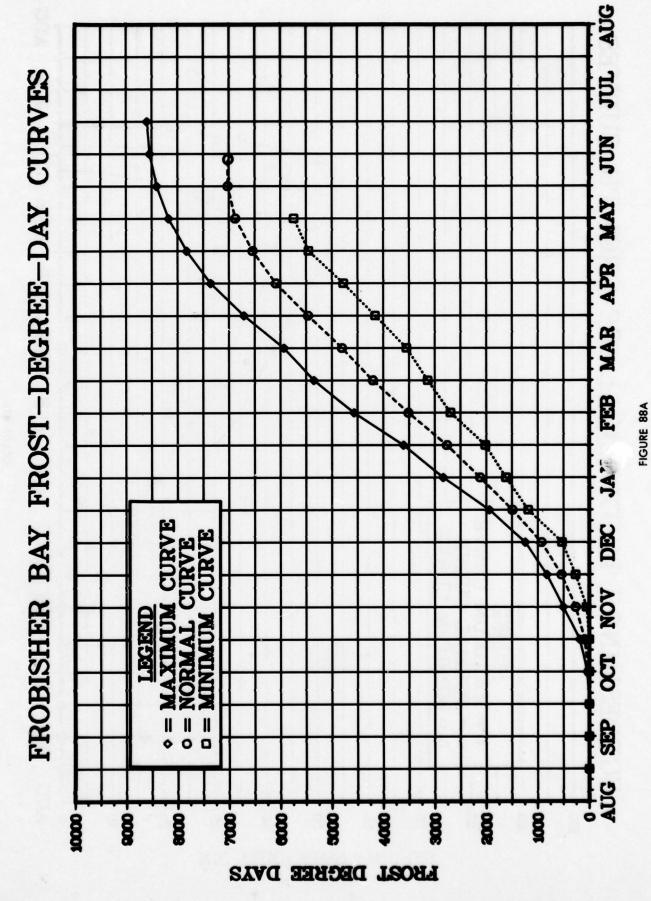


FIGURE 87A





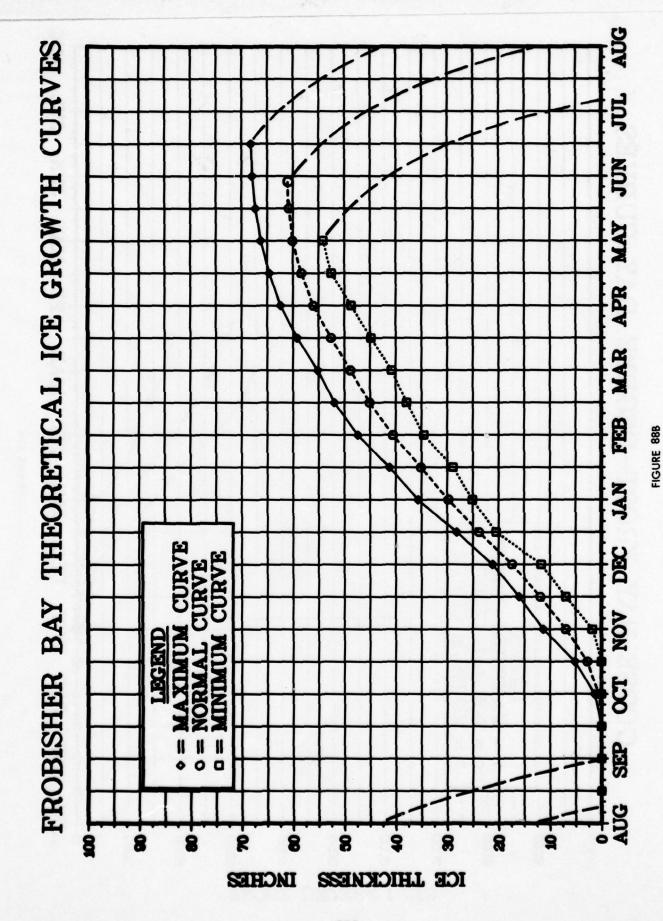


FIGURE 89A

FIGURE 89B

HOPEDALE FROST-DEGREE-DAY CURVES

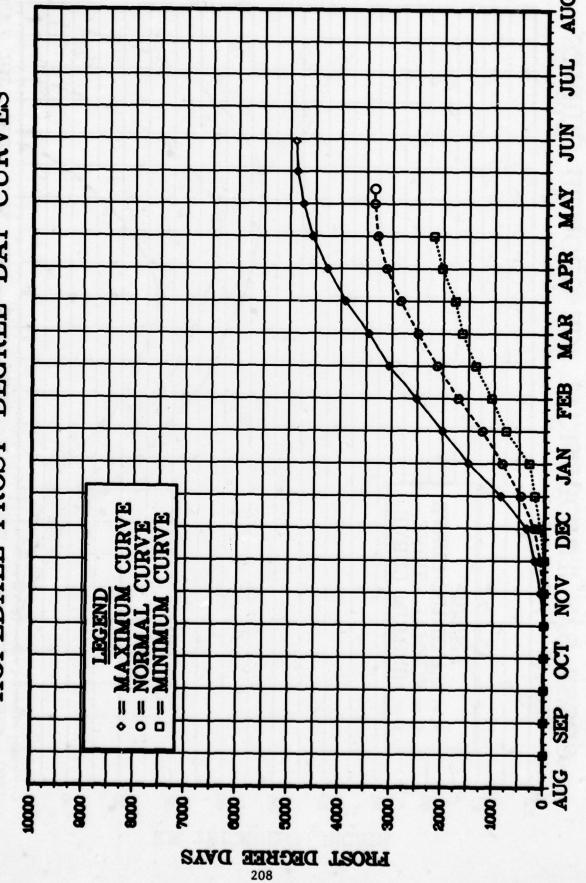


FIGURE 90A

209

FIGURE 91A

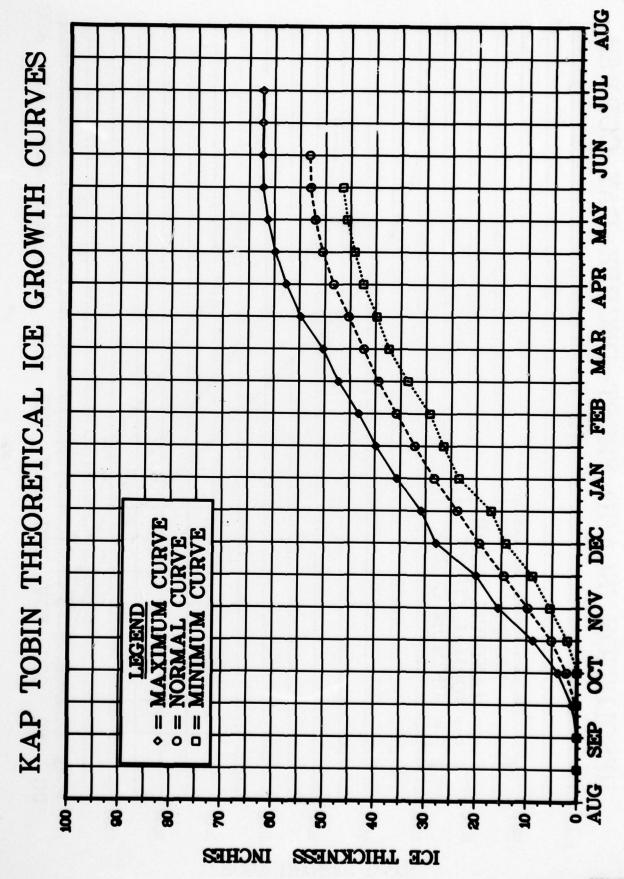


FIGURE 91B

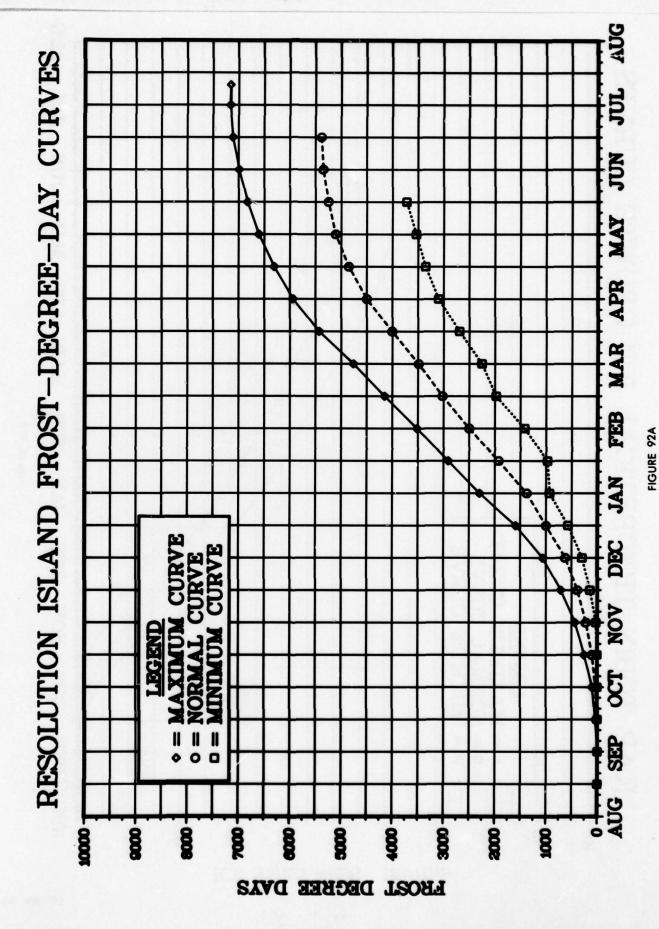
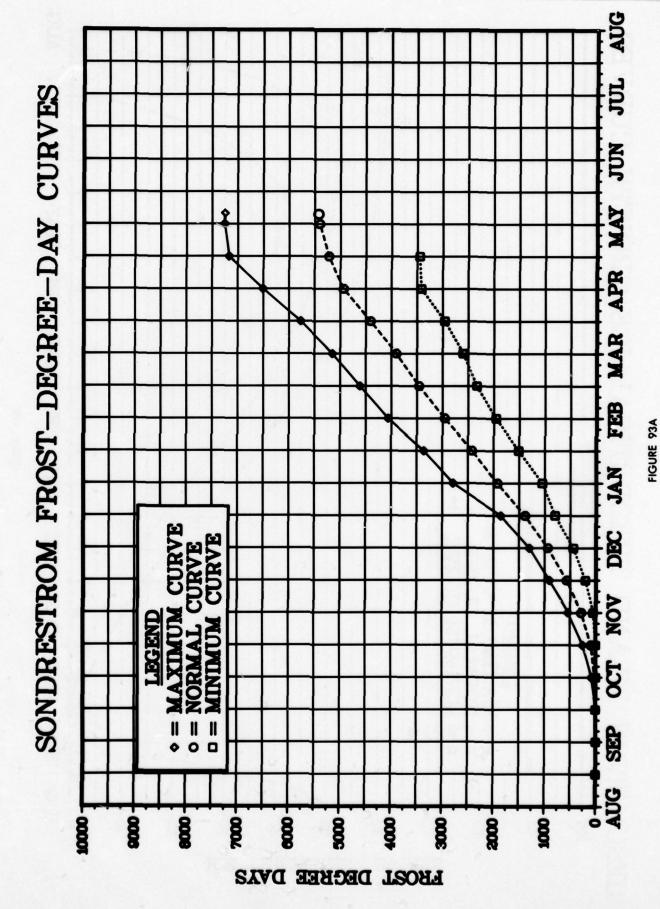
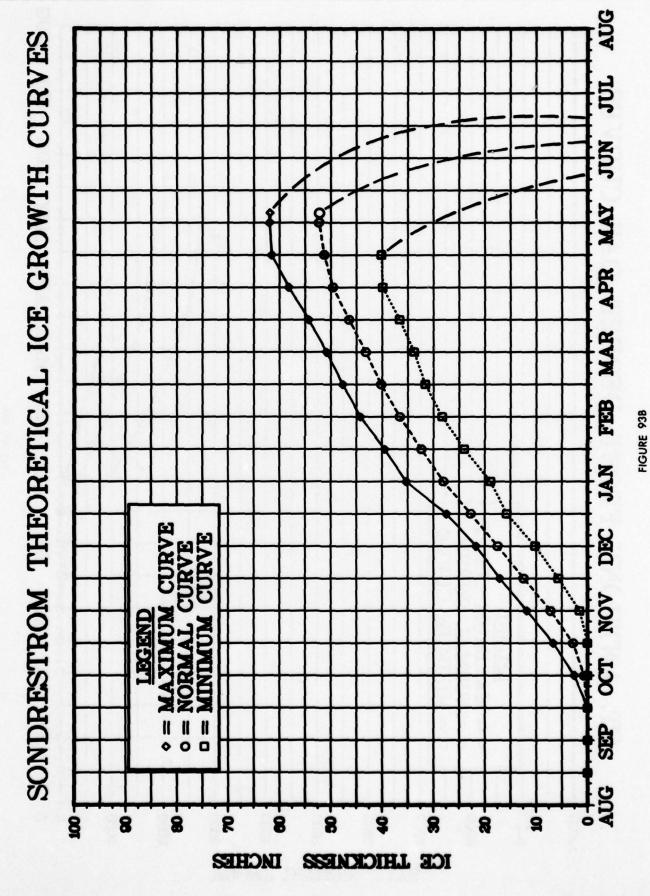


FIGURE 928

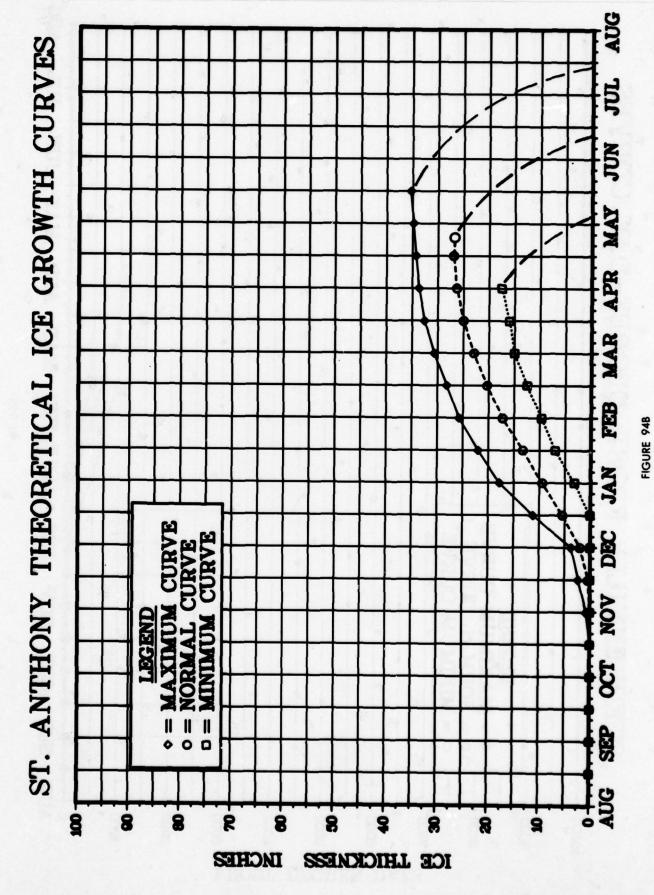




E E ST. ANTHONY FROST-DEGREE-DAY CURVES B Q APR EE CURVE CURVE DEC NOV g 11 SEP 0 900 9 9 8 8 9000 10000 8 8 8 FROST DEGREE DAYS

FIGURE 94A

216



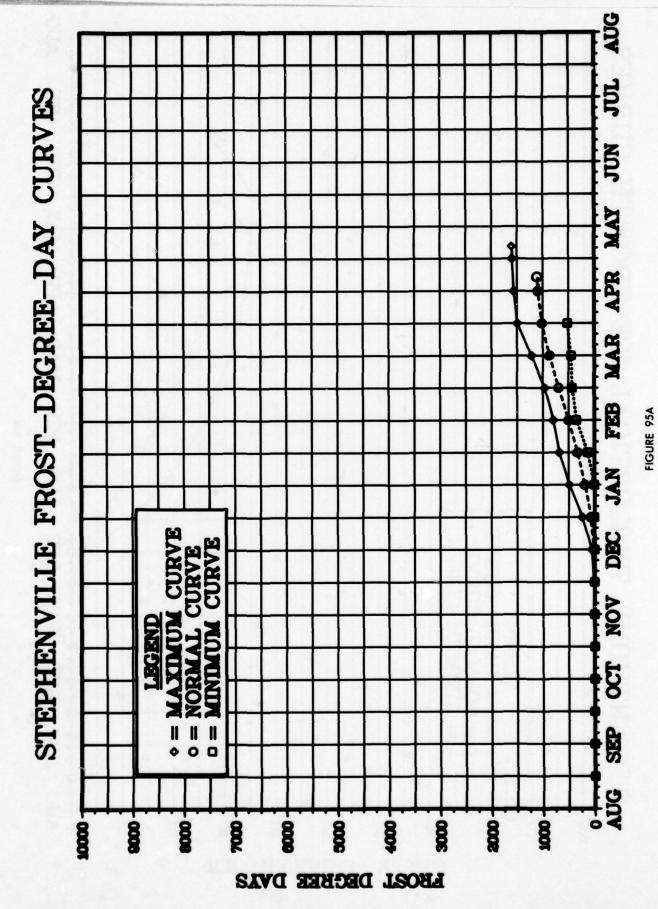


FIGURE 96A

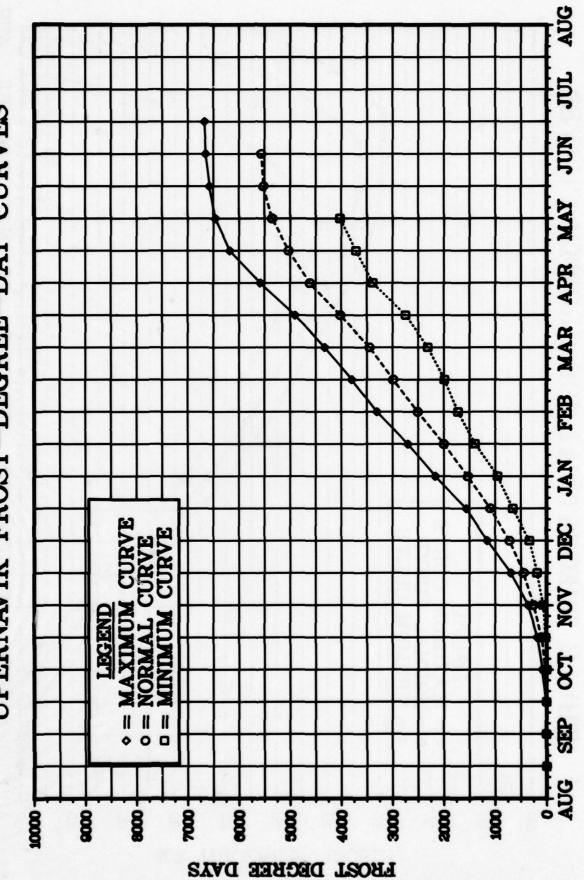


FIGURE 97A

223

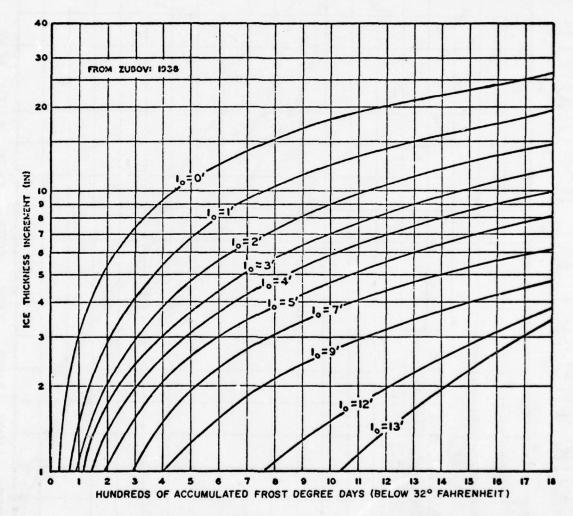


FIGURE 98 ICE-GROWTH GRAPH FOR VARYING ICE-THICKNESS AND SMALL DEGREE-DAY ACCUMULATIONS

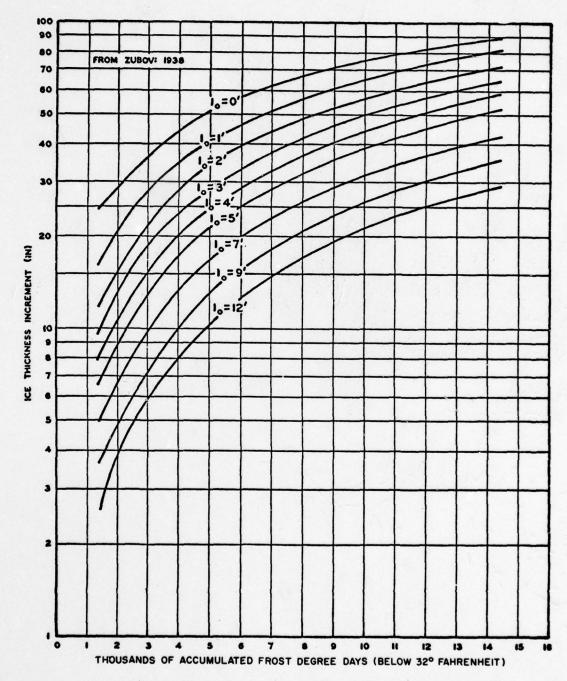


FIGURE 99. ICE-GROWTH GRAPH FOR VARYING ICE THICKNESS AND LARGE DEGREE-DAY ACCUMULATIONS

APPENDIX A

MEAN SEA LEVEL PRESSURE CHART (MB), JANUARY-DECEMBER

EASTERN NORTH AMERICAN ARCTIC AREA

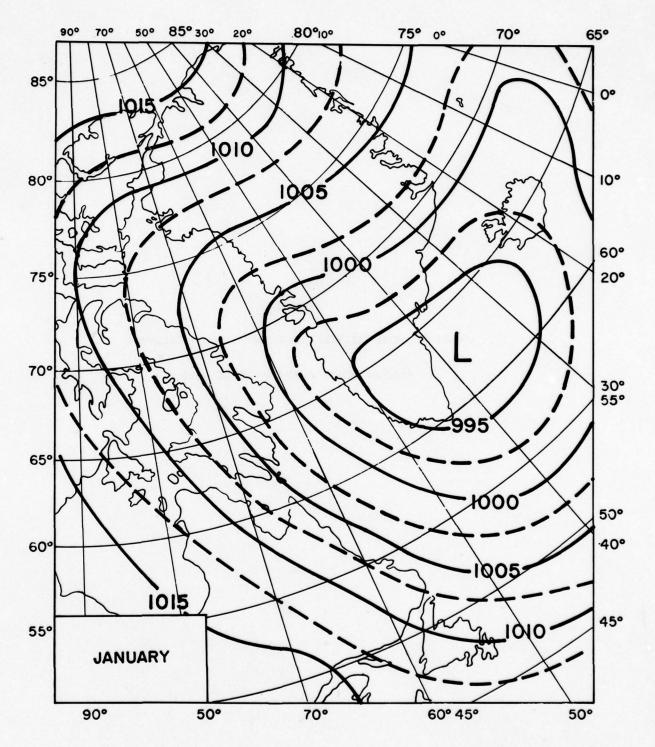


FIGURE A-1

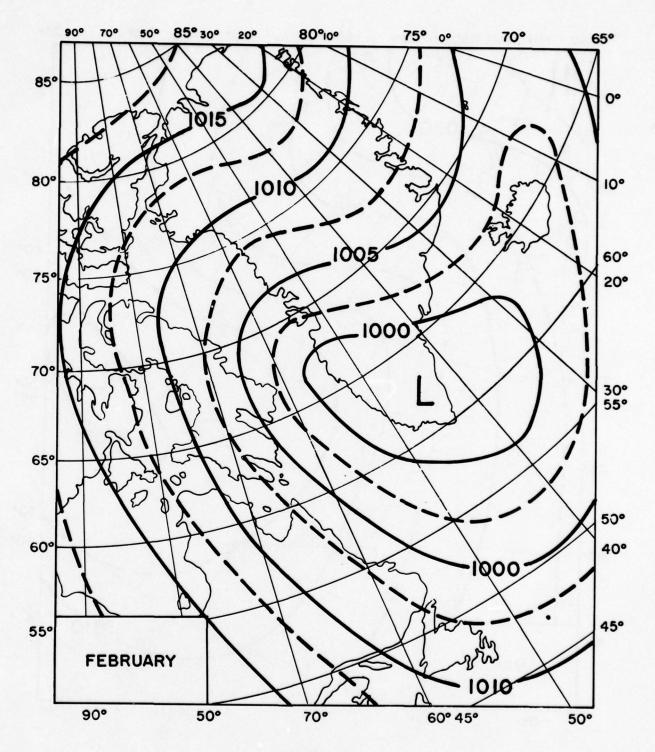


FIGURE A-2

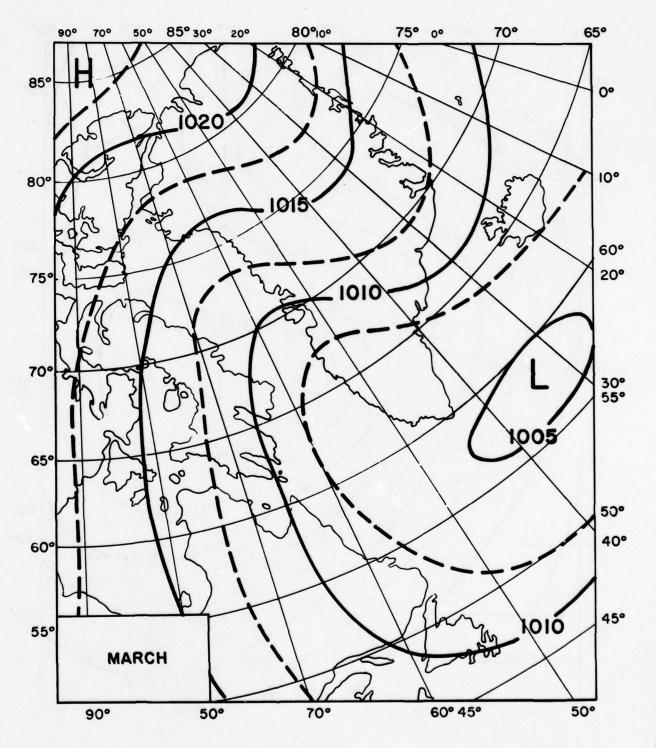


FIGURE A-3

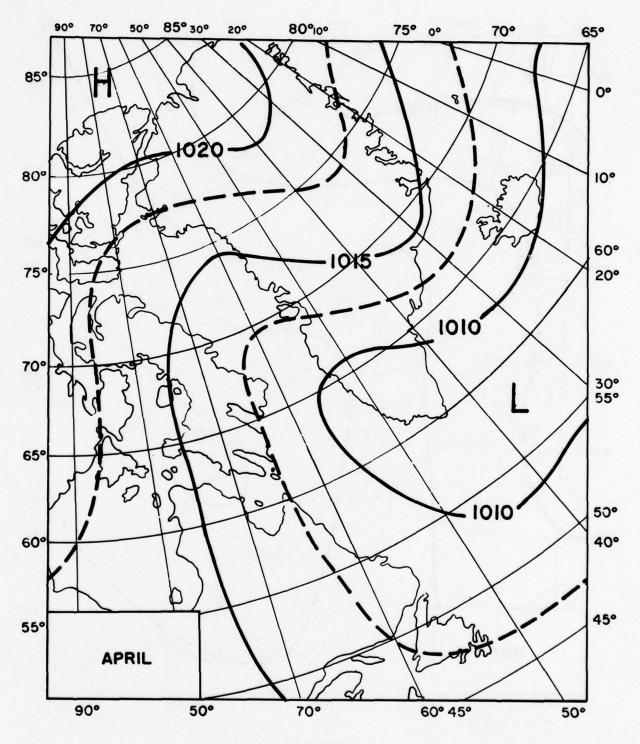


FIGURE A-4

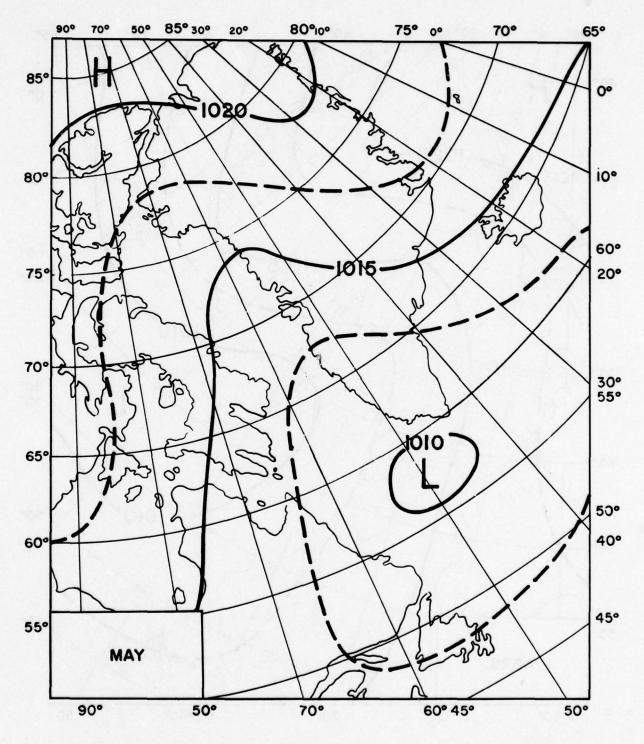


FIGURE A-5

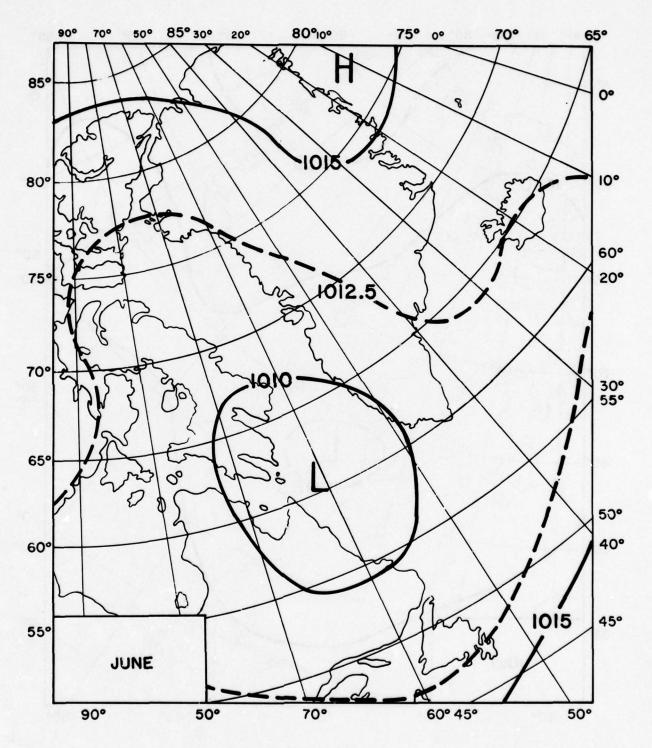


FIGURE A-6

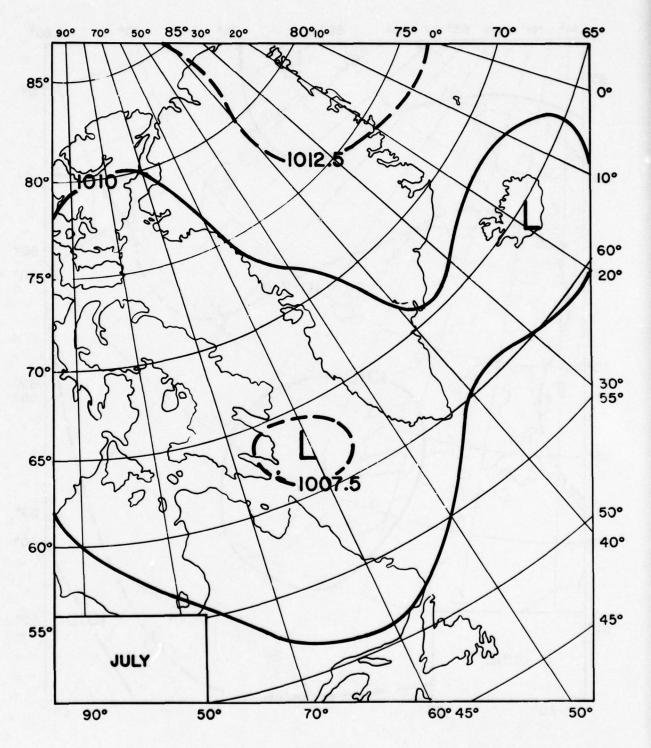


FIGURE A-7

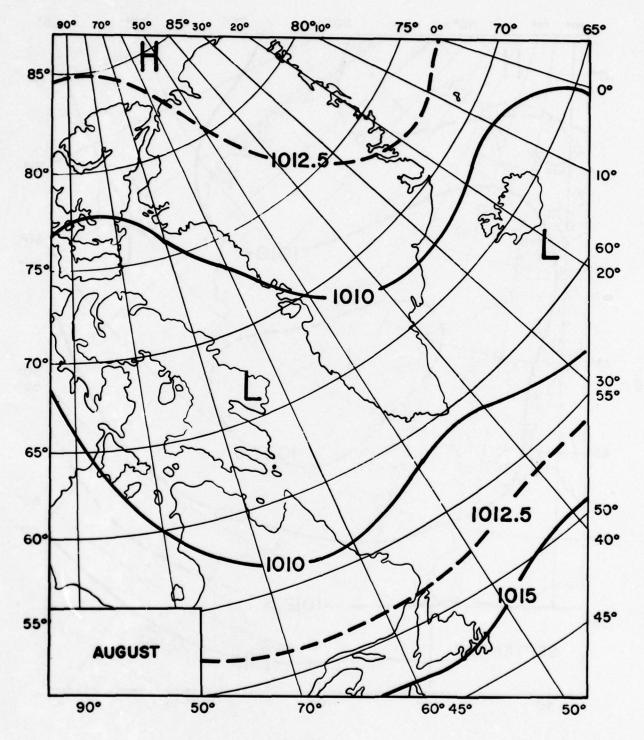


FIGURE A-8

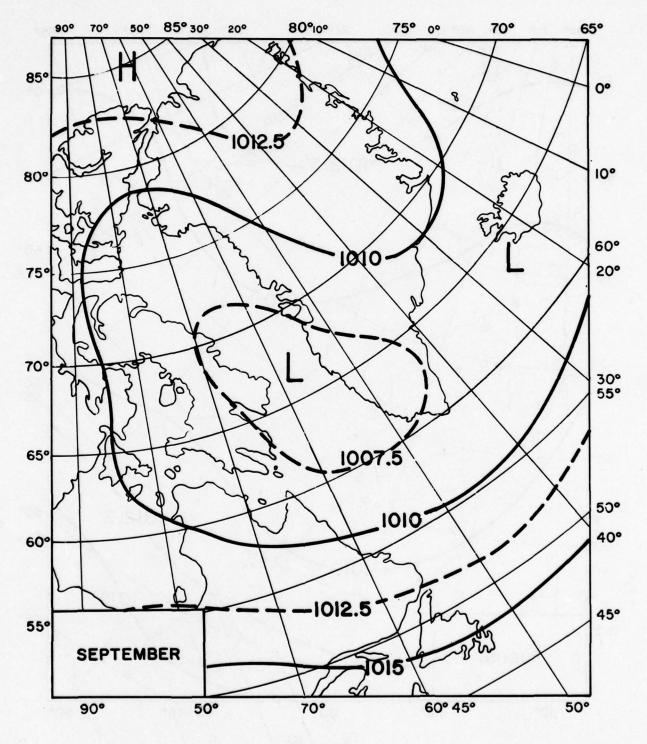


FIGURE A-9

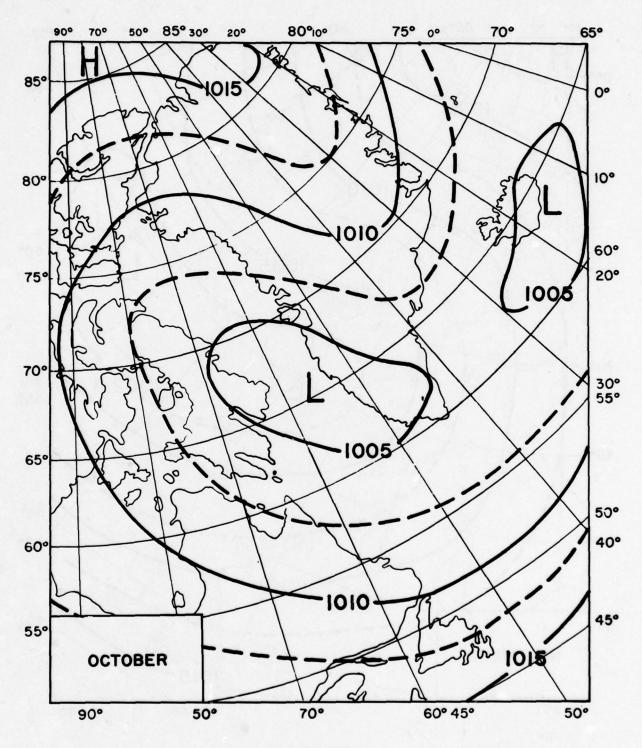


FIGURE A-10

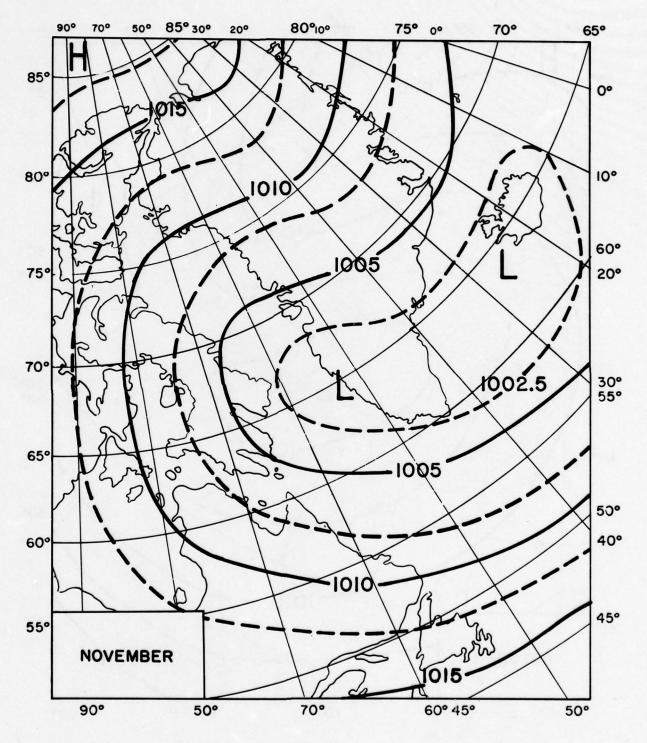


FIGURE A-11

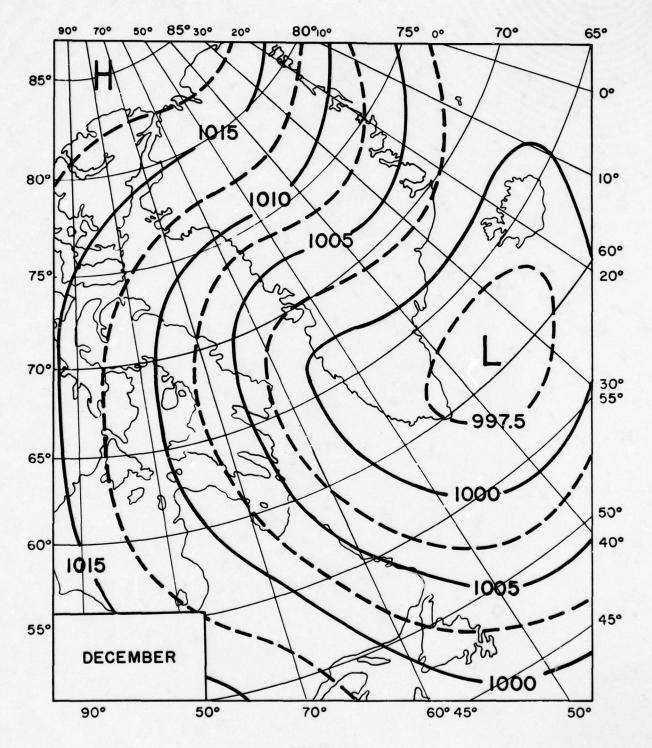


FIGURE A-12

APPENDIX B

MEAN MONTHLY SURFACE AIR TEMPERATURE CHARTS (°F), JANUARY - DECEMBER

EASTERN NORTH AMERICAN ARCTIC AREA

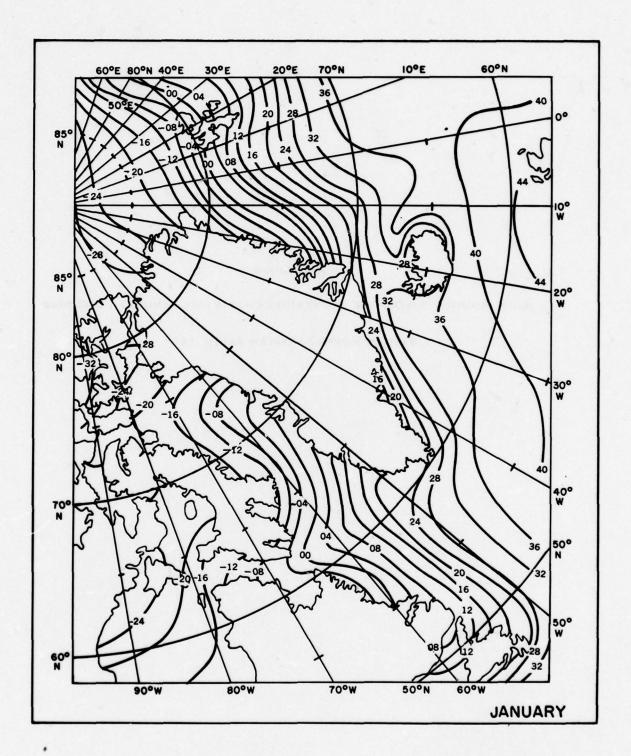


FIGURE B-1

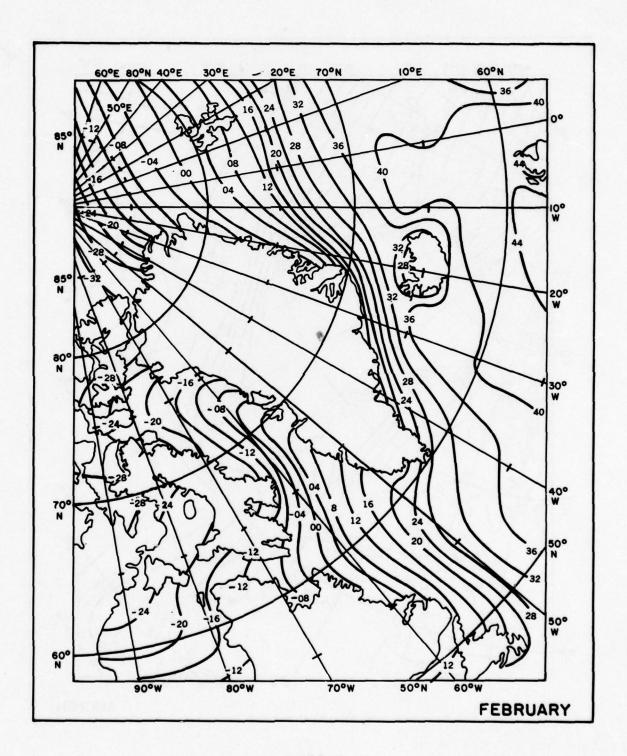


FIGURE B-2

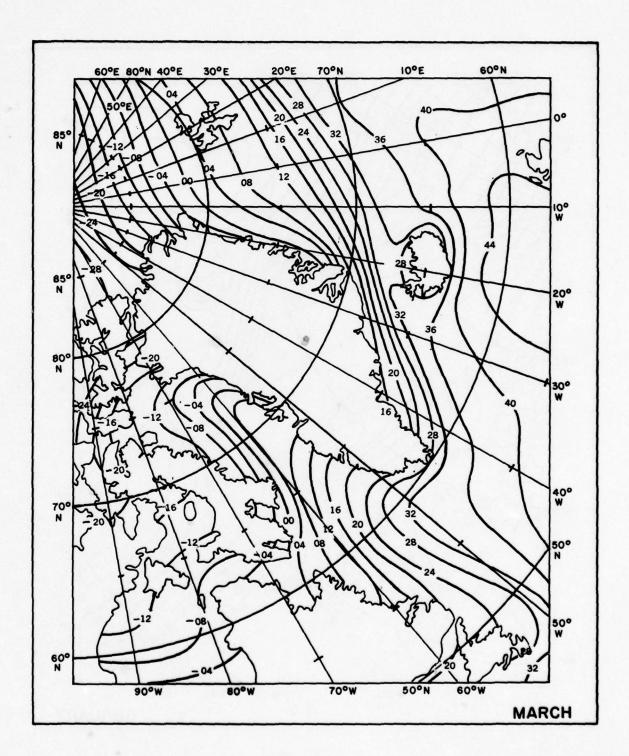


FIGURE B-3

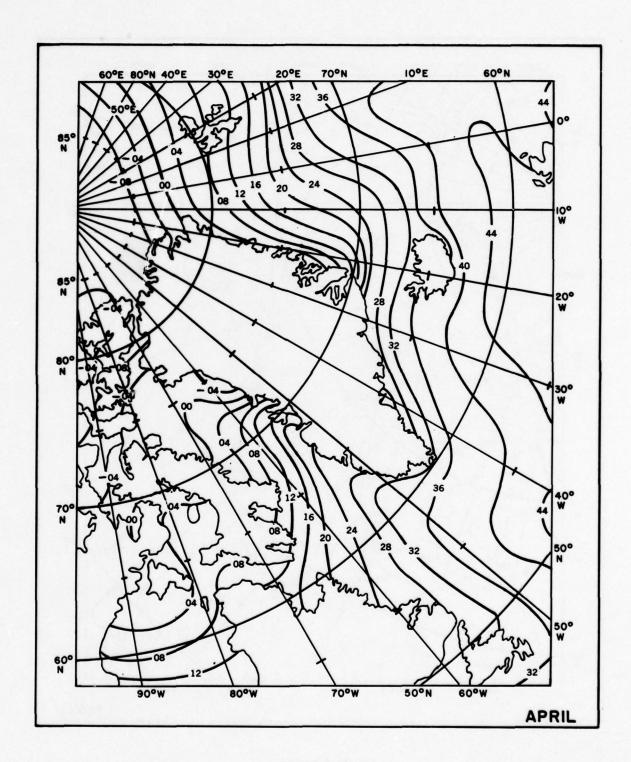


FIGURE B-4

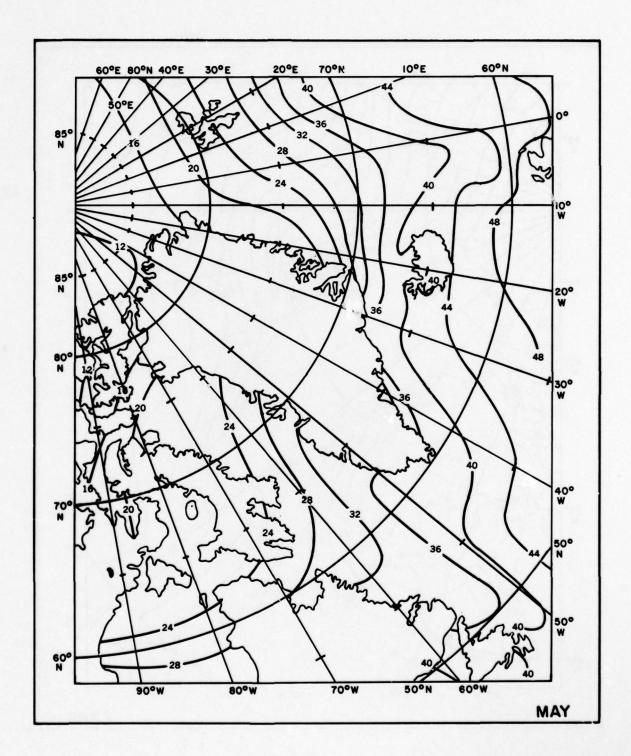


FIGURE B-5

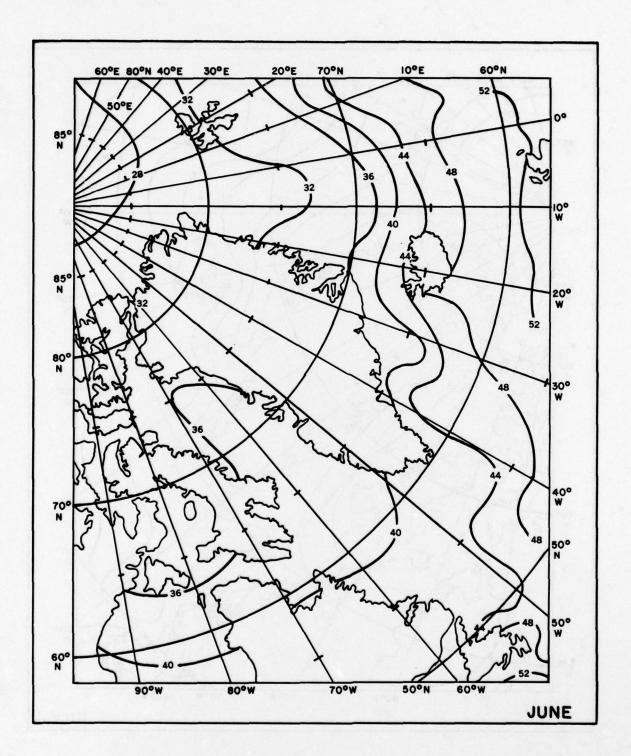


FIGURE B-6

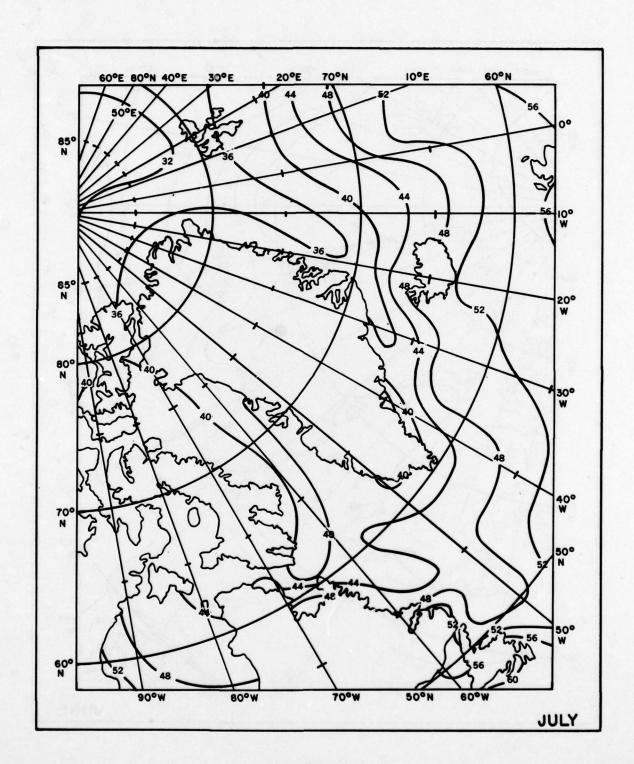


FIGURE B-7

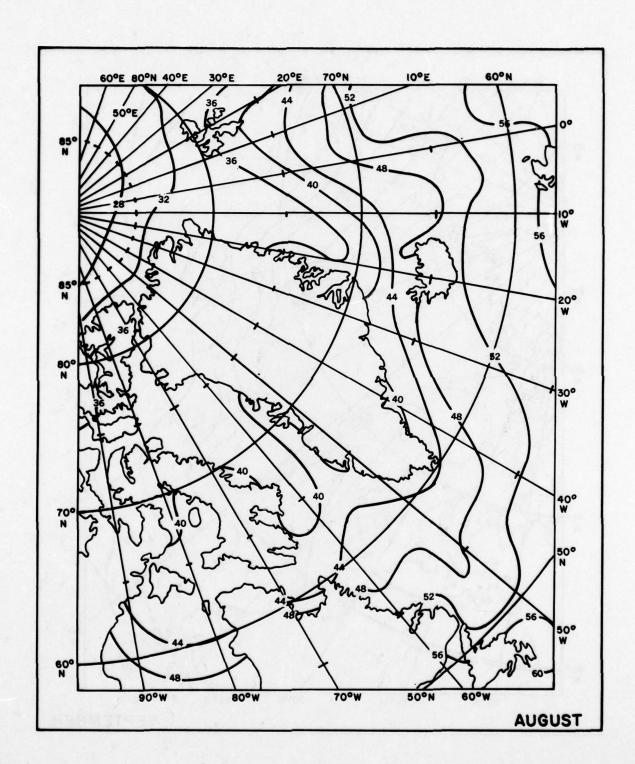


FIGURE B-8

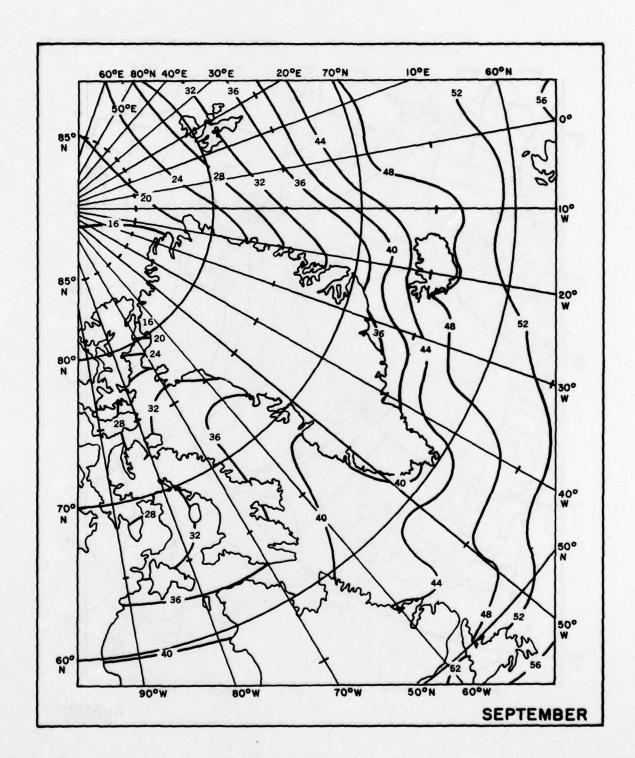


FIGURE B-9

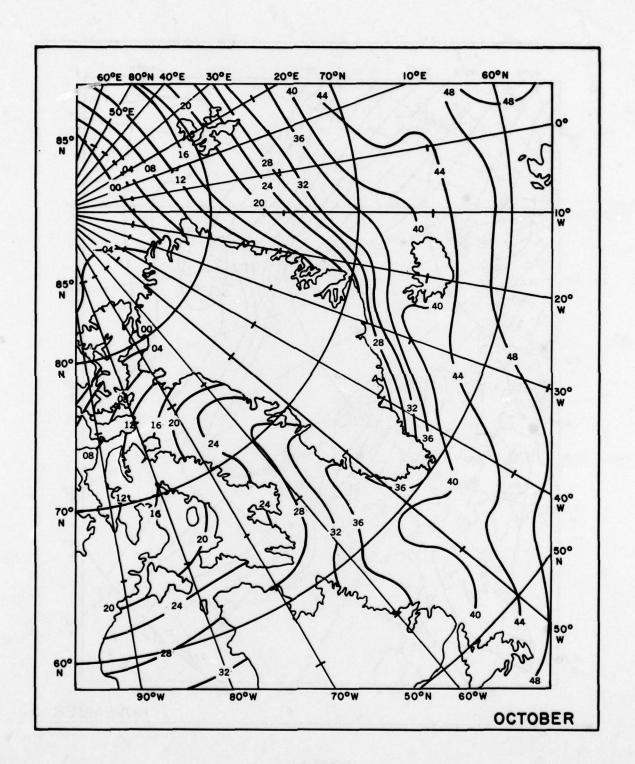


FIGURE B-10

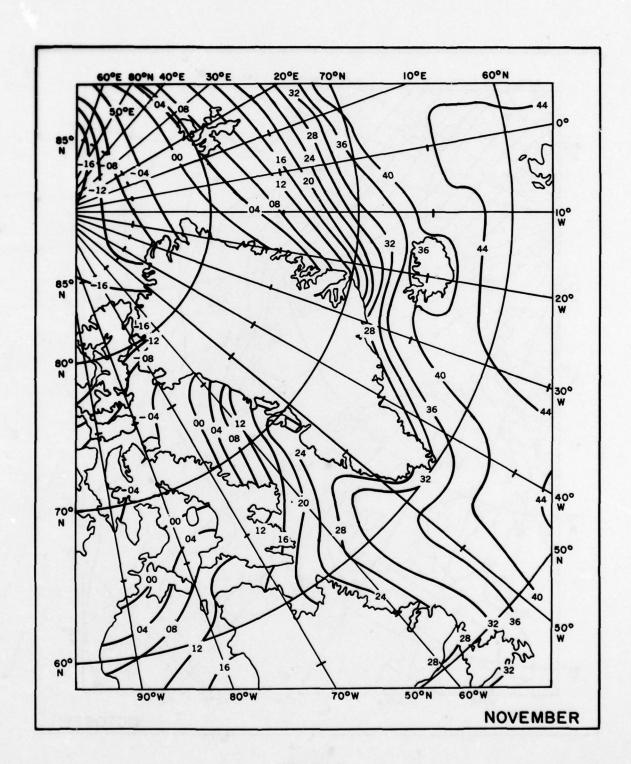


FIGURE B-11

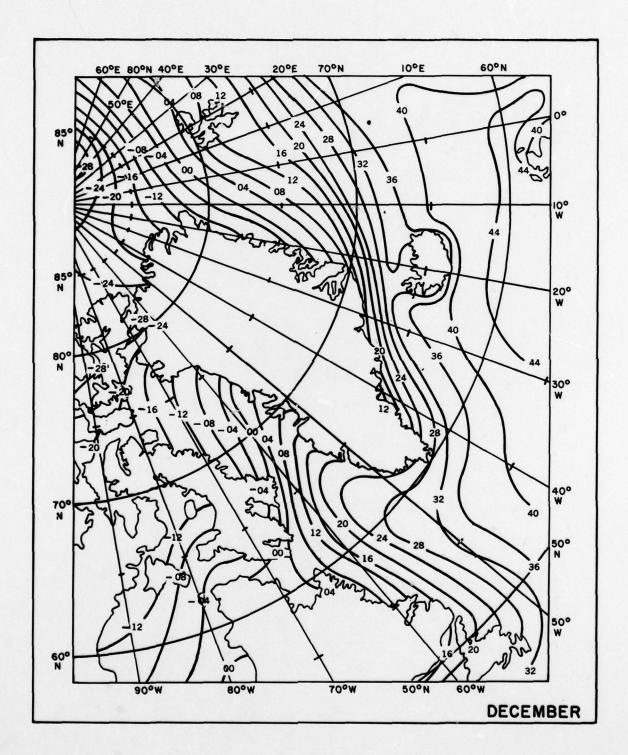


FIGURE B-12

APPENDIX C

700-MILLIBAR DEPARTURE-FROM-NORMAL THICKNESS DERIVATION AND

30-DAY DEGREE DAY MODIFICATION TABLE TO

PREDICTED TOTALS

To facilitate use of the 30-day mean 700-mb prognostic height D.N. charts produced on 12 December 1974 and thereafter, values on the charts are isoplethed for every 25 meters above or below normal. Therefore, if a specific station is located between isopleths interpolate to determine the correct value. The exact percentage of the departure-from-normal values given on the prognostic charts varies according to the conversion of D.N. values to mean virtual temperature.

The 1000- to 700-mb departure-from-normal thickness can be related to mean departure from normal and to virtual temperature by the following equation:

$$\Delta(\Delta h) = \Delta \overline{T}_v \frac{R}{g} \ln \frac{P}{P}$$

where $\Delta(\Delta h)$ = departure from normal in meters between the 700-mb height and the 1000-mb height

 $\Delta \overline{T}_{v}$ = change in mean virtual temperature (°C)

R = gas constant $(2.87 \times 10^6 \text{ ergs gm}^{-1} \text{ deg}^{-1})$

 $g = gravity (980 dynes gm^{-1}), and$

 $\ln \frac{P}{P}$ = natural log of the two isobaric surfaces (P = 1000 mb and P' = 700 mb).

Therefore, the change in the mean virtual temperature becomes

$$\Delta \overline{T}_{v} = \frac{\Delta(\Delta h)}{10.5}$$
 (°C,m)

If one were to use only the 30-day mean 700-mb prognostic height D.N. prediction, the relationship given above still can be used. Assuming that the variations of the 1000-mb level are small,

then

$$\Delta \overline{T}_{v} = \frac{\Delta_{700\text{mb}}^{h}}{10.5}$$

because the mean departure from normal is assumed to be uniform through the layer.

Table VIII takes into account the conversion of the mean virtual temperature from degrees Celsius to degrees Fahrenheit.

Table C-1

Number of Frost Degree-Days² to Add to or Subtract from Projected Totals (30-day Period) Using Meter Values from the 30-day Mean 700-mb Prognostic Height D.N. Chart

Meter Values +	0	10	20	30	40	50	60
Degree Days	0	16	31	47	61	77	93
Meter Values +	70	80	90	100	110	120	130
Degree Days	107	123	140	154	170	184	201

Use one-half of the degree-day values for a 15-day period.

When a positive meter value is predicted, subtract degree-days from the projected totals; when a negative meter value is predicted, add degree-days to the projected totals.

DISTRIBUTION LIST

NAVY

FLTWEACEN FLEWEAFAC NUPTLAB NUSC NAVWARCOL COMSUBDEVGRUTWO NATTC NAVAIRDEVCEN **USNA ANNA OCEANDEVRON** NAVSHIPRANDCEN NSWC NISC

CNO, Codes OP-32, 951E, 981 and 987T1

COMNAVWEASERV

NRL, Codes 2027, 8040 and 8310

NAVSEA, Code 06H1-4

NAVFACENGCOM

COMSC **OCEANAV**

ONR, Code 461 COMSUBLANT FLETRACEN

LANTFLEASWTACSCOL COMNAVAIRLANT COMSERVLANT

CINCPACFLT, Code 97

FLTASWSCOL

NELC

FLENUMWEACEN NAVPGSCOL

ENVPREDRSCHFAC/NAVPGSCOL

NSC/MSC NAVARCLAB

OTHER GOVERNMENT AGENCIES

USAF ETAC USAFCRL/L G Hanscom Field USA CRR&E LAB USCG/PSD USCGTC/MSS USCGC GLACIER USCGC NORTHWIND USCGC POLAR STAR USCGC POLAR SEA

USCGC WESTWIND INT ICE PAT NOAA/OTC HQAWS-AWVAS/TF NOAA, NWS/WSSO-SSD NOAA, NWS/W13 NOAA, S33 NOAA/EMP NOAA/NOS NOAA/TPB NOAA/NESS NAS/CPR DAMI/SD DA/Lib DMAHC, Code 506 CIA/CRD/ADD/STD DIST DLC/EG ODS/DDR&E-TWP, OC JCS/J3-38 USCGOU GPO/PDD NTIS CERC DDC, 12 copies NCC NMFS/ABFL

UNIVERSITIES

MIT, DOCS URI MLDS/SUNY, STONY BROOK CUIO, NY L-DGO OSU/IPS JHU/CBI GIF/AU AK OSU **HSC** SIO/UC

FOREIGN

AINA CANADA DAO NAV DIV CANADA DRB/DSIS CANADA DT/MOB CANADA DU/IO CANADA IFCES CANADA MC HDQTRS/HMS DOCKYARD CANADA CFH/M&O CANADA McG U CANADA EM&R/MB CANADA CINCLEASTLANTHQ/OFS-NATO, ENGLAND DMI DENMARK IOS ENGLAND SPRI ENGLAND GSPR GERMANY ORI/UT JAPAN US, Lib CANADA HMO JAPAN PRC/NSM JAPAN ILTS/HU JAPAN

PRIVATE

AINA OARI AGU UKSM WHOI

SHELF STOCK

DMADC/PHILA 150 copies
DMADC/CLEARFIELD 50 "
DMAODS 25 "

REPORT DOCUMENTATION PA	READ INSTRUCTIONS BEFORE COMPLETING FORM		
NOO SP-266	GOVT ACCESSION NO.	3. RECIPIENT'S CATALOG NUMBER	
EASTERN ARCTIC AREA 15- AND 30-DAY FORECASTING GUIDE	Special Publication 6. Performing org. Report number		
P.A. MITCHELL		8. CONTRACT OR GRANT NUMBER(*)	
Naval Oceanographic Office (NAVOCEANSTL Station Bay St. Louis, MS 39522	10. PROGRAM ELEMENT, PROJECT, TASK AREA & WORK UNIT NUMBERS		
1. CONTROLLING OFFICE NAME AND ADDRESS Naval Oceanographic Office (NAVOCEANSTL Station Bay St. Louis, MS 39522 4. MONITORING AGENCY NAME & ADDRESS(If different in	12. REPORT DATE 1979 13. NUMBER OF PAGES 259 15. SECURITY CLASS. (of this report) UNCLASSIFIED		
		15a. DECLASSIFICATION/DOWNGRADING SCHEDULE	
Approved for public release; distribution STATEMENT (of this Report) Approved for public release; distribution STATEMENT (of the abetract entered in			

18. SUPPLEMENTARY NOTES

19. KEY WORDS (Continue on reverse side if necessary and identity by block number)

Ice forecasting guide 15- and 30-day forecasts Eastern Arctic area Ice edge movement Advancement rates

Recession rates Ice growth Ice disintegration Frost degree days

Pack concentration

Breakup Freezeup

O. ABSTRACT (Continue on reverse side if necessary and identify by block number)

Procedures for preparing 15- and 30-day forecasts of ice conditions in the eastern North American Arctic which relate current and historical ice data to environmental parameters are given. Background data on the environmental factors which influence the growth, movement, and decay of sea ice in the eastern Arctic region are detailed and include primary and secondary storm tracks, sea level pressure, surface air temperature, and surface currents. Analyses of historical sea ice distribution data which have been observed

UNCLASSIFIED

LECURITY CLASSIFICATION OF THIS PAGE(When Data Entered)

ABSTRACT (continued)

over the 18-year period from 1954 through 1971 are presented and include the mean, median, mean maximum, mean minimum, absolute minimum, and absolute maximum eastern and western positions of the pack ice edges at half-monthly intervals. Advancement and recession rates of ice edge movement computed for the entire year and analyses of mean ice concentrations and percentage of large floe sizes for the western Labrador Sea, Baffin Bay/Davis Strait region, and the east Greenland coastal regions are included. Data also include frost degree-day, related ice-growth, and estimated ice disintegration curves for 17 eastern Arctic coastal stations. Statistical methods for forecasting ice growth, movement, distribution, and decay are presented since these methods have proven most successful.